
**Studies on lipid-induced mitochondrial dysfunction and
associated immune-metabolic perturbations: an approach
towards novel therapeutic interventions**

THESIS SUBMITTED FOR THE DEGREE OF
DOCTOR OF PHILOSOPHY (SCIENCE)

JADAVPUR UNIVERSITY



PROSENJIT DAS

METABOLIC DISORDER LABORATORY
CSIR-INDIAN INSTITUTE OF CHEMICAL BIOLOGY
4, RAJA S.C. MULLICK ROAD, KOLKATA 700032, INDIA

2024



सी.एस.आई.आर - भारतीय रासायनिक जीवविज्ञान संस्थान

वैज्ञानिक तथा औद्योगिक अनुसंधान परिषद की एक इकाई
विज्ञान एवं प्रौद्योगिकी मंत्रालय के अधीन, एक स्वायत्त निकाय, भारत सरकार
4, राजा एस. सी. मल्लिक रोड, यादवपुर, कोलकाता - 700 032

CSIR - INDIAN INSTITUTE OF CHEMICAL BIOLOGY

A Unit of Council of Scientific & Industrial Research
An Autonomous Body, under Ministry of Science & Technology, Government of India
4, Raja S. C. Mullick Road, Jadavpur, Kolkata-700 032



Dr. Sib Sankar Roy, Ph.D.
Chief Scientist

CERTIFICATE

This is to certify that the thesis entitled “**Studies on lipid-induced mitochondrial dysfunction and associated immune-metabolic perturbations: an approach towards novel therapeutic interventions**” Submitted by Sri Prosenjit Das who got his name registered on 07.12.2016 for the award of Ph. D. (Science) Degree of Jadavpur University, is absolutely based upon his own work under the supervision of Dr. Sib Sankar Roy and that neither this thesis nor any part of it has been submitted for either any degree / diploma or any other academic award anywhere before.

Dr. Sib Sankar Roy 04/6/24

Dr. Sib Sankar Roy
(Supervisor)
Head, Cell Biology & Physiology Division,
CSIR-Indian Institute of Chemical Biology,
4, Raja S.C. Mullick Road,
Kolkata-700032

डॉ सिब संकर राय / Dr. Sib Sankar Roy
मुख्य वैज्ञानिक / Chief Scientist
Head, Cell Biology & Physiology Division
सीएसआईआर - भारतीय रासायनिक जीवविज्ञान संस्थान
CSIR-Indian Institute of Chemical Biology
विज्ञान एवं प्रौद्योगिकी मंत्रालय, भारत सरकार
Ministry of Science & Technology, Govt. of India
कोलकाता-७०० ०३२ / Kolkata - 700 032

CERTIFICATE

This is to certify that the thesis entitled "**Studies on lipid-induced mitochondrial dysfunction and associated immune-metabolic perturbations: an approach towards novel therapeutic interventions**" Submitted by Sri Prosenjit Das who got his name registered on 07.12.2016 for the award of Ph. D. (Science) Degree of Jadavpur University, is absolutely based upon his own work under the supervision of Dr. Shampa Mallick and that neither this thesis nor any part of it has been submitted for either any degree / diploma or any other academic award anywhere before.

Shampa Mallick.
04/06/2024
Dr. Shampa Mallick
(Supervisor) *Retd.*

Dr. Shampa Mallick
Principal Investigator (DBT-BIO-CARe)
Indian Institute of Chemical Biology
(CSIR - Govt. of India), Kolkata-700032

Dedicated to “My Family”

ACKNOWLEDGEMENTS

First and foremost of all I thank Almighty God for “Everything”.

Today standing on the verge of completion of writing my Ph.D. thesis, when I look back through the path I came so far, it absolutely fills my heart with collages of memories. My writing would be incomplete without penning some of the names and thanking them for being in my life and enriching the whole experience while contributing in their own ways.

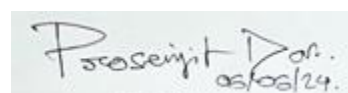
You cannot thank your **family** because it is all you have, undoubtedly unconditional. **Ma, Bapi**, I love you so much and am blessed to have you people in my life. **Riya**, my lovely wife, without you being there it would not have been possible for me to reach here today, thanks for making me complete. Blessings from my Baba-Ma (In-Laws), love and friendship of Tutun, Sourav, Tiya, Banguda, Subho & Golu made my journey smooth and filled gloomy days with rays of sunshine. Bhutu, your memory will be cherished.

Most importantly, I would like to convey my heartiest gratitude and reverence to my mentor, guide, and supervisor **Dr. Sib Sankar Roy**, Chief Scientist at CSIR-IICB for his constant support and technical help throughout my tenure. His continuous encouragement, constructive suggestions, and positive attitude greatly influenced me academically as well as personally. Thank you, Sir, for your esteemed guidance, financial and moral support, and for creating a conducive work environment for me.

This day I must thank my previous mentors, **Dr. Shailaja M. Dharmesh**, CSIR-CFTRI, and **Prof. Siddhartha Roy**, J C Bose Fellow, Ex. Director IICB for implanting the seeds of curiosity and being the motivation throughout my career. I am grateful to **Dr. Shampa Mallick** for her throughout guidance and helpful suggestions. I am honored to get a chance to collaborate with **Prof. Satinath Mukhopadhyay**, Professor at IPGMER, and enriched by his guidance and deep knowledge. I am indebted to **Dr. Deepak Kumar**, Scientist at CSIR-IICB for his mentorship and advice which greatly shaped my research interest and aptitude.

I am grateful to my friends and colleagues at the Indian Institute of Chemical Biology especially Anand, Anoy, Arijit, Abhishek, Kamran, and Nicky for their cordial support. I thank my past and present lab mates Eshani, Parash, Sampurna, Shreya (Jr.), Priti, Dipshikha, Eshayan, Suman, Bidisha, and the next generation stars Udit, Dev, Subhadeep & Pallabi for their support. I am grateful to Nabanita Di for all the help and guidance. I thank Prabirda, for his technical help and support throughout my tenure. I thank every staff and technician of the central instrumentation facility of IICB for their guidance. I am thankful to the past and present Directors of IICB. I am profoundly thankful to the Secretary, the Faculty Council of Science, and all the staff members of the Ph.D. cell of Jadavpur University for their cooperation.

I thank University Grant Commission and CSIR, for providing fellowship and necessary research infrastructure.

A handwritten signature in black ink that reads "Prosenjit Das" with the date "05/06/24" written below it.

PROSENJIT DAS

: List of Abbreviations:

ACC	Acetyl CoA Carboxylase
AFM	Atomic force microscopy
Akt	Protein B
ALT	Alanine aminotransferase
AST	Aspartate aminotransferase
ATP	Adenosine triphosphate
CPT-IA	Carnitine palmitoyltransferase IA
CYP26A1	Cytochrome P450 26A1
Cyt C	Cytochrome C
DAG	Diacylglycerol
DHA	Docosahexaenoic Acid
DMEM	Dulbecco's Modified Eagle Medium
DRP1	Dynamin-related protein 1
ECM	Extracellular matrix
ER	Endoplasmic reticulum
FA	Fatty acids
FAO	Fatty Acid Oxidation
FASN	Fatty acid synthase
FEN	Fenofibrate
FFAs	Free Fatty Acids
FGF21	Fibroblast Growth Factor 21
Fis1	Fission Protein 1
FOXO1	Forkhead Box Transcription Factor
FXR	Farnesoid X Receptor
GLP	Glucagon like peptide-1
GLUT4	Glucose transporter type 4
GPx	glutathione peroxidase
GSH	reduced glutathione
H ₂ O ₂	Hydrogen Peroxide
HCC	Hepatocellular Carcinoma
HE	Hematoxylin and Eosin
HFD	High Fat Diet
HOMA-	
IR	Homeostasis Model Assessment for Insulin Resistance
Hr	Hour
HSCs	Hepatic stellate cells
IF	Immuno-fluorescence
IHC	Immunohistochemistry
IKK	Inducer Kinase
IL	Interleukin

IR	Insulin Resistance
IRS	Insulin receptor substrate
JNK	c-Jun amino-terminal Kinase
JNK	Janus Kinase
LPA	Lysophosphatidic acid
LXR	Liver X Receptor
MAPK	Map Kinase
MDA	Malondialdehyde
MetS	Metabolic syndrome
MFN1/2	Mitofusin 1 and 2
MFN2	Mitofusin 2
Min	minutes
MnSOD	manganese superoxide dismutase
MRC	Mitochondrial Respiratory Chain Complex
MRS	magnetic resonance spectroscopy mTOR Molecular target of rap
mtDNA	Mitochondrial DNA
mTORC	Mammalian Target of Rapamycin Complex 1
NAD	nicotinamide adenine dinucleotide
NADP	Nicotinamide Adenosine diphosphate
NAFLD	Non-Alcoholic Fatty Liver Disease
NAO	Nonyl Acridine Orange
NASH	Non-Alcoholic Steatohepatitis
NEFA	Non-esterified Fatty acids
NF- κ B	Nuclear Factor κ B
OCR	Oxygen Consumption rate
OL	Oleate
Opal	Optic atrophy 1
OS	Oxidative stress
PA	Palmitic Acid
PBS	Phosphate Buffer Saline
PCR	Polymerase Chain Reaction
PDK1	phosphoinositide-dependent kinase 1
PGC1 α	Peroxisome proliferator-activated receptor gamma coactivator
PI3K	Phosphatidylinositol 3-kinase
PIP2	phosphatidyl-inositol-3, 4-bisphosphate
PIP3	phosphatidyl-inositol-3, 4, 5-trisphosphate
PK	Pyruvate kinase
PKC	Protein Kinase C
PPAR	Peroxisome proliferator-activated receptor
PPRE	Peroxisome proliferator responsive element
PRE	PPAR response elements

PREF1	Pre-adipocyte-factor 1
PUFA	Polyunsaturated fatty acid
RA	Retinoic Acid
RIPA	Radio Immuno Precipitation Assay
ROS	Reactive Oxygen Species
RT-PCR	Real Time Polymerase Chain Reaction
SARO	Saroglitazar
SCD	Steryl CoA desaturase
SDS	Sodium Dodecyl sulphate
SEM	Scanning Electron Microscopy
SIRT	Sirtuin Family
SIRT1	Sirtuin 1
SREBP	Sterol regulatory element-binding protein
STRA6	Stimulated by Retinoic Acid Gene 6 homolog
T2DM	Type 2 Diabetes Mellitus
TAG	Triacylglycerol
TBST	Tris-Buffered Saline containing 0.1% Tween-20
TFAM	Transcription factor A-Mitochondrial
TIMP	matrix metalloproteinases
TLR	Toll like receptor
TNF α	Tumor Necrosis factor- α
TZDs	Thiazolidinediones
VAD	Vitamin A Deficiency

Contents

1. Abstract.....	10
2. Review of Literature	13
2.1 Historical background:.....	14
2.1.1 Fatty liver disease:	14
2.1.2 Non-alcoholic steatohepatitis (NASH)	15
2.1.3 Fibrosis:.....	16
2.1.4 Cirrhosis.....	16
2.1.5 Hepatocellular carcinoma	16
2.2 Epidemiology:.....	17
2.3 Pathophysiology and Risk Factors:.....	18
2.3.1 Multiple hit hypothesis:	18
2.3.2 Genetic predisposition:	19
2.3.3 Diet:	19
2.3.4 Gut microbiota and oxidative stress:.....	19
2.3.5 Obesity:	20
2.3.6 Insulin resistance:.....	21
2.3.7 Dyslipidemia:	22
2.3.8 Metabolic syndrome:	22
2.4 Diagnosis and Management:.....	22
2.5 NAFLD associated molecular targets for intervention:	23
2.5.1 Oxidative stress (OS) in NAFLD:.....	23
2.5.2 The Role of SREBP in NAFLD:.....	25
2.5.3 The role of ChREBP in NAFLD:.....	25
2.5.4 The role of AMPK in NAFLD:.....	26
2.5.5 The role of SIRT1 in NAFLD:.....	27
2.5.6 The role of peroxisome proliferator-activated receptor (PPAR) α in NAFLD :	27
2.5.7 Inflammation in NAFLD:	28
2.6 Mitochondria in NAFLD:	30
2.6.1 Mitochondria Physiology:.....	31
2.6.2 Altered Mitochondrial Bio-energetics in fatty liver:.....	32
2.6.3 Mitochondrial reactive oxygen species, antioxidant defense:.....	33

2.6.4 Mitochondrial Dynamics in NAFLD:	34
2.6.5 Maintaining mitochondrial homeostasis by Mitophagy and Autophagy:	36
2.6.6 Role of mitochondrial fatty acid β -oxidation in NAFLD:	38
2.7 Therapeutic strategies in NAFLD:	39
2.7.1 Dietary changes:	40
2.7.2 Recommended drugs for NAFLD:	40
2.7.3 Antioxidant therapy in NAFLD:	41
2.8 Medicinal plants in NAFLD: Importance of <i>Wrightia tinctoria</i> :	42
2.9 <i>Wrightia tinctoria</i> : a potential medicinal plant and a possible NAFLD cure	43
2.9.1 Anti-ulcer activity :	43
2.9.2 Anti-fungal activity:	43
2.9.3 Anti-bacterial activity:	43
2.9.4 Anti-psoriatic activity:	44
2.9.5 Free radical scavenging activity:	44
3. General Introduction	45
4. Aims and Objectives	48
5. Materials & Methods	51
5.1 Materials:	52
5.2 Methods:	54
6. Chapter 1	63
Screening of different extracts of <i>Wrightia tinctoria</i> seeds and in vivo oral toxicity studies	63
6.1. Introduction:	64
6.2. Collection of plant material:	65
6.3. Extraction Procedure:	65
6.4. Results:	67
6.4.1. Effects on cell viability:	67
6.4.2. Anti-oxidant properties of WT extracts:	68
6.4.3. Effects on Hepatic Oxidative Stress:	69
6.4.4. Evaluation of different WT extracts on inhibition of lipid accumulation:	69
6.4.5. Evaluation of WT extracts on inhibition of NO ₂ production in mouse macrophage cells:	71
6.4.6. The effect of WT extracts on glucose uptake using 2-NBDG in HepG2 cells:	72
6.4.7. Acute oral toxicity test details:	74

6.4.8. General sign and behavioral analysis:.....	74
6.4.9. Hematology parameters:	75
6.4.10. Liver tissue toxicity:.....	76
6.4.11. Kidney tissue toxicity:	76
6.4.12. Spleen tissue histology:.....	77
7. Chapter-2	79
Role of <i>Wrightia tinctoria</i> seed hydro-ethanolic extract in ameliorating mitochondrial dysfunction and associated disorders in <i>in vitro</i> and <i>in vivo</i> model of NAFLD	79
7.1. Introduction:.....	80
7.2. Results:.....	81
7.2.1. Wrightia hydro-ethanolic extract (WTEC) abrogates PA-mediated reduction in mitochondrial membrane potential:	81
7.2.2. Wrightia hydro-ethanolic extract (WTEC) rescues altered mitochondrial respiration and glycolytic flux in palmitic acid-induced HepG2 cells:.....	82
7.2.3. PA mediated Disruption of mitochondrial morphology was protected by wrightia hydro-ethanolic extract:	84
7.2.4. Effect of wrightia extracts on expression of mitochondrial OXPHOS complexes upon PA treatment:	87
7.2.5. WTEC improves palmitic acid abrogated mitochondrial biogenesis via PGC1 α -TFAM dependant manner:	88
7.2.6. Evaluation of SIRT1 as a modulator of mitochondrial biogenesis behind the activity of wrightia hydro-ethanolic extract:	89
7.2.7. Evaluation of mitochondrial dynamics parameters implicated by WTEC treatment in response to saturated fatty acid stress scenario:	90
7.2.8. Evaluation of autophagy-mitophagy parameters in the regulation of mitochondrial quality control with WTEC treatment:.....	91
7.2.9. Exploring time kinetics study related to mitochondria-mitophagy-autophagy crosstalk imparted by WTEC in maintaining mitochondrial homeostasis:	93
7.2.10. Wrightia hydro-ethanolic extract ameliorates mitochondrial dysfunction through activation of AMPK α :.....	100
7.2.11. Evaluation of wrightia extract in the regulation of lipid metabolism in the context of fatty acid stress in hepatic cells:.....	101
7.2.12. High-fat diet (60% Kcal) feeding induces obesity and subsequent pathogenesis of non-alcoholic fatty liver disease:	104
7.2.13. Effect of wrightia hydroethanolic extract on mitochondrial and cytosolic enzyme activities responsible for maintaining bioenergetic and oxidative status:	109

7.2.14. Mitochondrial Biogenesis enzyme and autophagy gene expression were increased by WTEC in HFD-fed liver tissue:	110
7.2.15. Validation of AMPK α mediated amelioration of mitochondrial dysfunction by WTEC in HFD induced fatty liver model:	112
7.3. Discussion:	113
8. Chapter-3	116
Role of <i>Wrightia tinctoria</i> seedpod extracts in mitigating inflammation and characterization of compounds:	116
8.1. Introduction:	117
8.2. Results:	118
8.2.1. Extraction and isolation procedure of extracts from <i>Wrightia</i> seed pods:	118
8.2.2. Evaluation of cytotoxicity of seedpod extracts in macrophage cells by MTT assay:	118
8.2.3. Role in inhibition of total cellular oxidative stress:	120
8.2.4. Evaluation of reduction in pro-inflammatory cytokines expression by ELISA and RT-PCR:	120
8.2.5. Anti-inflammatory activities of hydro-ethanolic extract (50:50) of <i>wrightia</i> seedpods:	123
8.2.6. Characterization of phytoconstituents present in hexane fraction (Fr-B) and hydro-ethanolic extract of <i>Wrightia tinctoria</i> :	125
8.3. Discussion:	133
9. General Discussion	135
10. Bibliography	144
Publications	161

Abstract

Introduction:

In recent time sedentary lifestyle, poor food habits, and reduced physical activity are leading cause towards increase in obesity, insulin resistance, and dyslipidemia. Western diets, saturated fats, and adulterated oil contribute to the accumulation of free fatty acids inside hepatic cells, causing hypertension, mitochondrial dysfunction, and type-2 diabetes. Nonalcoholic fatty liver disease (NAFLD) affects over 30% of the general population and if untreated progresses to steatohepatitis, fibrosis, cirrhosis, and end-stage hepatocellular carcinoma. *Wrightia tinctoria*, also known as Indrajao, is used in traditional medicine for controlling jaundice, hyperglycemia, bowel diseases, and psoriasis. This study aimed to investigate the potential of *Wrightia tinctoria* seed extracts in improving lipid stress-induced metabolic diseases like NAFLD and associated mitochondrial anomalies.

Methodology:

The study used palmitic acid as a lipid stress inducer in an in-vitro model using hepatoma (HepG2), adipocyte (3T3L1), and macrophage (RAW264.7) cell lines. Phyto-extracts were extracted using various solvents (Hexane, ethanol, 50:50 ethanol: water and water). Molecular biology techniques like quantitative PCR, western blotting, and confocal microscopy were used. Mitochondrial morphology and integrity were studied using fluorescent probes such as Mito tracker red. Extracellular flux analyzers were used to measure mitochondrial bioenergetics parameters. The extract was then orally administered for 28 days to mice fed on a high fat diet (20weeks), and molecular experiments were conducted to validate its effect on mitochondrial dysfunction.

Results:

Based on the screening of four extracts, we can see the (50: 50) hydro-ethanolic extract (WTEC) of *Wrightia tinctoria* seedpod did not exhibit any cytotoxicity on human liver cell line in a broad range of concentration as well as in *in vivo* acute oral toxicity experiments. Consistently this fraction showed significant antioxidant activity and hindered lipid accumulation upon giving high saturated fatty acid stress and also improved mitochondrial bio-energetic function. This fraction along with hexane fraction (Fr-B) from ethyl acetate extract also effectively lowered pro-inflammatory markers often associated with NAFLD progression. WTEC significantly boosted mitochondrial biogenesis through activation of PGC 1 α , SIRT 1 and TFAM expression. Mitochondrial dynamics was also improved by inhibition of phospho-DLP1 (Serine 616) mediated mitochondrial fragmentation. *Wrightia* seedpod extract also activated mitophagy maintaining quality control. PARKIN and PINK1 level was restored and LC3B expression was augmented in palmitic acid treated hepatoma cells. Lipid metabolism was

also boosted as PPAR α , CPT1A level increased and fatty acid uptake was down by lowered CD36 level. WTEC also alleviated abnormal lipid levels, fasting blood glucose and collagen deposition in HFD model of NAFLD improving gross hepatic steatosis. Thus, WTEC at 1 to 10 μ g/ml dose range (*in vitro* hepatoma cells) and 250 -500mg/kg bodyweight (*in vivo* animal model) efficiently reversed the distressed mitochondrial physiology imparted by lipotoxic stress.

Conclusion:

Wrightia tinctoria is well acknowledged herb used in many traditional and ayurvedic treatment. However, the detailed mechanistic study on the mechanism of action of its specific extracts responsible for its positive effects, are still lacking. After comparing different extracts of wrightia seeds, the hydro-ethanolic extract (WTEC) showed the most potential beneficial effect in ameliorating the deregulated metabolic parameters. This particular extract improves the overall mitochondrial health as shown in hepatic lipotoxicity model employing palmitic acid and high fat diet, making it a safe and potential candidate against NAFLD. Characterization of compounds revealed presence of ω -3 poly unsaturated fatty acids (PUFA) in hexane fraction and phenolic compounds in WTEC, mainly responsible for bio-activity. Thus, wrightia seedpods hold an immense potential to generate an effective therapeutic lead against lipid-induced mitochondrial dysfunction and associated immune-metabolic perturbations in diseases like NAFLD.

Review of Literature

2.1 Historical background:

A range of fatty liver syndromes that do not arise from excessive alcohol intake (less than 30 grams of alcohol/per day in men; less than 20 grams of alcohol per day in women) is known as non-alcoholic fatty liver disease (NAFLD) (Chalasani et al., 2018).

Thomas Addison first described liver steatosis in 1836, a pathological buildup of intrahepatic fat content and Carrol Leevy classified the severity into five categories: normal, irregular, mild, moderate, and severe (Ayonrinde, 2021). In 1980, Jurgen Ludwig coined the term non-alcoholic steatohepatitis (NASH), and Elizabeth Brunt developed a standardized grading and staging technique for NASH diagnosis. Dietary changes have a strong chance of reversing fatty liver. More recently, a new term was coined as metabolic dysfunction associated fatty liver disease (MAFLD) in proposition to the widespread involvement of metabolic abnormalities associated with fatty liver (Pipitone et al., 2023).

2.1.1 Fatty liver disease:

Liver illnesses, including hepatic steatosis and fatty liver disease (FLD), are a growing global health concern. Alcohol-induced fatty liver disease (AFLD) and non-alcoholic fatty liver disease (NAFLD) are two major forms, with AFLD characterized by alcohol misuse and NAFLD influenced by other factors.

Nonalcoholic fatty liver disease (NAFLD) is a type of liver disease (FLD) caused by environmental factors such as a high-fat diet (HFD), drugs, HIV infection, and autoimmune disorders such as hepatitis triggered by the hepatitis B virus (HBV) and C virus (HCV) (Akinyemiju et al., 2017, Wahlang et al., 2019, Xanthakos et al., 2006). In the dearth of other potential causes of fatty liver, NAFLD is defined as lipid aggregation that exceeds 5% to 10% of the weight of the liver (Montecucco & Mach, 2008).

According to recent research, lipid buildup directly damages hepatocytes. This leads to a cascade of events including oxidative stress, cytokine generation, inflammatory response, aberrant cellular signaling, and stellate cell activation (Zisser et al., 2021). While the advancement rate of nonalcoholic fatty liver disease (NAFLD) may be slower than that of other liver diseases, its prevalence is rising alarmingly globally in tandem with the obesity pandemic. Moreover, NAFLD has no approved pharmaceutical treatment (Sumida & Yoneda, 2018). Therefore, dietary and lifestyle changes are presently the primary line of treatment for nonalcoholic fatty liver disease (NAFLD) (Zelber-Sagi et al., 2016).

Using different techniques for histopathological examination, NAFLD may be classified as macrovesicular or microvesicular steatosis qualitatively and as mild, moderate, or severe quantitatively. Hematoxylin and eosin (H&E) staining is frequently used to distinguish between two types of vesicular steatosis: (a) microvesicular steatosis and (b) macrovesicular steatosis (Takahashi, 2014).

(a) Microvesicular steatosis

Microvesicular steatosis is an unusual variant of fatty liver disease, characterized by larger hepatocytes with tiny lipid droplets and centrally placed nuclei. It is often associated with severe mitochondrial dysfunction, increased liver markers, and either with or without hepatic encephalopathy. It can affect the entire liver lobule or be predominant in centriportal, midzonal, or periportal hepatocytes.

(b) Macrovesicular steatosis

Macrovesicular steatosis is the most common type in humans, characterized by visible distinct gaps in hepatocyte cytoplasm by H&E staining. It is a fatty liver condition with a single large lipid droplet vacuole. Causes include obesity, diabetes, dyslipidemia, and alcohol consumption. A little elevation in blood transaminase levels, an enlarged liver, and hyper-reflective hepatomegaly on ultrasonographic evaluation may also be significantly linked to macrovesicular steatosis.

2.1.2 Non-alcoholic steatohepatitis (NASH)

Non-alcoholic steatohepatitis (NASH) is the second progressive phase of non-alcoholic fatty liver disease (NAFLD) (Akter, 2022) with abnormally increased liver enzymes. Histologically, NASH is distinguished by hepatocellular fat infiltration with ballooning, polymorphonuclear invasion, and sinusoidal fibrosis, with or without Mallory hyaline. (Sakhuja, 2014). High blood triglyceride and cholesterol levels are common in NASH patients. Metabolic diseases like hyperglycemia, obesity, T2DM, hyperlipidemia, and insulin resistance are the most common conditions responsible for the development of NASH.

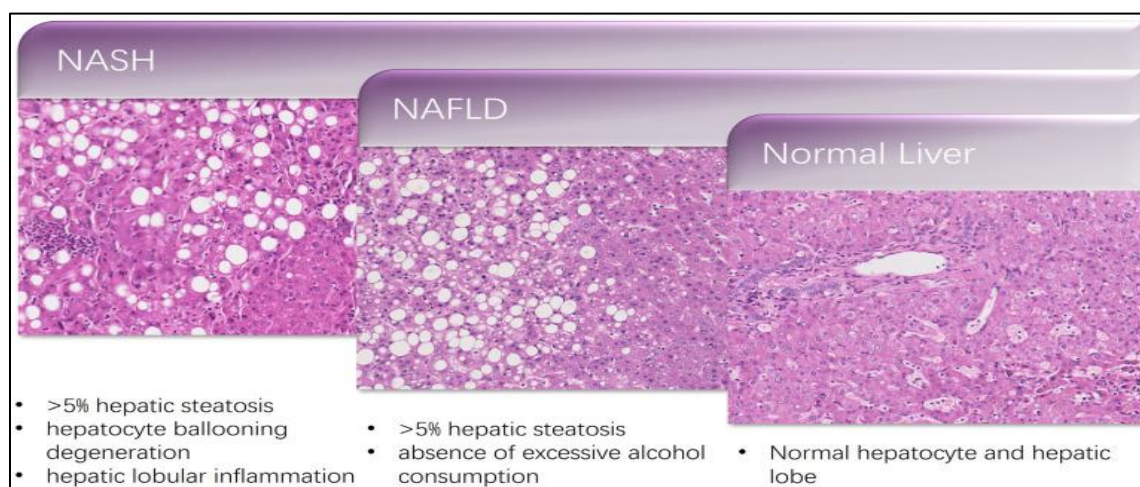


Figure 1: Histologic parameters of NAFLD doi: 10.3390/healthcare11010117

2.1.3 Fibrosis:

Liver fibrosis, a third progressive stage of NAFLD, is often clinically linked to insulin resistance and systemic hypertension in obese NASH patients. Higher levels of transforming growth factor- β 1 (TGF- β 1) and angiotensinogen (AT) with deposits of type 4 collagen 7S domain and hyaluronic acid are useful biochemical markers (Acharya et al., 2021) to determine the severity of fibrosis and distinguish between NASH patients with non-severe and severe fibrosis.

2.1.4 Cirrhosis

Liver cirrhosis an irreversible chronic condition and fourth stage of nonalcoholic fatty liver disease (NAFLD), marked by fibrosis and regenerating nodules is the basic definition of liver cirrhosis (Tanwar et al., 2020) with a propensity to worsen and lead to portal hypertension, hepatic dysfunction, and hepatocellular carcinoma (HCC). It is a global health challenge with no viable treatment options, leading to morbidity and death in undiagnosed NAFLD patients. It is more common in older, obese NASH patients with a history of T2DM.

2.1.5 Hepatocellular carcinoma

Hepatocellular carcinoma (HCC) is the leading cause of cancer-related mortality globally, with 30% linked to obesity, type 2 diabetes, and metabolic disorders like NASH and insulin resistance. Hepatic lipid accumulation with cirrhosis mediated by NASH is a key risk factor. Obese diabetics and non-diabetics can develop HCC, and a diet rich in saturated fat acids is the most likely cause of food-triggered metabolic disorders and liver cancer (Kanwal et al., 2020).

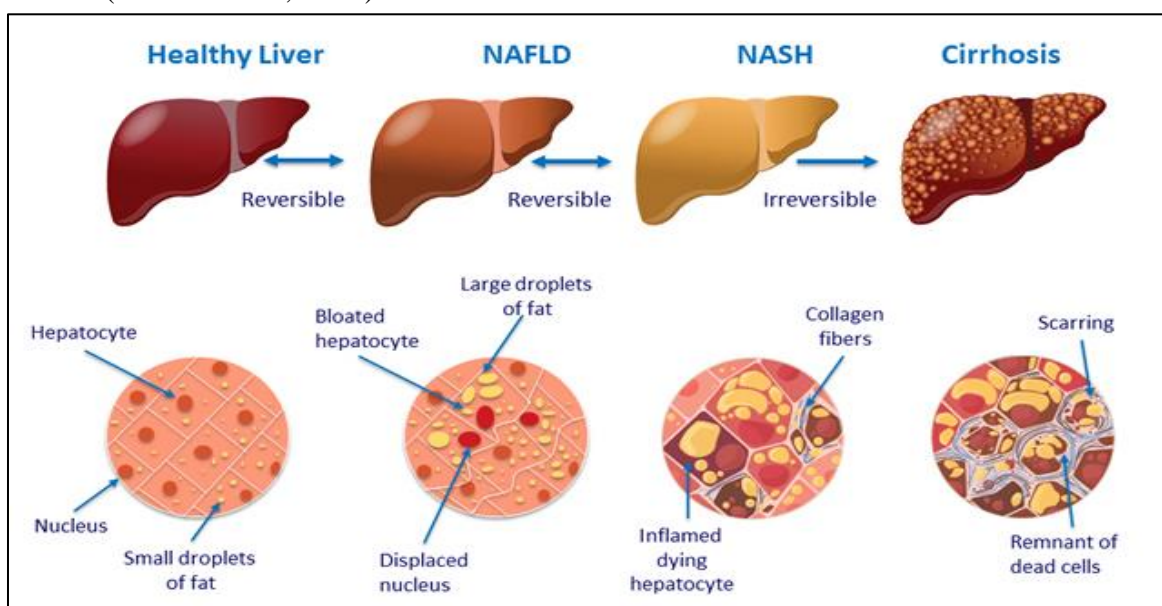


Figure 2: NAFLD progression stages <http://www.hcv-trials.com/nash/NAFLD-NASH.asp>

2.2 Epidemiology:

A recent meta-analysis (Riazi et al., 2022) found that there are 46.9 incidences of NAFLD for every thousand people per year, with males having a greater incidence than females. 32% of adults globally have NAFLD, with Southeast Asia having the greatest prevalence at 42%. Japan had the lowest pooled NAFLD prevalence at 22.28%, while Iran had the highest prevalence at 38.07%. The prevalence rate of non-alcoholic fatty liver disease (NAFLD) in South Asian countries like India (25.7–32.74%), Bangladesh (26.2–33.86%), and Sri Lanka (24.74%) are considered as moderate to high (Teng et al., 2023). The overall incidence of NAFLD in Southeast Asia was reported by Le et al. to be 38.5% in Malaysia, 51.04% in Indonesia, and 40.43% in Singapore. 10. A distinctive feature of the NAFLD epidemic in Asia is the high incidence of lean NAFLD (where body mass index <23) and non-obese non-alcoholic fatty liver (BMI <25). Using subgroup data from four research totaling 18,356 participants, Le et al., 2022 calculated that 35.3% of North Americans were estimated to have NAFLD. The National Health and Nutrition Examination Surveys recent 2017–2018 data were used to estimate the prevalence of NAFLD, which was 46.2% in non-Hispanic Blacks, 56.8% in Non-Hispanic Whites, and 63.7% in Hispanics (Zhang et al., 2021, Teng et al., 2023). Mathematical modeling studies predict that the worldwide burden of NASH and NAFLD will increase over the next ten years, with NAFLD prevalence predicted to increase to 55.4% by 2040. This raises concerns about the need for more financing and governmental will to address and mitigate metabolic risk factors for NAFLD at local, state, and federal levels.

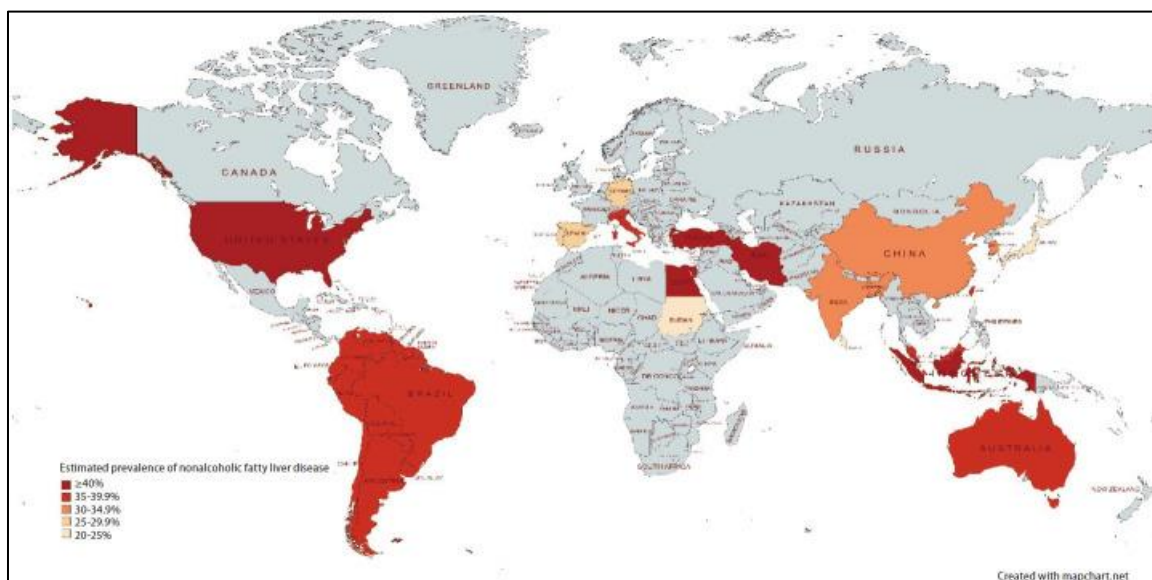
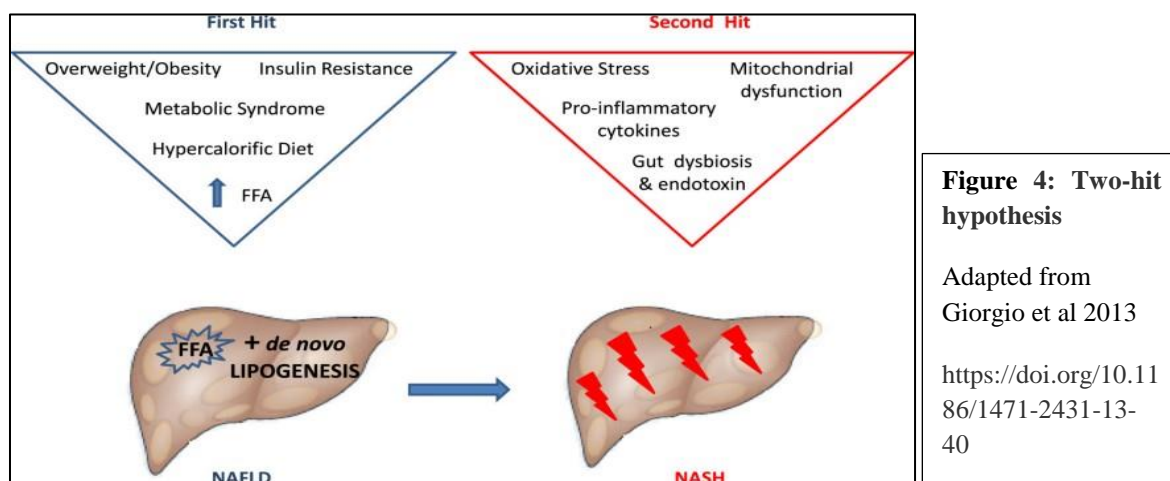


Figure 3: Global prevalence of NAFLD Adapted from Teng et al 2023 doi: [10.3350/cmh.2022.0365](https://doi.org/10.3350/cmh.2022.0365)

2.3 Pathophysiology and Risk Factors:

Nonalcoholic fatty liver disease (NAFLD) is a complex disease characterized by a combination of factors. After hepatic triglyceride accumulation, or "first hit," the liver becomes more vulnerable to damage from "second hits" such as oxidative stress accompanied by mitochondrial dysfunction and inflammatory cytokines/adipokines, which can cause steatohepatitis and/or fibrosis (Giorgio et al., 2013). The "two-hit" theory is no longer valid since it does not take account of the various molecular and metabolic alterations that occur in non-alcoholic fatty liver disease (NAFLD) and in recent times often gets replaced by the "multiple hit" theory.



2.3.1 Multiple hit hypothesis:

The "multiple hit" theory offers a more precise explanation of the pathophysiology of NAFLD by taking into account several insults operating in concert on genetically susceptible people to develop NAFLD (Buzzetti et al., 2016). Insulin resistance, metabolic disorders, adipokines, the function of FFA, dietary variables, gut microbiota, and genetic and epigenetic factors are examples of such hits.

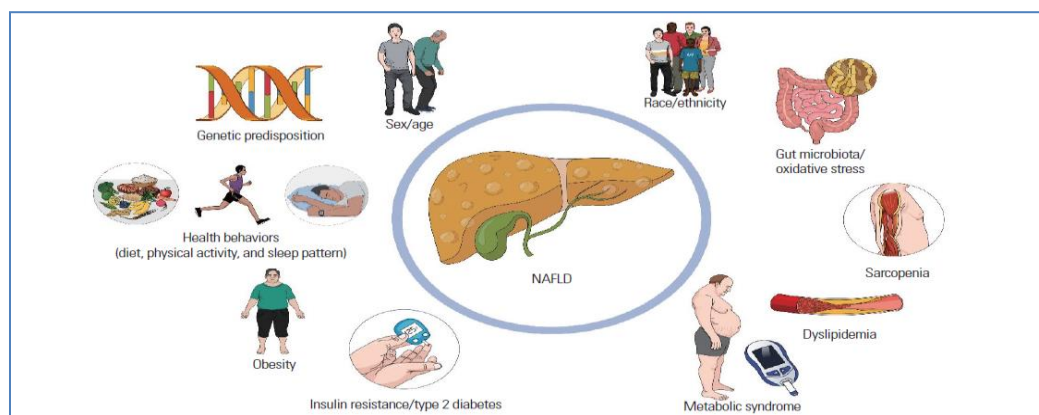


Figure 5: Risk factors of NAFLD Adapted from Huh et al 2022

2.3.2 Genetic predisposition:

In the recent decade, genetic variations have emerged as an important factor in the pathophysiology of NAFLD and also a focus of research, notably the identification of single nucleotide polymorphisms (SNPs), (Sulaiman et al., 2022). At least five or six significant variations in the unique genes linked to NAFLD have been recognized thus far:

Patatin-like phospholipase domain containing 3 (PNPLA3), which affects the development and progression of the NAFLD), membrane-bound O-Acyltransferase domain containing 7 (MBOAT7), glucokinase regulator (GCKR), transmembrane 6 superfamily, member 2 (TM6SF2), and collagen type XIII alpha 1 (COL13A1, significantly linked to increased fibrosis severity (J. Wang et al., 2021).

2.3.3 Diet:

Research has shown that certain macronutrients, such as animal proteins, trans fats, simple carbohydrates, and saturated fatty acids, can contribute to the development of non-alcoholic fatty liver disease (NAFLD). These macronutrients influence insulin sensitivity, lipid metabolism, and hepatic buildup of triglycerides. A significant rise in liver fat was linked to the SFA diet, most likely as a consequence of escalated adipose tissue lipolysis and de novo hepatic lipogenesis. Consuming unsaturated fat can reduce fat accumulation in the liver (Berná & Romero-Gomez, 2020). Fructose's hepatic metabolism promotes the liver's de novo lipogenesis, increasing liver fat. Using the c-Jun-N-Terminal pathway, sugars stimulate de novo lipogenesis and set off an inflammatory cascade that results in hepatocyte apoptosis. Polyunsaturated fats, particularly $\omega 3$ and $\omega 6$ fats, play a crucial role in the development of NAFLD. The ratio of fats to proteins ($\omega 6/\omega 3$) is crucial in increasing the incidence of long-term metabolic disorders. Omega-3 fatty acids have been found to decrease hepatic fat buildup in NAFLD patients (Jump et al., 2018).

2.3.4 Gut microbiota and oxidative stress:

Research suggests a link between non-alcoholic fatty liver disease (NAFLD) and gut microbiota dysbiosis. In NAFLD patients, specific microbiota families like Proteobacteria, Enterobacteriaceae, Lachnospiraceae, Escherichia, and Bacteroidetes increase, while Prevotella and Firmicutes decrease (V. W.-S. Wong et al., 2013). Studies show that non-alcoholic fatty liver disease (NAFLD) is influenced by the gut microbiota in a number of ways. Among these mechanisms some important are the following: a) The endocannabinoid system is modulated; b) fermentation of carbohydrates to short-chain fatty acids (SCFAs) regulates the energy homeostasis which influences de novo lipogenesis in the liver (Woodhouse et al., 2018); c) choline metabolism is regulated, which is necessary for the synthesis of VLDL, and export of hepatic lipids; d) regulation of bile acid metabolism; and e) endogenous synthesis of ethanol as a metabolic byproduct

is somehow modulated in the context of resident gut bacteria (Poeta et al., 2017). Also, an increase in abundance of bacterial lipopolysaccharide (LPS), activating the production of pro-inflammatory cytokines in liver macrophages, leading to inflammation of hepatocytes and progression of NAFLD (Jasirwan et al., 2019).

2.3.5 Obesity:

Nonalcoholic fatty liver disease (NAFLD) is a growing global health concern, with an estimated 200 million men and 300 million women overweight. 51% of people with NAFLD also have obesity, with prevalence ranging from 50% to 90%. Metabolic syndrome (MetS) and comorbidities like type 2 diabetes, hypertension, hyperlipidemia, and NAFLD are associated with obesity and increased mortality (Godoy-Matos et al., 2020). Weight loss strategies, such as diet and exercise, can lower overall mortality in obese individuals. Three sources account for the majority of the triglyceride pool in the livers of individuals with NAFLD: i) adipose tissue ii) chylomicrons, primarily derived from dietary sources iii) liver de novo lipid synthesis and also the instigator effect of inflammatory cytokines, which hasten the rate at which the illness progresses and causes damage.

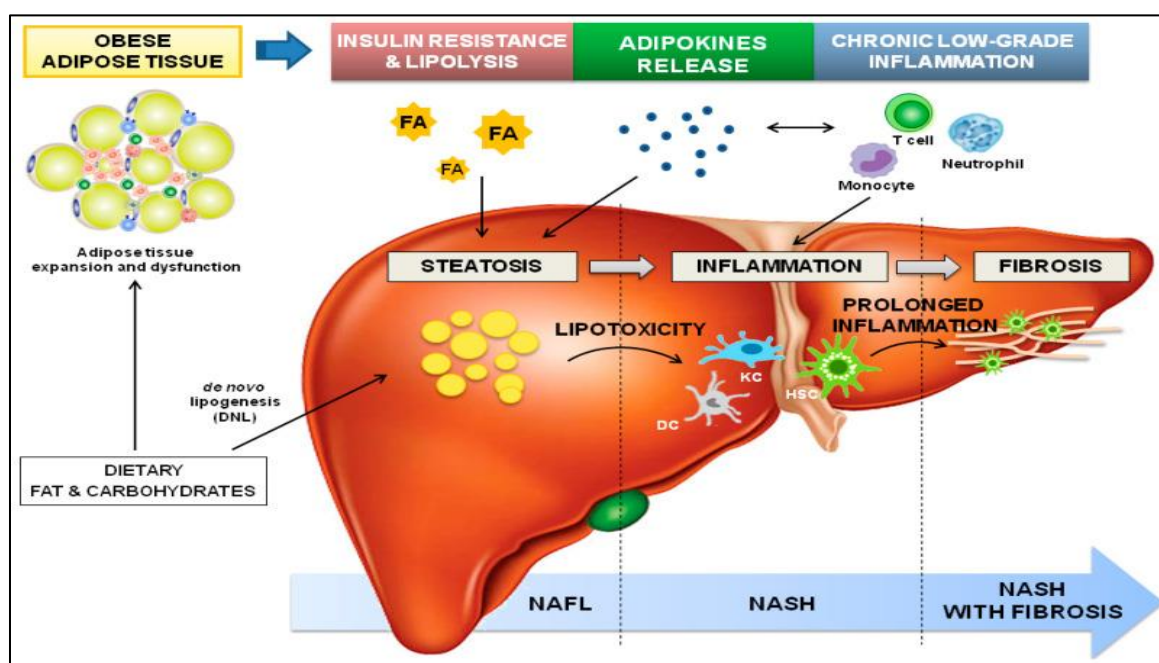


Figure 6: Adipose tissue dysfunction in NAFLD Adapted from Francisco et al 2022
doi: [10.3390/biology11081237](https://doi.org/10.3390/biology11081237)

Hepatocyte cells are exposed to high amounts of fat and carbohydrates, leading to lipotoxicity and glucotoxicity conditions. Mitochondrial abnormalities, endoplasmic reticulum stress, and oxidative stress all contribute to the pathophysiology of lipotoxicity

and glucotoxicity processes in NAFLD and NASH (Mota et al., 2016). Obesity and associated low-grade inflammation impacts the liver through adipokines and activated Kupffer cells, macrophages, dendritic cells, and hepatic stellate cells (HSCs) which can shift towards a more steatogenic, inflammatory, and fibrogenic character and also (Francisco et al., 2022).

2.3.6 Insulin resistance:

Insulin resistance is a significant contributor to non-alcoholic fatty liver disease (NAFLD), encouraging adipose tissue lipolysis, releasing free fatty acids into the bloodstream and depositing them in the liver, resulting in steatohepatitis. Patients with type 2 diabetes have a higher prevalence of NAFLD, with a prevalence of 30-70% (Sinha & Bankura, 2023, Younossi et al., 2019). NAFLD is also linked to a higher risk of cardiovascular disease. Insulin sensitivity in obese individuals is linked to elevated levels of pro-inflammatory cytokine $\text{TNF-}\alpha$, which can lead to insulin resistance (Hotamisligil et al., 1995).

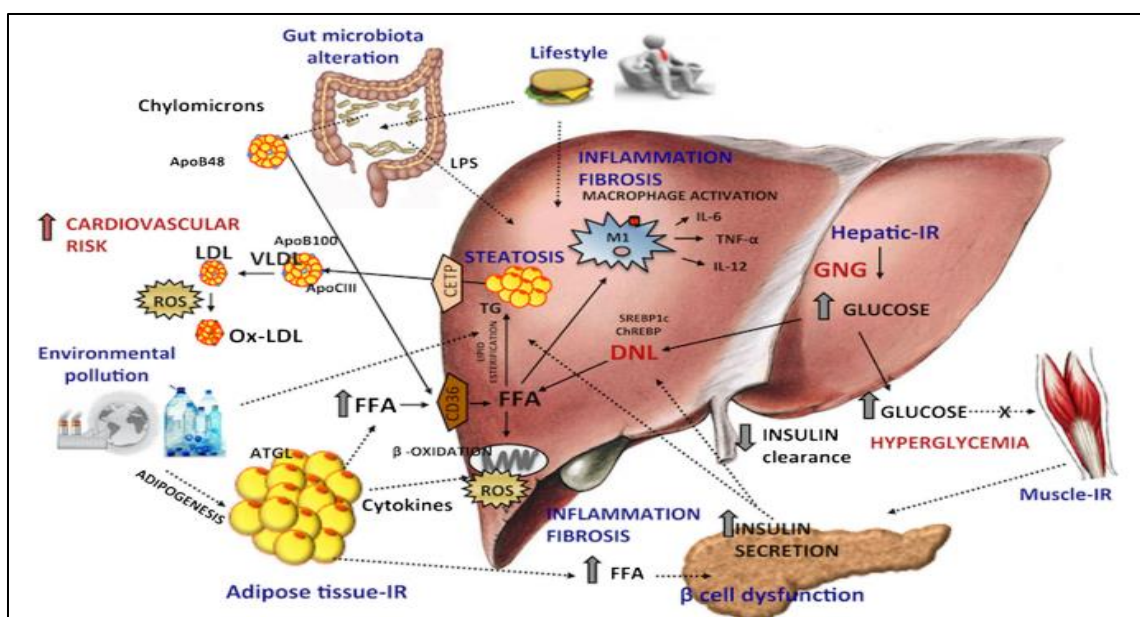


Figure 7: Pathophysiology of IR in NAFLD Adapted from Saponaro et al 2015 DOI:[10.1007/s11892-015-0607-4](https://doi.org/10.1007/s11892-015-0607-4)

Anti-diabetic drugs like pioglitazone have been shown to improve histological or metabolic abnormalities in NASH patients (Aithal et al., 2008). Insulin resistance (IR) in NAFLD patients stimulates gluconeogenesis by decreasing hepatic glycogen storage, increasing circulating FFAs, and adipocyte lipolysis. Systemic IR may cause hyperinsulinemia via increasing hepatic DNL. Hepatic IR is marked by elevated plasma insulin and hepatic glucose, leading to elevated fasting hyperglycemia and higher concentrations of FFAs. It is well acknowledged that IR plays a crucial

pathophysiological role in NAFLD. Phosphorylation of tyrosine residue in Insulin receptor substrate 1/2 (IRS1/2) is impaired by hepatic IR, which leads to NAFLD steatosis (Palma et al., 2022).

Skeletal muscle and adipose tissue manage blood glucose levels by insulin-stimulated glucose transport, mainly by glucose transporter GLUT4. Insulin resistance is a major problem in Type 2 Diabetes Mellitus (T2DM). Excess fatty acid supply causes insulin resistance and lipid deposition, subsequently leading to poor insulin signaling caused by lipid-derived metabolites such as diacylglycerols (Chadt & Al-Hasani, 2020). Insulin resistance is a major problem in Type 2 Diabetes Mellitus (T2DM) due to excess fatty acid supply and poor insulin signaling caused by lipid-derived metabolites.

2.3.7 Dyslipidemia:

Non-adipose tissues build up fat, leading to lipotoxicity, which triggers inflammatory pathways and lipoapoptosis in non-alcoholic fatty liver disease (NAFLD) patients. High triglyceride levels, hypertriglyceridemia, and elevated VLDL and IDL are associated with fatty liver pathology (Mendez-Sanchez et al., 2018). Proprotein convertase subtilisin/kexin type 9 (PCSK9) is correlated with steatosis severity and increases with hepatic fat deposition (Grewal & Buechler, 2022). Lipid-lowering drugs, such as statins, have been shown to improve NASH histological characteristics and lower the risk of liver cancer (Kamal et al., 2017).

2.3.8 Metabolic syndrome:

Metabolic syndrome (MetS) is a group of metabolic disorders including dyslipidemia, abdominal obesity, hypertension, and altered glycemia. Over 33% of adult Americans have MetS, with obesity increasing its prevalence. There may be a vicious loop between NAFLD and MetS, where NAFLD both causes and is a sign of MetS (Wainwright & Byrne, 2016). Hypertension is a significant risk factor for MetS, and obesity is the most prevalent ally of chronic liver disease. and Type 2 diabetes makes itself a significant risk factor for NAFLD.

2.4 Diagnosis and Management:

Nonalcoholic fatty liver disease (NAFLD) is diagnosed by confirming an excessive accumulation of triglycerides in hepatocytes. Liver biopsy is the gold standard for diagnosing NAFLD, providing information on hepatic steatosis, hepatocellular inflammation, and fibrosis. Non-alcoholic fatty liver disease activity score (NAS) is a composite score which is calculated on the degree of hepatocyte ballooning, lobular inflammation, and steatosis excluding fibrosis for assessing disease grade in NAFLD patients (Obika & Noguchi, 2012). Nevertheless, there are certain drawbacks, such as inter-observer variability, risk, complications, and variability in sample error. Low HDL levels

and elevated serum TG are typical hematology results for NAFLD patients, with normal transaminase levels found in 25% to 50% of NAFLD patients. Elevated blood ferritin levels are also linked to NAFLD. In the blood of patients with biopsy-proven NASH, the cleaved cytokeratin-18 (CK-18) fragment (produced after apoptosis) is dramatically raised while adiponectin, an anti-inflammatory cytokine, is reduced. Imaging modalities like MRI, CT, and abdominal ultrasonography (US) are used to identify NAFLD and NASH subtypes. Ultrasound (US) is a popular imaging modality for identifying elevated fibrosis and steatosis, but its sensitivity declines in obese individuals. Conventional ultrasonography, such as grayscale abdominal ultrasound, is most commonly used for detecting moderate to severe degrees of steatosis (Schwenzer et al., 2009). CT, MRI, and magnetic resonance spectroscopy (MRS) are generally detectable for hepatic steatosis, with sensitivity rates of 33, 50, and 88%, and specificity of detecting steatosis at 100, 83, and 63%, respectively (Borra et al., 2009).

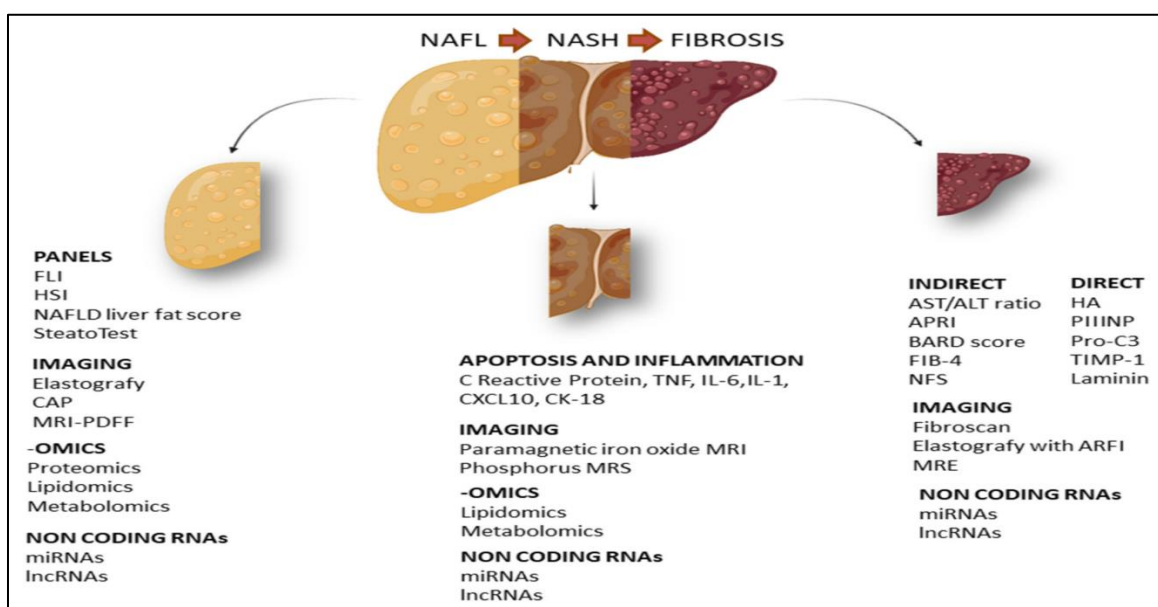


Figure 8: Clinical and Molecular Biomarkers for of NAFLD Adapted from Stefania Di Mauro et al *Int. J. Mol. Sci.* 2021, 22(21), 11905; <https://doi.org/10.3390/ijms222111905>

2.5 NAFLD associated molecular targets for intervention:

2.5.1 Oxidative stress (OS) in NAFLD:

Oxidative stress occurs when the antioxidant system's ability to scavenge reactive oxygen species (ROS) is out of balance with ROS production. Liver cells create ROS due to energy metabolism, and hepatic lipid excess alters ROS-generating pathways, leading to liver damage (Koek et al., 2011). Uncontrolled oxidative biomolecular damage and dysfunctional redox signaling may contribute to the advancement of non-alcoholic fatty

liver disease (NAFLD) (Delli Bovi et al., 2021). ROS and RNS are generated through a chain of enzymatic and nonenzymatic reactions, with major categories including alkoxyl/alkyl peroxy ($\text{RO}\cdot/\text{ROO}\cdot$), nitric oxide ($\text{NO}\cdot$), nitrogen dioxide ($\text{NO}_2\cdot$), superoxide anions ($\text{O}_2^{\bullet-}$), hydroxyl radicals ($\text{HO}\cdot$). ROS clearance mechanisms include glutathione peroxidase (GPX) decomposition of H_2O_2 , $\text{O}_2^{\bullet-}$ conversion to H_2O_2 by SOD and subsequently catalase breaking down H_2O_2 to H_2O and O_2 , and detoxification of xenobiotics by glutathione S-transferase (GST).

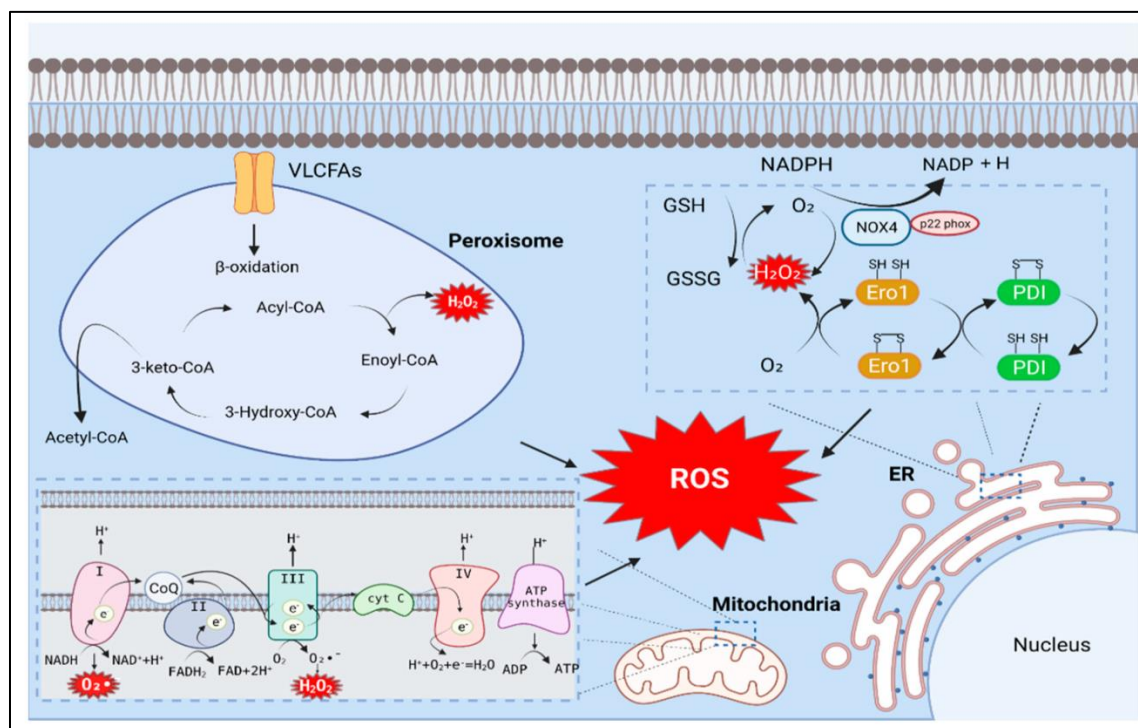


Figure 9: Sources of oxidative stress in lipotoxicity Adapted from Y Ma et al
Antioxidants 2022, 11(1), 91; <https://doi.org/10.3390/antiox11010091>

The most characterized location of mitochondrial ROS formation is the electron transport chain (ETC) in the mitochondrial inner membrane, where several complexes (I, II, and III) can undergo monoelectronic oxygen reduction, producing $\text{O}_2^{\bullet-}$ and other products derived from it (Pérez-Carreras, 2003). However, recent studies have also demonstrated the importance of other mitochondrial Reactive oxygen species producers, including pyruvate dehydrogenase, α -ketoglutarate dehydrogenase, glycerol phosphate dehydrogenase, and monoamine oxidases are considered noteworthy. Fatty acid oxidation (FAO), which is aided by the ACOX superfamily, results in the physiological production of H_2O_2 by peroxisomes.

Reactive oxygen species (ROS) are generated intracellularly in the endoplasmic reticulum (ER), providing an ideal oxidative redox environment for protein folding.

Three approaches are commonly used for evaluating oxidative stress: quantifying oxidative damage to biomolecules, directly measuring ROS levels, and evaluating antioxidant status. Indirectly evaluating the parameters of oxidative damage the radicals inflicted on proteins, lipids, and nucleic acids is a useful alternative to direct detection of ROS. Lipid peroxides, 4-hydroxynonenal (4-HNE), and malondialdehyde (MDA) are the most often measured oxidative damage products of lipids. Additionally, protein damage products (nitrotyrosine, hydroxyproline, and protein carbonyl) and DNA damage products (8-OH-dG) function as redox biomarkers (Martín-Fernández et al., 2022).

2.5.2 The Role of SREBP in NAFLD:

Sterol regulatory element-binding proteins (SREBPs) are transcription factors produced and processed in the Golgi and endoplasmic reticulum, influencing the expression of fatty acid synthesis genes (Moslehi & Hamidi-zad, 2018). SREBP-1c is the main isoform present in the liver, controlling enzymes that catalyze the synthesis of TG, NADPH, and fatty acids taking an important part in cholesterol, triglyceride, phospholipid synthesis as well as overall cellular lipid homeostasis. Elevated lipogenesis caused by SREBP-1c overexpression may lead to hepatic steatosis (Knebel et al., 2012). Some noteworthy genetic targets controlled by SREBP-1c are fatty acid synthase (FAS), ATP-citrate lyase, acetyl-coenzyme A carboxylase (ACC), desaturases and glucose 6-phosphate dehydrogenase. SNPs in the SREBP-1c gene have been linked to metabolic diseases, such as type 2 diabetes, insulin resistance, obesity, and hypercholesterolemia. Liver X receptors (LXRs) are crucial nuclear receptors controlling fatty acids and cholesterol metabolism. LXR α enables the induction of SREBP-1c, leading to hepatic lipogenesis and hypertriglyceridemia. ACC1, FAS, LXR- α , and SREBP-1c were all elevated in NAFLD patients (Higuchi et al., 2008). Insulin's regulation on hepatic lipogenesis is partly regulated by SREBP-1c, which lowers Insig-1/2 levels to increase SCAP/SREBP complex export towards Golgi bodies. ACC1, FAS, LXR- α , and SREBP-1c were all elevated in NAFLD patients. Metformin has been shown to attenuate hepatic steatosis in diet-induced insulin-resistant LDL receptor-deficient mice by stimulating AMPK activity and suppressing SREBP-1c cleavage with subsequent nuclear translocation via Ser372 phosphorylation (Pinyopornpanish et al., 2021). However, SREBP-1c induces lipogenic enzymes and fat accumulation linked to insulin resistance.

SREBP-2 activation may be essential for improving cholesterol absorption and production, controlling cell cholesterol metabolism, and preserving cholesterol homeostasis. Genetic polymorphisms of the SREBP-2 gene have a major impact on the onset of nonalcoholic fatty liver disease (NAFLD) (Y. Wang et al., 2014).

2.5.3 The role of ChREBP in NAFLD:

Carbohydrate-responsive Element Binding Protein (ChREBP) is a crucial transcription factor in hepatic metabolism, activating targeted genes through de novo lipogenesis

(DNL). ChREBP, a 94Kd protein containing 864 amino acids, is a member of the MONDO family of transcription factors that are expressed in various tissues, including the liver, muscle, adipose tissue, gut, and pancreatic islets. Fructose, a triglyceride, is more quickly converted into triglycerides than glucose, leading to weight gain and fatty liver. Research has focused on the role of ChREBP in the effects of sucrose and fructose on liver fat accumulation and weight gain. Overexpression can lead to fatty liver and lower plasma glucose levels. ChREBP regulates the absorption and catabolism of fructose, and its overexpression can result in fatty liver and lower plasma glucose levels (Iizuka et al., 2004). High-sucrose diets increase xylulose-5-phosphate and fructose-2,6-bisphosphate, prominent activators of ChREBP. Glucose-derived metabolites, Glucose 6-phosphate, Xylulose 5-phosphate, and Fructose 2,6-bisphosphate activate ChREBP and regulate gene expression in the fructose breakdown pathway via ChREBP dephosphorylation. ChREBP regulating FGF21 at the transcriptional level forms a feedback loop by maintaining a glucose/fructose-ChREBP-FGF21 axis and thereby regulating the sugar-consumption behavior in humans (von Holstein-Rathlou et al., 2016). Deleting ChREBP can prevent obesity and fatty liver. cAMP, a metabolite that is produced in greater amounts during starvation, phosphorylates ChREBP and deactivates transcription. Moreover, AMP-activated protein kinase (AMPK) functions as an allosteric inhibitor to limit ChREBP transcription activity, through phosphorylation and allosteric inhibition (Sato et al., 2016).

2.5.4 The role of AMPK in NAFLD:

5'-Adenosine monophosphate-activated protein kinase (AMPK) is an important coordinator of glucose metabolism, hepatic lipid dysfunction, and cellular energy homeostasis. It is allosterically regulated by adenosine nucleotides and is essential for survival under marginal energy supply conditions. With a conserved serine/threonine protein kinase complex, AMPK is an obligate heterotrimer consisting of two regulatory subunits and one catalytic (α) component forming a heterotrimeric holoenzyme complex. The α -subunit's N-terminal region requires phosphorylation of a conserved threonine-172 residue for full activation (Mihaylova & Shaw, 2011).

AMPK activation lowers the AMP: ATP ratio impacts cellular energy homeostasis, and regulates mitochondrial homeostasis by stimulating biogenesis and controlling autophagy/mitophagy. It affects vasculature by activating endothelial NO synthase, influencing blood flow and cellular nutrient supply. AMPK activation is thought to be a promising therapeutic approach. It can inhibit ACC dimerization, increase the activity of malonyl CoA decarboxylase (MCD), and enhance the activity of SIRT1, a class III histone deacetylase (Smith et al., 2016). AMPK can alter the intracellular AMP/ATP ratio, perturbing the NAD⁺/NADH balance, to promote Sirt1 activity. A feedback loop of regulation occurs, where the AMP/ATP ratio can cause LKB1 to stimulate AMPK phosphorylation, which further activates sirt1 (Long et al., 2019). This leads to the

deacetylation of gene targets downstream, increasing mitochondrial biogenesis through PGC1 alpha and suppressing lipid synthesis genes like FAS and ACC (Chau et al., 2010).

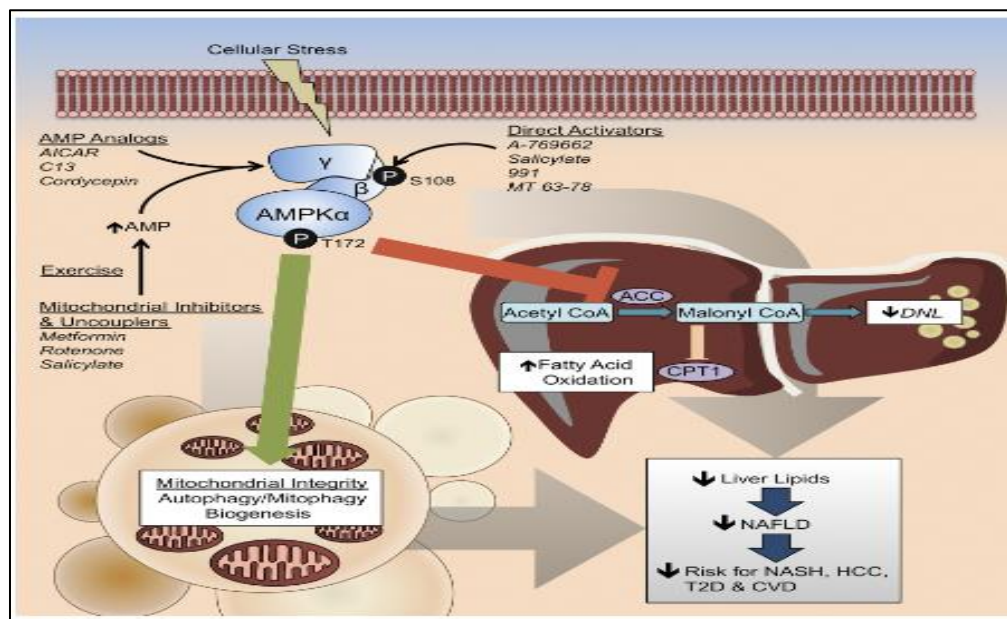


Figure 10: Role of AMPK in NAFLD

Smith et al
2016
<https://doi.org/10.1152/ajpen.00225.2016>

2.5.5 The role of SIRT1 in NAFLD:

Sirtuin 1 (SIRT1) or Silencing information regulator 1, a member of the sirtuin family is a nicotinamide adenosine dinucleotide (NAD)-dependent deacetylase. It plays an important role in the management of hepatic energy metabolism, lipid homeostasis, insulin resistance, and inflammation in the liver as well as skeletal muscle, adipose tissue (Wu et al., 2022). Its deacetylation activity has been reported to positively impact the pathogenic signaling mechanisms of non-alcoholic fatty liver disease (NAFLD). According to studies, SIRT1 may influence lipid and cholesterol metabolism in NAFLD. In NAFLD patients, liver SIRT1 expression generally declines (Mariani et al., 2015), whereas overexpression of this protein prevents hepatic steatosis in mice fed a high-fat diet, proving its potential in alleviating NAFLD (Pfluger et al., 2008).

2.5.6 The role of peroxisome proliferator-activated receptor (PPAR) α in NAFLD :

PPARs (Peroxisome proliferator-activated receptors), a subset of the nuclear receptor superfamily, maintain the expression of numerous lipid and glucose metabolism genes acting as ligand-activated transcription factors (Cave et al., 2016). As a ligand such as FFAs or eicosanoids binds to the target gene promoter, it binds with retinoid X receptor (RXR) forming a heterodimer, which then subsequently targets binding to specific response elements (PPRE) (Pawlak et al., 2015) that regulate a myriad of genes expressing enzymes or proteins involved in different metabolic activities including fatty

acid absorption, beta-oxidation, fatty acid synthesis, adipocyte differentiation, ketogenesis, triglyceride homeostasis, and insulin resistance (Wang, 2010).

Mammals often have been found to contain three different PPAR isoforms: α , beta/delta, and gamma. PPAR α promotes the mitochondrial and peroxisomal fatty acid β -oxidation pathways, facilitating lipid transport and metabolism. Additionally, constitutive genes encoding enzymes that metabolize fatty acids and mitochondrial FA oxidation activity are regulated by PPAR α , mostly in the liver. In human primary hepatocytes, it directly suppresses NF- κ B-driven inflammatory genes and decreases C-reactive protein expression produced by IL-1. Treatment with fenofibrate reduced the expression of acute phase response genes triggered by IL-6 in normal mice, but not observed in PPAR α -deficient mice. PPAR α activators, such as fibrate medications, improve mitochondrial FAO in mice, hence reducing hepatic steatosis (Lakhia et al., 2018). PPAR γ is abundantly expressed in adipocytes and muscle tissues, to increase fat storage and decrease inflammation (Corrales et al., 2018). The insulin-sensitizing medicines namely pioglitazone and rosiglitazone target PPAR γ , making it a key receptor in treating type 2 diabetes (Orasanu et al., 2008).

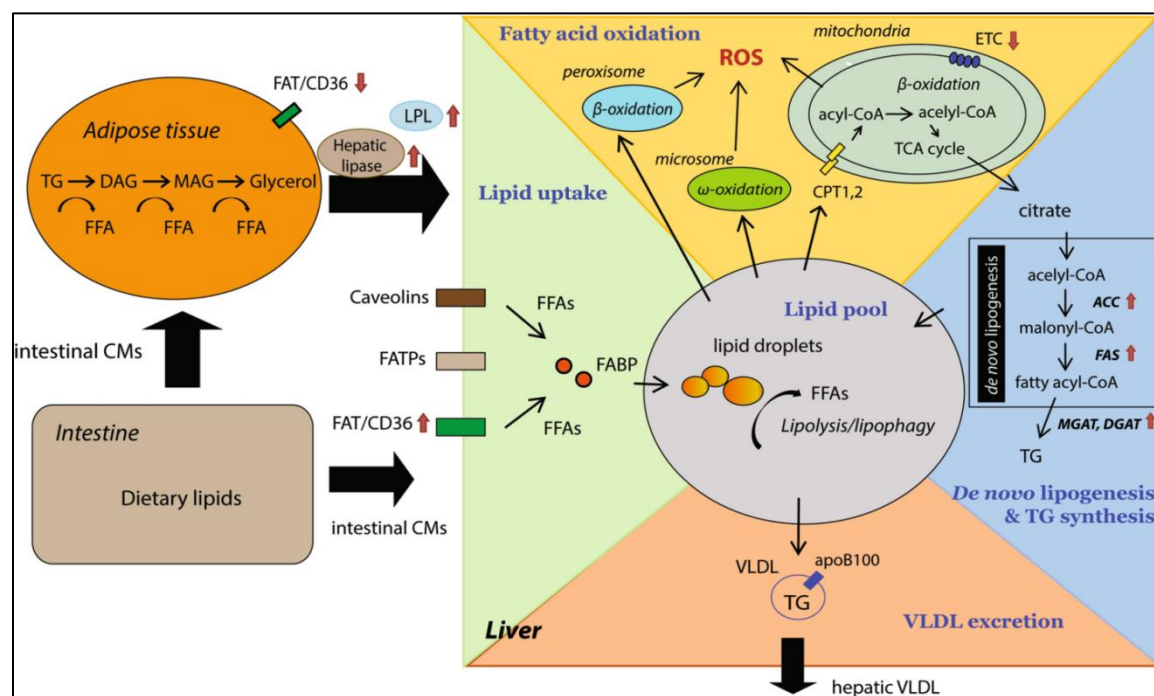


Figure 11: Altered Hepatic lipid metabolism in NAFLD Adapted from Geng et al 2021

<https://doi.org/10.1007/s12072-020-10121-2>

2.5.7 Inflammation in NAFLD:

The hepatic inflammatory response is a significant factor in the pathogenesis of non-alcoholic fatty liver disease (NAFLD), with obesity playing a key role. Obesity increases adipocyte size, leading to hypertrophy of fat tissues and a local inflammatory phenotype,

activating immune cells like macrophages and T-cells (Kawai et al., 2021). This leads to fat buildup, lipotoxicity, insulin resistance, and persistent low-grade inflammation, ultimately leading to liver fibrosis. Gut microbiota imbalance is often considered an important mediator of obesity-induced systemic inflammation. Lipopolysaccharide (LPS) is a major molecular pattern of bacterial pathogenicity, involved in hepatic inflammation and macrophage polarization during NAFLD (Fukunishi et al., 2014). LPS reaches the liver and induces hepatic inflammation following a dysbiosis. The TLR-4 receptor on the plasma membrane of liver cells recognizes LPS and passes on a downstream proinflammatory signaling cascade, producing inflammatory cytokines like TNF- α , interleukin-1 β , and interleukin-6. Nuclear factor- κ B (NF- α) and protein kinase c-Jun N-terminal kinase (JNK) are the two primary downstream pathways after macrophage activation (Heida et al., 2021, Singh et al., 2009, Kodama et al., 2009). Cholesterol crystallization, saturated free fatty acids, and reactive oxygen species all trigger The JNK pathway whereas NF- κ B is activated by TLRs, IL-1 β , and TNF- α . High-fat diet (HFD) mice with pathophysiological characterization of NAFLD show considerable macrophage infiltration, and inflammatory upregulation with tissue remodeling (Thibaut et al., 2022) within their adipose tissue. Furthermore, saturated fatty acid intake predisposes animals towards the development of M1 polarization with necrotic adipocytes that regulate Ly6C⁺ monocyte migration upregulated chemokine ligand (CCL2) receptor (Puengel et al., 2022).

Immune cells like macrophages and T-lymphocytes play a crucial role in metabolic tissues. Adipose tissue is a complex unit regulating versatile metabolic activity and is home to several immune cells, including adipose tissue macrophages (ATMs), T-helper cells, cytotoxic T lymphocyte cells, regulatory B-cells, and T-cells. M1 and M2 macrophages express different markers in adipose tissue, with M1 macrophages secreting pro-inflammatory cytokines like IL-1 β , IL-6,8 ,12, and TNF- α and M2 macrophages secreting anti-inflammatory cytokines (Viola et al., 2019).

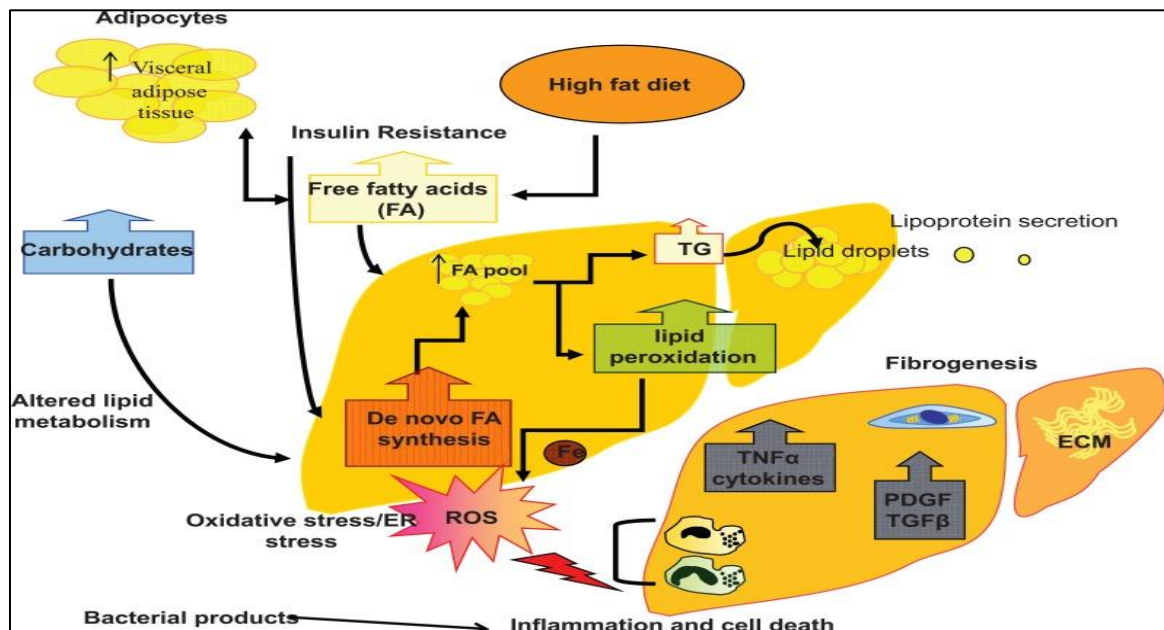


Figure 12: Sources of inflammation in NAFLD Adapted from Dongiovanni et al 2013
doi: 10.2174/13816128113199990381

Kupffer cells (KCs) which make up 80–90% of total tissue macrophages residing in the human body are essential to innate immunity and are found in the hepatic sinusoids (Chen et al., 2020). TLR ligands induce KCs to become immunogenic, triggering T lymphocyte activation and cytotoxic T-lymphocyte reactions. Nitric oxide (NO) produced by inducible nitric oxide synthases (iNOS) can combine with O_2^- to form peroxynitrite, a potent physiological oxidant. It can trigger KCs to become M1 phenotype-active and has been of particular interest in relation to NAFLD and metabolic syndrome. M1 macrophages are well recognized for their induction of iNOS, which results in the generation of oxidative stress although there is a debate on the pro-inflammatory role of iNOS in hepatic steatosis development (Anavi et al., 2015, Qiao et al., 2019).

2.6 Mitochondria in NAFLD:

The liver is a vital organ responsible for controlling carbon metabolism in foods like glucose, lipids, and protein. It is rich in mitochondria, which are crucial in hepatic metabolism. Mitochondria account for 18% of hepatocytes and use 15% of the organism's oxygen. They regulate blood glucose levels, maintain lipid homeostasis through fatty acid oxidation, and regulate blood pressure. The proper coordination of mitochondrial biosynthesis, fission/fusion, and autophagy is necessary for mitochondrial homeostasis. Disrupting mitochondrial homeostasis may jeopardize cellular processes and be responsible for exacerbating many metabolic diseases like NAFLD (Ramanathan et al.,

2022). NAFLD is the accumulation of extra fat in the liver, with lipid droplets accounting for 5-10% of total liver weight.

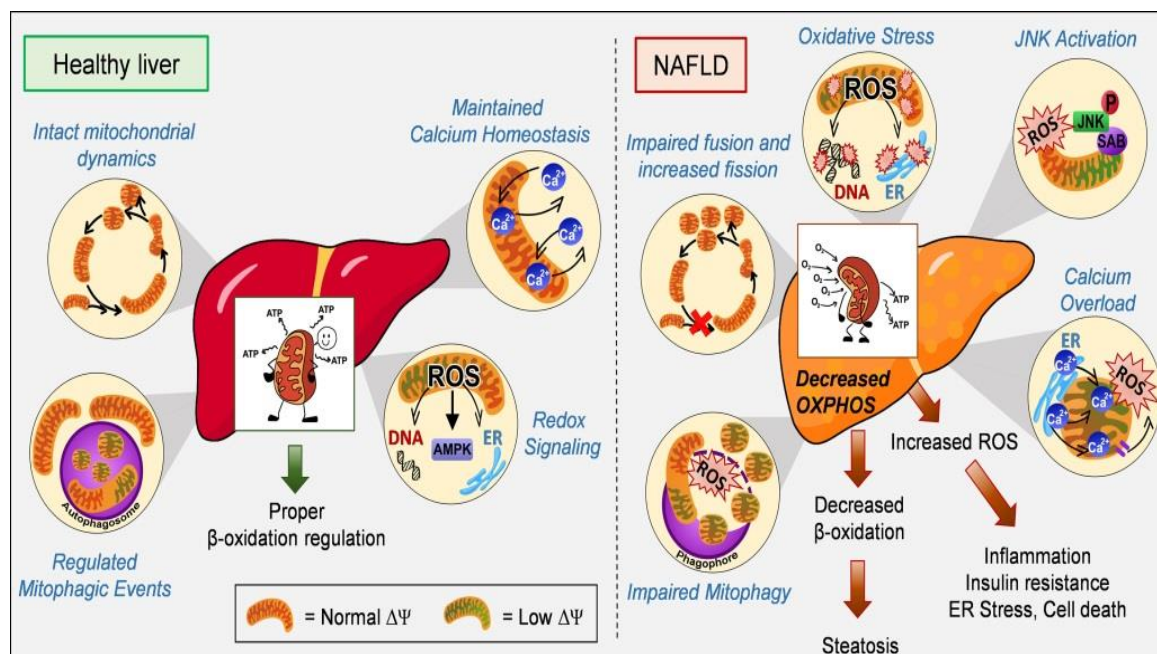


Figure 13: Differential physiology of Mitochondria in NAFLD

Michael Shum et al 2021 doi: [10.1016/j.jmolmet.2020.101134](https://doi.org/10.1016/j.jmolmet.2020.101134)

Mitochondria are organelles with dual membrane-bound structures. The outer mitochondrial membrane (OMM) allows passive diffusion of solutes, while the inner mitochondrial membrane (IMM) is selective for ion and molecule passage. Cristae are formed to accommodate mitochondrial respiratory function, whereas cristae junctions (CJs) regulate ion and protein transport. The IMM architecture is influenced by phospholipid composition, cardiolipin, and phosphatidylethanolamine, which cause membranes to curve negatively, affecting organelle morphology (Blum et al., 2019). The ATP synthase, a terminal chain complex involved in oxidative phosphorylation, shapes cristae borders and forms dimeric complexes. Mitochondria contain their own genome, mtDNA, which encodes respiratory complex components, tRNAs, and rRNA. The mitochondrial genome encodes 13 polypeptides, 22 transfer RNA (tRNA), and two ribosomal RNAs. The genome is packed in a nucleoid assembly within the mitochondrial matrix, transcribed and translated there. Furthermore, the import and export of proteins in and out of mitochondria is specifically controlled by the TIM, and TOM complexes are positioned on the IMM and OMM, respectively. The placement and organization of these depots are tightly linked and regulated. Also, there are several ion channels and transporters like VDAC, CPT1, and CPT2 which also facilitate the smooth exchange of ions, solutes, and nutrients in and out of mitochondria (Friedman, 2022).

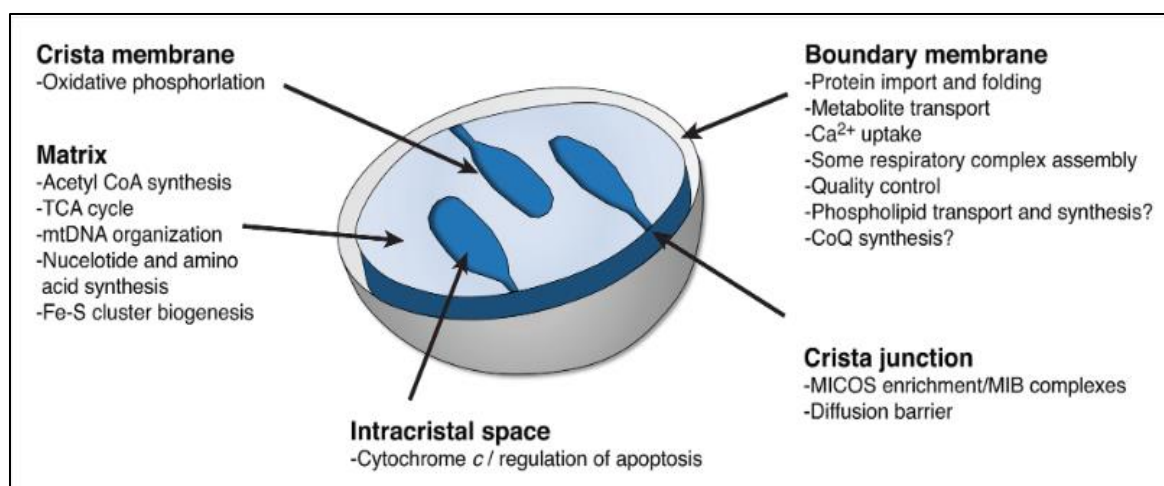


Figure 14: General mitochondrial morphology Adapted from Friedman et al 2022

<https://doi.org/10.1177/25152564221133267>

2.6.2 Altered Mitochondrial Bio-energetics in fatty liver:

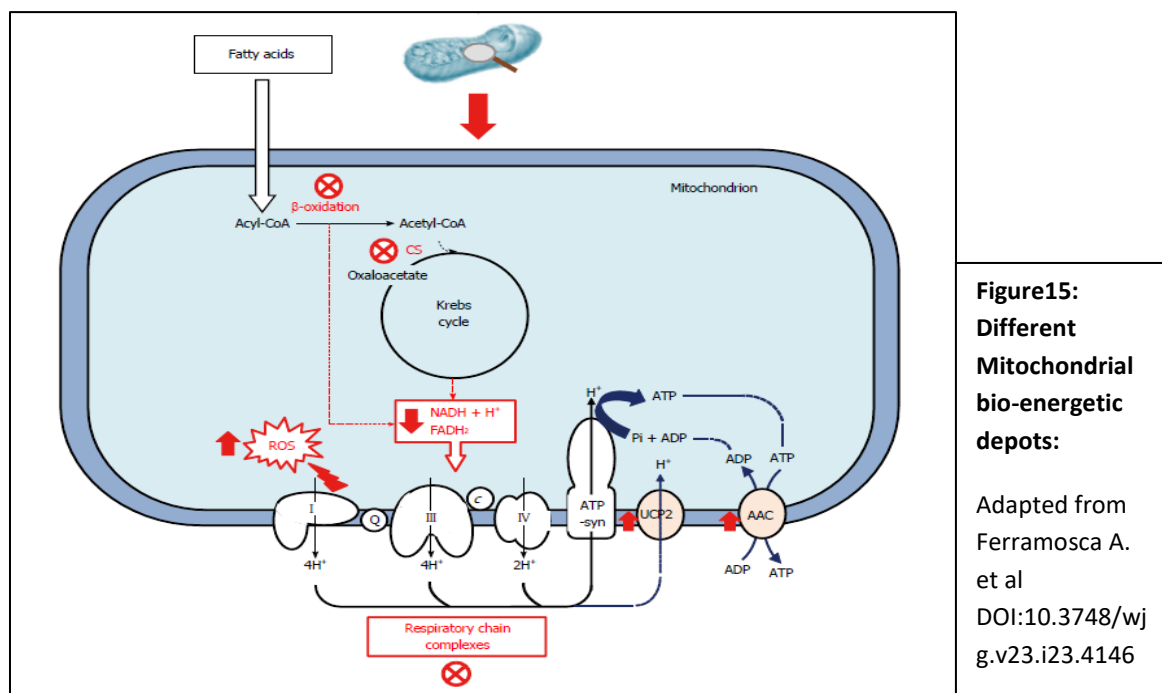
The human liver consumes 15% of oxygen even though it makes up just 4% of the body weight. Hepatocytes consume oxygen and generate ATP meeting 60% of the ATP needed for glucose synthesis and ureagenesis, with the kidney providing the remaining 40% (Rolfe & Brown, 1997). When nutrients are scarce, the liver serves as the main organ for producing glucose and ketone bodies.

A 10-fold increase in mitochondrial fat oxidation occurs during fasting. During the fed state, hepatocytes use insulin to promote glucose storage and transform dietary glucose into lipids to save and store nutrients and energy. The oxidation of glucose-derived pyruvate in mitochondria increases the production of citrate. After which, citrate is used to produce malonyl-CoA, the carbon precursor of newly produced fatty acids, which is subsequently esterified to produce triglycerides and lipid droplets. The primary metabolic functions of mitochondria, like the TCA cycle, fatty acid oxidation, ETC activity, ketone body, and ATP generation, regulate hepatic energy homeostasis (Morio et al., 2021). Mitochondrial bioenergetic efficiency assesses ATP production per nutrient molecule, while mitochondrial ATP synthesis capacity measures ATP production/unit time.

Fatty liver disease is linked to structural and functional perturbations in mitochondria, including DNA depletion, mutation, epigenetic modification, and morphological abnormalities (Zhao et al., 2023). These alterations cause reduced ATP levels, release of reactive oxygen molecules, and elevated fat storage. FFA overflow to hepatocytes promotes mitochondrial bio-energetic processes, meeting altered energy requirements for TG storage and droplet formation. Mitochondria serve as organelles for oxidative phosphorylation, involving the electron transport system, which connects electron mobilization to ATP production. The tricarboxylic acid (TCA) cycle generates electron carriers such as NADH and FADH₂, the reducing component and electron donors playing an integral part in the generation of membrane potential leading to ATP

synthesis. Hepatocytes are rich in mitochondria, essential for various hepatic processes such as digestion, cholesterol production, and ammonia elimination (Degli Esposti et al., 2012). A drop in redox potential propels electrons at the mitochondrial respiratory complexes (MRC) through many multi-subunit proteins (Complexes I–IV) before arriving at oxygen as the final acceptor.

Fatty livers experience decreased mitochondrial respiration efficiency due to a putative uncoupling effect between ATP generation and transport across respiratory complexes, possibly due to altered expression patterns of proton conductive mitochondrial carrier proteins (Demine et al., 2019). Variations in mitochondrial metabolic pathways such as OXPHOS efficiency, overall mitochondrial respiration, ATP production, and MRC enzymatic activity have been reported with different models of fatty acid overload in the liver (Begrich et al., 2013), potentially due to variations in oxidative stress and associated metabolic and physiological factors.



2.6.3 Mitochondrial reactive oxygen species, antioxidant defense:

Cells maintain homeostasis by modulating oxidant and antioxidant species. Oxidizing substances absorb electrons, while antioxidants delay or prevent oxidation by scavenging free radicals, quenching singlet oxygen, inhibiting lipoxygenase-like pro-oxidative enzymes, and chelating oxidative metals. Free radicals have an unpaired electron in an atomic orbital and have a limited lifespan. Basal cell metabolism produces reactive species (RS), some of which have legitimate physiological roles. Xanthine oxidase, NOS, and NADPH oxidase are examples of enzymes generating ROS; on the other hand

respiratory chain of the mitochondria is one non-enzymatic generator of ROS. Oxidative stress can result from excessive ROS generation or insufficient ROS clearance in a variety of pathological conditions (Arroyave-Ospina et al., 2021). Mitochondria are the primary root of cellular reactive oxygen species in human cells, playing crucial roles in metabolic regulation, inflammatory response, growth arrest, and apoptosis. Complex I and Complex III are the two main locations in mitochondria where $O_2^{\bullet-}$ is generated (Kausar et al., 2018).

Oxidative stress can result from excessive ROS generation or insufficient ROS clearance in various pathological conditions. Reactive oxygen species react with iron-sulfur clusters within mitochondria including SDH, fumarase, and complex I. Gpx may remove H_2O_2 by reducing it to H_2O , a process that needs glutathione (GSH) (Napolitano et al., 2021) [115, 119]. Glutathione reductase (GR) activity converts oxidized GSH (GSSG) to GSH, which is essential since GSSG cannot be delivered into the cytosol. Under pathological scenarios, MnSOD, glutathione reductase, and glutathione peroxidase functions are inhibited by ROS and RNS, leading to further damage. The oxidative state of mitochondria continues to be influenced by several other ROS generation depots, such as pyruvate dehydrogenase (PDH), succinate dehydrogenase (SDH), and alpha-ketoglutarate dehydrogenase (KGDH). The activities of PDH and KGDH are suppressed by oxidative stress, which leads to the accumulation of pyruvate and KG. H_2O_2 -mediated non-enzymatic decarboxylation of KG increases succinate as well as acetate from pyruvate. Elevated succinate levels in the cytoplasm promote anaerobic metabolism, increased glycolysis, and fat storage (Mailloux, 2020, Chalifoux et al., 2023).

The high quantity of phospholipids containing polyunsaturated fatty acids (PUFAs) in mitochondria enhances their sensitivity to oxidative damage, resulting in lipid peroxidation, diminished respiratory chain function, decreased ATP generation, and ROS overproduction. Lipid peroxidation also produces cytotoxic lipid peroxides, like, 4-hydroxy-2-nonenal (4-HNE), malondialdehyde, and other lipid peroxides, which tend to form protein adducts and inhibiting critical enzymes like ACN, ATP synthase, and ALDH (Ayala et al., 2014, Mattson, 2009).

2.6.4 Mitochondrial Dynamics in NAFLD:

Mitochondrial dynamics and morphological structure vary across different cellular types and tissues. Different nutrient and cellular insults trigger a signaling cue directing modification of outer and inner membranes through fission or fusion. Uncontrolled fission can lead to mitochondrial fragmentation, which in turn can cause metabolic dysfunction and disease. A balance between these physiological processes is crucial for maintaining overall mitochondrial health by shaping the metabolic needs of cells and ensuring the programmed removal of damaged organelles (Molina et al., 2009). Mitochondrial dynamics are essential for cellular homeostasis, mitochondrial health, bioenergetic functioning, quality management, and intracellular signaling. A critical

balance between energy demand and supply is always required for cellular homeostasis. The organization of mitochondrial dynamics regulation is controlled either by fusion (mediated by MFN2 and OPA1) or fission (Dynamin-related protein 1; DRP1), whereas malfunction causes mitochondrial hyper tubulation or fragmentation. Fusion and fission events allow mitochondria to share and reorientation of the different mitochondrial inner components. Often different cellular metabolic dysfunction like cardiovascular and neurological disorders, cancer, and obesity is reported to show enhanced mitochondrial fission as it also helps in autophagic clearance of the damaged organelle by mitophagy as well as meeting the altered physiological energy demand (Dorn & Kitsis, 2015). Fusion necessitates the coordination of three GTPases: Mfn1 and Mfn2 for OMM fusion and OPA1 for IMM fusion (Schrepfer & Scorrano, 2016). Drp1, a major GTPase, is used in the fission process to produce an oligomeric chain-like structure around OMM, which is then constricted and segregated of mitochondria.

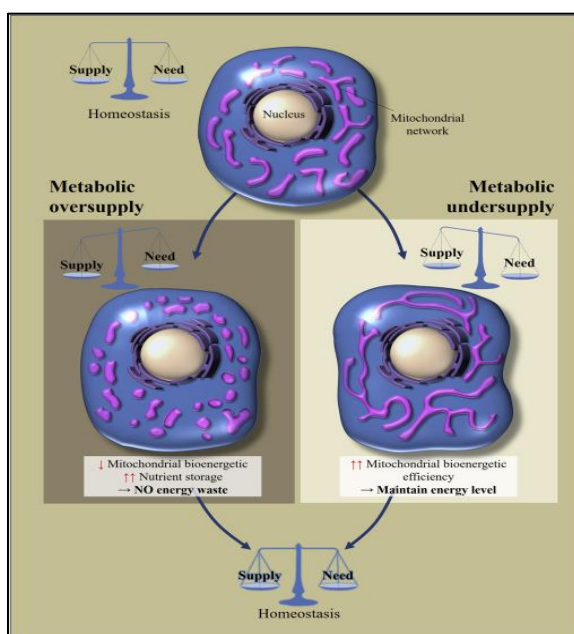


Figure 16: Mitochondrial dynamics with nutrient availability Schrepfer et al
<https://doi.org/10.1016/j.molcel.2016.02.022>

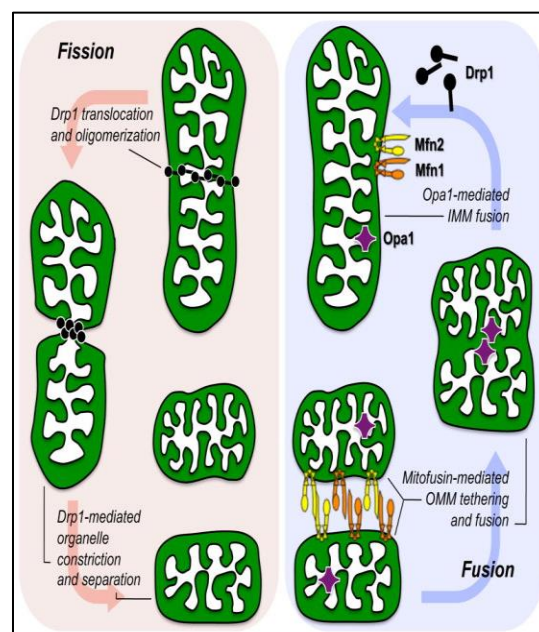


Figure 17: Mitochondrial fission-fusion process 10.1161/CIRCRESAHA.116.303554 Dorn et al 2015

DRP1 is a protein that translocates to mitochondrial OM (organisms of the mitochondria) in response to specific cellular signals and pathogenic stimuli. It oligomerizes into a ring-like structure, guided by ER and cytoskeletal components. DRP1 deletions can lead to premature embryo death, abnormalities in the heart, liver, and neural tube, and dilated cardiomyopathy and cardiac necrosis (Ishihara et al., 2009). In some cases, reducing DRP1 expression can help protect against diet-induced obesity and associated disorders (Galloway et al., 2014).

Dynamin-like GTPases, particularly mitofusins 1 and 2, are required for the fusion of mitochondrial OMs and IMs. Mitofusin synthesis and degradation are controlled by transcriptional and post-transcriptional regulation, phosphorylation, and ubiquitination. In mice, deletion of either protein or inhibition of GTPase activity impairs mitochondrial fusion, resulting in cell fragmentation and embryonic death.

Studies on obesity and non-alcoholic fatty liver disease (NAFLD) have validated the role of altered mitochondrial dynamics in various pathophysiological manifestations (Legaki et al., 2022). Palmitate treatment fragments hepatocytes, enhances ROS activity and leads to cytochrome C release and apoptosis. Hepatic fission inhibition can prevent liver steatosis and reduce oxidative stress. Reintroducing Mfn2 in liver-specific Mfn2 knockout animals can relieve illness, emphasizing the role of Mfn2 in NAFLD pathogenesis (Hernández-Alvarez et al., 2019).

2.6.5 Maintaining mitochondrial homeostasis by Mitophagy and Autophagy:

Autophagy is a self-destruction process that maintains cellular homeostasis in response to nutritional deficiencies, low oxygen, ATP stress, genotoxicities, and other stressors and recycles metabolic resources. It is involved in various medical conditions such as hepatic ischemia-reperfusion injury, liver cancer, NAFLD (Raza et al., 2023), and dementia. Mitochondria use quality-checking proteases to clear damaged proteins and respond to unfolded protein stress via chaperone expression in the UPR pathway. Autophagy has three types: macroautophagy, microautophagy, and chaperone-mediated autophagy. Macroautophagy involves engulfing cellular components and damaged organelles into autophagosomes, while microautophagy focuses on directing intracellular materials to lysosomes without invaginating vesicular structures (L. Wang et al., 2023). Chaperone-mediated autophagy targets proteins with the “Lys-Phe-Glu-Arg-Gln (KFERQ) motif for direct destruction in lysosomes mediated by specific chaperon complex HSC70 and translocation to the lumen of the lysosome by LAMP2A. Lipophagy is a selective autophagic clearance of lipid droplets from lipo-stressed cells with malfunctioning lipid metabolism. Autophagy regulation is influenced by the mammalian target of rapamycin (mTOR) and AMPK proteins. In a nutritional surplus scenario, growth factor (insulin) stimulation activates the PI3K/AKT pathway, which then activates mTOR. In starvation, increased catabolic activities enhance the cellular AMP/ATP ratio, activating AMPK and inhibiting mTOR, which promotes autophagy. A beclin-1/VSP34-interacting complex initiates phagophore production whereas the elongation step is regulated by the ATG5-ATG12-ATG16L1 complex and thereafter promotion of autophagosome formation subsequently by ubiquitin-like adaptor protein light chain 3 (LC3). ATG7 contributes to vesicle maturation and cytosolic LC3 (LC3-I) conjugates with phosphatidylethanolamine in the autophagosomal membrane to produce LC3-phosphatidylethanolamine conjugate (LC3-II), making both an effective and intriguing target for this process (Kuramoto & He,

2022). The transcription factor EB (TFEB) plays a crucial role in autophagy and lipid metabolism.

Autophagy plays a crucial role in cellular homeostasis, dysregulation in this process can lead to cellular injury in NASH, and hepatocellular carcinoma (HCC). While activation of this process is often linked to the elimination of pathogenic patterns and suppression of inflammatory mediators on the contrary autophagy gene knockouts result in macrophage infiltration, pro-inflammatory cytokines, obesity, and glucose intolerance. Autophagy exerts a dual role in tumorigenesis, acting as a tumor suppressor in normal tissue and aiding the survival of tumor cells by supplying nutrients when a tumor has developed.

Mitophagy is the selective autophagic removal of damaged mitochondria in the body that maintains mitochondrial quality by obliteration of diseased organelle in pathologic conditions also governing mitochondrial regeneration in response to metabolic demand (Suomalainen & Battersby, 2018). It is divided into three types: basal mitophagy, programmed mitophagy, and stress-induced mitophagy. Basal mitophagy governs cell fates, while programmed mitophagy regulates cell maturation and differentiation. BNIP3 and BNIP3L/Nix, are two important proteins responsible for mitochondrial turnover. Stress-induced mitophagy enhances the clearance of defective mitochondria, which can contribute to various human disorders. Mitophagy deregulation inhibits the production of healthy mitochondria and accumulates faulty ones, which are linked to various illnesses. Stress-induced mitophagy is categorized into PTEN-induced putative kinase 1 (PINK1)/Parkin-dependent and independent mitophagy. The PINK1-Parkin E3 ubiquitin ligase-mediated pathway is the most extensively deciphered pathway of damaged mitochondrial obliteration regulating mitophagy. Loss-of-function mutations in these proteins have been linked to dysfunctional mitochondria leading to pathological conditions like Parkinson's disease (Kitada et al., 1998).

In normal physiological conditions, PINK1 is a serine/threonine kinase that translocates to the intermedium matrix (IMM) and is cleaved by mitochondrial processing peptidase (MPP) and Presenilin-associated rhomboid-like protein (PARL). However, mitochondrial stress and depolarization inhibit PINK1's proteolytic cleavage. When stabilized, it accumulates on the MOM and is ubiquitinated and autophosphorylated at serine (Ser)65 residue. Two ways exist for PINK1 to activate Parkin: first, by directly phosphorylating Parkin on S65 in its ubiquitin-like domain, which causes conformational changes that enable binding of the charged E2 ligase, and second, by competing with an autoinhibitory domain within Parkin to stabilize it in an active conformation.

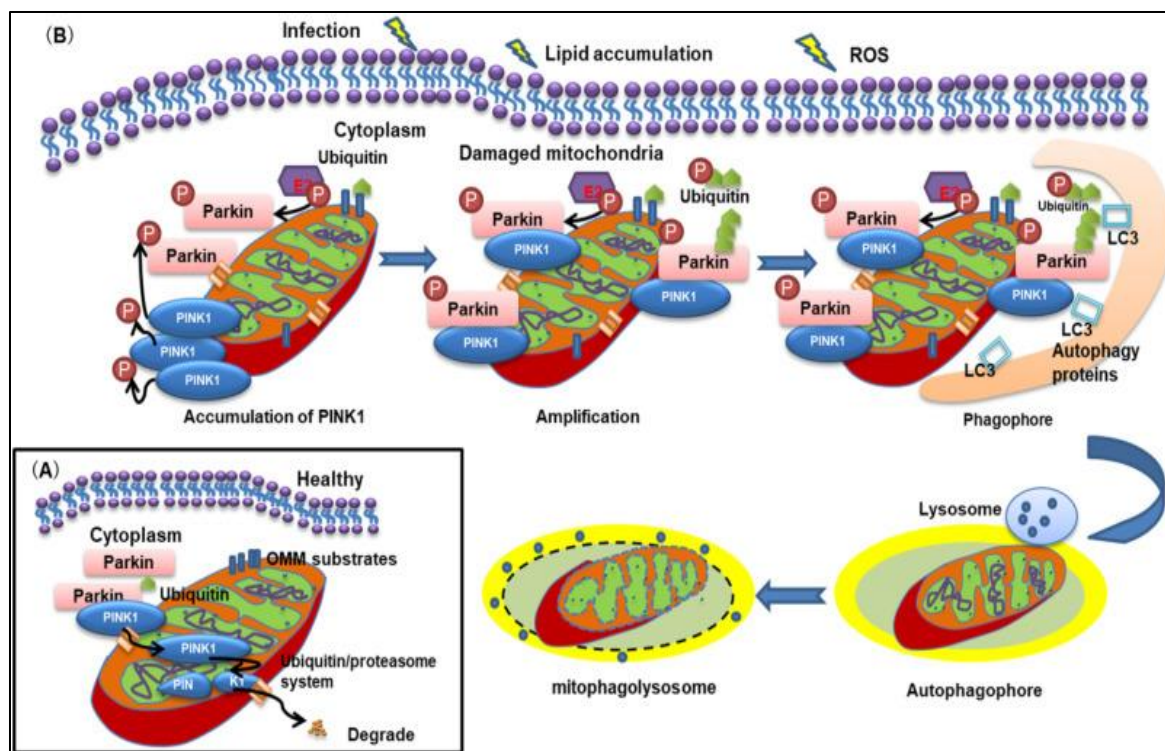


Figure 18: Mitophagy and autophagy for mitochondrial quality control: Adapted from Lihui Zhu et al 2023 <https://doi.org/10.1016/j.lfs.2022.121162>

Once activated Parkin exerts its activity by ubiquitinating the pool of OMM, matrix proteins, and thereafter IMM proteins as well as some cytosolic targets like AIMP2, Parkin Interacting Substrate (PARIS) (Quinn et al., 2020).

One of the primary triggers of NAFLD's advancement is mitochondrial dysfunction, and mitophagy is a defense mechanism that lessens the severity of the illness (Kwanten et al., 2016). According to in vitro studies Mice on a high-fat diet (HFD) have increased fat buildup, higher Oxidative potential, inflammation, and reduced mitophagy. When Parkin is genetically deleted in NAFLD mouse models exacerbation of the diseased pathology was seen. Hepatocyte-specific deletion aggravated fatty liver disease and IR, although some alternative protective effects on NAFLD were also reported (Edmunds et al., 2020).

2.6.6 Role of mitochondrial fatty acid β -oxidation in NAFLD:

The mitochondrial fatty acid oxidation (mtFAO) pathway is crucial for maintaining energy homeostasis, especially during fasting. It involves β -oxidation of long-chain fatty acids, which are essential for cardiac and skeletal muscle energy, and the generation of ketone bodies as an alternative source of energy (Bartlett & Eaton, 2004). β -oxidation occurs in peroxisome and mitochondria, with peroxisomal FAO primarily degrading VLCFAs (longer than C22) while mtFAO can oxidize different lengths of fatty acids including short, medium, and long chain fatty acids (Schrader et al., 2015). Long-chain acyl-CoA synthetase (ACS) does the activation step by adding a coenzyme-A moiety into

the fatty acid acyl chain creating acyl-CoA thioesters in the outer mitochondrial membrane (OMM), which are loaded with carnitine group by carnitine palmitoyltransferase-1 (CPT1) in OMM synthesizing fatty acyl-carnitines and subsequently regulating the crucial entry steps in mitochondrial fatty acid oxidation with the help of carnitine-acylcarnitine translocase (CACT) residing at IMM, ultimately translocating the acyl carnitines in the mitochondrial matrix. CPT2 then gives back the acyl moiety to acetyl-coA.

Endogenous fats are oxidized in acetyl-CoA molecules, resulting in reduced NADH and FADH₂. These molecules transfer electrons to the mitochondrial respiratory chain (MRC), producing FAD and NAD⁺ molecules. FAD-dependent dehydrogenases, such as medium-chain acyl-CoA dehydrogenase (MCAD) and long-chain acyl-CoA dehydrogenase (LCAD), catalyze two important mitochondrial beta-oxidation processes (Houten et al., 2016).

The transcriptional control of enzymes involved in mtFAO and ketogenesis is predominantly influenced by peroxisome proliferator-activated receptor α (PPAR α), which can be triggered by natural fatty acids or other external stimulations (Pawlak et al., 2015). Malonyl-CoA, an intermediary in de novo lipogenesis, can inhibit CPT1A, increasing mitochondrial FAO of long-chain fatty acid metabolism during fasting and repressed after eating. Impaired mtFAO can also affect hepatic gluconeogenesis, resulting in hypoglycemia, since low acetyl-CoA levels inhibit the activity of pyruvate carboxylase, a critical regulatory enzyme in the gluconeogenesis cascade. When mtFAO is impaired due to MRC inefficiency, lactic acid builds up in the system causing hyperlactatemia and lactic acidosis because the transformation of surplus pyruvate to lactate by lactate dehydrogenase enzyme is facilitated by the excess NADH buildup. Furthermore, mtFAO may trigger intracytoplasmic lipid accumulation, with extreme inhibition mostly resulting in microvesicular steatosis and intermediate inhibition often associated with macrovesicular steatosis (Diao et al., 2018).

2.7 Therapeutic strategies in NAFLD:

NAFLD is a liver condition and the risk factors associated with this immuno-metabolic pathophysiological condition are a sedentary lifestyle, insulin resistance, type 2 diabetes, elevated hepatic lipogenesis, and gut microbiome imbalance. There is no such specific established therapy for NAFLD, but clinical guidelines from the European Association for the Study of Liver (EASL) and the American Association for the Study of Liver Diseases (AASLD) suggest that lifestyle changes can result in a 5-10% weight loss in overweight or obese patients (Mantovani & Dalbeni, 2021). NAFLD therapy requires lifestyle optimization through food and exercise and combining medicines that manage glucose and lipid metabolism while simultaneously decreasing liver inflammation and fibrosis.

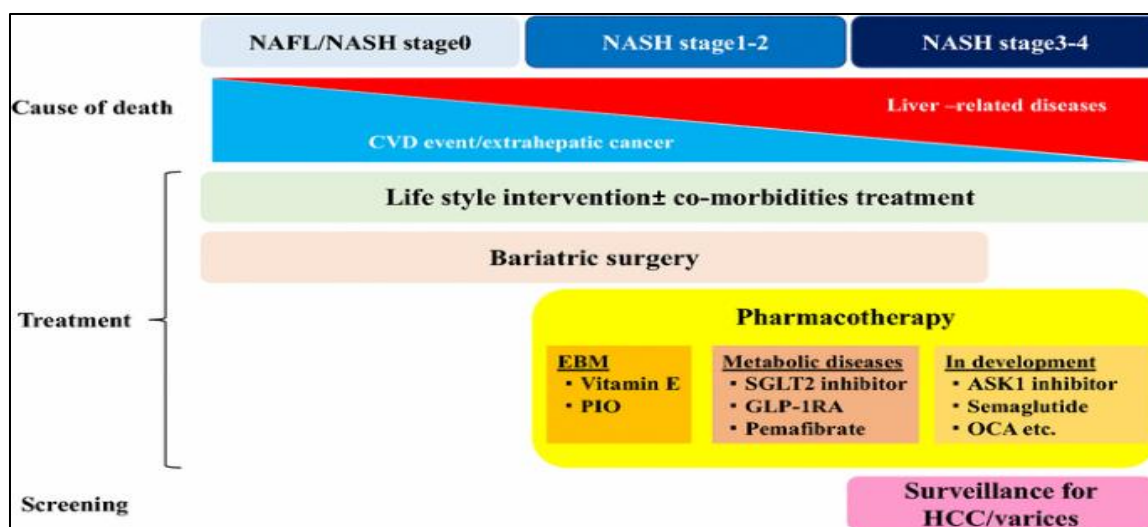


Figure 19: Strategies for NAFLD Treatment Adapted from Sumida et al 2017
<https://doi.org/10.1007/s00535-017-1415-1>

2.7.1 Dietary changes:

The National Institute for Health and Care Excellence (NICE) recommends a sedentary lifestyle modification as the primary treatment for nonalcoholic fatty liver disease (NAFLD) (Leoni et al., 2018, V. W. Wong et al., 2018). Dietary treatments, such as limiting calories, promoting ketosis, reducing sugar intake, and limiting carbohydrates, can improve liver protection. A Mediterranean-style diet and a ketogenic diet are recommended for treating NAFLD. A recent study revealed that Western lifestyle and food pattern exacerbate the chances of NAFLD development by 56%, while a plant-based Mediterranean diet reduces this risk by 23% (Hassani Zadeh et al., 2021). Exercise, along with dietary changes, can improve glucose and lipid metabolism, reduce hepatic fat deposition, and treat metabolic dysfunction.

2.7.2 Recommended drugs for NAFLD:

Currently, there is no specific drug recommended as a pharmacological guideline from the USFDA or EMA to treat NAFLD. However medical advisors often recommend some drugs for insulin resistance and dyslipidemia as an adjunct therapy (Rong et al., 2023). So there is an overwhelming need for specific pharmacological targets that can be used for the treatment of this disease. NAFLD or NASH goes hand in hand with other associated metabolic abnormalities, making this disease a critical one.

	Mechanism of action	Side effects	Recommendation to treat NAFLD	
			AASLD ⁷	EASL ⁸
Pioglitazone	PPAR γ agonist, decreases insulin resistance	Weight gain, fractures, may precipitate heart failure	Yes (use in patients with biopsy proven NASH, with/without type 2 diabetes mellitus)	Yes (use in patients with NASH, especially in diabetics)
Vitamin E	Antioxidant	Increase in overall mortality, hemorrhagic stroke, prostate cancer	Yes (use in nondiabetic patients with biopsy proven NASH)	Yes (use in nondiabetic, noncirrhotic patients with NASH)
Statins	HMG CoA reductase inhibitor	Hepatitis (serious liver injury is rare)	No (Can use to treat dyslipidemia. Avoid in decompensated cirrhosis)	No (can use to treat dyslipidemia)
Metformin	Decreases insulin resistance	Lactic acidosis	No	No
Ursodeoxycholic acid	Decreases TNF- α , reduces oxidative stress and insulin resistance	Headache, GI side effects	No	No

PPAR γ : peroxisome proliferator activated receptor gamma; HMG CoA: 3 hydroxy 3 methyl glutaryl coenzyme A; TNF- α : tumor necrosis factor alpha

Figure 20: Current Pharmacological Therapies for Nonalcoholic Fatty Liver Disease Adapted from Deepu David et al, 10.1016/j.jceh.2020.09.001

2.7.3 Antioxidant therapy in NAFLD:

Oxidative stress is a significant contributor to nonalcoholic fatty liver disease (NAFLD), leading to the research of antioxidants for treating NAFLD patients. Plant-derived and synthetic antioxidants and vitamins, such as silymarin, silybin, N-acetylcysteine (NAC), Betaine, resveratrol, and vitamins A, C, and E, have been tested against experimental and clinical NAFLD scenarios (Ezhilarasan & Lakshmi, 2022). Vitamin E, a lipophilic antioxidant found in vegetables, oils, meat, and eggs, has been found to alleviate fibrosis, diminish mitochondrial lipid peroxidation, and correct oxidative stress (Perumpail et al., 2018, Bril et al., 2019, Podszun et al., 2020). Nutritional intervention strategies centered on vitamins A, C, and E have been aimed at NAFLD patients, with studies showing that consuming these vitamins and supplements can lower the risk of NASH. Resveratrol, a photo-based antioxidant, has been used in research and clinical studies to treat NAFLD. It restores lipid stress-triggered steatosis in Hepatoma cells, reduces oxidative stress in mice, and enhances lipid metabolism and redox balance in rats with NAFLD (Huang et al., 2020). Betaine, a glutathione restorative substance, has been shown to reduce elevated liver enzyme levels, hepatic steatosis, and fibrosis in NASH patients (Abdelmalek et al., 2009).

Despite its numerous benefits for liver health and general body homeostasis, antioxidant treatment has been controversial. Some of the reasons are as follows:

- Due to its redox-sensitive properties, it can operate as a pro or anti-oxidant depending on the physiological circumstances.
- Redox oxygen species (ROS) are essential for maintaining homeostasis and producing an adaptive response to oxidative stress. Antioxidants frequently

compensate for weakened endogenous defenses by increasing antioxidant enzyme expression. However, externally contributed sources frequently undergo a difficult procedure and do not always achieve the desired outcome.

- Exogenous antioxidants frequently fall short in terms of target specificity since the oxidative harmful effect is generally restricted to certain cell types and organelles such as mitochondria and ER, and for pharmacological activity, target-based accumulation is required in the disease-initiating phases.
- Furthermore, their bioavailability in biological systems is poor, as impacted by endogenous variables such as dietary matrix, physicochemical qualities, and intake. Many dietary antioxidants fail in preclinical and clinical studies due to stability and bioavailability issues.

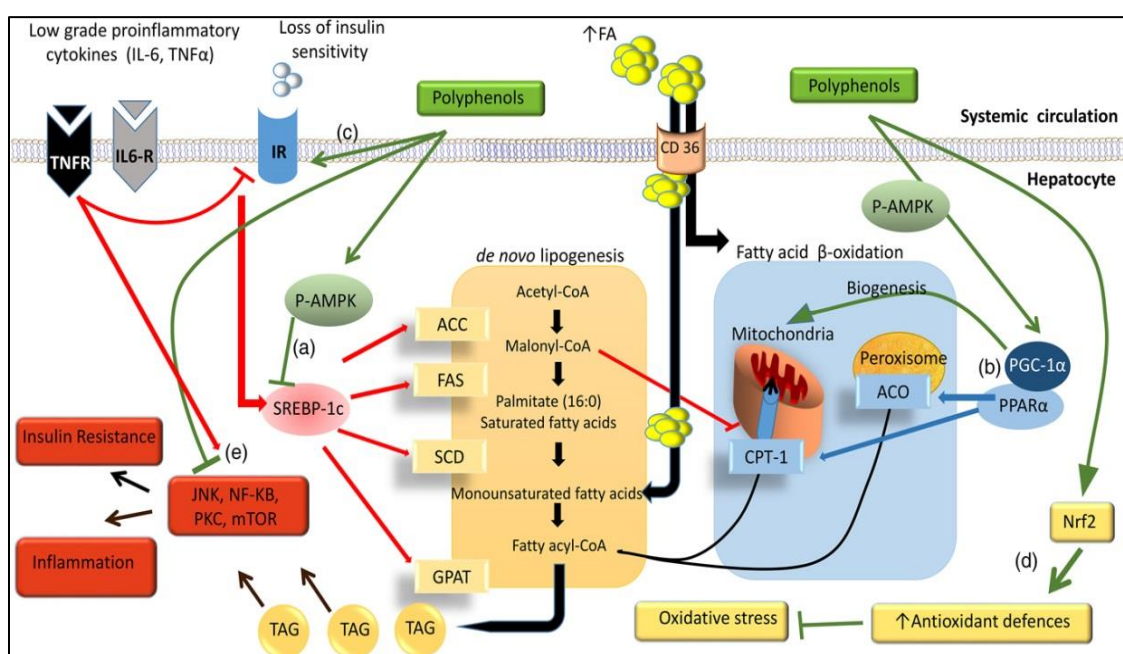


Figure 21: Polyphenols in Treating NAFLD: Adapted from Rodriguez-Ramiro et al 2016
DOI: 10.1017/S0029665115004218

2.8 Medicinal plants in NAFLD: Importance of *Wrightia tinctoria*:

Medicinal herbs are well known for their traditional usage and medicinal properties. They are regarded as an excellent source of bioactive chemicals, which can potentially be converted into medications. They have been listed in pharmacopeias from many nations for quality control purposes and are utilized in healthcare due to their low toxicity and fewer negative effects. Polyherbal treatments include many active components that work together to provide a combined synergistic effect within the human body.

2.9 *Wrightia tinctoria*: a potential medicinal plant and a possible NAFLD cure

Wrightia tinctoria is a medium-sized deciduous plant native to India, Australia, Myanmar, Nepal, and Vietnam (Kale et al., 2021). It produces milky white latex and has been traditionally used to treat various health problems, including diarrhea, seizures, wounds, jaundice, leukemia, gynecological diseases, toothache, headache, dandruff, diarrhea, and skin conditions like psoriasis, eczema, and scabies. The plant contains alkaloids, triterpenoids, steroids, flavonoids, lipids, and carbohydrates, with a wide range of pharmacological qualities. It has also been used for the management of breast cancer (Ganga Rao Battu et al., 2018). The Siddha medical system uses Oil 777, made from fresh leaves, as an effective treatment for psoriasis.

Taxonomical classification Kingdom: Plantae, Angiosperms, Eudicots, Asterids Order: Gentianales Family: Apocyanaceae Genus: *Wrightia* Species: *tinctoria*

2.9.1 Anti-ulcer activity :

A recent study evaluated the anti-ulcer properties of *Wrightia tinctoria* leaves on albino rats using a methanolic extract and a 70% ethanolic extract. The methanolic extract at 200 mg/kg showed strong gastroprotective action of 65.89%, compared to the conventional medication famotidine, which exhibited 75.34% (Divakar Madhu.C & Devi. S Lakshmi, 2011). Hydroxychloric acid extract of *W.tinctoria* bark also showed considerable anti-ulcer efficacy at 1000 mg/mL. Further research is needed to gain more insights.

2.9.2 Anti-fungal activity:

Wrightia tinctoria leaves have anti-dermatophytic properties against Basidiomycetes, Trichophyton, and Epidermophyton species. They also inhibit fungal species like *Curvularia*, *Botrytis*, and *Aspergillus*. The antifungal activity was tested using spore germination, agar dilution, and broth microdilution techniques. The hexane extract and chloroform extract were found to be effective against most dermatophytes (Ponnusamy et al., 2010).

2.9.3 Anti-bacterial activity:

A study found that methanolic seed extracts were more effective against gram-positive bacterial pathogens like *Staphylococcus aureus* and *B. cereus*, while aqueous extracts had moderate effects against fungal strains. Brown seeds showed greater pharmacological action than beige seeds. Both aqueous and methanol extracts of *W.tinctoria* leaves and flowers showed potent antibacterial activity against both gram-positive and gram-negative bacteria (Nagalakshmi et al., 2012).

2.9.4 Anti-psoriatic activity:

A study on *Wrightia tinctoria* leaves' anti-psoriatic activity showed a potency of 70.18%, above the norm of 57.43% (Dhanabal Sp et al., 2012). The extract also showed strong antioxidant activity. Traditional medicine, 777 oil, a mixture of *Wrightia tinctoria* and *Oleum Cocus nucifera* leaf extract, has been used for psoriasis treatment.

2.9.5 Free radical scavenging activity:

Wrightia tinctoria bark and flower extracts show potential as antioxidants, efficiently converting Fe^{3+} to Fe^{2+} and scavenging superoxide radicals (Kumar D Lakshman, 2011). The hydroalcoholic extract of *W. tinctoria* leaves showed strong antioxidant activity in tests like DPPH, H_2O_2 , and nitric acid scavenging (Dhanabal Sp et al., 2012, Khan et al., 2021).

2.9.6 Anti-diabetic activity:

Research on *Wrightia tinctoria* extracts has shown significant anti-diabetic properties in rodent models. In a diabetic rat model, methanolic (300 mg/kg/b. wt) and ethyl acetate (200 mg/kg/b. wt) fruit extracts showed significant hypoglycemic and anti-hyperglycemic effects. The methanolic and ethyl acetate extracts showed the greatest decrease in blood glucose levels after 4 hours (Rani M. Sandhya et al., 2012). *Wrightia tinctoria* leaf chloroform extract also showed strong anti-diabetic effects compared to glibenclamide. The leaf petroleum ether extract showed hypocholesterolemic and hypotriglyceridemic effects, suggesting a potential role in diabetes prevention and lipid resolution (Raj R et al., 2009).

General Introduction

In the dawn of the 21st century with recent socio-economic advances, technological revolution, and busy lifestyle a drastic change in the mass style of living, food intake, quality of nutrition, and also deterioration of sound mental-physical coordination is very much prominent. With the food and industrial revolution and newer methods of agriculture, the introduction of genetically modified plant products, uncontrolled use of pesticides, adulterants, and chemical processing of natural foods for petty monetary profits marked up a deep curse in the stomach of the whole human population. With the day-by-day degrading quality of food, the choice of food and culinary habits also pull human health towards unwanted development of cardiovascular and metabolic diseases. Western diets are a type of food characterized by highly processed, calorie-rich, nutrient-poor refined products with added sugar, salt, and saturated fats. High intake of processed red meat, carbonated sugar-rich beverages, and use of cheap oils loaded with saturated and trans fat in the preparation of food greatly increases the incidences of hypertension, colorectal cancer, cardiovascular diseases, and type 2 diabetes (Anand et al., 2015, Sami et al., 2017, Kumar et al., 2023). In the United States, a whopping increase in the prevalence of male obesity from 27.5% to 43.0% can be seen, also affecting children and women with an increase from 33.4% to 41.9% in the last two decades (Li et al., 2022). Nonalcoholic fatty liver disease (NAFLD) is an umbrella term defining a plethora of fatty liver diseases without influences of excessive alcohol intake and the most common form of chronic liver disease with a general prevalence of greater than 25% of the total population. South Asian countries and the Middle East reported a higher occurrence with $\geq 30\%$. (Riazi et al., 2022, Le et al., 2022) Obesity is the most prominent risk factor behind the pathogenesis of NAFLD with developing other comorbidities like type-2 diabetes, inflammation, and metabolic dysfunction and a higher propensity towards progression to steatohepatitis (NASH) henceforth making this pathological condition a global hot topic of research with no current specific clinical treatment (Fabbrini et al., 2010). NAFLD is pathologically defined as having $\geq 5\%$ hepatic fat. If left untreated this disease can rapidly progress towards developing fibrosis, cirrhosis of the liver and subsequently hepatocellular cancer. After detection by liver histology, or advanced imaging (MRI, CT) the common therapeutic strategies involve lipid-lowering drugs and/or anti-diabetic medication (statins, pioglitazone, rosiglitazone) with common anti-oxidant therapies (Vitamin C, Vitamin E supplements) (Smeuninx et al., 2020). Mitochondria being the power generator of the cell, control different aspects of the metabolic turnover while a deregulation in any aspect provokes metabolic anomalies and thus can have a major impact on NAFLD progression. Not only in the initiation step but with progressive deterioration by enhanced production of ROS, uncontrolled oxidative stress, disorganization in the mitophagy and lipid metabolism genes and overproduction of pro-inflammatory mediator secretion results in a surge of dysfunctional mitochondria. Different studies have reported the effect of restoring the impaired or decreased mitochondrial regulation in alleviating the occurrence as well as aggressiveness of fatty

liver disease (Nassir, 2014, Mansouri et al., 2018, Zhu et al., 2023). An overall coordination between liver, adipose tissue, pancreas, skeletal muscle tissue and their network of nutrient-signaling mediator exchange make the scenario more complicated. Obesity, insulin resistance and uncontrolled inflammation, all corroborate the pathogenesis of this liver disease triggered by mainly lipid stress. So taking a superficial approach by employing anti-obesity or anti-diabetic drugs can bring down the severity of the clinical manifestation but from root, it can't hit the bull's eye and eradicate the disease.

Natural products and/or phytochemistry were the most important sources of pharmacology and therapeutic research from its inception. Recent advances in technology, drug designing approaches, and synthetic chemistry have taken a front seat in today's drug development but carry a burden of toxicity, ill effects of long-term usage, non-specificity as well as bioavailability. Traditional medicine has long been silently walking down on its own path of safely treating multiple ailments effectively. Many aspects, information, and methods have been lost or undervalued for several socio-economic reasons despite of having immense potential in this field. Time has come to once again dig into this oldest and well-acknowledged but disorganized sector of medicine like Ayurveda, Unani, and Siddha style and collect specific molecular cues with the help of innovative modern research methodologies and software advancement. Thus by bringing the traditional knowledge and modern technologies hand in hand with proper validation and analysis, a newer and simpler solution to our long unmet need of therapeutic solution could be met. Walking down this path we gathered some background information, read literature, and consulted some experts of traditional medicine about the effective strategies to treat liver problems and diabetes in ayurvedic medicine which led our way towards *Wrightia tinctoria*, commonly known as Indrajao and its seeds are locally available in grocery stores but doing wonders in treating hyperglycemia, psoriasis, jaundice, and bowel problems. Several studies in the literature reported its anti-fungal, anti-bacterial, anti-diabetic, and anti-inflammatory activities but no proper validation and detailed work targeting mechanism of action was there (Ganga Rao Battu et al., 2018, Kale et al., 2021, Raj R et al., 2009, Rani M. Sandhya et al., 2012, Nagalakshmi et al., 2012, Ponnusamy et al., 2010). So we took the seeds of this plant and conducted a thorough research on NAFLD pathogenesis in cell culture as well as *in vivo* model. Stress was given to unravel the mitochondrial aspects of regulation revealing detailed molecular mechanism in controlling hepatic fat accumulation, mitochondrial dysfunction and inflammation in disease scenario. Cultivating more pathways with detailed pharmacokinetic study and characterization of responsible molecules present could pave a promising avenue in unraveling specific therapeutic lead towards the development of a permanent cure of NAFLD and associated disorders.

Aims and Objectives

The current research was focused on the pathophysiology of diet-induced Non-alcoholic Fatty Liver Disease and the search for a therapeutic intervention from natural resources. Excessive intake of a calorie-rich diet high in saturated fat, a sedentary lifestyle, and obesity predisposes a large proportion of the current human population in developing Fatty liver disease (Non-alcoholic). It also raises the chances of associated T2DM, cardiovascular abnormalities as well as progression towards NASH, Cirrhosis of the liver ultimately developing hepatocellular carcinoma. Building up of oxidative stress by abnormal accumulation of fats in hyperlipidemic condition, increased de Novo lipogenesis, and impaired fatty acid oxidation work together with dysfunctional mitochondrial bioenergetics as well as dynamics and mitophagy to result in pathogenesis of NAFLD. Peripheral Insulin resistance further aggravates the disease scenario. Currently, no such specific medicine is available for NAFLD due to its asymptomatic progression in primary forms with the scarcity of diagnosis markers as well as unawareness of its potentially damaging effect. Some antioxidants and lipid-lowering drugs are the sole candidates available till date which also comes with a burden of side effects and other associated complexities. The generation of a therapeutic lead from natural resources as well as a search for an effective phyto-formulation for lowering the pathophysiological parameters of NAFLD and NASH will fill in a long unmet gap. *Wrightia tinctoria* has long been used in traditional medicine in the Asiatic subcontinent to treat a range of diseases like jaundice, psoriasis, dysentery, and diabetes but its use in NAFLD and associated immune metabolic perturbation as well as mechanism of action is never explored. Seeds of *Wrightia tinctoria* are consumed after soaking in water or in dried powder form but a detailed study starting from extraction towards validation of the effects exerted by the extract on mitochondrial parameters, lipid metabolism and inflammation was long overdue. This study will not only help in understanding the mechanism of action of the compounds of this traditional medicine but also uncover a new possibility towards the development of a therapeutic lead or even a nutraceutical well-validated in *in vitro* and *in vivo* model.

The specific objectives of this study were as follows:

Objective 1:

Preparation and screening of different extracts of *Wrightia tinctoria* seeds and acute oral toxicity studies in mice (Chapter 1)

Objective 2

Role of *Wrightia tinctoria* seed hydro-ethanolic extract in ameliorating mitochondrial dysfunction and associated disorders in *in vitro* and *in vivo* model of NAFLD. (Chapter 2)

Objective 3:

Role of *Wrightia tinctoria* seedpod extracts in mitigating inflammation and characterization of compounds. (Chapter 3)

Materials & Methods

5.1 Materials:

Serial no	Name	Make	Catalogue Number
1	AMPK ALPHA	Abcam	ab137304
2	AMPK ALPHA (THR172)	SCBT	sc166897
3	PPAR α	Sigma Aldrich	P0369
4	PGC1 alpha	SCBT	sc552
5	NF κ B	(CST)	C22B4
6	CPT1A	SCBT	sc20514
7	MFN2	(CST)	D2D10
8	MFN1	(CST)	14739
9	PGC1 α	CST	2178
10	LC3B	CST	3868
11	PHDRP1(SER616)	(CST)	4060
12	BETA ACTIN	Sigma	2125
13	DRP1	CST	8570
14	TFAM	CST	8076

HRP- tagged Secondary Antibodies

1	HRP Tagged Anti-Rabbit secondary antibody	(CST)	7074
2	HRP tagged Anti-mouse secondary antibody	(CST)	7076
3	HRP tagged Anti-goat secondary antibody	(SCBT)	sc-2354

	Fluorophore-tagged SecondaryAntibodies	Company	Catalog no:
1	Anti-Rabbit Alexa Fluor 488	Invitrogen	A11008
2	Anti-Rabbit Alexa Fluor 555	Invitrogen	A48283
3	Anti-mouse Alexa Fluor 488	Invitrogen	A32723
4	Anti-mouse Alexa Fluor 633	Invitrogen	A21052
5	Anti-goat Alexa Fluor 488	Invitrogen	A11055
6	Anti-rabbit Alexa Fluor 633	Invitrogen	A21070

Reagents and Kits:

	Reagent Name	Company	CatalogNo:
1	iScript cDNA synthesis kit	Biorad	1708891
2	RNAiso Plus Reagent	Takara	9109
3	MitoStress kit	Agilent	103015-100
4	ECL reagent	Biorad	1705062
5	Biorad Sybr green	Biorad	1725120
6	MitosoxTM red	Invitrogen	M36008
7	MitoTracker Red CMXRos	Invitrogen	M7512
8	Palmitic acid	Sigma Aldrich	P500
9	JC-1 dye	Sigma Aldrich	T3168
10	DAPI	Sigma Aldrich	D9542
11	Fenofibrate	Sigma Aldrich	F6020
12	Hoechst stain	Sigma Aldrich	14533
13	Bovine Serum Albumin (BSA)	SRL	85171

5.2 Methods:

Cell culture and treatments:

HepG2 a human hepatoma cell line, were cultured in Dulbecco Modified Eagle Medium (AL007S HIMEDIA) containing low glucose with 10% FBS, 100U/I penicillin/streptomycin (Invitrogen), and 5% CO₂ humidified atmosphere in a Heracell CO₂ incubator maintained at 37°C. BSA conjugated Palmitic acid stock solution was prepared at a concentration of 2 millimolar (Palmitic Acid, Sigma) (BSA Sigma); For saturated fatty acid treatment serum-starved cells were subjected to a working 0.40 mM concentration of PA for 24 hours (Lee et al 2022, Seo M.H et al 2016). Inhibitor pre-treatment for AMPK- α was done with compound C (5 μ M, Sigma) for 2hour followed by co-incubation with PA. Raw 264.7 macrophage cells were maintained in DMEM high glucose medium supplemented with 10% FBS 100 U/I penicillin/streptomycin (Invitrogen) and maintained in 5 % CO₂ incubator. LPS for inflammation stimulation were prepared in PBS and used in one μ g/ml concentration for shorter periods (30mins-2 hr) and 100 ng/ml concentration for longer duration (18hr). Treatment for plant extracts were given with mentioned concentrations for six hours prior to addition of PA stimulation. SN50 was used as NF κ B inhibitor and TAK 242 (2 μ M) was used as TLR 4 inhibitor. PPAR agonist fenofibrate (50 μ M) was used as control drug in the lipid stress experiments and also in in vivo model (50mg/kg bodyweight). 3T3L1 adipocyte cells were grown in DMEM high glucose medium supplemented with 10% FBS and penicillin/streptomycin in 5% CO₂ humidified chamber. In order to differentiate the pre adipocyte cells into mature adipocytes a differentiation protocol was as followed: After confluence 3T3L1 adipocyte cells were grown in DMEM medium supplemented with 150 μ g/ml of insulin for 48 hours then differentiation medium was added consisting dexamethasone, IBMX, and insulin for 48 hours. After this a maintenance medium with DMEM supplemented with 10% FBS was added and left for another 48 hours for full maturation of adipocytes. For *in vitro* experiments extracts were pretreated with cultured cells for 6 hour, then stimulation (Palmitate/ LPS) was added and further incubation (according to mentioned time) was done with presence of extracts in the medium.

Animal studies for in vivo model:

Male C57BL6 mice (6-8) weeks were maintained in aerated cages and fed a normal rodent diet and water at libitum maintaining a 12-hour day and night cycle in a animal facility of Indian Institute of Chemical Biology, Kolkata accredited by the Association for Assessment and Accreditation of Laboratory Animal Care International. All animal experiments were carried out in maintaining CPCSEA guidelines, Government of India, with approval from the institutional animal Ethics Committee. During the experimental procedure, to establish the animal model mice were fed with fatty diet (Cat no: Research

diets D 12492 60% fat Kcal) for 20 weeks, simultaneously maintaining one control group fed on regular diet. On completion of 20 weeks feeding regimen, mice taking fat diet exhibited a considerable increase in body weight when compared to the typical chow diet. Consequently, blood glucose levels were assessed in all animals on day zero of therapeutic intervention and Oral glucose tolerance test was performed. Prior getting randomly assigned, the animals were separated according to their body weights and blood glucose levels and divided into designated treatment groups. For the next 28 days, animals were fed with plant extract by oral gavage in two dosages (250 milligrams per kilogram body weight for the lower dose LD and 500 milligrams per kilogram body weight for the higher dose HD), as well as with vehicle in control group. Fenofibrate was used as a control drug at 50mg/kg bodyweight dose and given by oral gavage. The day before the final day, an insulin tolerance test and an oral glucose tolerance test were done. On the last day, after an 8-hour fasting, blood was obtained by retro orbital method and mice were euthanized. The serum was isolated and analyzed for AST, ALT, cholesterol, triglyceride, HDL, LDL levels. Tissues were collected and either fixed in 10% formalin or otherwise snap frozen in liquid nitrogen as per requirement.

RNA isolation and Quantitative PCR:

The cells' total RNA was harvested using RNA isolation solution (RNAiso Plus, TaKaRa Bio) according to standard isolation technique. In short, Cells were vigorously mixed and ruptured with RNAiso Plus and further incubated at room temperature for 15 minutes. Following that, chloroform was added and vigorously mixed and kept at room temperature for 15 minutes for phase separation. The resulting mixture was spun down at 12000g for fifteen minutes at 4 degrees Celsius. The top most clear solution was aspirated and mixed with 2.5 fold iso-propanol and subsequently left for a further 20 minutes at room temperature before another round of centrifugation at 12000g for 15 minutes at 4°C. The supernatant layer was removed, and the remaining pellet was extensively cleaned with 75% ethanol (Merck) by rotating at 7500g for 10 minutes at 4°C. The RNA pellet was subsequently air dried at RT before being dissolved in DEPC-treated water. Gel electrophoresis alongwith a 260nm/280nm absorbance ratio was used to assess RNA purity. To synthesize cDNA, 0.5ug of RNA and the Bio-Rad iScript cDNA synthesis kit were used. To prepare a 20µl reaction mixture, the reagent ratios are as follows: cDNA synthesis buffer (4µl), reverse transcriptase enzyme (0.5µl), and nuclease-free water for the rest of the volume. The PCR cyclet layout was as follows: (a) 5 min of priming at 25°C, (b) 20 minutes of reverse transcription at 46°C, and (c) RT inactivation: 1 minute at 95°C (d) hold at 4°C. Real-time PCR was used to further quantify the relative mRNA expression levels of various genes (Applied Biosystems 7500, Foster City, CA) using SYBR green (Invitrogen) after normalization to endogenous housekeeping genes like 18S rRNA. The comparative Ct method was utilized to determine the relative gene expression profile, and fold change was evaluated as:

$$[2-(\Delta CT(\text{sample}) - \Delta CT(\text{calibrator}))]$$

Where ΔCT is calculated on subtraction of the C_t values of desired gene expression from the C_t value of the housekeeping genes respectively the relative fold change in gene expression is depicted as fold change in Y axis. Primer Express 3.0 software (Applied Biosystem) was used to create the primers, which were purchased from Integrated DNA Technology. The table contains a list of primer sequences used in experiments.

Gene	Forward Primer (5'-3')	Reverse Primer (5'-3')	T _m (°C)
18s rRNA	GATTCCGTGGGTGGTGGTGC	AAGAAGTTGGGGGACGCCGA	60
IL-1 β	TGAAGCTGATGGCCCTAAACA	GTAGTGGTGGTTCGGAGATTCG	59
IL-6	CCTGACCCAACCACAAATGC	CCTTAAAGCTGCGCAGAATGA	59
PGC1 α	TGCCCTCGGTTCATTGTC	GATTCTGATTGGTCGCTGTA	60
PPAR α	GCCCCCTCCTCGGTGACTTAT	CCCCGCAGATTCTACATTCG	59
SIRT1	CGGGAATCCAAAGGATAA	CCTCGTACAGCTTCACAGTCAACT	59

MTT Assay:

Cellular cytotoxicity was measured by employing MTT reagent colorimetric assay. Cells were first seeded in 96 well cell culture treated plates and subsequently treatment was given. After completion 20 μ l of MTT (5 milligram/ ml) was added to 180 μ l of fresh medium/well and incubated for 3 hours. After completion of incubation MTT reagent was discarded and 100 μ l DMSO was added to solubilize the formazan crystals and absorbance was recorded at 570 nm using multimode reader (Hidex; Sense Microplate Reader).

Griess assay for measurement of NO:

Employing the Griess reagent, the amount of nitric oxide (NO) produced in cell culture supernatants was measured, and the findings were represented in μ M nitrite. In summary, equal volumes of Griess reagent (1% sulfanilamide and 0.1% N-1-naphthylethylene diamine hydrochloride in 50% H₃PO₄) were combined with 100 μ l of culture supernatants, and the mixture was incubated for 10 minutes at room temperature. After then, absorbance was calculated at 540 nm. Using NaNO₂ as a standard, a calibration curve was created.

DPPH assay for assessing free radical scavenging activity:

DPPH was utilized as a free radical scavenging reagent to estimate the test samples' free radicals scavenging capacity. DPPH has a consistent purple color in the methanolic solution. The plant solutions' ability to scavenge radicals by respective change in the purple color was investigated using the DPPH assay (for plant extracts). In a 96-well microplate, 100 μ L of DPPH solution (0.008% w/v DPPH in methanol) was combined with 100 μ L of plant extract at different concentrations, and the mixture was incubated for 30 minutes at 25 °C. Following incubation the absorbance was measured at 517 nm using a microplate reader.

Cellular ROS measurement by DCFH-DA:

The cells were grown in a 60 mm cell culture treated plate and appropriate treatments were given. After treatment completion spent medium was discarded then scraped cells were washed with PBS. Approximate 1×10^6 cells were stained for 15 minutes with 5 μ M H₂DCF-DA fluorescent reagent as an indicator of total cellular ROS (CM-H₂DCFDA, Invitrogen Cat# C6827). Three 5-minute washes with PBS were then carried out. The labeled cells were resuspended in 300 μ L of PBS and subjected to flow cytometry (excitation/emission 488nm/520nm) for detection and the results were processed by Using BD FACSDiva Software (RRID: SCR_001456).

Measurement of Mitochondrial membrane potential by JC1 dye:

Cells were grown in 60mm plate and plant extracts were pretreated for 6 hours. Thereafter PA stimulation was given and after incubation cells were washed twice with PBS at 5-minute intervals. This was followed by staining with JC-1 dye dissolved in PBS (stock conc: 5 μ g/ml, Invitrogen, cat# 3168) for fifteen minutes at 37°C incubator. Further cells were scraped, washed two times with PBS before resuspending in cold 300 μ L PBS followed by detection with flow cytometer (Excitation/Emission for Red 535nm/590nm; and Green Excitation/Emission 485nm/535nm) using BD FACSDiva Software. The ratio of the shift from the red JC1 aggregates towards green monomers was used to evaluate mitochondrial membrane potential.

Staining of Mitochondria using Mito-tracker red (MTR):

To investigate mitochondrial morphology, cultured cells were seeded in the treated cover plate and after completion of treatment stained with fluorescent probe MitoTracker Red CMXRos (100 nM, Invitrogen; Cat No. M7512) for 15-20 minutes at 37 °C. Following this, cells were fixed in 4% paraformaldehyde (PFA) for 15 minutes before being permeabilized in 0.1% Triton X-100 for 10 minutes. Then further processing steps for confocal microscopy was followed and finally after counter staining with nuclear stain DAPI, slides were observed under microscope.

Glucose uptake assay using 2-NBDG:

The fluorescent D-glucose analog 2-NBDG was utilized as a tracer to monitor the absorption of glucose in the cells during the glucose uptake experiment. Glucose Uptake Cell-Based Assay Kit (CAYMAN 600470) was used. In short, the cells seeded in 96-well plates were treated with plant extract in glucose free DMEM and after fatty acid treatment incubated with or without insulin (150 nM) for 15 mins. Thereafter 2-NBDG was added to cells and further incubated for 45 mins at final concentration of 100 µg/ml. Following the treatment, 150 µl of cell assay buffer was added to each well and the plate was centrifuged at 400g for 5 mins. 100 µl of supernatant medium was taken in black microplate and fluorescence intensities were measured at 485 nm for excitation and 538 nm for emission using a Thermo microplate fluorescence reader.

Immuno-cytochemistry study by confocal microscopy:

1x10⁵ cells were cultured in a 6-well plate with collagen-treated cover slips for 24 hours in complete DMEM medium. After reaching 70% confluence, cells were pretreated with plant extracts and stimulated with 400 µM PA for 20 hours. Following incubation, cells were rinsed with PBS, and 4% paraformaldehyde was applied drop by drop to a cover slip for cell fixation. The cells were then permeabilized with 0.1% Triton X for 10 minutes. Cells were washed three times with PBS and then placed in PBS containing 5% BSA for one hour before being incubated with the primary antibody (dilution 1:200 for CST) overnight at 4°C. Following two PBS washes, the cover slip was incubated with Alexa Fluor 488-647 labeled secondary antibody for one hour. Then DAPI was used as nuclear counter stain and mounted with prolong glod-antifade reagent (Thermo) for observation. Scalebar is 10 µm. The images were visualized and acquired using SP8 Lighting super resolution confocal microscope (Leica, Germany; RRID: SCR_008960) with objective lens (oil immersion 63X, NA 1.4) and processed by using LAS X software (LAS X, RRID: SCR_013673).

Isolation and Estimation of protein by LOWRY method:

After treatment the cells were harvested and further washed twice with saline followed by centrifugation at 2000rpm for 5 mins. RIPA lysis buffer with freshly added DTT, PMSF, and a protease inhibitor cocktail was used to prepare the cell lysate and extract the proteins. The cell lysate was sonicated four times with a 20-second pulse and a 10-second pause after being incubated in ice for 20 minutes (Nicholas et al., 2019). After centrifuging the lysate for 11 minutes at 13,000 g, the supernatant was recovered. Using Lowry-Folin's technique, the protein concentration was estimated. Alkaline copper sulfate reagent was added to the protein samples and incubated for 15 minutes followed by addition of falling cycle to reagent and further incubation at room temperature for 20 minutes in dark after completion of the incubation. The absorbance was taken at 660

nanometer wavelength. Laemmli buffer containing bromophenol blue, beta-ME was freshly prepared and utilized to prepare 40-60 ug of protein aliquots for every sample.

Western Blotting of protein:

Cell lysates or tissue homogenates were prepared according to standard protocol. After estimation of the protein samples it was run in SDS-PAGE with restrained marker for proper separation and subsequently western blot was performed using PVDF membrane which was activated first using methanol. Wet transfer (Constant volt: 85 at 4°C) was done for $\pm 2-4$ hr was done depending on the molecular weight of the target proteins. After wet transfer the membranes were subjected to blocking for 3 hrs in a 5% blocking solution (BSA/skimmed milk in TBS-T) and then incubated with antibodies specific for the protein overnight at 4°C. After washing HRP tagged secondary antibody was added at the membrane was kept in a slow shaking for 1-2 hr. Detection was executed employing ECL chemiluminiscent detection reagent (Bio-Rad Catalogno:1705062) and densitometry analysis of the band were done using ImageJ software.

Analyzing the morphology of mitochondria employing atomic force microscopy :

For Atomic Force Microscopy (AFM) mitochondria was separated from cell lysate employing mitochondria isolation kit (Thermo) and subsequently the mitochondrial pellet was serially dilute in PBS and mounted on mica sheets and visualized using a Pico plus 5500 AFM (Agilent Technologies, USA) equipped with a piezo scanner (range of 10 μ m) at the institutional facility. The image was processed with PicoView Image software Version 1.20 (Agilent Technologies, USA).

Measurement off mitochondrial respiration and glycolytic flux by Sea Horse flux analyser:

24 well XFe cell plates (Seahorse bioscience) were used for cell plating. HepG2 cells were seeded at a density of 5×10^4 cells /well in 100 μ l DMEM growth media containing 10% FBS and incubated at 5% CO₂ for three hours. Another 150 μ l of growth medium was topped up to the cells and incubated at 37°C with CO₂ till 60-70% confluency. Treatment was given, and the next day, after discarding the spent medium the basal medium was prepared by adding 2 mM glutamine to basal DMEM (Seahorse bioscience), and added to the cells and further incubated for an hour in a 37°C normal incubator. The XFe cartridge's three injection ports A-C were injected with 1 μ M Oligomycin, 2 μ M FCCP, and 1 μ M Rotenone-Antimycin A, followed by 12 minutes of instrument equilibration and calibration. After calibrating the cartridge, the cell plate was loaded to begin measuring the oxygen consumption rate (OCR) using preset parameters (Three-minute main, Two-minute mix, and Three-minute wait,) cycle. Protein estimation was done using Folin-lowry's principle for normalization of the the resulting OCR values. Oxygen consumption rate was indicated in picomol/mint/mg of protein.

For the glycolytic flux test, three injection ports of A to C of the cartridge were filled with glucose 10 mM, oligomycin 2 μ M, and 2-deoxyglucose 100 mM, respectively which were then equilibrated and calibrated in the instrument for 12 minutes before measuring the extracellular acidification rate. ECAR was measured by preset cycle of three-minute wait, two-minute mix, and three-minute measurement. Protein estimation was done using Folin-Lowry's principle to normalize the ECAR results with cellular protein content. ECAR rate was expressed as mpH/mint/mg of protein.

Estimation of fasting glucose, serum AST, ALT triglyceride and cholesterol level:

After 8 hour of fasting blood was collected by retro orbital method and serum was isolated following standard protocol. Fasting glucose was measured by Contour Plus strip employing glucose oxidase method. Serum AST, ALT was measured by standardized method using Commercial kits (Roche Diagnostic Germany) and expressed as IU/L. Triglyceride and cholesterol were also measured using standard kit (Roche) and expressed as milligram /dl.

Oral glucose tolerance test and Insulin tolerance test:

To determine glucose intolerance in animal's oral glucose tolerance test was executed on penultimate day of sacrifice. Mice were fasted overnight for eight hour and were given 2 gram/kg bodyweight of oral glucose solution and blood samples were taken at indicated time points for 120 minutes after glucose administration by severing the tip of the tail. Insulin was peritoneally injected and blood sugar levels were detected at 0, 30, 60, 120 mint time point for measuring ITT.

Oil red O staining:

Following cell fixation in 10% formalin solution for 30 mints and then dehydration in 60% isopropanol solution cells were flooded with 60% oil red O stain at room temperature for 45 mints. After this 2 wash with PBS/water the cells were ready for microscopy. The image was captured by Olympus inverted imaging system.

Study of tissue histology:

For histological staining freshly isolated liver tissues were store in 10% formalin for minimum 24 hours and subsequently paraffinized. Liver and fat tissues were sliced approximate 5 micrometer thickness in a micotome and stained with hematoxylin eosin general physiology and picrosirious red for fibrosis staining. The images were captured in Olympus BX51 Brightfield microscope. After imaging the samples were graded for severity of steatosis by scoring for tissue ballooning, inflammation, and fibrosis.

Immunohistochemistry followed by immunofluorescence based detection:

Isolated liver tissues were fixed by 10 % formalin and paraffin block were prepared using standardized protocol. The five micrometer thickness paraffin sections were cut by a micotome and placed on poly lysine coated glass plates. After deparaffinization with xylene and rehydration with consecutive decreasing concentration off alcohol starting from 100% - 90% - 70% then 50% and then running water wash tissues were blocked in 5% BSA prepared in PBS for 30 minutes and incubated for two hour with primary antibody. The slides were then washed and incubated with secondary antibody tagged with Alexa fluorescent probes(488 and 637) followed by staining of nucleus for 5 minutes DAPI stain. Slides were observed under a Leica confocal microscope.

Extraction of mitochondria from liver:

The tissue samples of liver were washed and subsequently homogenized in chilled Na-phosphate buffer (50 mM) containing (50mM Tris, 250 mM sucrose, 1m M EDTA pH 7.4) with a Potter Elvenjem glass homogenizer (Belco Glass, IncUSA). To extract the mitochondrial fraction, the homogenates (10%) were centrifuged at 3000 rpm for 10 minutes. The resulting supernatant was then spun again at 14000 rpm for 40 minutes. The pellet was used to measure the activity of mitochondrial enzymes by resuspending it in Tris-sucrose buffer (pH-7.8).

Measurement of mitochondrial respiratory chain enzyme activity:

The technique of Chretien et al., 1995 was used to quantify pyruvate dehydrogenase activity with a few minor adjustments. In summary, spectrophotometric measurement of NAD⁺ to NADH was performed at 340 nm with a substrate (0.5 mM sodium pyruvate in 50 mM phosphate buffer, pH 7.4) present. The protein activity produced by the enzyme was represented as U/mg during the 90-second recording of the increase in optical density at 10-second intervals.

The activity of citrate synthase enzyme was measured spectrophotometrically in the mitochondria of the liver tissue using the Srere, 1969 method. For 120 seconds, at 10-second intervals, the interaction between CoA-SH and DTNB was measured as a rise in optical density. At their final concentrations, the reaction mixture contained 10mM oxaloacetate, 1.01mM DTNB, 0.124mM acetyl CoA, and Tris-HCl buffer (pH-8.0). Units/mg protein was used to express the enzyme activity.

The activity of succinate dehydrogenase (SDH) was determined by applying the technique of (DERVARTANIAN & VEEGER, 1964) . The absorbance change was monitored at 420 nm for 120 seconds, with 10-second intervals, using a UV/VIS spectrophotometer. 200mM succinate was used as the substrate and 25mM potassium ferricyanide (III) was

added to reaction mixture to check the rate of potassium ferrocyanide (II) formation. Activity was expressed in U/mg protein.

NADH-Cytochrome c oxidoreductase activity was determined following method of (Goyal & Srivastava, 1995) and observing the change in absorbance spectrophotometrically at 565nm. The change in absorbance was recorded for 90 seconds at 10 seconds interval in presence of 20 μ M oxidised cytochrome C and 0.5 μ M NADH in the reaction mixture. Enzyme activity was expressed as U/mg protein.

Estimation of NADH Oxidase activity:

NADPH oxidase activity was spectrophotometrically measured at 340nm and the oxidation of NADH to NAD⁺ was recorded, following the method of Reusch & Burger, 1974. The reaction mixture contained 51mM potassium phosphate, 0.07mM NADH, 0.1mM FAD and 0.03% (w/v) BSA as final concentration in 1ml. reaction mixture. Enzyme activity was expressed as U/mg protein

Lipid peroxidation assay:

The tissue was suspended in 0.9% NaCL buffer and lysate was prepared. After adding the thiobarbituric acid-trichloroacetic acid reagent to the solution, it was heated for 20 minutes at 80⁰C for color development. To measure the absorbance at 532 nm, a SHIMADZU UV/VIS spectrophotometer was used.

Statistical Analysis:

Every experiment described above was carried out using a minimum of three biological triplicates, unless otherwise stated, GRAPHPAD PRISM-8 (San Diego, CA, USA) was used for the statistical analyses. The data were shown graphically as Mean \pm SEM. A two-tailed Student's t-test was used to determine the P-value for paired sample and in case of more than two sample sets one-way ANOVA was used for statistical analysis before Tukey's Multiple Comparison Test was applied. A 95% confidence interval, or $\alpha = 0.05$, was used to calculate the significance threshold. Significance was calculated with respect to Palmitic Acid or HFD group unless mentioned. The following was a representation of the degrees of significance: *P-value<0.05, **P-value<0.01, and ***P-value<0.001; ****P-value<0.0001 ns (non-significant).

Chapter 1

**Screening of different extracts of *Wrightia tinctoria*
seeds and in vivo oral toxicity studies**

Screening of different extracts of *Wrightia tinctoria* seeds and in vivo oral toxicity studies:

6.1. Introduction:

Wrightia tinctoria is known by the names “pala indigo” and “indrajao,” and belongs to the Apocyanaceae family mainly used in traditional medicine. It is extensively used in the treatment of skin diseases and liver disorders, jaundice, and psoriasis and possesses a broad spectrum of many other biological activities. It has been reported that Indrajao is mainly comprised of saponins and polysaccharides and has pharmacological activities, including immune promotion, anti-aging, blood glucose regulation, and lipid regulation (Kumar & Sinha, 2004, Anusharaj; et al., 2013). In addition, several previous studies indicated that Indrajao prevented type 2 diabetes. However it is not clear whether Indrajao can alleviate NAFLD. The pharmacological effects and underlying mechanisms of Indrajao in protecting against obesity and fatty liver disease remain to be identified.

High saturated fat induced lipid accumulation and subsequent metabolic dysfunction was mimicked in well-established in vitro model with HepG2 hepatoma cell line with Palmitic acid (400uM) treatment. Different extracts were prepared using solvents of varied polarity, starting from non-polar hexane towards maximum polar aqueous solvent. Ethanol and ethanol: Water (1:1) mix was also used for gradation of polarity in extraction with solvents. Resulting extracts cytotoxicity was checked and subsequently oxidative stress, nitrosative stress lowering capacity was screened for all four extracts. Cellular toxicity upon fatty acid overload and inhibition of fat accumulation was also screened between the extracts. Glucose uptake was also checked as insulin resistance is another important pathophysiology apart from increased oxidative, nitrosative stress and intracellular lipid accumulation. Oral toxicity was also checked for the most promising extract for effect in blood parameters as well as vital organs like liver, spleen and kidney using mice model. Acute oral toxicity of a compound or extract is often tested to rule out any adverse effect of the agent on the biological system. After feeding the animal immediate and after effect is recorded such as behavioural, haematological, biochemical or histological alteration along with mortality if any. LD₅₀ dose is calculated and according to the results, categorization of compound in terms of safety is allocated. Indrajao or *Wrightia* seeds are consumed from long back by people as therapeutic in herbal medicine making it easier to establish its safety profile and negate any significant toxicity. A precise study to determine the LD₅₀ and pinpoint any specific toxic effect on major sensitive organs like liver, kidney, spleen with overall physical, haematological parameters is required to establish the potency of *Wrightia* extract as a biologically safe lead to proceed upon. Therefore, in this study, we prepared and screened the promising alleviating effect of Indrajao extracts against lipid stress and also investigated the impact of high oral doses on tissue level toxicity in mice.

6.2. Collection of plant material:

Wrightia tinctoria was procured from local market of two locations namely Jadavpur and Sonarpur (West Bengal) and assessed for seed quality, texture etc. The seed pods were authenticated by Central National Herbarium, Howrah (IICB/DK/012). More greener and good textured source was chosen (it yielded more concentrated turbid aqueous layer and in ayurvedic treatments it is normally taken after soaking in water).



6.3. Extraction Procedure:

Coarsely powdered seeds of *Wrightia tinctoria* were successively extracted with the solvents of increasing polarity i.e. hexane, ethanol, ethanol-water (50:50 v/v), and water (48 hrs). The obtained extracts were evaporated under reduced pressure at 45-48°C to obtain solvent-free residues. 60 grams of dried seed were taken and coarsely in a grinder and then soaked in approx. 200 ml of solvent for 48 hours and this process was repeated for twice to get the best possible extraction of compounds into the solvents. Now the resulting filtrate was filtered through a whatman filter paper and further dried at 45-50 degree temperature to get the final extracts. The obtained fractions were analyzed by HPLC (Ascentis RP18, 25 cm x 4.6 mm, 5µm Supelco column; mobile phase A: water containing 0.1 % formic acid and B: acetonitrile, 0-1 min 90:10 v/v; 1-20 min 5:95 v/v; 20-25 min 5:95 v/v; 25-26 min 90:10 v/v and 25-30 min 90:10 v/v at 254 and 210 nm).

60 grams of seed after extraction with hexane yielded 7.4 gram of yellowish sticky extract nomenclature as 186A (WTEA) whereas 60 grams of seed when extracted with 100 % ethanol gave a yield of 3.8 gram greenish extract (186B or WTEB). Thirdly, a 1:1 hydro-ethanolic mixture of solvent was used for extraction of 60 gram of wrightia dried seeds which subsequently yielded approximately 7 gram of dry brownish textured extract (186C or WTEC). Lastly the most polar solvent i.e. water was used as a solvent and after extraction it yielded 11.4 gram of brownish thick textured extract (186D or WTED).

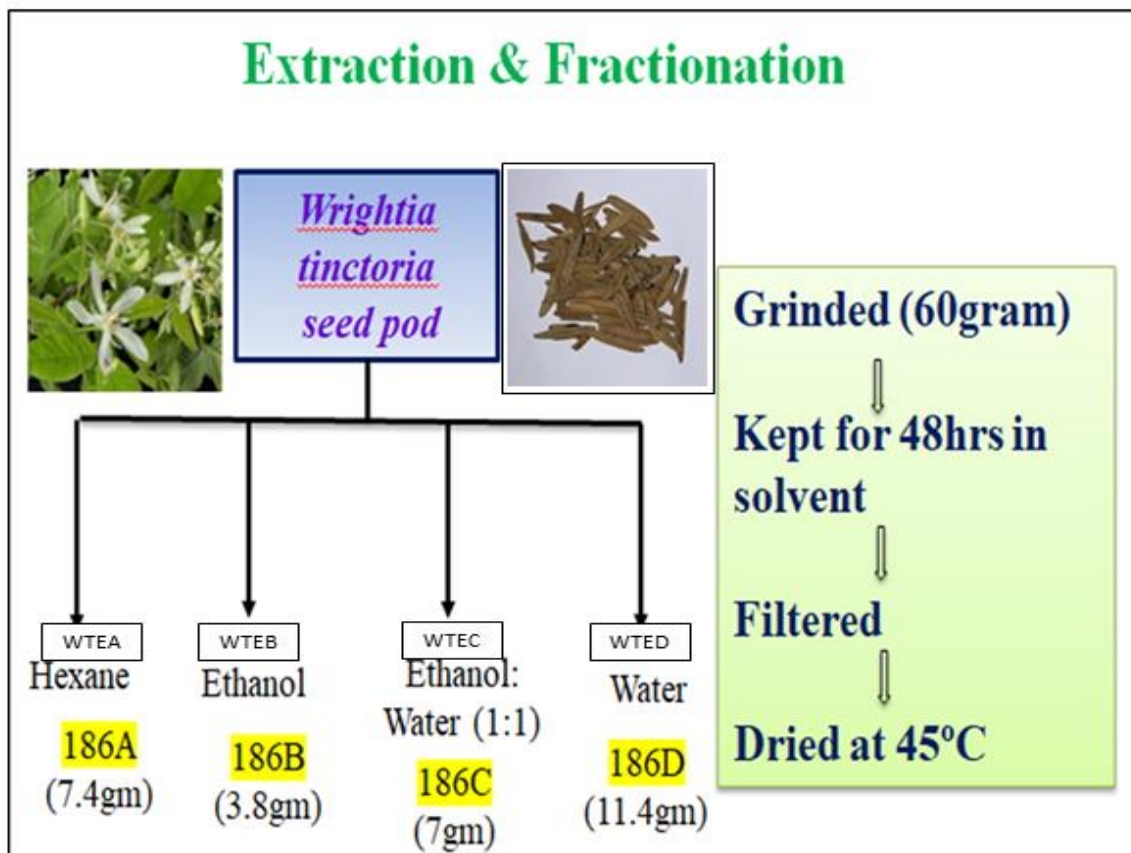
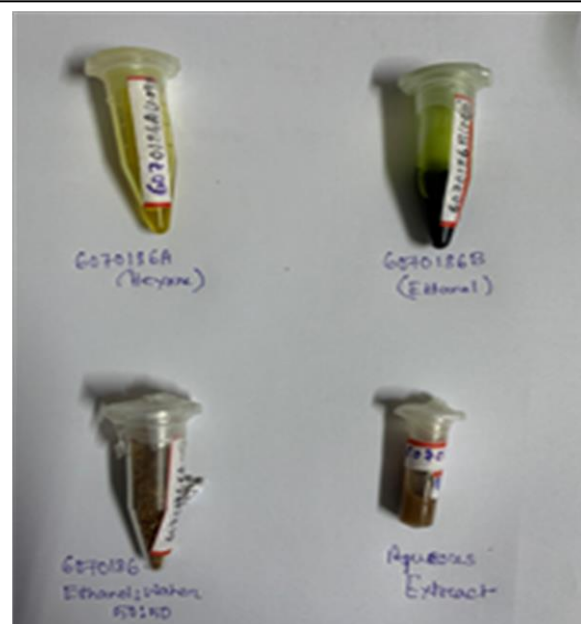


Figure 1: Procedure of preparation of extracts of *Wrightia tinctoria* (WT) seedpod and their nomenclature (Plant picture taken from Khyade et al 2014)

So after extracting with these solvents we got four extracts of *Wrightia tinctoria*:

- 1) Hexane extract- 6070186A (WTEA)
- 2) 100% Ethanol extract- 6070186B (WTEB)
- 3) Ethanol: H₂O (50:50) extract- 6070186C (WTEC)
- 4) Aqueous extract- 6070186D (WTED)



6.4. Results:

Screening of different *Wrightia tinctoria* (WT) extracts for bio-activities:

6.4.1. Effects on cell viability:

The in-vitro cytotoxic effects of *Wrightia tinctoria* extracts comprising of (WTEA), (WTEB), (WTEC), (WTED) were assessed on hepatoma cells at doses between 1.0 and 300 $\mu\text{g/mL}$ by MTT assay after 24 hours of incubation. The extracts at a concentration of up to 300 $\mu\text{g/mL}$ for 24 hour did not show any significant decrease in cell viability of HepG2 cells with a cell viability index of $\geq 95\%$ at highest doses thus proving its non-cytotoxicity (Figure 2).

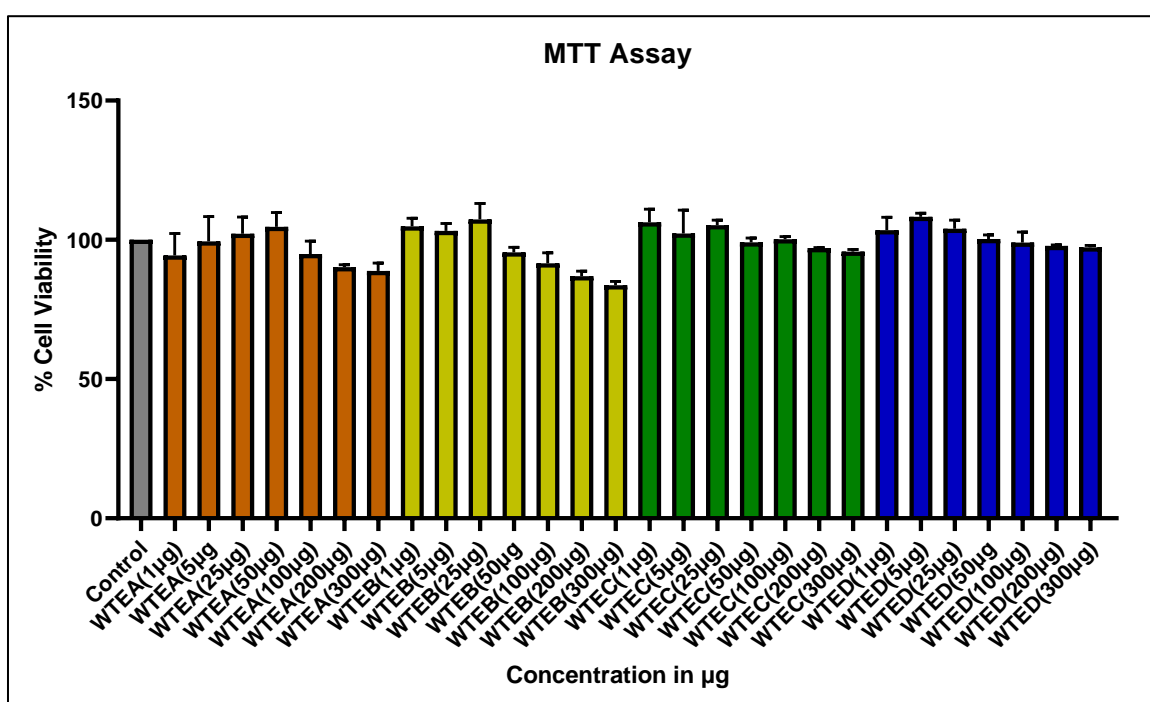


Figure 2: Determination of cytotoxicity of different WT extracts on HepG2 (hepatoma) cells after 24 hours.

For in vitro experiments to generate lipotoxic stress by lipid overload, Palmitic acid at a concentration of 400 μM was used. In the presence of saturated fatty acid stress the effect of this extracts on hepatoma cells were evaluated by pretreating the extract for 6 hours followed by incubation with or without palmitate for 24 hours. With 0.4 mM PA treatment a 20-25% decrease in overall cell viability was seen which was rescued by WTEC and WTED treatments (Cell viability $\geq 90\%$) whereas WTEA and WTEB showed viability loss likewise that of palmitic acid treated cells (Cell viability index around 80%). WTEB in 50 $\mu\text{g/mL}$ and 100 $\mu\text{g/mL}$ concentration showed a marked decrease in viability (Viability index at 70%) suggesting a toxicity at $\geq 50\mu\text{g/mL}$ concentration for

100% ethanolic extracts. So a cyto-protective effect of 50:50 hydro-ethanolic extract (WTEC) and aqueous extract (WTED) of wrightia seedpod was noted employing the viability assay by means of measuring mitochondrial dehydrogenases in hepatoma cells in a lipid stressed environment (**Figure 3**).

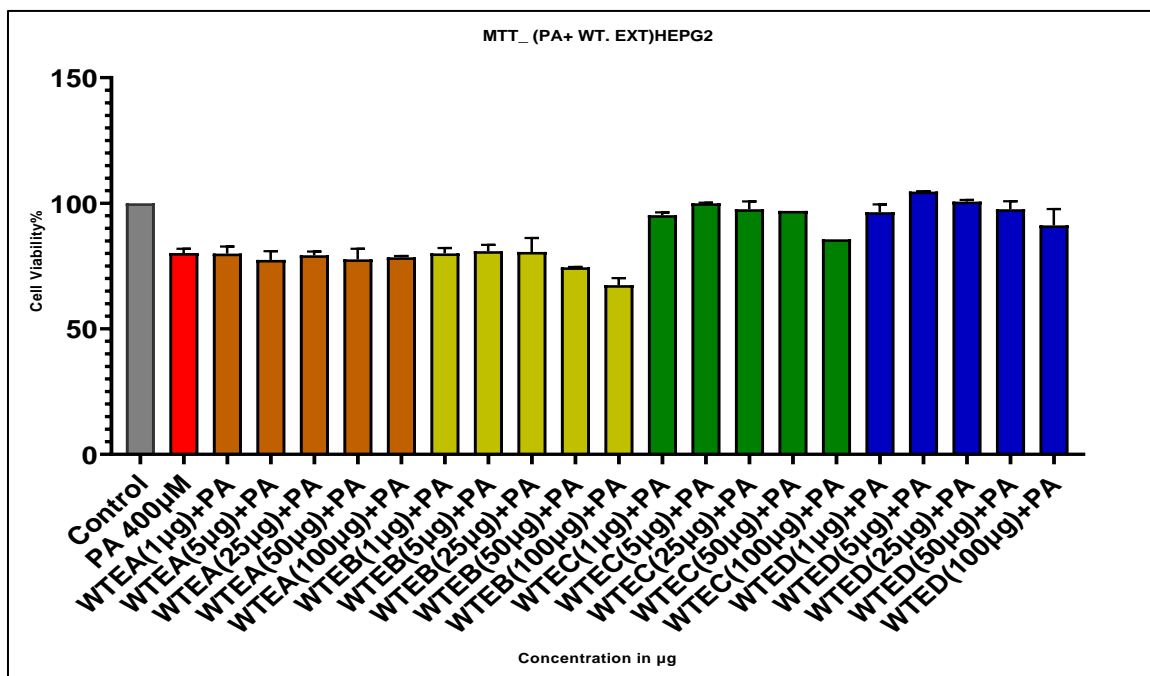


Figure 3: Effect on cytotoxicity while co-incubation with palmitic acid (400µM) for 24 hours after pretreatment with four WT extracts.

6.4.2. Anti-oxidant properties of WT extracts:

The ability to scavenge free radicals were evaluated using 2,2-diphenyl-1-picrylhydrazyl (DPPH) assay. WTEA (hexane extract) showed 20% scavenging activity at 0.8 µg/ml whereas the highest dose of 100 µg/ml showed 28% inhibition. 100% ethanolic extract (WTEB) inhibited approximate 18% -34% radical scavenging effect at same concentration range of 0.8-100 µg/ml. Both WTEA and WTEB showed weak radical scavenging effect whereas WTEC was very effective in quenching the radicals with 68% inhibition at 100 µg/ml. WTED showed little less inhibitory activity at the highest concentration of 100 µg/ml proving significant antioxidant properties of WTEC and WTED as evidenced by the effective scavenging of DPPH radicals (Figure 4A). Ascorbic acid was used as the positive control which produced 80% scavenging effect at dose of 25µM. These results indicate the ability of the hydro-ethanolic extract and aqueous extracts potential to protect the liver cells from oxidative damage, which might be correlated to their radical scavenging effect.

6.4.3. Effects on Hepatic Oxidative Stress:

Hepatic oxidative stress marks as a major contributor to NAFLD, so the attenuating effect of total cellular ROS levels was checked by DCFDA fluorescent dye (Figure 1c). The mean fluorescent intensity of the treatments was correlated with the generation of reactive oxygen species. Palmitic acid in HepG2 cells conferred an oxidative stress increasing the fluorescence intensity of CM-H2DCFDA by approximately 2 fold whereas after pretreatment with extract for 6 hours WTEA at 1, 5, 25 $\mu\text{g/ml}$ concentration lowered the ROS production by 28%, 38%, and 47% respectively. WTEB on the other hand reduced this stress by 12%, 34%, and 38% by 1, 5, 25 $\mu\text{g/ml}$ concentration respectively. WTEC pre incubation for 6 hours followed by stimulation with PA showed the most significant effect with 1, 5, and 25 $\mu\text{g/ml}$ of extract inhibited the ROS production by 38%, 53% and 64% respectively. WTED effect was at per hydro-ethanolic formulation showing 53% inhibition of fluorescence intensity at 25 $\mu\text{g/ml}$ dose (**Figure 4B**).

While macrophage cells are one of the main immune effectors of inflammation and related oxidative surge in biological systems we employed the RAW264.7-LPS model of inflammation to validate the anti-oxidative capacity of our extracts. At 25 $\mu\text{g/ml}$ dose WTEA inhibited 50% of ROS production whereas WTEB exerted a 65% inhibitory effect. Interestingly WTEC at 25 $\mu\text{g/ml}$ and 50 $\mu\text{g/ml}$ showed 84% and 95% inhibition of ROS production by LPS while WTED also showed similar effects (**Figure 4C**).

6.4.4. Evaluation of different WT extracts on inhibition of lipid accumulation:

Hepatic lipid accumulation is the main etiological factor on development of lipotoxicity and associated metabolic Disorders like NAFLD, NASH. A significant increase in the lipid droplets was observed after stimulating the hepatoma cells with 400 μM PA for 18 hours but when co-incubated with extracts after pretreatment for 6 hours a significant reduction in lipid droplet formation was observed as measured by BODIPY fluorescent dye which specifically binds neutral fat in cells. Flow cytometric analysis of lipid droplets showed that 50:50 Ethanol: water extract (WTEC) showed the highest lipid-lowering activity of 30% and 45% at concentrations of 5, 25 $\mu\text{g/ml}$ respectively followed by 24% and 34% reducing effect by WTED. WTEA showed lesser activity in prevention of formation of lipid aggregates as 5 $\mu\text{g/ml}$ and 25 $\mu\text{g/ml}$ of extract inhibited 12% and 30% when compared with palmitic acid treated cells. WTEB at 5 $\mu\text{g/ml}$ showed 26% relative reduction but at higher concentrations no such effects were seen. So as measured by the fluorescence intensity of stained neutral lipid, the hydro-ethanolic extract prevented the most hepatic fat accumulation followed by aqueous and hexane extracts (**Figure 5A**).

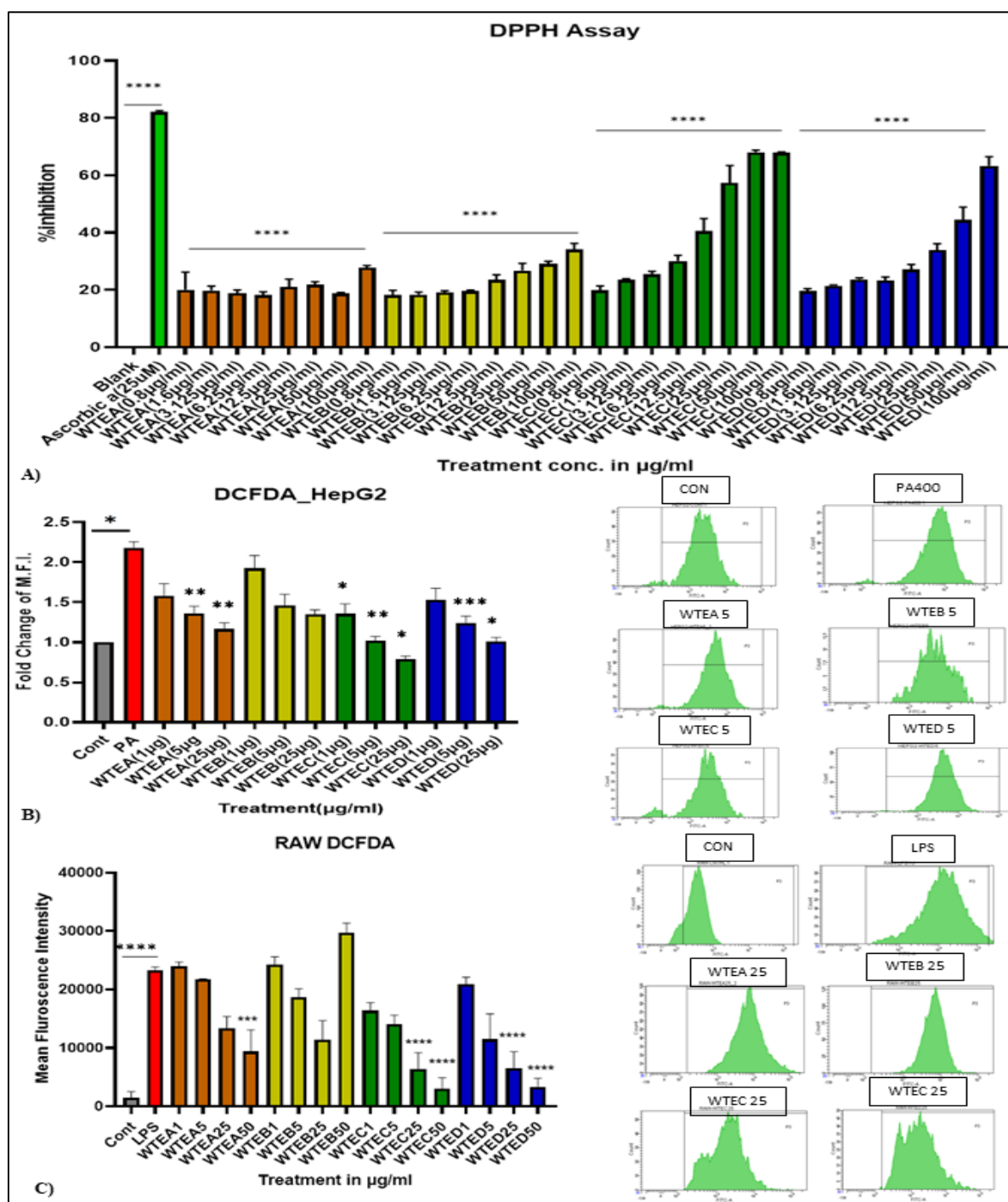


Figure 4: Screening of different Wrightia extracts on basis of antioxidant capacity and inhibition of cellular oxidative stress : A) Evaluation of antioxidant activity of different concentrations (0.8µg/ml to 100µg/ml) of WT extracts by DPPH radical scavenging assay B) Estimation of total cellular ROS by DCFHDA reagent by flow cytometry employing 1µg/ml to 25 µg/ml of four WT extracts using palmitic acid for lipotoxic stress in HepG2 cells C) Determination of ROS inhibition by WT extracts on RAW264.7 cells after LPS stimulation by flow cytometry using DCFHDA. Respective histograms on right side(selected conc.).Data represented as Mean±S.E.M. ****P<0.0001, *** P<0.001, ** P<0.01, * P<0.05, ns= non-significant

6.4.5. Evaluation of WT extracts on inhibition of NO₂ production in mouse macrophage cells:

Increased nitric oxide(NO) levels and its stable intracellular intermediate like nitrite(NO₂⁻), nitrate(NO₃⁻), and peroxynitrite (ONOO⁻) as a pro-inflammatory mediator marks as an important function in hepatic disease progression, So the effect of various extracts on attenuating the production of the NO level(measured by nitrite production) was measured in RAW264.7 cells upon inducing LPS (100ng/ml) stimulation.

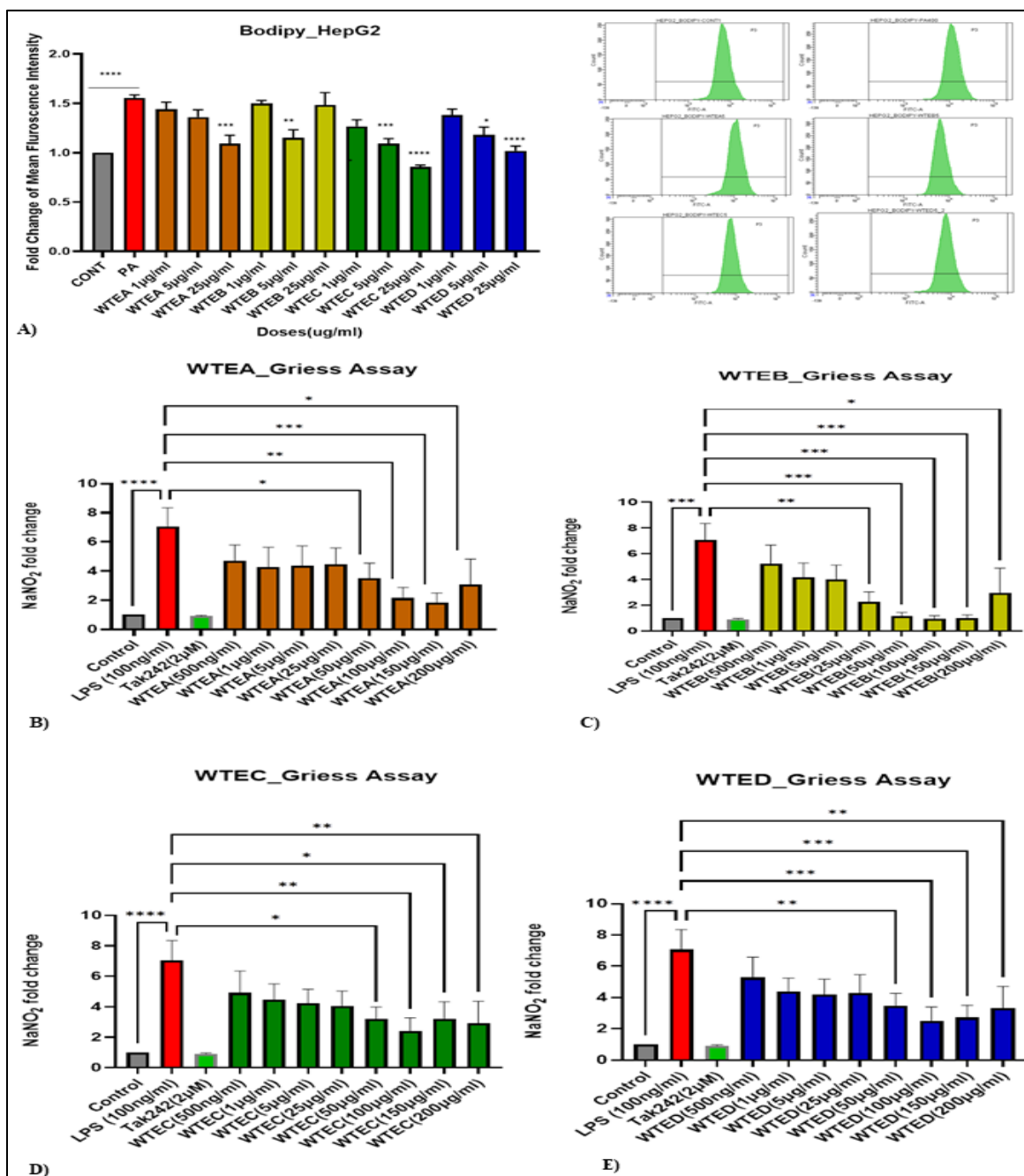


Figure 5: Evaluation of WT extract on intracellular lipid accumulation and nitric oxide (RNS)

production: A) Effect of four WT seed pod extracts on inhibition of lipid accumulation by PA mediated fatty acid stress on HepG2 cells tagging neutral lipid droplets with BODIPY fluorescent reagent measured by flow cytometry (Histogram for 5 µg/ml doses) B) Effect on nitric acid production inhibition by Griess assay performed on LPS treated RAW264.7 macrophage cells after pretreating with extracts for 6 hours. Data represented as Mean±S.E.M. ****P<0.0001, *** P<0.001, ** P<0.01, * P<0.05, ns= non-significant

NaNO₂ was used as a standard and TAK242 (2 µM), a TLR4 inhibitor was used as a positive control. LPS treatment increased NO production by approx. 7 fold of untreated control cells whereas WTEA pretreatment reduced the production by 50% at a concentration of 50 µg/ml whereas at a concentration of 150 µg/ml, it showed approx. 74% reduction. WTEB ethanolic extract manifested a good effect in lower concentrations till 25 µg/ml (68% reduction relative to LPS group) by gradually decreasing NO formation with respect to increasing concentration but at 50 µg/ml significant cell death happened after LPS induction which resulted in an erroneous lower signal of NO formation by griess reagent. WTEC and WTED both showed similar effects while inhibiting 30-35% at 1 µg/ml toward a gradually increased 65% at 100 µg/ml doses. At higher doses, a slight reduction in affectivity was observed for both WTEC and WTED. TAK242 (2µM) inhibited the LPS effect by almost 87% in RAW264.7 macrophage cells (**Figure 5B, 5C, 5D, 5E**).

6.4.6. The effect of WT extracts on glucose uptake using 2-NBDG in HepG2 cells:

Chronic high saturated fat exposure puts the hepatic cells at the risk of lipotoxicity and subsequent inflammatory pathogenic manifestations like type 2 diabetes and fatty liver. Insulin resistance followed by lowered glucose uptake potential is another major risk factor in developing NAFLD. The effects of *Wrightia* extracts on glucose uptake by hepatoma cells were evaluated by co-incubating with palmitic acid to induce insulin resistance and employing a fluorescent glucose analog, 2-NBDG. Palmitate treatment for 24 hours resulted in a 50% decrease in glucose uptake compared to control cells. WTEA treatment showed a consecutive increase (15 to 42% increases in 1-50 µg/ml doses) in glucose uptake percentage with respect to the PA group with increasing doses. WTEC pretreatment at 1 µg/ml increased uptake by 52% whereas 5 µg/ml doses rescued the palmitate effect by 92% showing glucose uptake as much as untreated control. 25 and 50 µg/ml doses of the hydro-ethanolic extract also showed a good response (63% and 43% rescue) but lower than previous doses. WTED treatment effect saturated with the highest decrease of 58% at both 5 and 25 µg/ml and then decreased to 33% increase compared to the PA group in the highest dose of 50 µg/ml. So these comparative screening study showed the best positive effect by WTEC around 1 to 5 µg/ml of treatment doses in HepG2 cells (**Figure 6**).²²

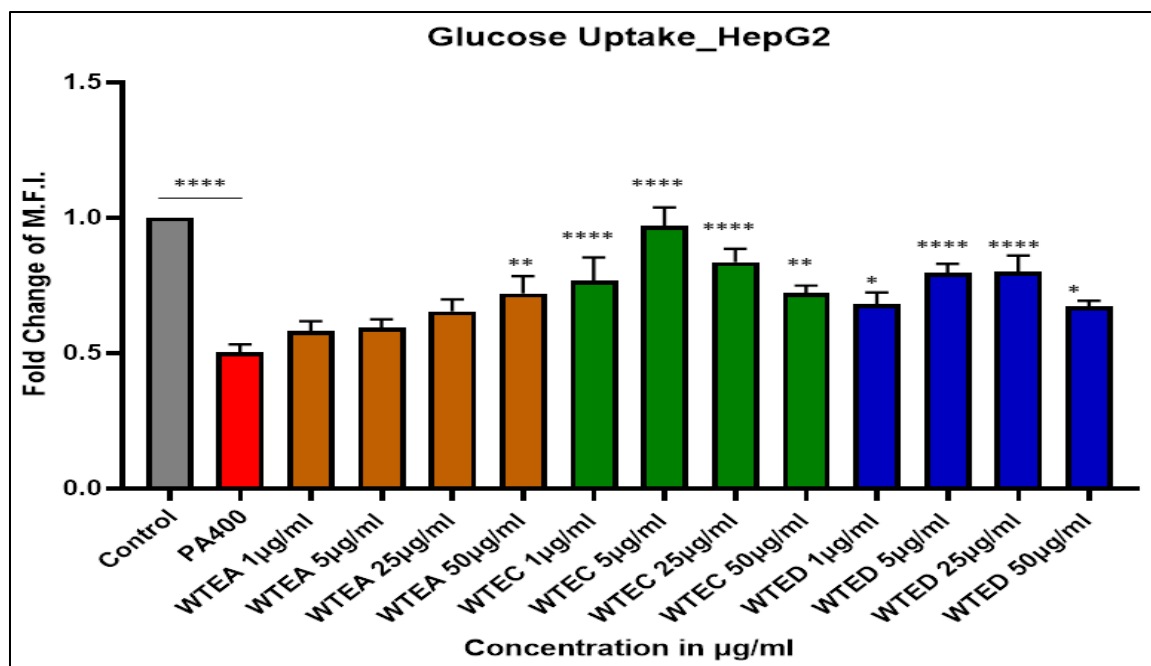


Figure 6: Screening of WT extracts on basis of glucose uptake: Evaluation of different concentrations of WTEA, WTEC, and WTED on rescue of reduced glucose uptake affected by saturated fatty acid stress measured by fluorescent spectrometry employing 2-NBDG dye(a glucose analog) Data represented as Mean±S.E.M. ****P<0.0001, *** P<0.001, ** P<0.01, * P<0.05, ns= non-significant

Acute oral toxicity study:

6.4.7. Acute oral toxicity test details:

50% aqueous ethanolic extract was prepared according to the previously described process. Dried extracts were powdered and dissolved in water and orally given at a dose of 3 gram/kg body weight. C57BL6J male mice (n=3/group) were maintained in animal facility of IICB, Kolkata with 12 hour dark/12 hour light cycle and normal chow diet was given as food before oral gavage of wrightia extracts. The mice were 8-10 weeks of age weighing 22-25 grams were acclimatized for 7 days before starting the toxicity study: prior to oral gavage mice were starved for 6 hrs and fed with extracts (3500mg /kg bodyweight and given gavage in a volume of 1ml/100gram bodyweight) for treatment group and water for control group using a proper intubation cannula. After 2 hours of treatment food was given and any sign of immediate toxicity or change in fur, eyes, or behavioural pattern were observed for 3-4 hours and thereafter daily for the next 14 days. Post intubation weight were taken weekly and on day 15 all animals were euthanized and internal organs were grossly observed , liver spleen and kidney were washed in PBS and fixed in 10% formalin for minimum 24 hours and thereafter processed for histopathological sectioning for Hematoxylin & Eosin staining. Blood was collected by retro orbital method for hematological testing in EDTA vial, and serum was isolated for any biochemical testing. Throughout the experiment, animals were constantly monitored for mortality, and behavioral or physical appearance changes to rule out any chances of manifestation of toxicity. (Jain et al., 2011)

6.4.8. General sign and behavioral analysis:

Oral administration of WTEC (50% hydro-ethanolic extract) didn't cause any immediate toxic effect as evidenced by the absence of any abrupt behavioural changes nor any changes in skin fur, movement or tremor, salivation. After an observation period of 14 days no treatment-related mortality was neither seen nor any abrupt significant difference in body weight with respect to control group was recorded after extract treatment. No lesions or physical abnormalities were found upon gross macroscopic observational analysis of the internal organs after sacrificing the animals on day15.

6.4.9. Hematology parameters:

After the collection of blood by retro-orbital method blood hematological parameters were checked in the control and treatment group.

Parameters	CONTROL	TREATED
RBC (x10⁶/ μl)	9.31 \pm 0.646	8.846 \pm 1.363346
HGB (g/dl)	14.95 \pm 0.894	13.166 \pm 1.901
WBC (x10³/ μl)	6.925 \pm 0.297	6.453 \pm 0.663
NEU (%)	6.3 \pm 1.270	8.066 \pm 1.940
LYMPH (%)	91.6 \pm 1.789	90.366 \pm 2.218
MONO (%)	0.45 \pm 0.202	0.433 \pm 0.384
BASO (%)	1.15 \pm 0.375	0.866 \pm 0.352
PLT (x10³/ μl)	996.5 \pm 66.106	857 \pm 368.557
MPV(μm³)	6.65 \pm 0.259	6.4 \pm 0.326
HCT (%)	55.75 \pm 6.783	47.966 \pm 8.950
MCV (μm³)	59.2 \pm 3.117	54.1 \pm 4.235
MCH (pg)	16.15 \pm 0.144	14.966 \pm 0.296

Biochemical parameters were assayed for liver enzymes and protein as well as renal function was evaluated. Apart from a mild increase in AST level in the treatment group, no such significant alteration was observed with respect to control animals

Parameters	Control	Treated
AST (U/L)	106.1 \pm 8.6	127.6333 \pm 25.56
ALT (U/L)	77.6 \pm 4.3	70.433 \pm 4.25
ALP (U/L)	66.8 \pm 1.3	62.333 \pm 5.49
BILLIRUBIN (Total)(mg/dl)	0.4 \pm 0.01	0.36 \pm 0.03
Protein (g/dl)	5.865 \pm 0.08	6.033 \pm 0.14
Albumin (g/dl)	3.49 \pm 0.01	3.4 \pm 0.12
Globulin (mg/dl)	2.375 \pm 0.06	2.633 \pm 0.19
Urea (mg/dl)	42.7 \pm 6.63	38.266 \pm 3.16
Creatinine (mg/dl)	0.645 \pm 0.02	0.496 \pm 0.052

6.4.10. Liver tissue toxicity:

Overall gross physical evaluation of the organ didn't show any abnormalities like liver enlargement, patches, or discoloration of any sort. After paraffinization approx. 5µM sections were cut and hematoxylin & eosin stain was done for observation of the histology of the organ. Microscopic observations showed no abnormal tissue architecture compared with control group. Proper arrangement of hepatocytes and sinusoids were seen without any neutrophilic intrusion or hemorrhagic zone. Any such necrotic region were not found upon comparison with normal tissue organization.

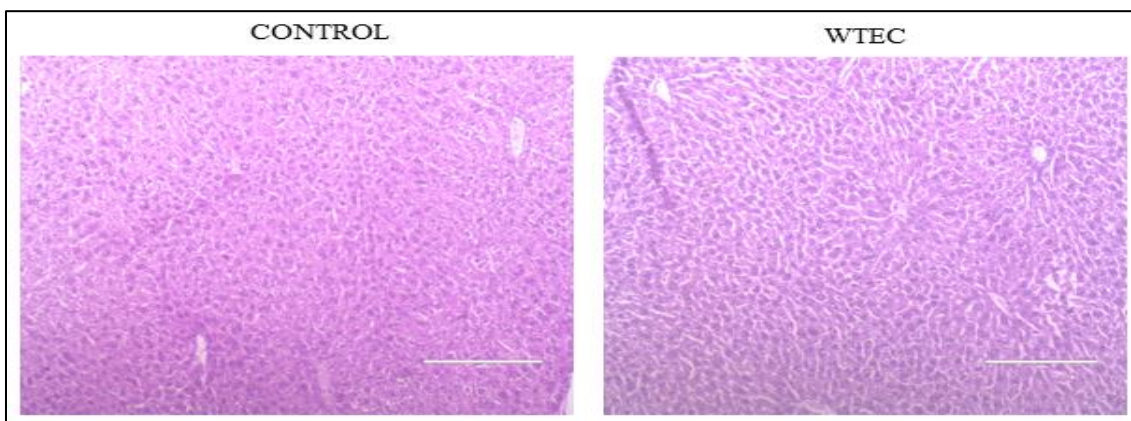


Figure7: Hematoxyline & eosin staining of liver tissue samples of control mice and WTEC (3500 mg/kg) fed mice for acute toxicity testing.

6.4.11. Kidney tissue toxicity:

Both kidneys on average showed no abnormalities on gross outside physical structure. Upon deeper microscopic evaluation of histological sections no such pathological deformities was found in the extract fed group. The proximal and distal tubules and

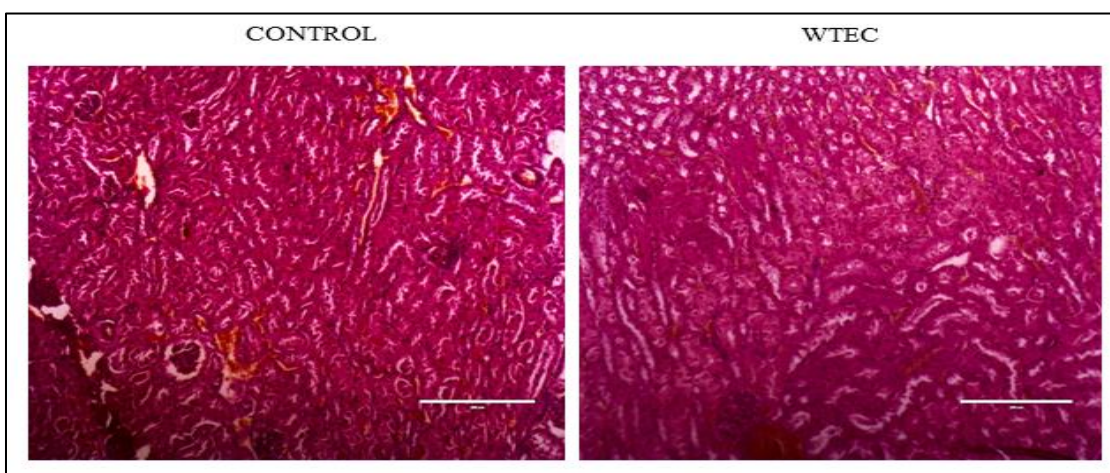


Figure8: Hematoxyline & eosin staining of kidney tissue samples of control mice and WTEC (3500 mg/kg) fed mice for acute toxicity testing.

glomerular corpuscles appeared normal architecture. No tubular anomalies, necrosis, or neutrophilic infiltration were seen. Nephron cells were seen with normal physiology without any degenerative zones in the treatment as well as control group.

6.4.12. Spleen tissue histology:

Spleen is the primary organ to clear any impurities in the blood caused by any inner or outside stress to biological system. Hematoxyline and Eosin staining of mice spleen tissue of Extract treated as well as control group didn't show any significant alterations other than some neutrophilic infiltrations in tissue architecture and proper organization of the white and red pulp zones were seen with well-defined lymphoid follicles.

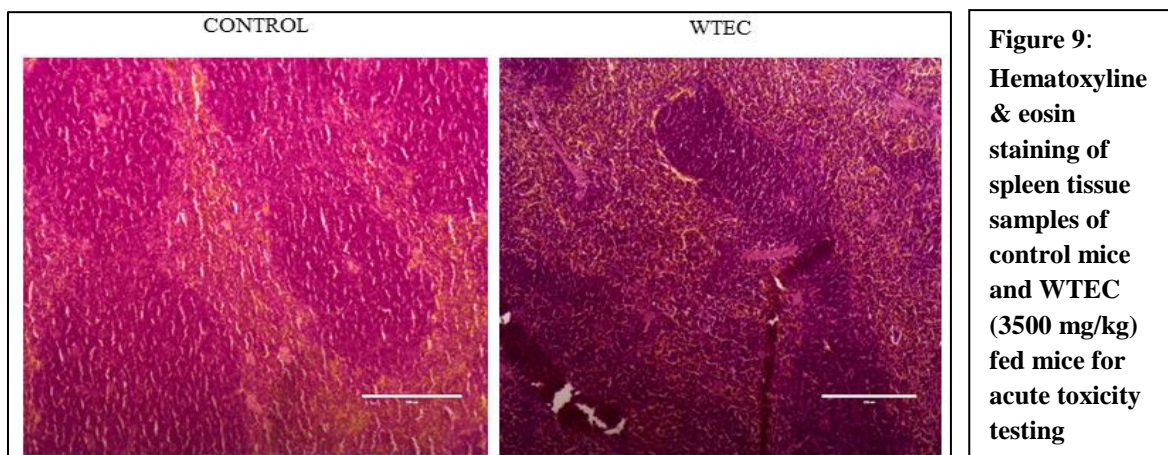


Figure 9:
Hematoxyline
& eosin
staining of
spleen tissue
samples of
control mice
and WTEC
(3500 mg/kg)
fed mice for
acute toxicity
testing

Discussion:

Wrightia tinctoria(WT) is long been used for its medicinal properties. Every part of this plant like leaf, bark, root, seed has biological activities. Seedpods of WT are well acknowledged for improving liver health in diseases like jaundice, and diabetes in traditional medicine. Here in this study we tried to screen different extracts of wrightia seeds and check for their bio-activities in curing fatty acid stress induced liver diseases like NAFLD, NASH and associated metabolic perturbations. To get the maximum varieties of phyto-constituents from the seedpods of these plant different polarity solvents were used for maximum extraction. Enhanced oxidative and nitrosative stress generated by over accumulation of fats in liver works as the main pathogenic factors leading to fatty liver disease. So basic screening of extracts was done based on this parameters. While none of the extracts showed cytotoxicity towards Hepg2 hepatoma cells hydro-ethanolic extract (WTEC) and aqueous extract (WTED) showed cytoprotective effect when imparted with lipotoxic stress by palmitic acid (400 μ M). 100% ethanolic extract showed cytotoxicity at higher doses (≥ 50 μ g/ml) whereas hexane extract didn't show much protective effect. WTEC and WTED both showed commendable anti-oxidant activity by scavenging 70% DPPH radicals at a conc of 100 μ /ml whereas WTEA and WTEB also showed mediocre effect by 30% inhibition at the highest concentrations. Significant

attenuation of cellular ROS in hepatoma and macrophage cells were also achieved by WTEC followed by WTED and WTEA. WTEB on the other hand increased the ROS generation at higher concentrations (50 µg/ml) may be due to its cytotoxicity at these concentrations. Inhibition of neutral fat aggregation in response to saturated fatty acid stress was also another interesting attribute of *Wrightia* seedpod extracts where WTEC showed the maximum effect of 45% inhibition by 25 µg/ml dose. Retardation of nitric oxide generation by LPS in macrophage cells also supported a dose-dependent positive effect by WTEC WTEA and WTED while maintaining the viability of the treated cells. Based on this preliminary assays WTEA, WTEC and WTED was selected for further screening and 100% ethanolic extract was scraped for its cytotoxicity and oxidative stress enhancement activities. A dose range of 1 µg/ml to 50 µg/ml was selected on the basis of the linearity of effects for further assays which was evaluating the effect on glucose uptake by HEPG₂ cells after lipid overload. Insulin resistance is a major risk factor associated with fatty liver and decreased glucose uptake instigates the pathogenesis of the disease. Among three tested WTEC in treatment dose of 1 µg/ml and 5 µg/ml doses showed excellent rescue (up to 90%) in decreased uptake exerted by palmitic acid treatment. So based on these preliminary screening experiments it was very obvious that the hydro-ethanolic extract (WTEC) of *Wrightia tinctoria* seedpod showed the most potent activity and for this reason it was selected for further exploration of in-vivo toxicity studies and detailed therapeutic activities related to fatty liver diseases unraveling the mechanism of action in search of a new lead for treatment of metabolic diseases like obesity, NAFLD and Type 2 Diabetes.

The typical aim of the toxicity study relies on the identification of the LD₅₀ dose of an extract. LD₅₀ is calculated by measuring the amount of extract treatment causing 50% mortality in the experimental animals. In our experiment, a dose of 3500 mg/kg body weight of mice didn't yield any mortality or any sort of major toxicity making it to be classified as Class 5 (LD₅₀ > 2000 mg/kg body weight) group of a compound according to the classification of the acute systemic toxicity doses of the compound set by OECD. This is the lowest toxicity group which makes hydro-ethanolic extract of *Wrightia tinctoria* safe to consume without any significant adversity. Apart from mortality any immediate physical or behavioral changes (like hyper or hypo activity) often helps to predict the acute toxicity of any compound. Besides hematological parameters, liver enzyme expression also gets altered as a means of defense against genotoxic compounds. Continuous observation for 14 days after administration of extract no such adverse effect was noted, tissue histology and blood parameters results also certified the efficacy and non-toxicity of this extract without developing any significant adverse side effect thus establishing its potency of being a therapeutic lead safe for human consumption.

Chapter 2

**Role of *Wrightia tinctoria* seed hydro-ethanolic extract
in ameliorating mitochondrial dysfunction and
associated disorders in *in vitro* and *in vivo* model of
NAFLD**

7.1. Introduction:

NAFLD is a metabolic disease affecting 20-40% of global population(Rinella et al 2015). It is an umbrella phrase covering a plethora of pathological condition accompanying hepatic fat accumulation without major alcohol intake. To elucidate its involvement in perturbing metabolic function of cell often a new term, “Metabolic dysfunction associated fatty liver syndrome” (MAFLD) has been proposed (Eslam et al 2020, Mendez-Sanchez et al 2022). Multiple researches have pinpointed the association of physiological, morphological, biochemical perturbation of mitochondria in pathogenesis of NAFLD. There are currently no FDA recommended specific drug available for NAFLD/Nonalcoholic steatohepatitis(NASH). Absence of particular biomarker and overlapping general symptoms with lack of professional expertise in detection and diagnosis is a major hurdle in treating this metabolic syndrome. So search for therapeutic leads which eliminate the underlying mechanism like mitochondrial dysfunction seems like a lucrative treatment option. In our study we have taken cue from traditional medicine and wanted to explore the role of *Wrightia tinctoria* seedpod extracts in mitigating the mitochondrial abnormalities in fatty liver unravelling a probable mode of action.

Deregulated lipid metabolism in obese population often leads to abnormal fat accumulation in hepatic cells. Insulin resistance, increased *de novo* lipogenesis, impaired fatty acid oxidation and increment of fatty acid uptake create a oxidative environment leading to disorientation of mitochondrial physiology. Mitochondrial respiration is often deteriorated in course of disease progression accompanied by modulation of mitochondrial respiratory chain (MRC) enzyme activities. Mitochondria reshuffle its internal contents by means of fusing two mitochondria to form a longer fibril like structure. On the other hand various physiological stresses generate fragmentation of mitochondria mainly by Dynamin related protein 1 (DRP1). A healthy balance of this fusion and fission is crucial for maintaining mitochondrial homeostasis. Metabolic disease like NAFLD often disrupts this balance. Mitochondrial has its own genome inside cell which can synthesis important mitochondrial proteins of oxidative phosphorylation for efficient ATP generation. In response to any distress or energy deficiency mitochondrial biogenesis pathway is one of the main factors to be up regulated to meet the increased ATP need. Mitophagy is another important protective pathway for specific clearance of severely damaged mitochondria and thus restrict generation of ROS.

Here in this part of our study we will concentrate on deciphering the potential of wrightia hydro-ethanolic extract (WTEC) on amelioration of mitochondrial dysfunction (MD). We will encompass various aspects of MD including altered morphological features, deregulated mitochondrial dynamics, mitochondrial bio-energetic maintenance and mitophagy –autophagy process to get a picture of this extracts mechanism of action.

7.2. Results:

7.2.1. Wrightia hydro-ethanolic extract (WTEC) abrogates PA-mediated reduction in mitochondrial membrane potential:

Lipotoxic overload in hepatic cells results in disruption of mitochondrial membrane integrity and subsequently develops alteration in membrane potential generating an abrupt amount of superoxide followed by mitochondrial ROS increment. Increased oxidative burden compromises cellular health often manifested by different pathologic conditions like fatty liver, liver cirrhosis, etc. Changes in membrane potential can be detected employing JC 1 dye which changes in fluorescence emission upon changes in membrane potential. Normally JC1 resides in aggregated form and emits red fluorescence but after membrane disruption, it shifts to monomeric form emitting green fluorescence. So the ratio of population emitting RED/GREEN fluorescence often serves as a measure to assess the mitochondrial health pinpointing the mitochondrial membrane potential (MMP).

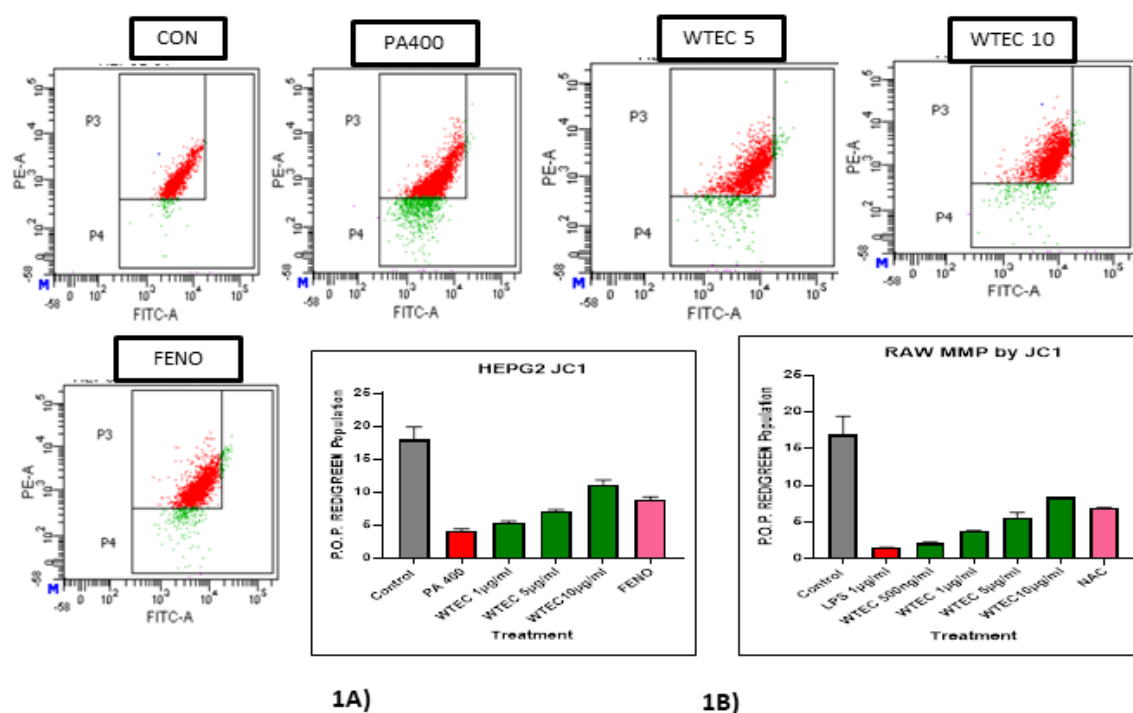


Figure 1: Wrightia hydro-ethanolic extract improves PA induced disruption of mitochondrial membrane potential: HepG2 and RAW264.7 cells were treated with WTEC for 6 hours prior to PA or LPS treatment for subsequent 24 hours and mitochondrial membrane potential was detected by JC1 staining (1A and 1B)(Red/Green ratio) Data are expressed (percent of parent population) as mean \pm SEM and significance was calculated w.r.t. PA group, using one way ANOVA **** $P < 0.0001$, *** $P < 0.001$, ** $P < 0.01$, * $P < 0.05$, ns= non-significant

We used LPS-induced macrophages and palmitic acid stimulated hepatoma cell model to evaluate the protective effect of wrightia hydro-ethanolic extract (WTEC) in mitigating the alteration of membrane potential. A range of concentrations of extracts (from 500 ng/ml to 10µg/ml) were preincubated for 6 hours and then stimulation was given. In RAW264.7 macrophage cells, 85-90% reduction of membrane potential compared to control after stress induction for 24 hours was abrogated dose-dependently by extracts. The lowest dose failed to show a significant effect with 4% rescue in MMP compared to the LPS group whereas, at 10µg/ml, it showed 55% rescue in reduction which was almost the same (59%) as shown by positive control NAC (N-acetylcysteine) (Figure 1B). PA treatment to HepG2 cells generated 4.8-fold reductions in MMP whereas by a dose of 10µg/ml, it was rescued by almost 62%. Fenofibrate was used as a drug control which showed a response of almost 60% reduction to altered membrane potential comparable to our extract (WTEC) (Figure 1A).

7.2.2. Wrightia hydro-ethanolic extract (WTEC) rescues altered mitochondrial respiration and glycolytic flux in palmitic acid-induced HepG2 cells:

Reduced mitochondrial membrane potential with altered membrane integrity was also reflected in mitochondrial bioenergetics parameters of fatty acid-overloaded hepatocytes by palmitic acid treatment under lipo-toxic conditions. Impaired mitochondrial basal and maximal respiration parameters with saturated fatty acid treatment were partially rescued when the cells were co-incubated with different doses of WTEC extract for 24 hours. Disrupted mitochondrial functioning due to lipid overload also resulted in reduction of ATP production and trans-membrane proton leakage. PA treatment caused a 50% reduction in maximal respiration rate which was reversed by almost 82% at 5 µg/ml dose of WTEC. In basal conditions also same trend was seen as PA treatment caused 45% reduction in basal respiration and subsequent dose-dependent increase of stress retrieval by 72-102% in dose regimen of 1-10 µg/ml (WTEC). As the mitochondrial bioenergetics efficiency was hampered by saturated fatty acid treatment the rate of ATP production and proton leak was also reduced by 45 to 50% which was subsequently rescued by WTEC treatment (92 and 100% respectively by WTEC 5 µg/ml) (Figure 2B-F). At the highest dose of 10 µg/ml mitochondrial respiratory parameters were comparable to untreated cells proving the efficacy of WTEC in improving mitochondrial oxidative phosphorylation and respiratory chain (MRC) parameters.

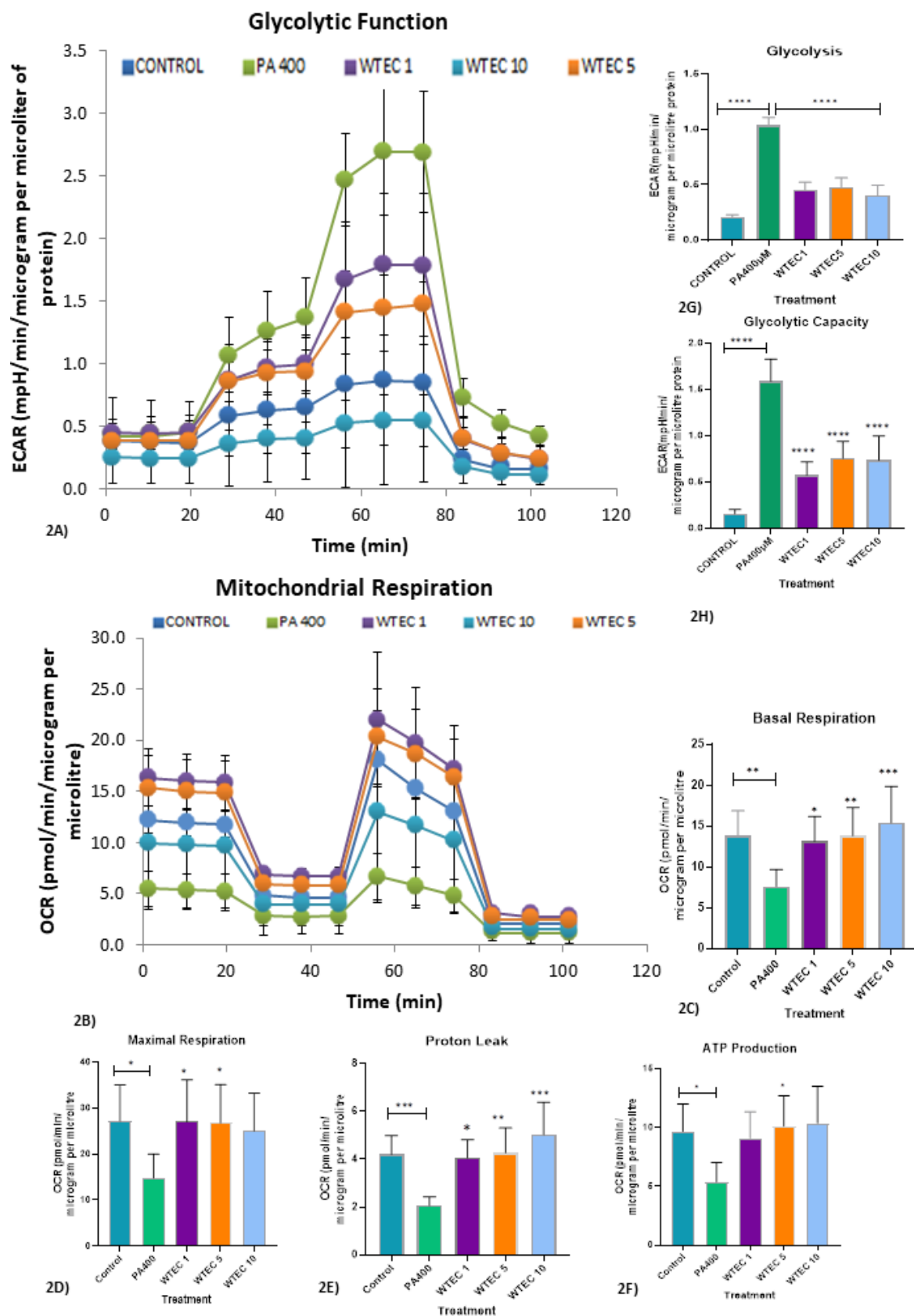


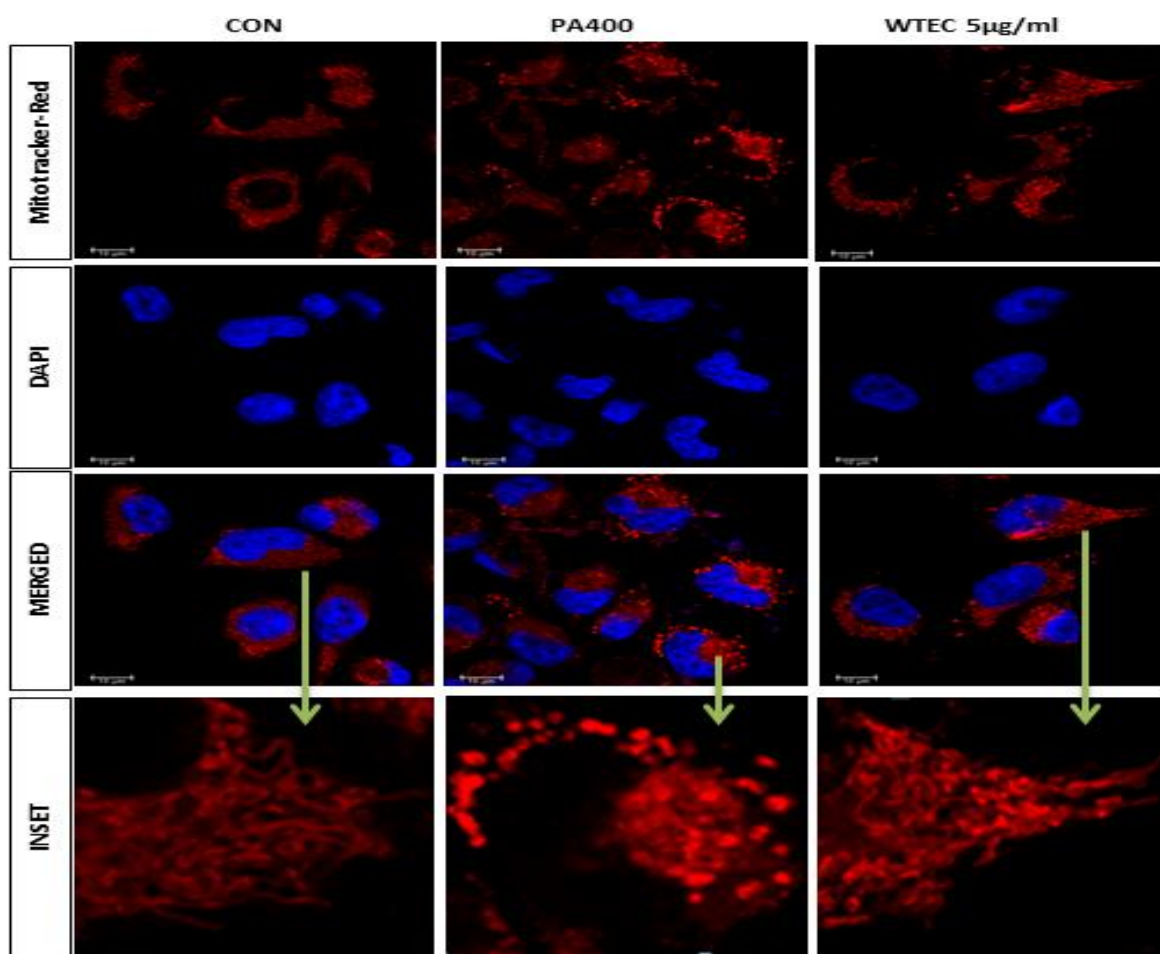
Figure 2: WTEC protects against PA mediated impairment of mitochondrial respiration and glycolysis in hepatocytes: HepG2 cells were treated with WTEC for six hour prior to PA treatment for subsequent 24 hours and assessed for different mitochondrial respiratory parameters(**2B**). Basal and maximal mitochondrial respiration, proton leak, levels of ATP production (**2 C-F**) was measured. Different parameters of glycolysis under stress conditions were analyzed (2A). Glycolysis rate (2G)and overall glycolytic capacity (2H) was calculated. Data are expressed as mean \pm SEM and significance was calculated w.r.t. PA group, using one way ANOVA **** $P < 0.0001$, *** $P < 0.001$, ** $P < 0.01$, * $P < 0.05$, ns= non-significant

The reduced ATP yield with disrupted MRC triggered an increase in glycolysis parameters as noticed by a surge in anaerobic glycolysis with an attempt to increase the production of acetyl co-A as measured by cellular acidification rate in the seahorse metabolic analyzer. Palmitic acid stress for 24 hours resulted in 5 fold increase in glycolysis rate while WTEC pre-incubation for 6 hours with co-incubation with SFA reduced 56% and 60% of increment at 1 and 10 $\mu\text{g/ml}$ doses. Abruptly Increased Glycolytic capacity (10 fold) with PA (400 was μM) was also brought down by about 50% providing a relief in cellular acidification and subsequent toxicity (Figure 2A, 2G , 2H)). Thus WTEC co-treatment helped in the recovery of damaged mitochondrial bioenergetics and simultaneously improved the exacerbated glycolytic conditions proving its potential in combating mitochondrial dysfunction followed by hepatic lipotoxicity.

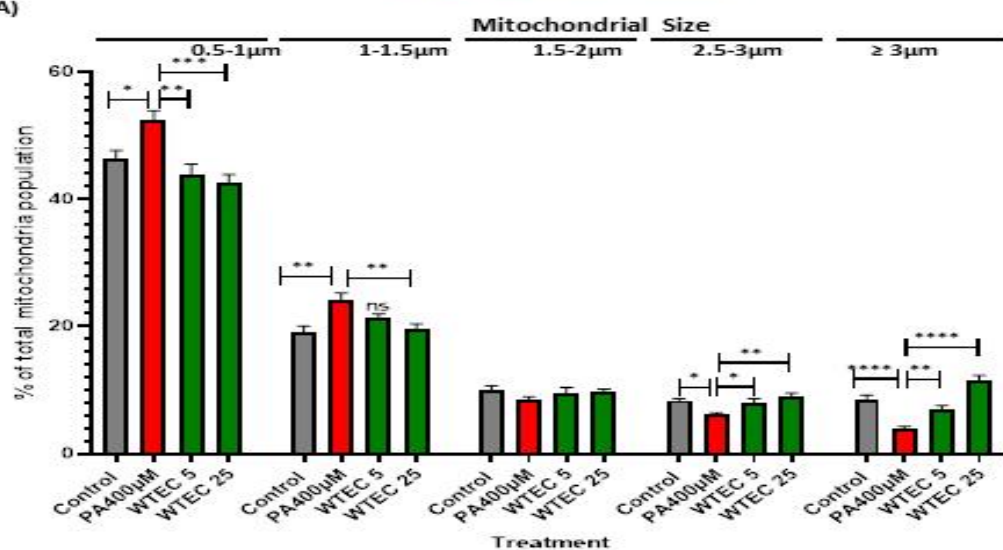
7.2.3. PA mediated Disruption of mitochondrial morphology was protected by wrightia hydro-ethanolic extract:

Saturated fatty acid treatment in hepatoma cells not only perturbs the mitochondrial energetics but also has a profound effect on overall structural integrity altering the mitochondrial morphology. Mitotracker red is a fluorescent cell-permeant dye that is used to label mitochondria in cultured cells after experimental treatments. In normal conditions, HepG2 cells are seen to have a fairly large network of fused mitochondrial structures with the presence of a smaller counterpart. PA treatment for 24 hours resulted in increased smaller, fragmented mitochondria with a probable increase of mitochondrial fission machinery upon lipotoxic stress as measured by LAS X Leica imaging software (Figure 3A). 0.5 μm -1 μm and 1-1.5 μm sized population of mitochondria was increased by 10-15% in the PA group which was abrogated in the WTEC 5 $\mu\text{g/ml}$ and 25 $\mu\text{g/ml}$ dose groups. WTEC showed almost the same or reduced percentage of fragmented/ smaller sized mitochondria as compared to untreated control group but when 2-3 μm or ≥ 3 μm population were analyzed a marked increase in longer fused mitochondrial population was seen in WTEC treated groups (Figure 3B). Atomic force microscopy technique was employed to get a perspective of the gross morphological and topographical features. WTEC 5 $\mu\text{g/ml}$ dose pre-incubation for 6 hours Palmitic acid treatment was given in HepG2 cells and after next 24 hours mitochondria were isolated from the cultured cells and processed for microscopy. As evident from pictographs, after

palmitate treatment mitochondria were swelled with uneven membrane topography. WTEC 5 treatment rescued this morphological transformation to some extent (Figure 3C).



3A)



3B)

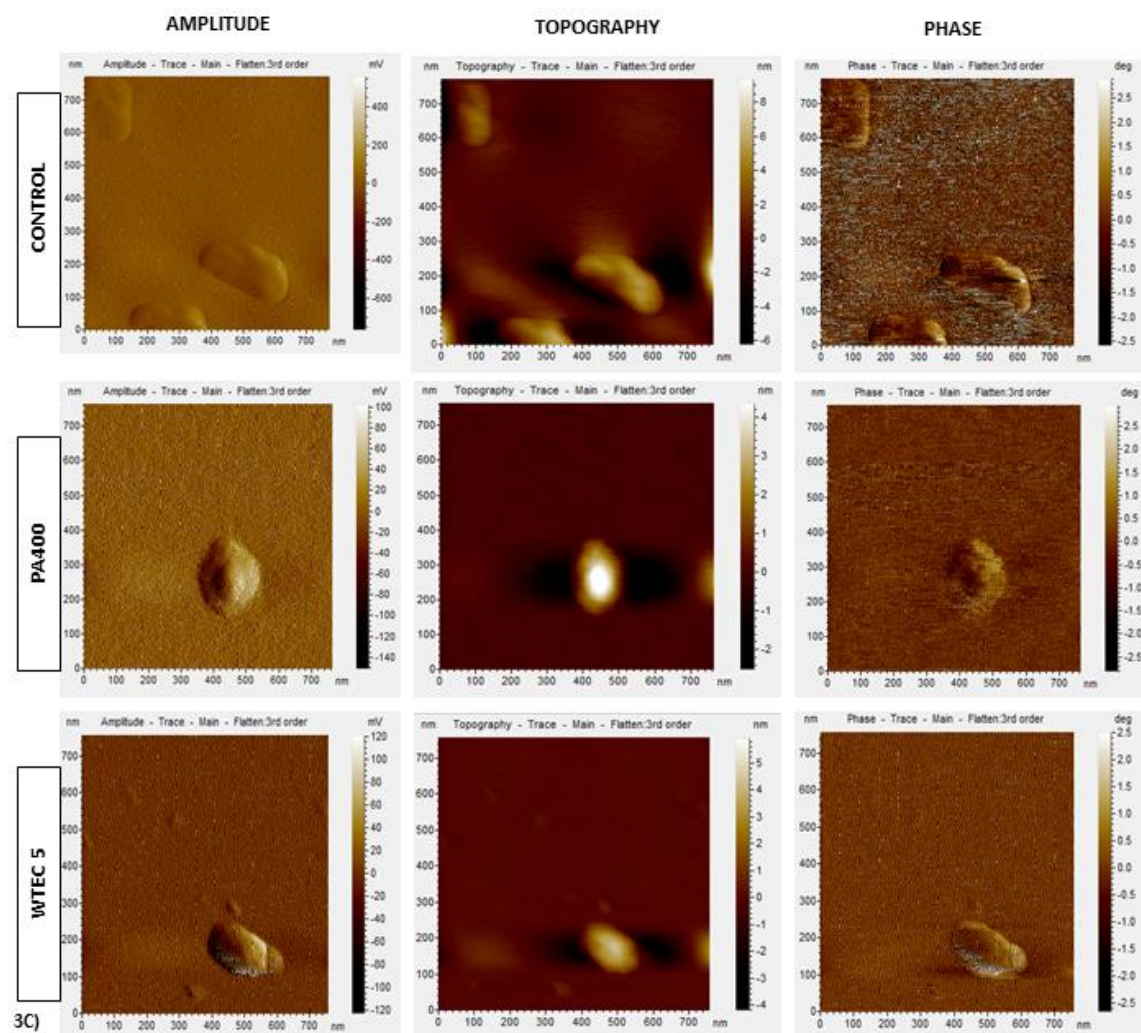


Figure 3: Effect of wrightia extract on mitochondrial morphology in hepatic lipotoxicity model: WTEC (dose 5 and 25 $\mu\text{g/ml}$) pre-treatment in PA stimulated HepG2 cells rescued mitochondrial fragmentation (3A). Reduction in smaller sized mitochondrial population compared to PA group was accompanied by increased longer mitochondria ($\geq 2\mu\text{m}$) quantified by LASX software(3B). Representative pictures of isolated mitochondria by Atomic Force Micrography in control , PA400 μM , and WTEC 5 $\mu\text{g/ml}$ dose group(13C) Data are expressed as mean \pm SEM and significance was calculated w.r.t. PA group, using one way ANOVA **** $P < 0.0001$, *** $P < 0.001$, ** $P < 0.01$, * $P < 0.05$, ns= non-significant

7.2.4. Effect of wrightia extracts on expression of mitochondrial OXPHOS complexes upon PA treatment:

Mitochondrial oxidative complexes are an integral part of MRC and contribute majorly to ATP generation and any abnormalities in the abundance or activity of these complexes result in reduced energy production as well as increase in mitochondrial superoxide and subsequent debilitating conditions. Expressions of mitochondrial complexes were checked upon PA-treated HepG2 cells after (6 hours) pre-treatment with WTEC and further stimulation for 24 hours. A cocktail of five MRC complexes was used to evaluate the effect by western blot experiment and fenofibrate was used as a drug control (Figure 4A). WTEC at a dose range of 1-10 $\mu\text{g/ml}$ doses dependently showed a positive trend in increase of complex II, III, and IV with no significant change in complex V expression (Figure 4B-F). This increase in the expression of major machinery complexes of the respiratory chain ultimately correlates to a surge in ATP production which gets majorly affected by palmitate treatment with lipid aggregation thus improving overall mitochondrial bio-energetics.

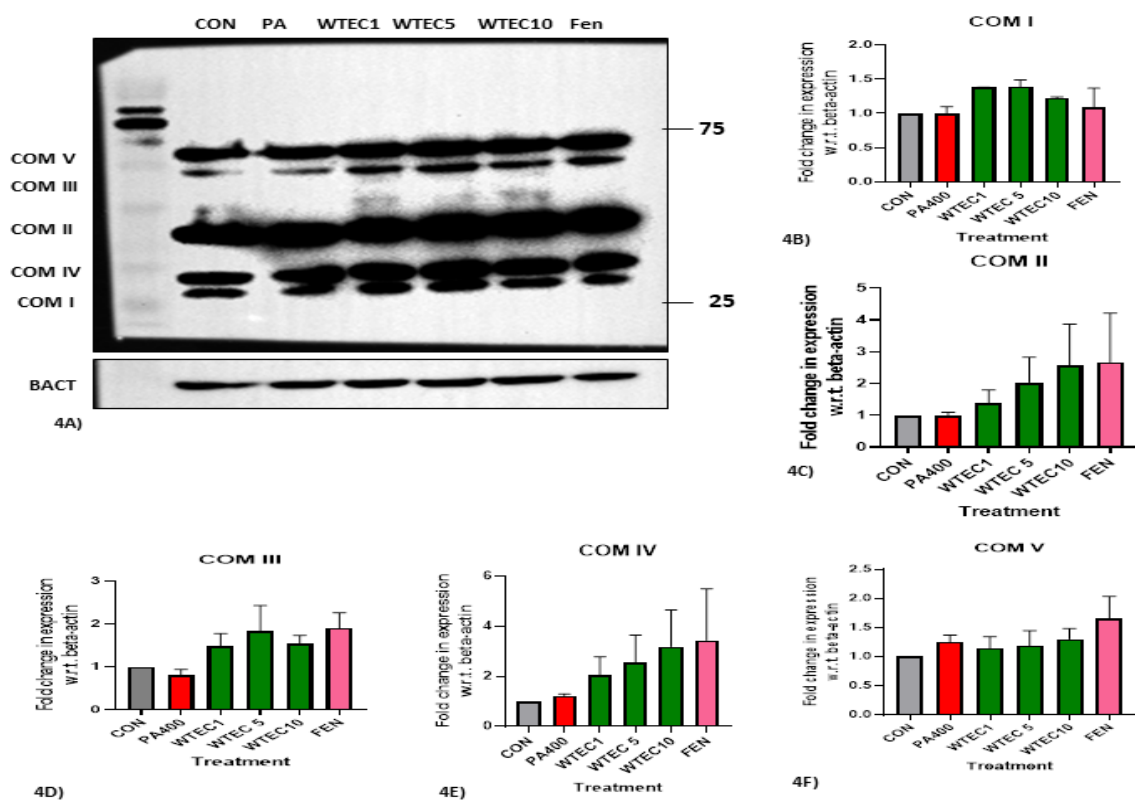


Figure 4: Effect of WTEC on expression of mitochondrial respiratory chain complex enzymes: WTEC at a dose range of 1 to 10 $\mu\text{g/ml}$ was pre-incubated for 6 hours followed by treatment with PA (400 μM), after 24 hours respiratory chain complexes expression was checked by human OXPHOS-complex cocktail antibody (4A) Complex I-Complex V expression (4B-F) was evaluated.

7.2.5. WTEC improves palmitic acid abrogated mitochondrial biogenesis via PGC1 α -TFAM dependant manner:

Mitochondrial number and load are interwoven with metabolic adaptation followed by stress leading to improved cellular energetic efficiency and maintenance of metabolic function. PGC1 α is a major nuclear protein acting as a nuclear receptor co-activator modulating the expression of various genes of mitochondrial synthesis and respiratory complexes. Saturated fatty acid overload in hepatic cells causes lipid accumulation and subsequent decrease in mitochondrial biogenesis attributed to reduced expression of PGC1 α expression.

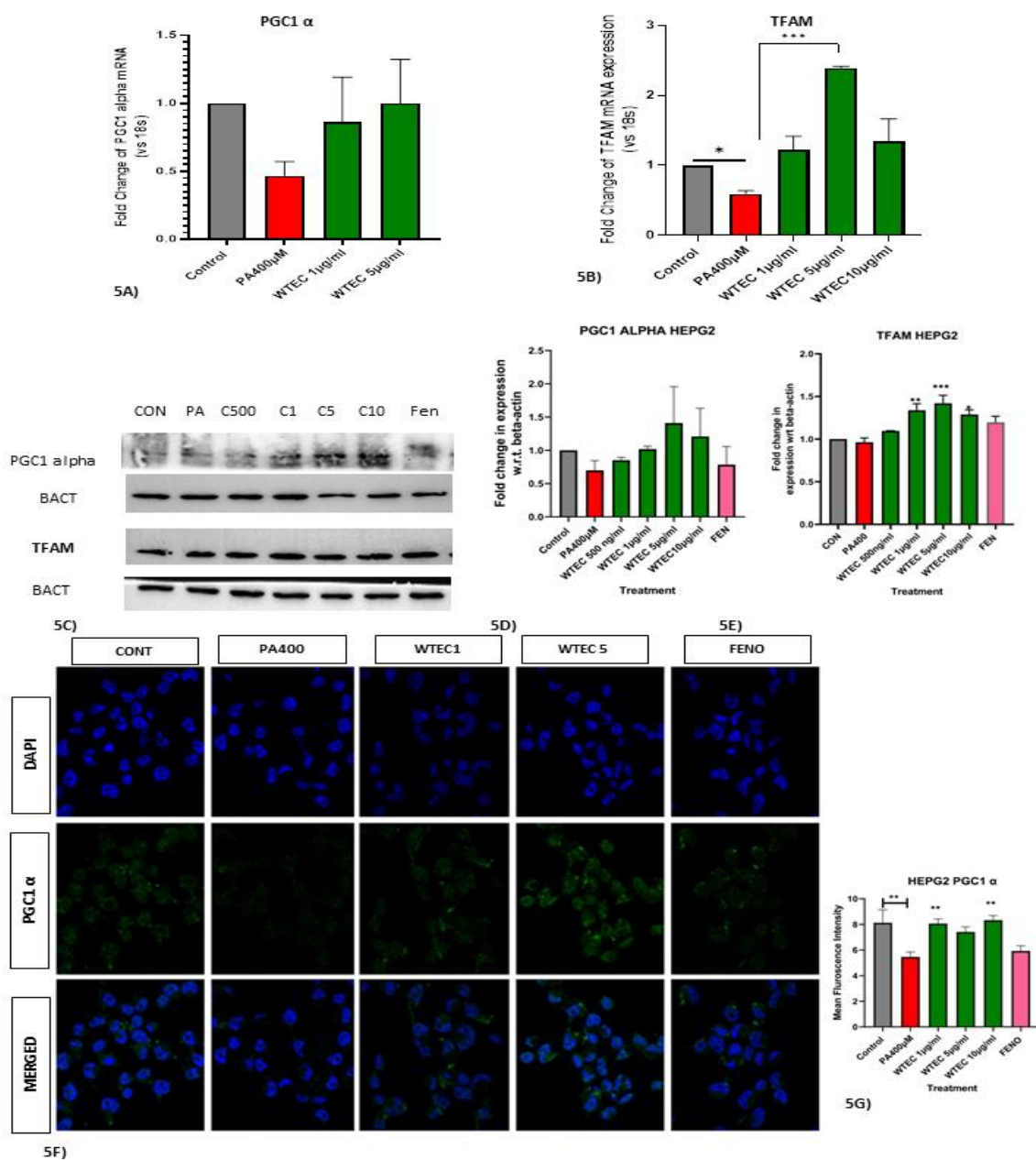


Figure 5: Wrightia extract (WTEC) activates PA abrogated mitochondrial biogenesis genes in HepG2 cells: HepG2 cells were treated with different doses (500ng/ml to 10µg/ml C500-C10) for 6 hour before stimulation with palmitate (24hr) and expression of genes responsible for mitochondrial biogenesis like PGC1 α and TFAM were checked by real time RT-PCR(5A-B) , western blotting (5D-F) and confocal microscopy by tagging PGC1 α with Alexa AF488 (green) and DAPI as nuclear stain.(5F-G). Data are expressed as mean \pm SEM and significance was calculated w.r.t. PA group, using one way ANOVA ****P<0.0001, ***P<0.001, **P<0.01, * P<0.05, ns= non-significant

We checked for the mRNA expression as well the protein abundance of PGC1 α in lipid lipid-mediated fatty liver model where we observed a dip in protein expression as well as mRNA abundance upon palmitic acid treatment in HepG2 cells but intriguingly when co-incubated with different doses of WTEC a dose-dependent increase of expression up to 5 µg/ml can be seen (Figure5A, 5C). PGC1 α is believed to impart this positive effect in mitochondrial biogenesis by ultimately coordinating with transcription factor TFAM, a major regulator of mitochondrial DNA (mtDNA) transcription and synthesis of mitochondrial proteins ultimately resulting in augmented mitochondrial mass. Fatty acid-induced steatosis model in hepatoma cells showed a decrease in TFAM protein expression as well as mRNA abundance (Figure5B-C)). WTEC treatment not only rescued by but at a dose range of 500 ng/ml to 10 µg/ml it showed a dose-dependent 4-5 fold increase in expression of this transcription factor thus validating the stimulating effect of mitochondrial synthesis by this extract (WTEC). Confocal microscopy of palmitate-treated HepG2 cells also corroborated this effect where we can see rescue of PA-mediated obliterating effect with a dose-dependent increase in expression of this protein along with nuclear localization (Figure5F-G).

7.2.6. Evaluation of SIRT1 as a modulator of mitochondrial biogenesis behind the activity of wrightia hydro-ethanolic extract:

SIRT1 is an NAD⁺ dependant deacetylase, well acknowledged for its positive role in mitigating lipid-induced mitochondrial dysfunction in the hepatic steatosis model. It increases mitochondrial mass through deacetylating PGC1 α . In our in vitro experimental model we can see a depletion of SIRT 1 protein expression upon SFA stress for 24 hours which was salvaged by WTEC treatment (1-10 µg/ml) (Figure6A,B). Extract treatment resulted in a far better increment in SIRT1 compared to fenofibrate (50µM). Relative gene expression by quantitative RT-PCR also showed a 70% reduction in SIRT1 gene expression whereas WTEC at a dose of 5-10 µg/ml increased 2.5-5 fold SIRT1 gene expression compared to PA treated group(Figure 6C). Confocal microscopy of HepG2 cells with Alexa-AF633 tagged SIRT1 antibody also validated the gene expression stimulatory activity of WTEC in response to lipotoxic stress (Figure6 D, E).

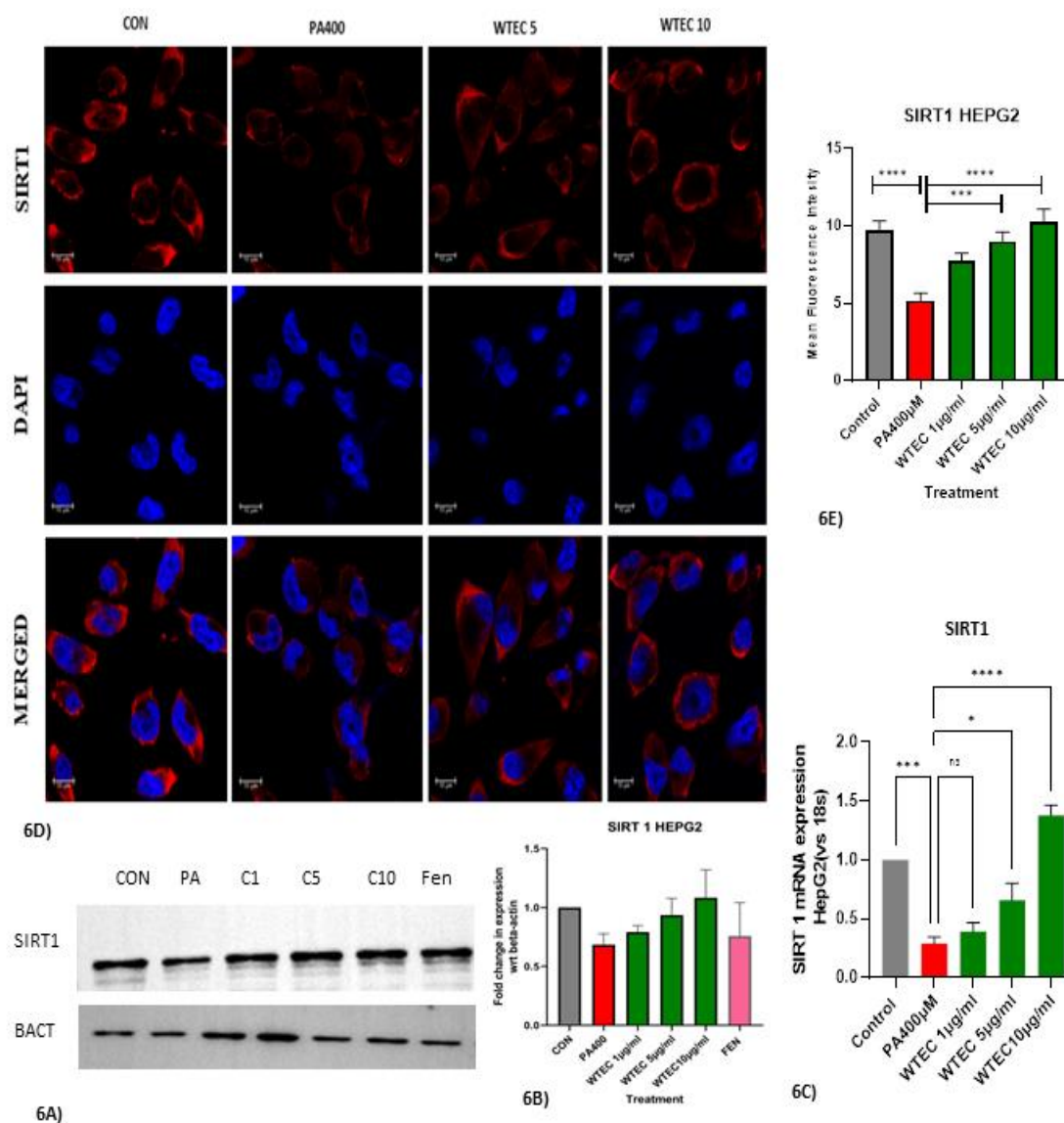


FIGURE 6:WTEC improves mitochondrial biogenesis through SIRT1 dependent manner: WTEC pretreated HepG2 cells with 1, 5 and 10 μg/ml doses (C1, C5, C10) were given fatty acid stress which resulted in rescue of the PA mediated dip in SIRT1 expression. Protein expression was checked by western blot (6A, B), mRNA expression was determined by real time RT-PCR (6C). Confocal microscopy was checked to follow the expression of SIRT1 using Alexa AF633 antibody (6D-E). Data are expressed as mean ± SEM and significance was calculated w.r.t. PA group, using one way ANOVA ****P<0.0001, ***P<0.001, **P<0.01, *P<0.05, ns= non-significant

7.2.7. Evaluation of mitochondrial dynamics parameters implicated by WTEC treatment in response to saturated fatty acid stress scenario:

Mitochondrial population in cell often oscillates between a balanced fission-fusion process in accordance with the bioenergetic need pertaining to the metabolic status of the cell. An elongated fibrillar network of fused mitochondria mediated by the conjugative

effect of MFN1 and 2 often generates a better bio-energetic yield and shuffling of internal contents whereas increased mitochondrial fission by DRP1 with the help of Fis 1 is often associated with mitochondrial dysfunction related to fatty liver, diabetes-like condition. PA treatment resulted in a significant increase in phosphorylation of serine 616 residue; an obligatory requisite to implicate the fission response as well as a slight increase in total DRP1 protein was also noticed. The ratio of phosphor-DRP1/DRP1 is often regarded as a reference to estimate the gross picture of the mitochondrial fission process which in our experimental condition showed a marked increase exemplifying the enhancement of the fission process. PA treatment resulted in a 12-15% increase in phosphor-DRP1 protein expression whereas increasing the dose of WTEC (500ng/ml - 10µg/ml) abrogated the expression by 37%-65% establishing a mitochondrial fission inhibitory effect of this extract which was also validated by a marked decrease in the ph-DRP1/DRP1 ratio(Figure7C,D). With inhibition of the exacerbated fission parameters we also checked fusion protein MFN1 and MFN2 expression in PA treated HepG2 cells with WTEC co-incubation. After a stress stimulation of 24 hours PA treated cells showed a marked decline in both MFN1 and 2 expressions as checked by western blotting but interestingly in extract treatment groups the fusion gene expression was elevated (Figure 7A,B) which reinforces the fusion promotion effect as already seen in increased fibrillar morphology by confocal microscopy . So in a nutshell besides mitigating the deleterious effect of increased fission by inhibiting phosphorylation on DRP1 serine 616 residue, WTEC at a dose range of 1-10 µg/ml enhances the fusion machinery balancing the mitochondrial dynamics and protect cells from potential damage.

7.2.8. Evaluation of autophagy-mitophagy parameters in the regulation of mitochondrial quality control with WTEC treatment:

The quality and quantity of active mitochondria in a particular cell at any particular time is maintained by the coordination of three important processes 1)mitochondrial biogenesis, 2)mitochondrial dynamics and mitochondrial turnover regulating 3) mitophagy-autophagy process. In our quest to elucidate the effect of wrightia hydro-ethanolic extract on maintaining mitochondrial health, we checked for the mitophagy-autophagy markers in WTEC pre-incubated hepatoma cells and subsequent fatty acid overload by palmitate treatment. As expected a significant deregulation in the mitophagy effector protein PINK1 and Parkin with autophagy marker LC3B was found in fatty acid-treated cells. After 24-hour treatment, a reduction in PINK1 and PARKIN expression of 27 and 20% respectively was observed in the PA group whereas WTEC treatment efficiently mitigated this decrease and showed a significant increase in mitophagic clearance of damaged organelle dose dependently compared to the PA group. In the fatty acid-only group a slight increase in autophagic marker LC3B(LC3BI+LC3BII) was observed but in extract-treated cells, in dose range of 500ng/ml-10, µg/ml a significantly

better increment of the marker was noted(Figure7E,F). A significant dose-dependent increase with almost 1.5-2 fold in 5 and 10 $\mu\text{g/ml}$ range of the WTEC treatment provided

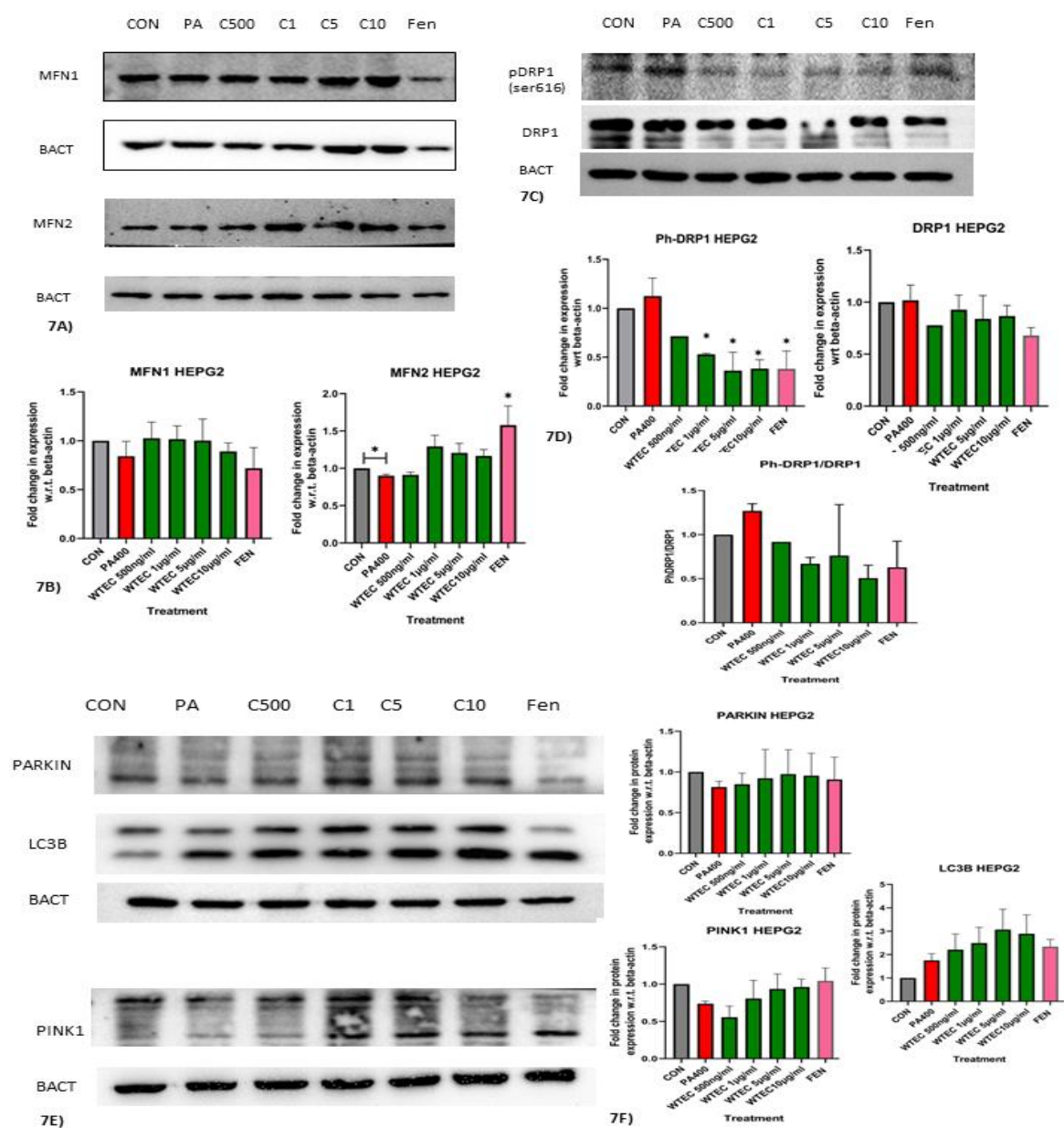
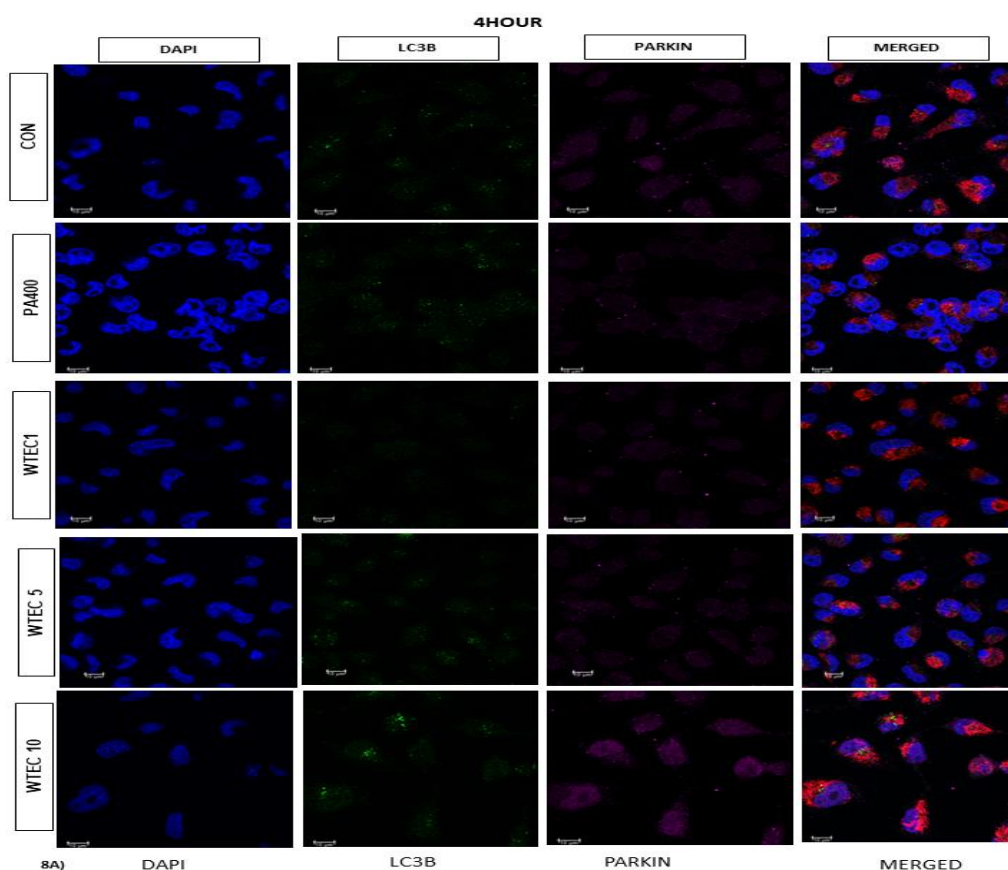


Figure 7:Wrightia improved palmitate worsened mitochondrial dynamics and mitophagy response: WTEC treatment in different dose range of 500ng/ml-10 $\mu\text{g/ml}$ (C500,C1,C5,C10) defended the lipotoxicity (PA400 μM) induced alteration in fusion protein MFN1 and MFN2 by western blot (7A-7B).Mitochondrial fission was checked by protein expression of ph-DRP1(ser616) and total DRP1 (7C-D).Expression of mitophagy marker protein PARKIN and PINK1 , as well as autophagy related LC3B was evaluated by western blotting (7E-F) Fenofibrate (50 μM) was used as drug control . Data are expressed as mean \pm SEM and significance was calculated w.r.t. PA group, using one way ANOVA **** $P < 0.0001$, *** $P < 0.001$, ** $P < 0.01$, * $P < 0.05$, ns= non-significant

7.2.9. Exploring time kinetics study related to mitochondria-mitophagy-autophagy crosstalk imparted by WTEC in maintaining mitochondrial homeostasis:

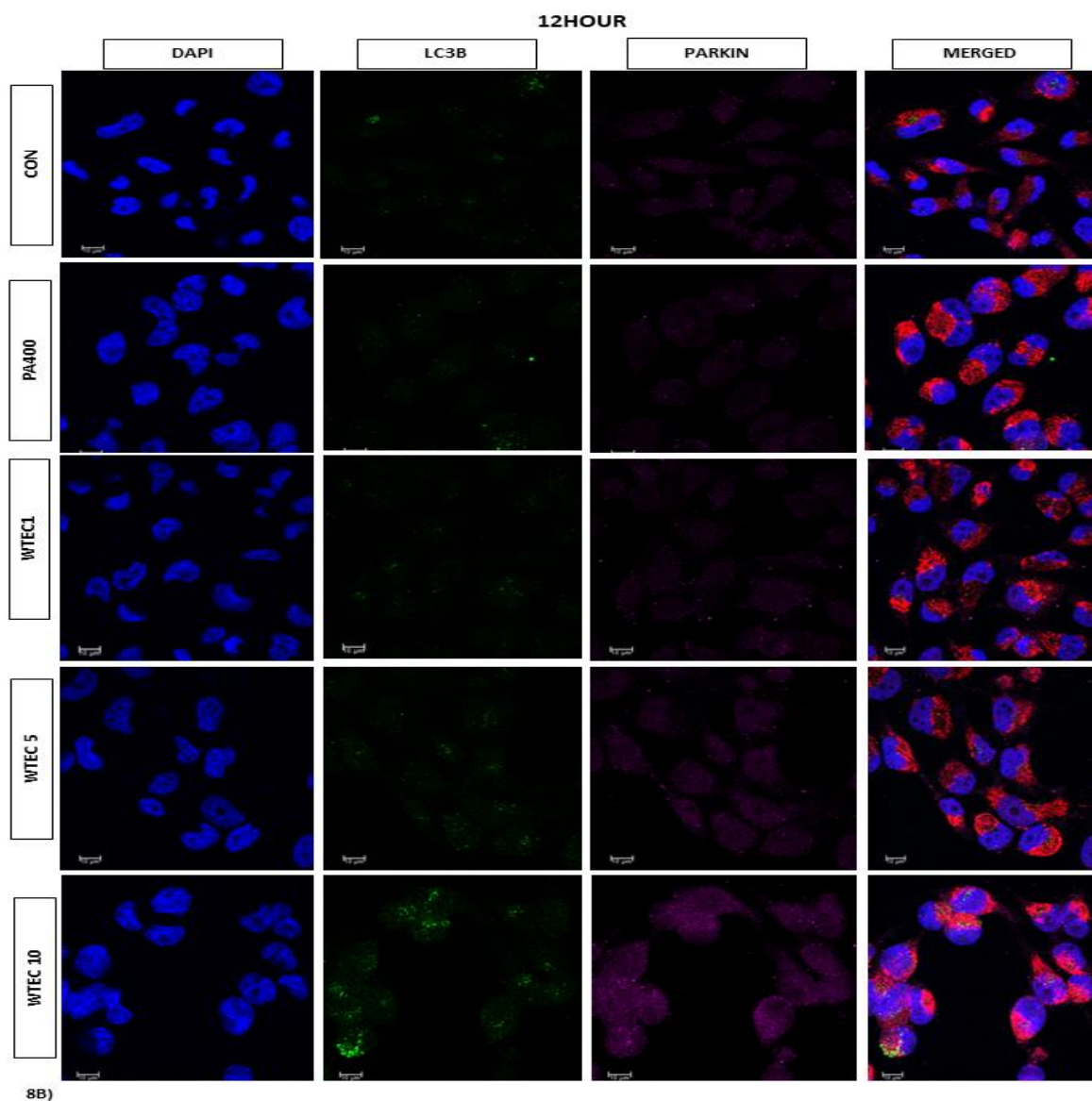
Autophagy is a general self-renewal process for the clearance of damaged or non-functional organelle whereas mitophagy is a specialized branch dealing with the clearance of damaged dysfunctional mitochondria preventing the role of deleterious ROS generation. Following induction of lipotoxic stress by overload of saturated fatty acid (generally abundantly found in western fatty diets) a plethora of debilitating mitochondrial disruptive mechanism follows causing molecular as well physiological damage to this organelle .so subsequent clearance by coordination of mitophagy marker Parkin with subsequent docking with autophagosome bound LC3B-p62 is a prime mechanism for effective clearance and maintaining cellular homeostasis. In this part of the study we marked the mitochondria with mitotracker red and subsequently with PARKIN and LC3B at different time points after palmitic acid-mediated lipotoxicity induction on WTEC pretreated HepG2 cells and followed the course of action in the expression of these proteins by confocal microscopy.



At 4hour, 12hour and 18hour time point expression of LC3B and parkin were checked and their colocalization in terms of Pearson's localization coefficient was quantitated

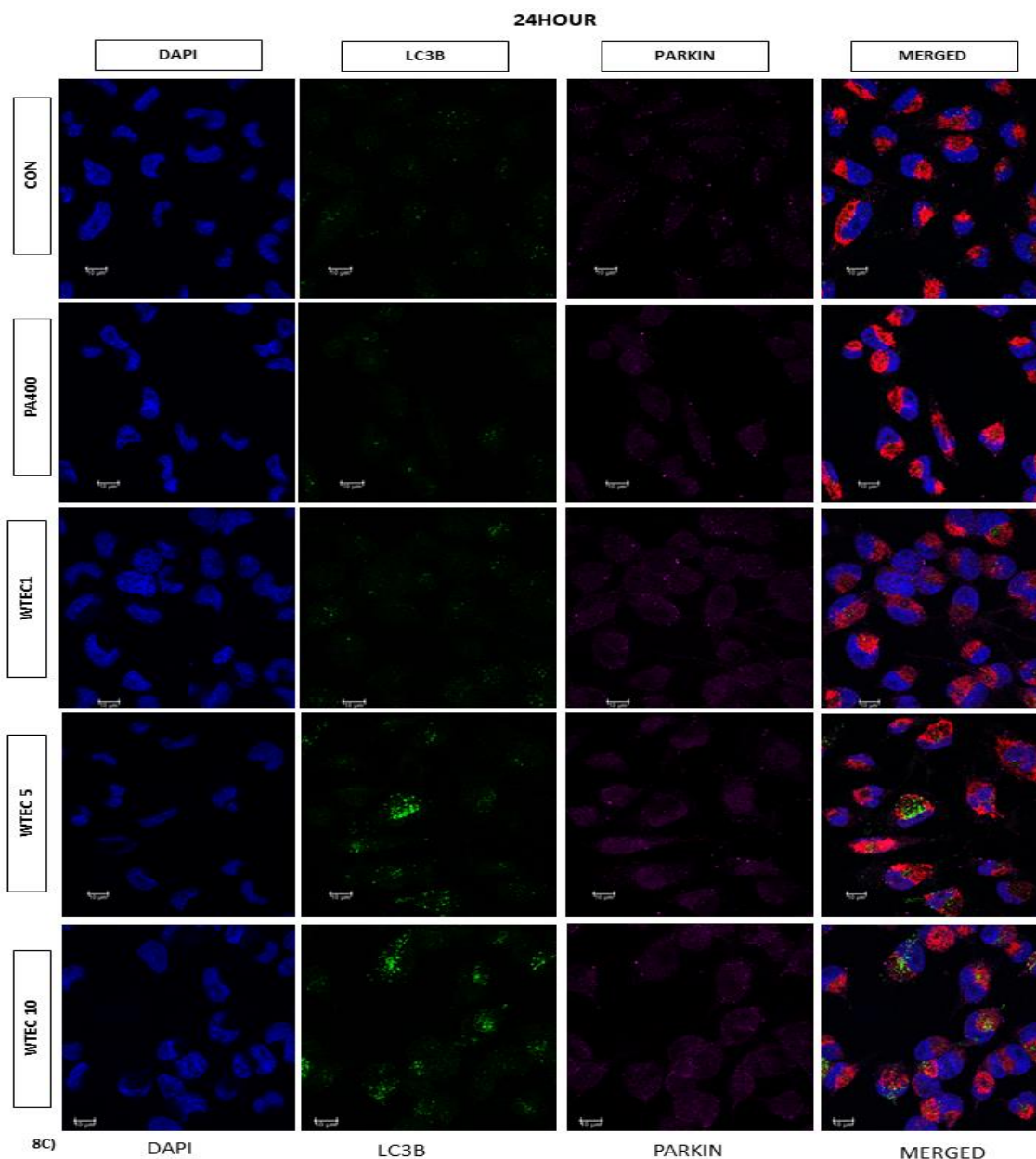
using 1, 5, and 10 $\mu\text{g/ml}$ dose of WTEC and fenofibrate as drug control (image not shown).

At the 4-hour time point, there was not so much variation with LC3B expression but PARKIN expression was reduced with PA treatment, and with a 10 $\mu\text{g/ml}$ dose of WTEC a rescue in PARKIN expression was seen. Interestingly significant increase in PARKIN fluorescence intensity was observed in fenofibrate(50 μM) treated group (Figure8A,8D).



At 12hour the PARKIN expression was significantly reduced in palmitate-treated cells but this time a significant dose-dependent elevation of PARKIN expression can be seen from the lowest dose of 1 $\mu\text{g/ml}$ and yielded the best response with 10 $\mu\text{g/ml}$. LC3B expression on the other hand did not show a significant reduction in the PA group but at

the highest dose of WTEC treatment, a rise in expression of this autophagic marker was noticed. LC3B-PARKIN co-localization increased 2-3 fold dose-dependently over a 12-hour timepoint (Figure 8B,8D).



After the 18-hour time point of fatty acid treatment, a low-level increase in PARKIN and LC3B expression was observed in the PA treatment group but on the contrary, the co-localization of these two markers decreased significantly. Although there was no significant difference in the increment of expression of these two markers relative to the PA group, a positive correlation was perceived signifying activation of mitophagy-related degradation of damaged organelle (Figure 8D: Image not shown).

At 24 hours Parkin expression increased in extract-treated cells and also in only PA-treated cells although to a lesser extent but expression of LC3B markedly increased in this time point with WTEC doses of 5 $\mu\text{g/ml}$ and 10 $\mu\text{g/ml}$ compared to palmitate only group which signifies an activation of the final stages of autophagic degradation in response to dysfunctional stressed mitochondria (Figure 8C,8D).

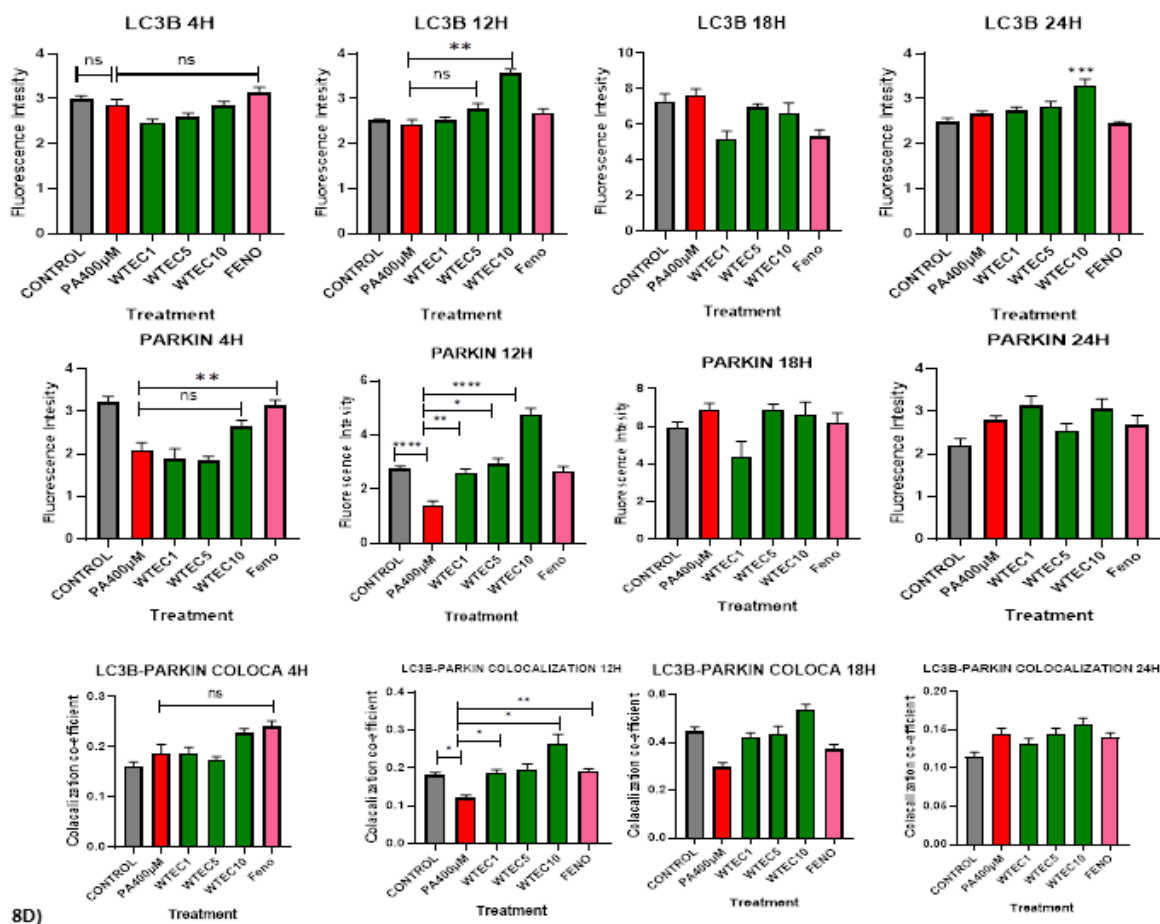
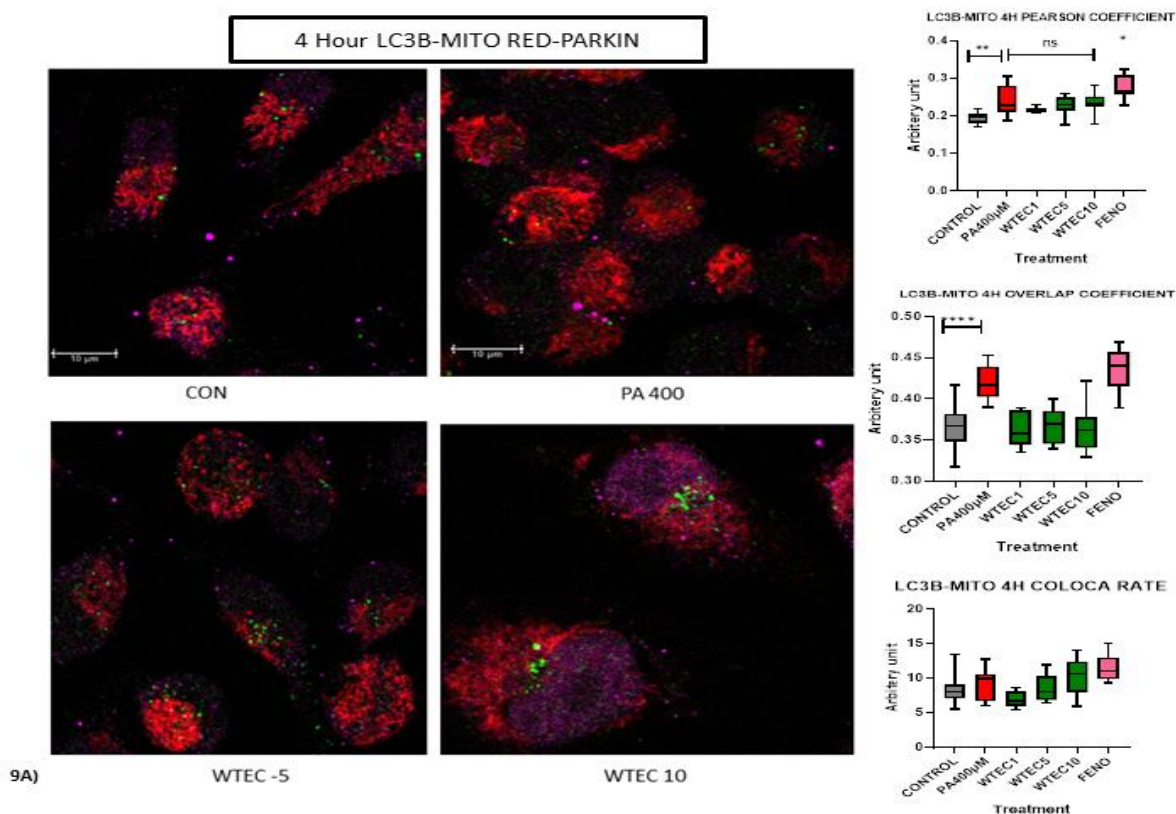


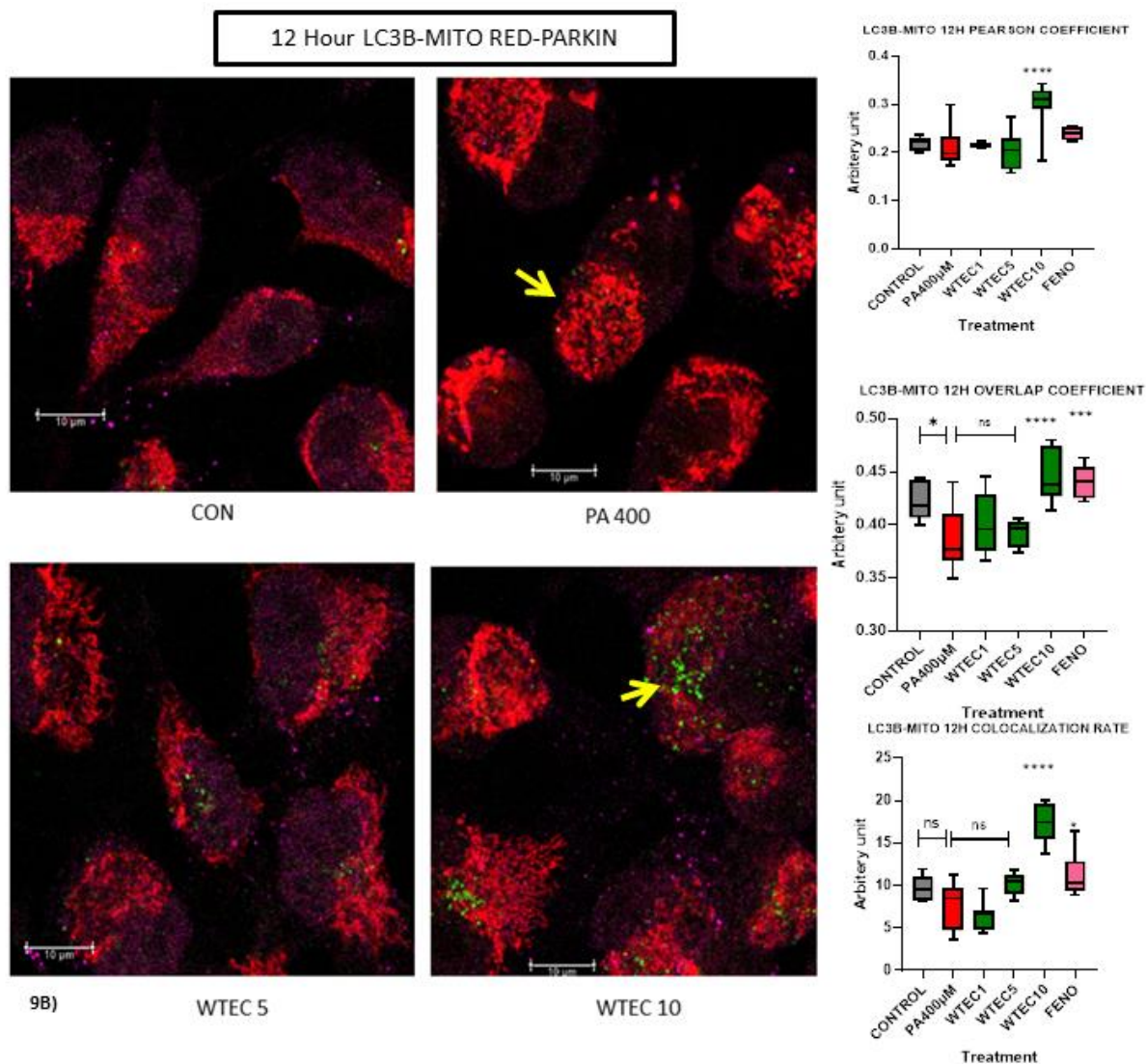
Figure 8: Time kinetics study of WTEC mediated expression and co-localization of mitophagy and autophagy related genes for dysfunctional mitochondrial clearance: WTEC doses of 1, 5, 10 $\mu\text{g/ml}$ was pretreated in hepatoma cells and incubated with saturated fatty acid (Palmitate). After 4hour, 12hour, 18hour(Image not shown), 24hour time point treatment were terminated and cells were processed for confocal microscopy using Mito-tracker red for mitochondrial staining, Alexa fluor 488 for LC3B(green) and Alexa fluor 565 for PARKIN(pseudo pink) visualization. DAPI was used for nuclear staining. Fluorescence intensity and Pearson correlation coefficient between PARKIN and LC3B was evaluated (4H, 12H, 18H and 24H) and expressed in bar diagram. Fenofibrate (50 μM) was used as drug control. Merged image shown with Mitotracker red. Data are expressed as mean \pm SEM and significance was calculated w.r.t. PA group, using one way ANOVA **** $P < 0.0001$, *** $P < 0.001$, ** $P < 0.01$, * $P < 0.05$, ns= non-significant

Nextly, we wanted to analyze the colocalization rate, localization status, and overlap coefficient between mitotracker red-tagged mitochondria with autophagic (LC3B-Alexa AF488) and mitophagy marker (Parkin -Alexa AF565, Pseudo color pink).

In 4hour we can see fibrilar elongated mitochondria in normal cells and very basal expression of LC3B and parkin. Upon fatty acid treatment, mitochondria were fragmented but no such response of mitophagy marker was seen but a rise in LC3B was noted which was also correlated with higher mitochondria-LC3B overlap coefficient in this early period. Surprisingly in the WTEC treatment group at the highest dose of 10 $\mu\text{g/ml}$, a significant increment of Parkin expression was seen with a little rise in LC3B expression hinting the potential of this extract in early activation of mitophagy (Figure 9A).

After 12 hours of incubation, most of the mitochondria in the lipotoxic group were fragmented with a dip in mitophagy-autophagy markers as evident from a significant dip in overlap coefficient and colocalization rate. Parkin was increased at lower doses at this time point whereas an increase in LC3B was also noted in the high-dose group of 10 $\mu\text{g/ml}$. In WTEC treated group where the extracts were co-incubated with palmitate, a marked increase in these two parameters with raised Pearson's coefficient authenticate the promotion of regulated clearance of damaged mitochondria by wrightia hydro-ethanolic extrac (Figure 9B).





At the 24-hour time point in WTEC treated group, an increased expression of LC3B with fragmented smaller mitochondria was noticed which was also validated by a significant increase in the co-localization rate and Pearson's coefficient starting from WTEC doses of 1 µg/ml towards the best effect with 10 µg/ml which suggest the potential of this extract in regulating a planned clearance of specific damaged mitochondria by up-regulating the autophagy pathway. In only the palmitic acid-treated group although there was an increase in autophagy noted but co-localization rate and Pearson's coefficient between mitochondria and LC3B were markedly decreased suggesting a gross deregulation of the distressed mitochondrial clearance (Figure 9C).

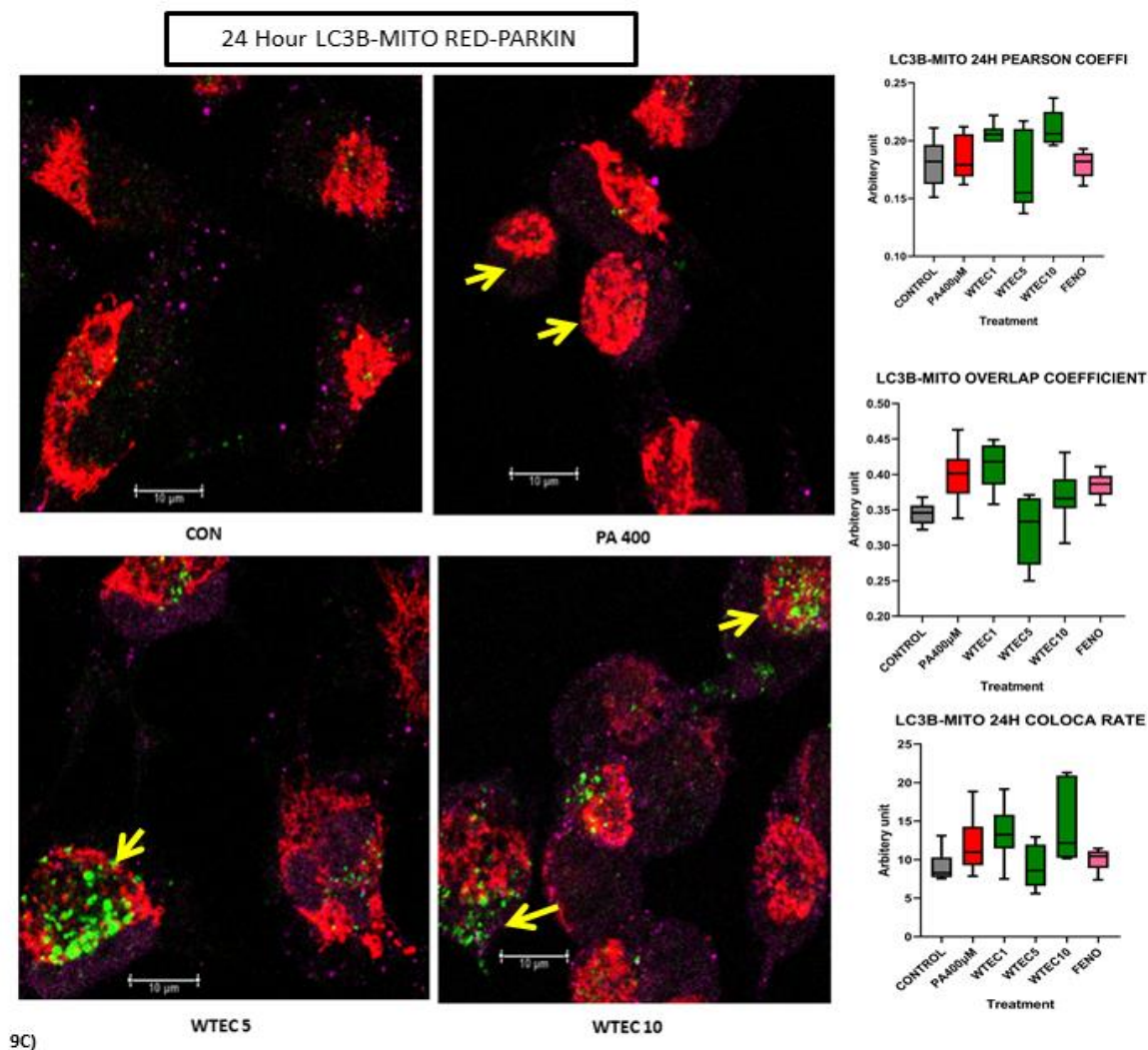


Figure 9: Evaluation of WTEC boosted colocalization of LC3B with damaged mitochondria was checked at different point of time in PA treated HepG2 cells: At 4hour, 12hour and 24 hour time point after introduction of lipotoxic stress in WTEC (1, 5 µg/ml and 10µg/ml and Fenofibrate) pretreated HepG2 cells LC3B, PARKIN and mitochondria was visualized by confocal microscopy. Fenofibrate (50µM) was used as drug control. Confocal representative image contains Mitotracker red –Alexa 488(LC3B) –Alexa565 (Parkin). Quantitated value plotted in graph depicting Colocalizaion rate, Pearson's colocalization coefficient and overlap coefficient was checked between Alexa 488 tagged LC3B(green) and Mitotracker Red stained mitochondria at 4hour(9A), 12hour(9B), 24hour(9C) in all treatments.. Parkin was stained for reference of expression by Alexa fluor 565(pseudo pink). DAPI was used as nuclear stain. Data are expressed as mean \pm SEM and significance was calculated w.r.t. PA group, using one way ANOVA ****P<0.0001, ***P<0.001, **P<0.01, * P<0.05, ns= non-significant

7.2.10. *Wrightia* hydro-ethanolic extract ameliorates mitochondrial dysfunction through activation of AMPK α :

AMPK is a metabolic master regulator responsible for the maintenance of cellular metabolic and bio-energetic status. It sits in the nodal position regulating major lipid metabolism pathways, maintaining mitochondrial health, and managing autophagy-mitophagy processes and often gets triggered by sensing the intracellular lower energetic status(ATP) in metabolic stress conditions. It has an important regulatory role in the coordination of mitochondrial dynamics while maintaining a balance between mitochondrial biogenesis and the mitophagy pathway. As WTEC showed a positive effect in the improvement of mitochondrial insult preserving mitochondrial homeostasis, we wanted health modulating to check the expression of AMPK α and also the phosphorylation at threonine172 residue which marks an important residue for activation of this protein. Upon palmitate insult for 24 hours in hepatoma cells, the phosphorylated AMPK α as well as total protein level reduced in response to lipotoxicity generated by abrupt lipid accumulation. WTEC co-incubation not only hindered the reduction in the expression but the Phospho- Threonine(172) AMPK α subunit expression increased up to 1.5-2 fold in response to increasing doses of wrightia. The phospho AMPK α / total protein ratio was also rescued by WTEC treatment (Figure 10A).

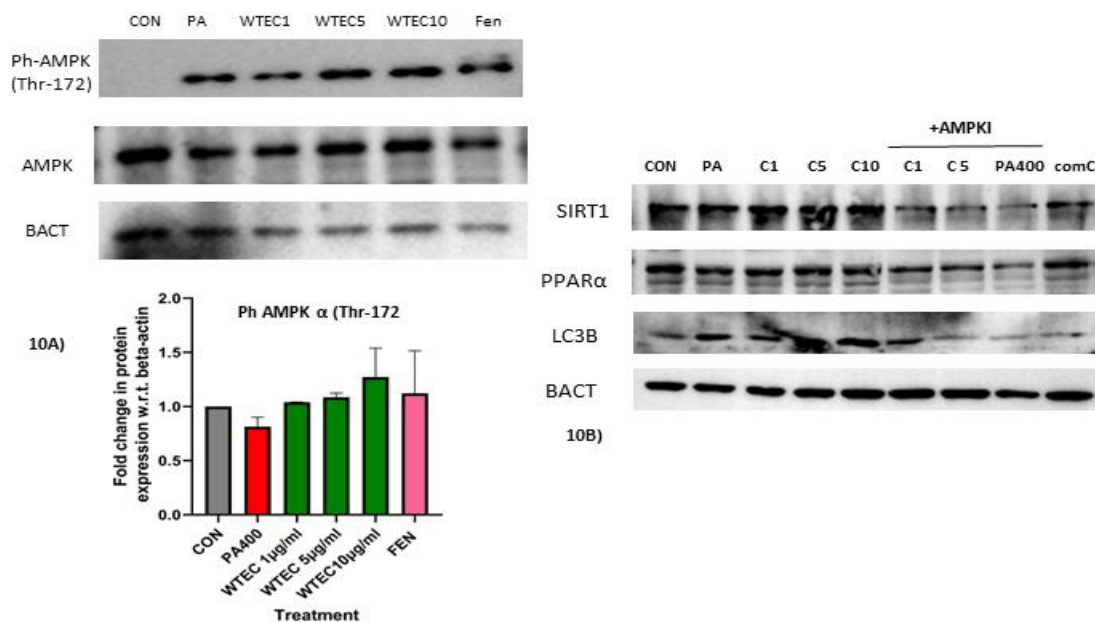


Figure 10: *Wrightia* hydro-ethanolic extract ameliorates mitochondrial dysfunction through activation of AMPK α : HepG2 cells are incubated with 1, 5, 10 μ g/ml doses of WTEC (C1, C5, C10) and subsequently Palmitate was added as stress inducer and both were co-incubated further for 24 hours. Protein expression of total AMPK α and phosphor- AMPK α (Thr-172) were checked by western blotting (10A). AMPK α inhibitor compound C was used (WTEC 1, 5 μ g/ml dose and with PA400 only) to check the dependence on AMPK α . Expression of SIRT1, PPAR α , and LC3B was checked with or without inhibitor and normalized to β -actin. All expression was normalized to β -actin (10B).

For affirmation of the dependence of WTEC in the manifestation of its mitochondrial health improvement towards AMPK a well-known AMPK inhibitor compound C was used to inhibit this protein and subsequently expression profiles of downstream target genes like SIRT1, PPAR α , and LC3B were checked with or without the addition of this inhibitor (5 μ M). Compound C treatment surprisingly abrogated all the positive increments in the downstream effector genes mentioned while without the addition of compound C, WTEC 1-10 μ g/ml doses showed the same protective role against biogenesis(SIRT1), lipid metabolism(PPAR α) and autophagy regulator(LC3B) genes attesting the role of AMPK in the regulation of its bio-activity (Figure 10B).

7.2.11. Evaluation of wrightia extract in the regulation of lipid metabolism in the context of fatty acid stress in hepatic cells:

Treatment with saturated fatty acids like palmitic acid in hepatoma cells like HepG2 serves as a perfect model of in-vivo fatty liver causing intracellular lipid accumulation and subsequent generation of ROS, causing downstream metabolic stress by alteration of fatty acid oxidation as well as synthesis genes, fatty acid uptake also modulating secretion of lipid particles and inflammatory mediators. Wrightia hydroethanolic extract in the dose range of 1-10 μ g/ml already manifested some wonderful results in protecting cells from oxidative stress and associated mitochondrial dysfunction with fatty acid insult. In this part, we wanted to check the effect of this extract in preventing lipid accumulation and metabolism genes.

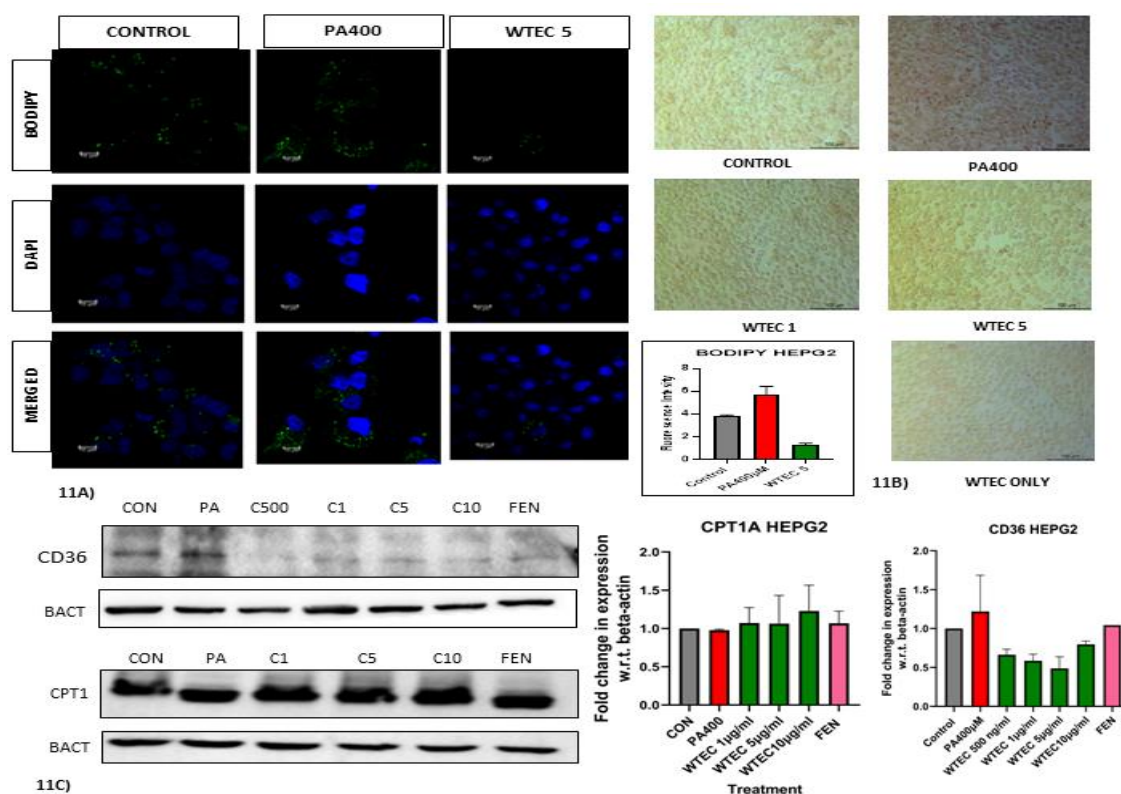


Figure 11: *Wrightia* hydro-ethanolic extract hinders palmitic acid mediated lipid accumulation in HepG2 cells and regulates fatty acid uptake and oxidation: Palmitate treatment for 24 hours in hepatoma cells resulted in lipid droplet formation. BODIPY fluorescent probe was used to stain the neutral lipid droplets and Oil Red O was used for bright microscopy. WTEC at 1 and 5 $\mu\text{g/ml}$ dose significantly reduced droplet formation as visualized by confocal (11A) and bright field microscopy (11B). Protein expression of CD36 was checked to estimate fatty acid uptake and CPT1A expression was checked by western blotting to evaluate the fatty acid β -oxidation status in WTEC pretreated HepG2 cells (500 ng/ml and 1, 5, 10 $\mu\text{g/ml}$ as C500, C1, C5, C10) with saturated fatty acid insult (11C). Protein expression was normalized to β -actin.

PA treatment for 24 hours resulted in substantial accumulation of lipid droplets in HepG2 cells which was observed by fluorescent BODIPY dye and oil red O stain by confocal and bright microscopy. A short pre-incubation of WTEC with 1-5 $\mu\text{g/ml}$ doses and then induction of fatty acid stress with palmitate with extracts prevented most of the accumulation of the lipid as can be seen by the microscopy results. At a dose of 5 $\mu\text{g/ml}$ WTEC can be seen effectively abolishing the green fat droplet aggregation by confocal microscopy (Figure 11A) as well as reduction of red dots of oil red O stained neutral lipids inside HepG2 cells by bright field microscopy (Figure 11B).

CPT1 is the main transporter of long-chain fatty acids to pass through the mitochondrial inner membrane towards the matrix and subsequently, they are oxidized by enzymes in the mitochondrial matrix by beta-oxidation process. So CPT1 catalyzes the rate-limiting step of fatty acid oxidation and serves as an important marker for estimation of cellular fatty acid oxidation status. After 24 hours of PA treatment in the presence of WTEC, we can see a rise in CPT1A expression certifying the increase of fatty acid oxidation process which will subsequently help in meeting the cellular energy requirement diminished by lipotoxic stress (Figure 11C).

CD36 is another major fatty acid transporter residing in the cell membrane and helps in uptake of fatty acid from outside. In the fatty liver condition, we can see an upregulation of fatty acid uptake by an increment of expression in CD36 expression. As in the obesity and fatty liver scenario, there is a surge of free-flowing fatty acid in the system a rise in uptake causes increased complexity generating more ROS and subsequent metabolic abnormalities. When WTEC dose from 1-10 $\mu\text{g/ml}$ was introduced with saturated fatty acid like palmitate a significant dose-dependent decrease in CD36 was noticed which certifies the role of WTEC in inhibition of fatty acid uptake (Figure 11C).

In adipose and muscle tissue, we can see a different situation with respect to lipid metabolism parameters when compared with the liver. Fatty liver manifests an increase in lipid accumulation through increased uptake whereas adipose tissue manifests a dip in the fatty acid uptake process. We have employed 3T3 adipocyte cells for the evaluation of some lipid regulation parameters and to check if our extract can have a positive impact in rescuing the altered metabolic scenario.

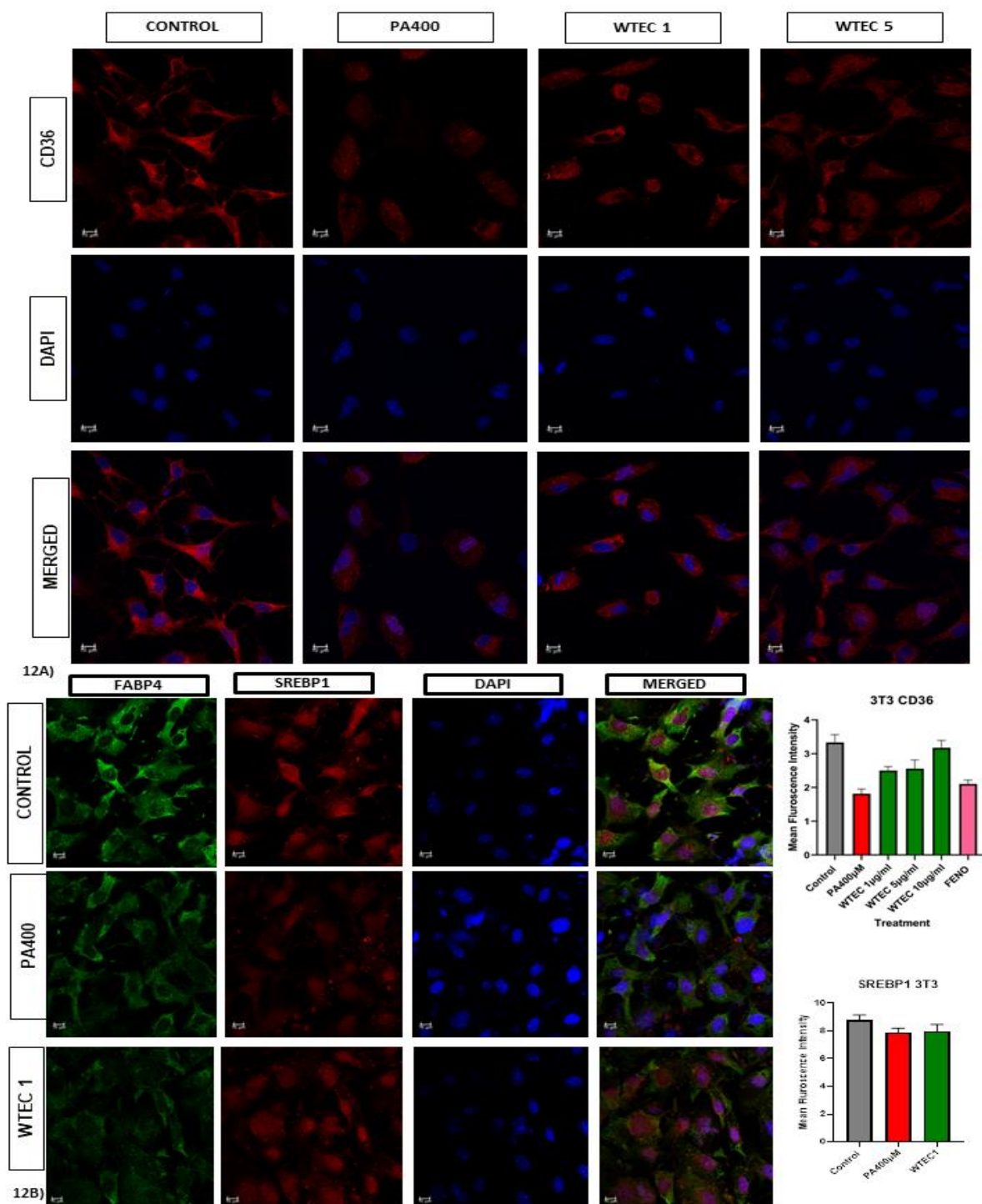


Figure 12: Assessment of WTEC regulation of fatty acid uptake and synthesis in PA treated 3T3 adipocyte cells: Adipocytes were treated with palmitate (400µM) and co-incubated with or without WTEC (1 and 5 µg/ml doses) for 24 hours and checked for expression of CD36 (Alexa 633) for fatty acid uptake . Differentiated adipocytes after fatty acid stress were evaluated for SREBP1 (Alexa fluor 633) and FABP4 Alexa fluor 488) expression by confocal microscopy. DAPI was used as nuclear counterstain. Bar diagram showing the quantitation of mean fluorescent intensity by LAS X software

3T3 adipocytes were given a pre-incubation of 1 and 5 $\mu\text{g/ml}$ of WTEC and then subsequently palmitic acid (400 μM) was added to the cell and incubated for 24 hours with extracts. By employing confocal microscopy we estimated the expression profile of CD36 for assessing the fatty acid uptake status and also checked for SREBP1 the main regulatory transcription factor for fatty acid synthesis along with FABP4 which is another fatty acid transporter mainly responsible for the secretion of lipid particles outside the cell. Palmitic acid treatment reduced the expression of AlexaAF633 tagged CD36 to a significant extent whereas the extracts rescued the decrease in expression implementing a positive role by increasing the fatty acid uptake by storage cells (Figure 12A). While fatty acid uptake was increased by extract administration in palmitate-stressed cells the fatty acid synthesis transcription factor SREBP1 expression was seen to be increased although at a low level by WTEC 1 $\mu\text{g/ml}$ dose (Figure 12B). FABP4 levels seemed to be decreasing with fatty acid treatment but at dose of 1 $\mu\text{g/ml}$ WTEC showed no change in effect on its expression compared to the PA group (Figure 12B).

7.2.12. High-fat diet (60% Kcal) feeding induces obesity and subsequent pathogenesis of non-alcoholic fatty liver disease:

C57BL6J male mice were fed a high-fat diet (Research diet D12492) for 20 weeks and after randomization allotted into five groups. *Wrightia* hydro-ethanolic extract was dissolved in water and fed to a high dose (500mg/ kg body weight) and low dose (250mg/ kg body weight) group for 28 days by oral gavage with a high-fat diet. Fenofibrate, an FDA-approved drug for dyslipidemia was used as a control drug (50mg/kg body weight) and fed by oral gavage to the drug control group. One group received a normal chow diet and served as a control group. The work plan is summarized in (Figure 13A).

High-fat fed mice gained significant weight but two doses of WTEC showed a positive effect preventing further increase of weight gain as well decrease in total body weight was reduced significantly. After sacrifice liver and epididymal fat (EPF) was collected and weighed. A decrease in liver weight as well as a significant dip in EPF was noted corroborating the positive effect of extract feeding on overall obesity management (Figure 13C). Upon gross physical evaluation the liver size and weight were increased in the HFD group as well as a pale yellowish coloration was observed which is an important signature characteristic of non-alcoholic fatty liver disease (NAFLD) (Figure 13B).

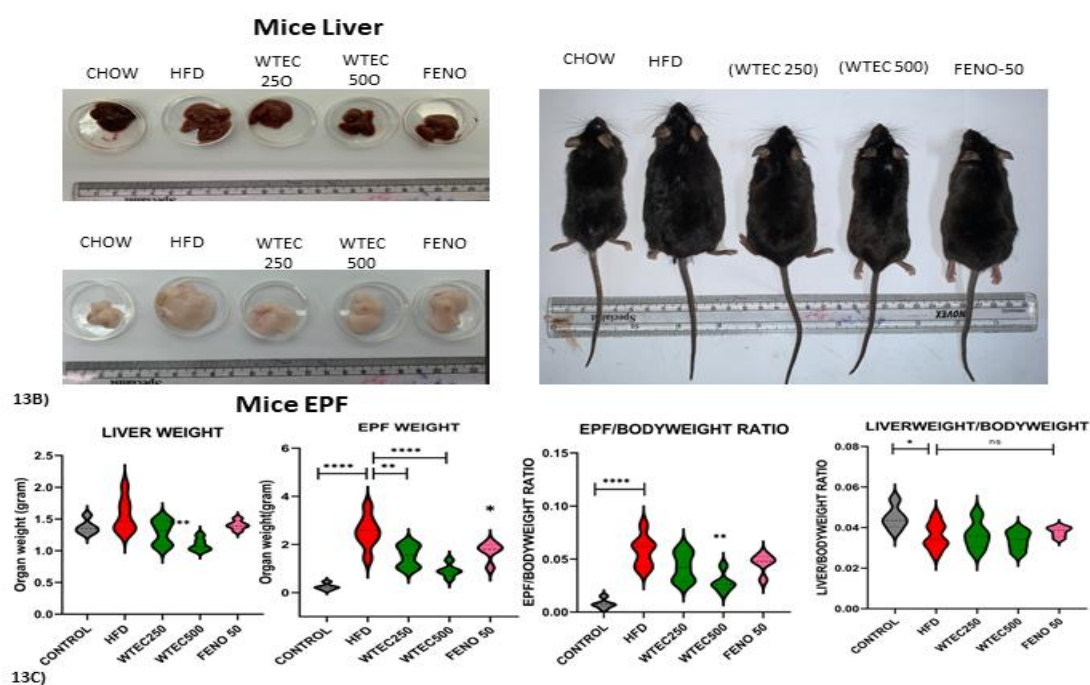
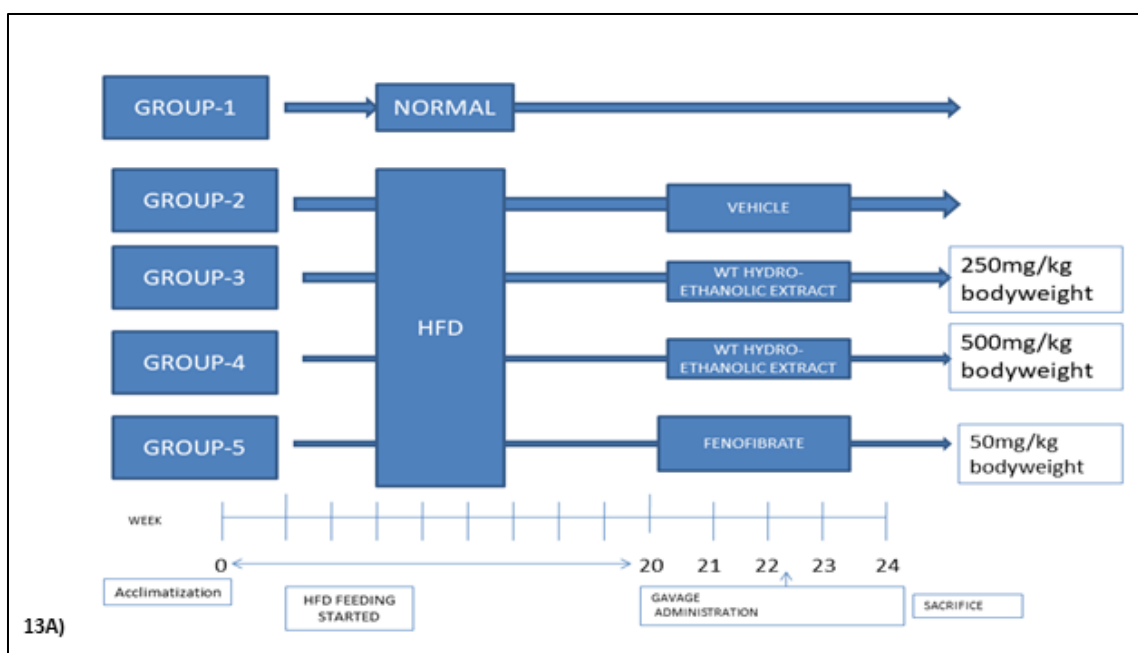


Figure 13: Experimental model of high fat diet feeding in C57BL/6J mice induces OBESITY and pathologic feature of NAFLD: C57BL6J male mice were fed with 60%Kcal highfat diet for 20 weeks and then therapeutic efficacy of two doses of WTEC (250mg/kg bodyweight and 500mg/kg of bodyweight) taking fenofibrate (50mg/kg) as drug control for another 28 days (13A) After sacrifice mice liver and epididymal fat was collected and grossly evaluated (13B). Organ weight was measured in each group and plotted (13C) Data are expressed as mean \pm SEM and significance was calculated w.r.t. HFD group, using one way ANOVA **** $P < 0.0001$, *** $P < 0.001$, ** $P < 0.01$, * $P < 0.05$, ns= non-significant

High fat diet with 60% Kcal energy from fat (mostly saturated lard fat) is an important trigger for the development of fatty liver and these high-fat-fed mice for a minimum of 12-16 weeks are considered as an ideal model of NAFLD/NASH. C57BL/6J male mice when fed with a high-fat diet for 20 weeks and for next 4 weeks with therapeutic intervention, displayed several characteristic features of fatty liver disease. HFD group mice showed significant body weight gain, and elevation in fasting blood sugar, cholesterol, LDL-cholesterol, and triglyceride levels compared to normal diet-fed mice which with treatment doses manifested a promising reduction (Figure 14 A-E). ALT level showed a slight increment in our HFD group but AST level didn't show any significant changes. WTEC 500mg/kg dose efficiently reversed the ALT level to normal whereas the AST level was slightly increased (Figure 14F, G). Fatty liver development with these abnormal blood parameters is often associated with hyperglycemia and subsequent development of insulin resistance. Oral glucose tolerance test (OGTT) was performed and an Insulin tolerance test (ITT) was also performed. HFD was seen to cause a sharp rise upon glucose feeding which was minimally reduced till 120 minutes after feeding whereas in WTEC treated group the fasting blood glucose level dropped within 60 minutes dose-dependently showing a better effect than fenofibrate (Figure 14H). In ITT, after intra-peritoneal administration of insulin, a sharp dip in the FBG level was noticed in the control and WTEC, drug group whereas a lower decrease was seen for full experimental time (120 minutes) compared to other group in case of the HFD group suggesting an involvement of insulin resistance (Figure 14I).

The degree of ballooning, fibrosis, inflammation, and hepatic steatosis in the specimens were graded using the grading system outlined by Kleiner et al. (2017). In a nutshell, hepatocellular steatosis is classified into four grades: grade 0 (no fat), grade 1 (steatosis comprising less than 33% of the hepatic parenchyma), grade 2 (34%–66%), and grade 3 (greater than 66%). Grades 0–3 indicate different levels of inflammatory cell infiltration: fewer than two foci per 200× field, three to four foci per 200× field, and more than four foci per 200× field. Grade 0: none; Grade 1: few balloon cells; Grade 2: many balloon cells. Hepatocellular ballooning. An analysis of histology was carried out by an experienced scientist (Figure 14J).

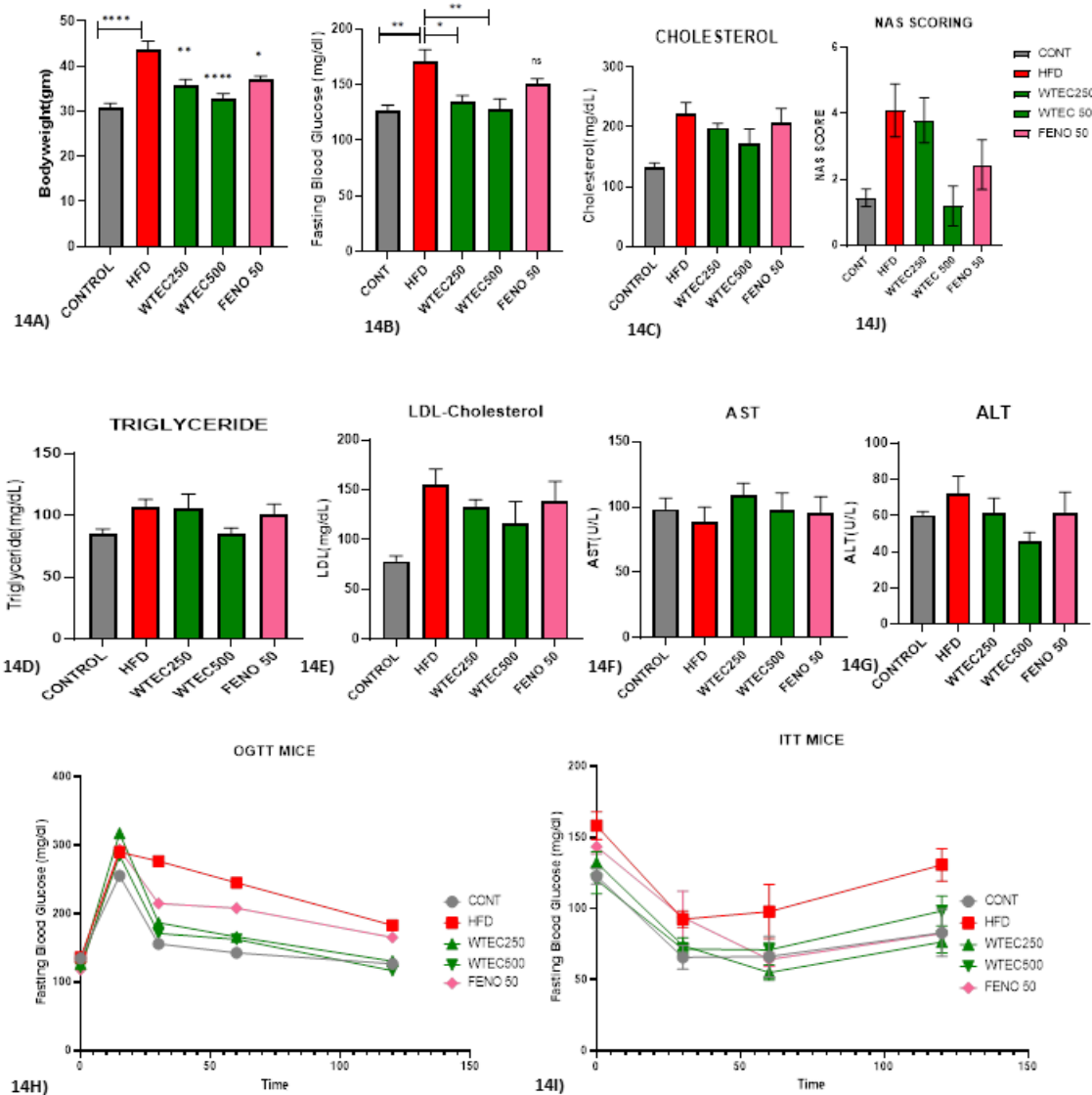
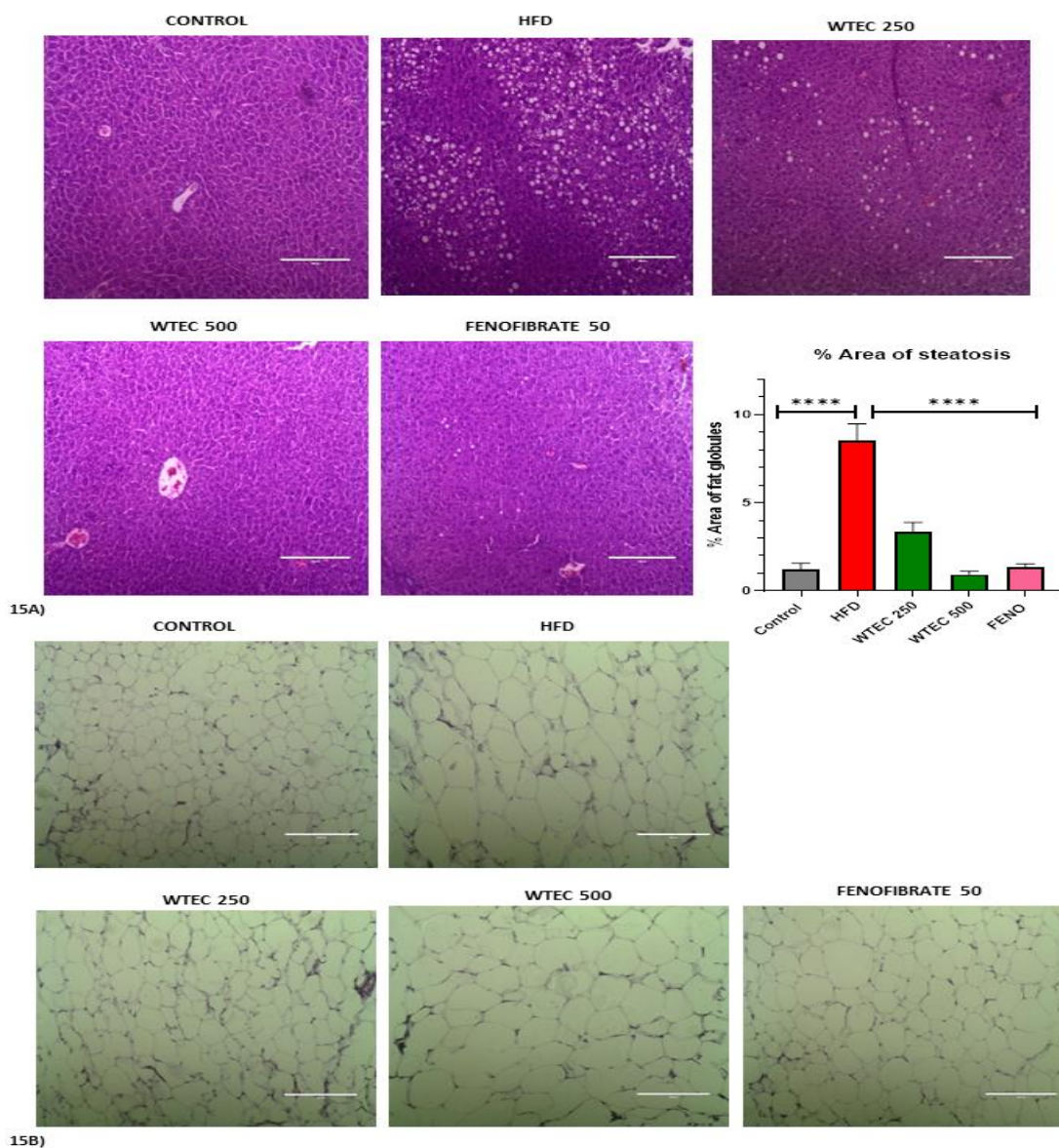


Figure 14: WTEC intervention ameliorated altered hematological features and insulin resistance in HFD fed mice model of NAFLD: 20 weeks of HFD fed mice were fed with wrightia hydro-thanolic extract by oral gavage (250 and 500mg/kg bodyweight). Fenofibrate (50mg/kg) was fed as control drug. Total mean bodyweight, fasting blood glucose level, cholesterol, triglyceride, LDL, ast and ALT level was checked in blood of each group of animals. Oral glucose tolerance test and Insuline tolerance test was performed at 0, 30, 60, 120 mint timepoint to evaluate the status of insulin resistance in experimental animals. Data are expressed as mean \pm SEM and significance was calculated w.r.t. HFD group, using one way ANOVA **** $P < 0.0001$, *** $P < 0.001$, ** $P < 0.01$, * $P < 0.05$, ns= non-significant

One of the main pathogenic features of the development of fatty liver disease is fat accumulation within liver cells. Steatosis (fat deposition) in $\geq 5\%$ hepatic cells with or without the presence of inflammatory cell infiltration and ballooning certifies the occurrence of fatty liver. Liver and epididymal fat were collected after sacrificed and after 10% formalin fixation a slice of the tissue was embedded in paraffin and

subsequently sectioned and stained by hematoxyline and eosine which stain the nucleus and cytoplasm respectively (Figure 15A). A nine-fold increase in the % area of fat accumulation was observed in the HFD group compared to normal whereas WTEC treatment dose-dependently reduced this steatosis showing almost the same effect as fenofibrate. The cell size of EPF was also grown significantly as noticed in the HFD group whereas WTEC doses of 250 and 500 mg/kg rescued this increment and showed a positive reduction in adipocyte size (Figure 15B)



Picrosirius red is used to stain the collagen deposition within the liver specifically in the sinusoidal area and endothelial wall of the portal veins. Higher collagen deposition is correlated with increased severity of disease. In some of the high-fat-fed tissue, we saw a prominent collagen fiber deposits but none of the WTEC 500mg/kg fed mice showed any

deposition which reinforces the fatty liver alleviating effect of wrightia hydro-ethanolic extracts (Figure 15C).

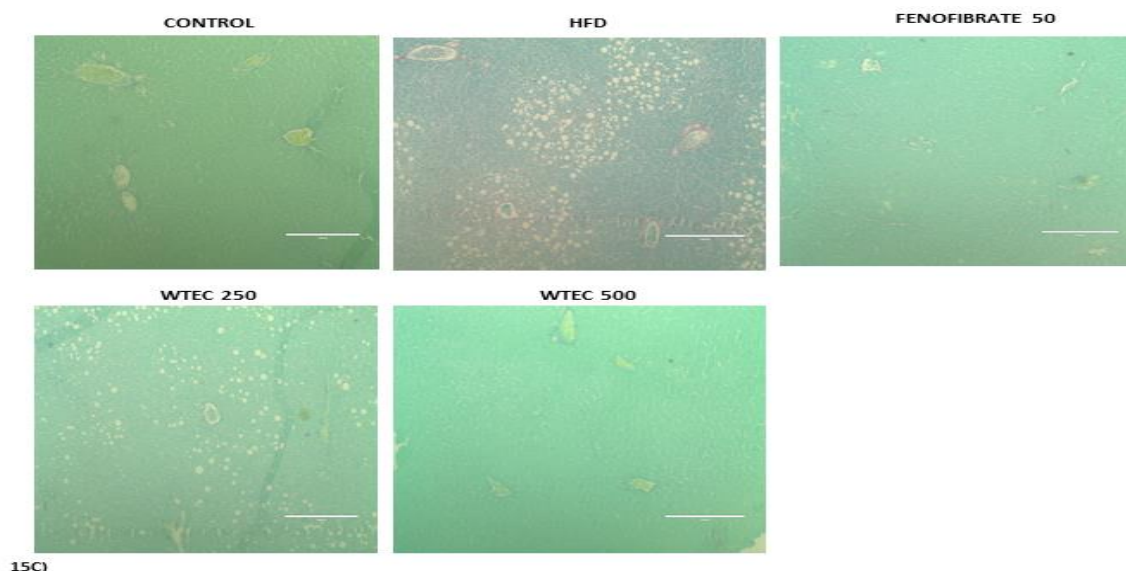


Figure 15: Wrightia reverses histological features of NAFLD and also reduces collagen deposition: H&E staining was done in liver section (15A) and EPF sections (15B) and subsequently evaluated for steatotic features. % of steatotic fat globules were quantitated using Image J software. Picrosirius red-Fast green staining was done in paraffin embedded liver sections to evaluate the effect of WTEC treatment on collagen deposition (15C) Data are expressed as mean \pm SEM and significance was calculated w.r.t. HFD group, using one way ANOVA ****P<0.0001, ***P<0.001, **P<0.01, * P<0.05, ns= non-significant

7.2.13. Effect of wrightia hydroethanolic extract on mitochondrial and cytosolic enzyme activities responsible for maintaining bioenergetic and oxidative status:

Accumulation of excess fat induces a rise in superoxide and other ROS in the hepatocellular environment. NADPH Oxidase is triggered by excessive ROS in distressed hepatocytes and further aggravates the pathophysiological condition by generation of reactive oxygen species. WTEC treatment successfully eliminated this ROS production by cytosolic NADH oxidase enzyme as can be seen by reduced activity in the treatment group measured spectrophotometrically by the method of Reusch and Burger(1974) (Figure 16A).

Pyruvate dehydrogenase is a mitochondrial enzyme mainly responsible for generating acetyl-coA from glycolysis towards TCA cycle and maintaining bio-energetic homeostasis. In the fatty liver, its expression often gets reduced generating an energy void and further deteriorating mitochondrial respiration. In the HFD group of mice, a significant dip in the enzyme activity was noticed in our case whereas WTEC fed group of mice dose-dependently increased its activity while the highest rescue was seen in the fenofibrate group(Figure 16D).

The MRC enzyme cytochrome c oxidoreductase activity was checked as the generation of fatty liver simultaneously destroys the mitochondrial respiratory complexes as a result of mitochondrial dysfunction. Indeed in the HFD group of our experiment, we can see a significant decrease in the activity of both of these enzymes which were dose-dependently rescued by wrightia extracts as well as fenofibrate (Figure 16E)..

Succinate dehydrogenase complex and citrate synthase, important TCA cycle enzyme residing in mitochondria was checked which also showed a dip in activity in the HFD group and efficiently rescued by WTEC 250-500(mg/kg)dose and fenofibrate (50mg/kg) (Figure 16B,C)..

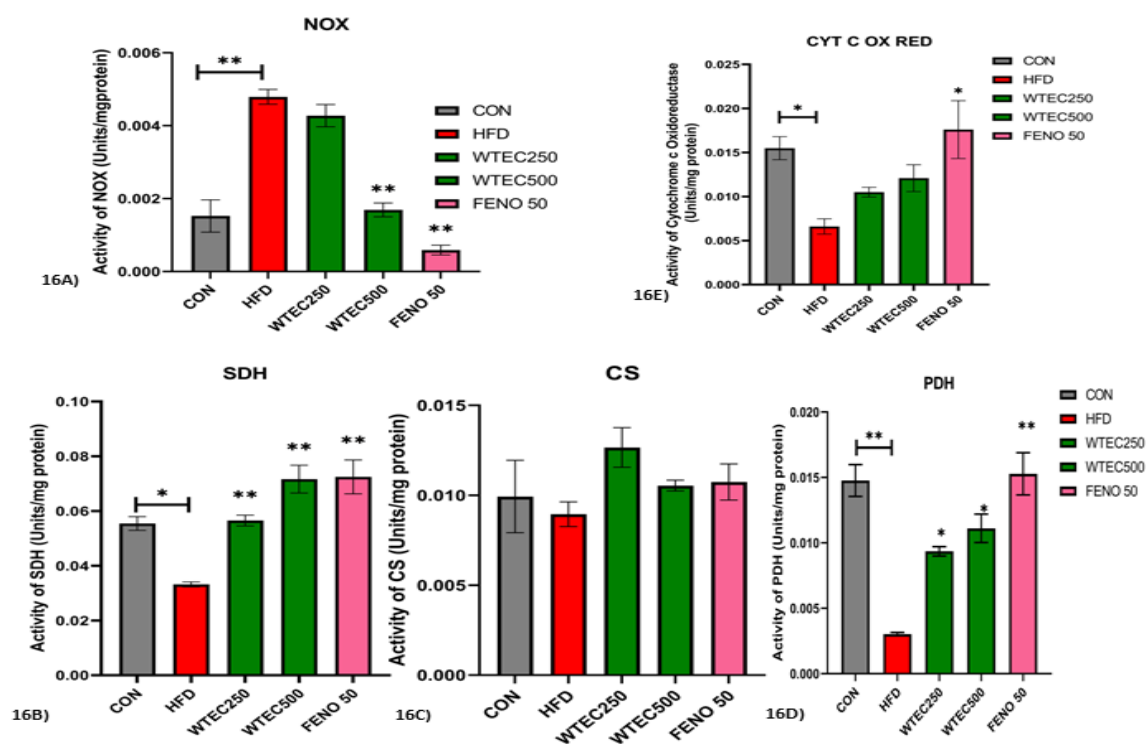
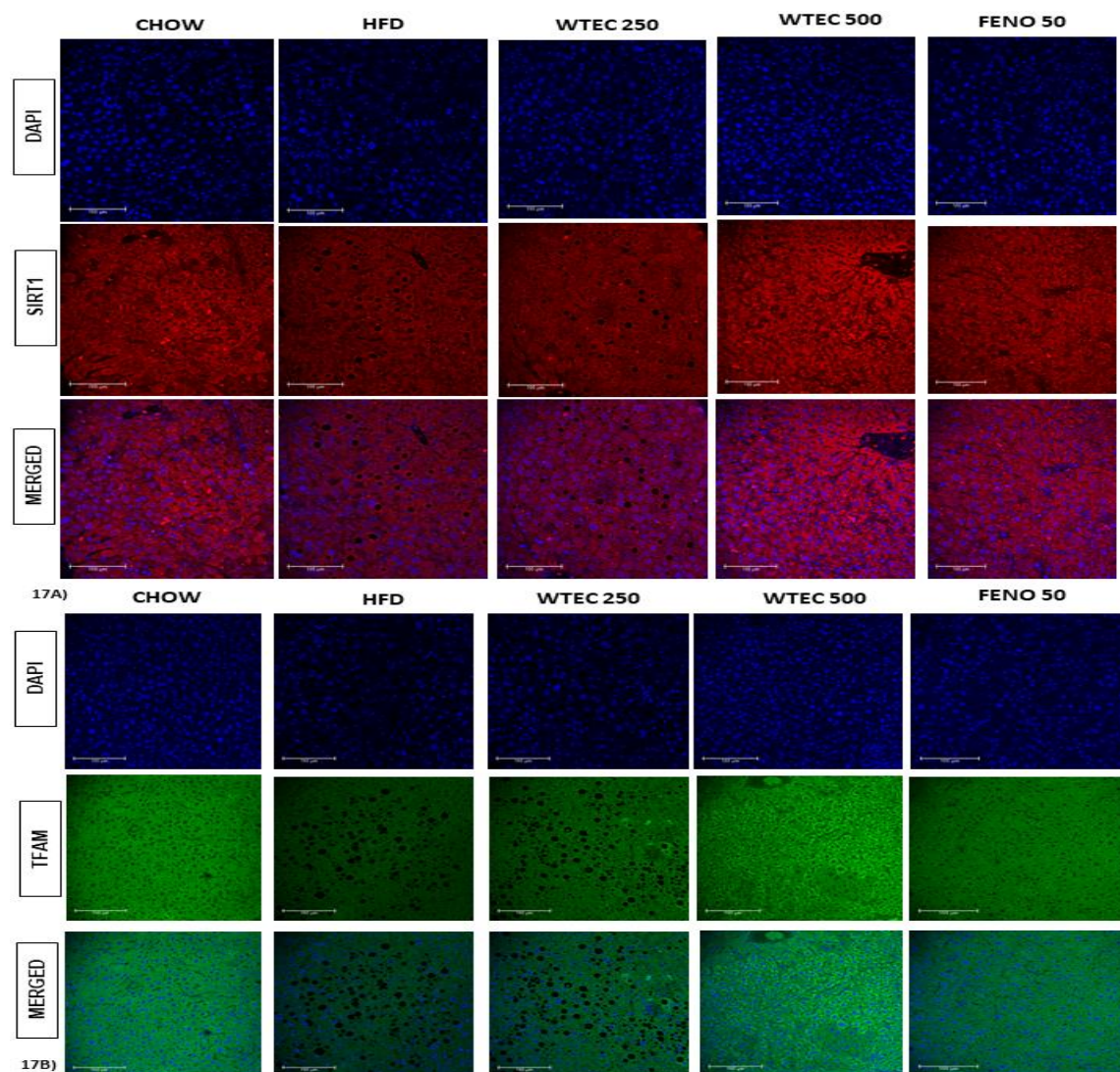


Figure 16: HFD feeding has deleterious effects on mitochondrial and cytosolic enzymes regulating bioenergetics homeostasis which is abrogated by WTEC: NADPH Oxidase enzyme activity were measured spectrophotometrically(16A).Succinate dehydrogenase, Citrate synthase, Pyruvate dehydrogenase enzymes activity were checked in the animal liver tissue spectrophotometrically (16B-D) Cytochrome C oxidoreductase enzyme activities were checked spectrophotometrically in liver tissue mitochondrial fractions. Data are expressed as mean \pm SEM and significance was calculated w.r.t. HFD group, using one way ANOVA ****P<0.0001, ***P<0.001, **P<0.01, * P<0.05, ns= non-significant

7.2.14. Mitochondrial Biogenesis enzyme and autophagy gene expression were increased by WTEC in HFD-fed liver tissue:

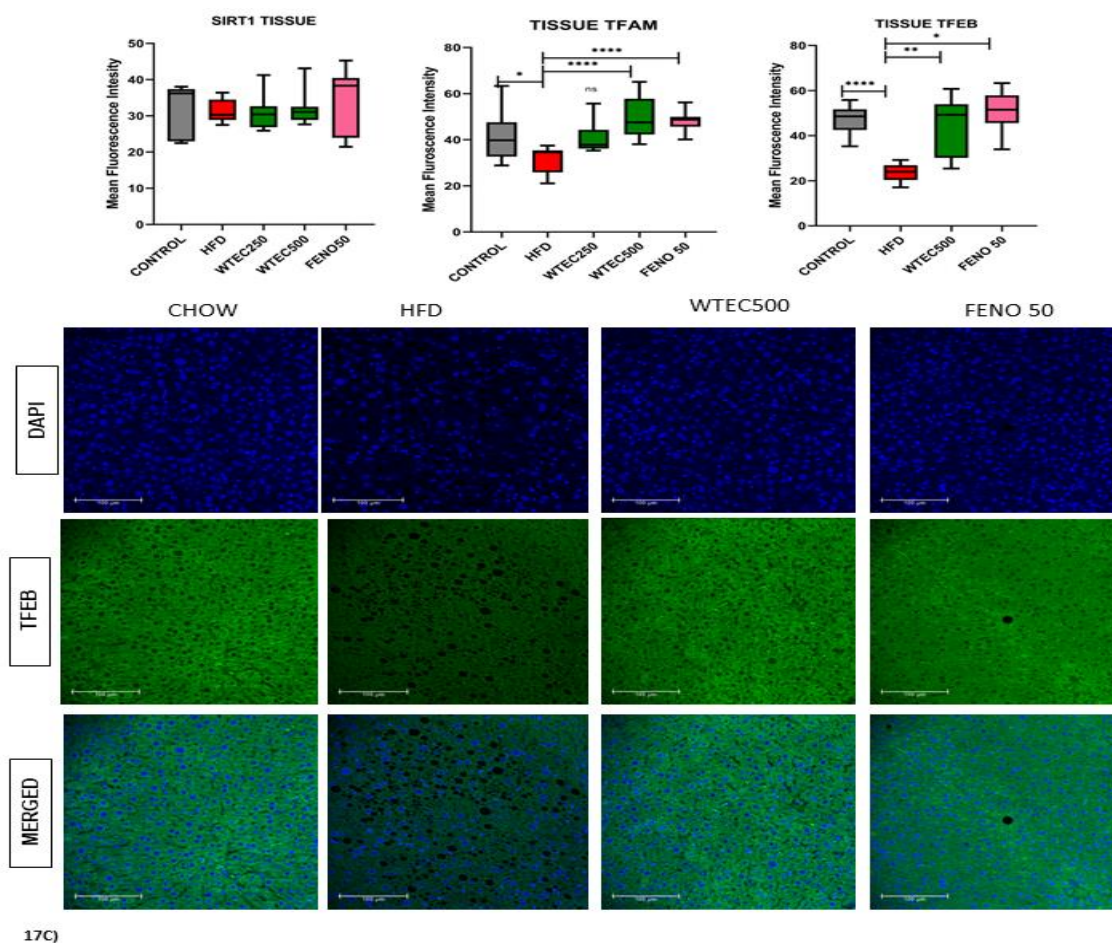
SIRT1 is an important deacetylase that mainly inhibits de novo lipogenesis and increases hepatic fatty acid oxidation which often gets reduced in stressed liver. Fat aggregates cause a reduction of its expression in hepatic tissue but upon activation of AMPK α it

gets induced and impacts beta-oxidation and mitochondrial biogenesis. TFAM is another end-point transcription factor responsible for mitochondrial protein expression and subsequent increase in mitochondrial mass. Both of these protein expressions were checked in liver tissue samples where the fatty liver model group fed with HFD showed a decrease in SIRT1 and TFAM which was intriguingly restored compared to HFD and interestingly in the WTEC 500 dose group was significantly higher than control mice suggesting a positive regulatory role of this extract in mitochondrial biogenesis (Figure 17A,B).



Next, we wanted to validate the activation of autophagic response of wrightia hydroethanolic extract in in the HFD model of fatty liver disease. This time we choose TFEB, a master regulator and major transcription factor of autophagy-lysosomal pathway. As expected highest dose of WTEC (500mg/kg bodyweight) significantly increased TFEB expression while we saw a dip in this transcription factor expression in

HFD mice when compared to the control checked by confocal microscopy. Fenofibrate also produced a commendable response elevating the expression of this transcription factor (Figure 17C).



17C)

Figure 17: Expression of Mitochondrial biogenesis and autophagy related genes were reduced in HFD fed mice group which was reversed and activated by WTEC: Expression of SIRT1 in liver tissue section (Alexa fluor 633) (17A) , TFAM expression (ALexa fluor 488) (17B) and TFEB expression (Alexa fluor 488) (17C) was checked by immunocytochemistry in liver sections by fluorescent tagged antibodies. DAPI was used as nuclear counterstain. Data are expressed as mean \pm SEM and significance was calculated w.r.t HFD group, using one way ANOVA **** $P < 0.0001$, *** $P < 0.001$,

7.2.15. Validation of AMPK α mediated amelioration of mitochondrial dysfunction by WTEC in HFD induced fatty liver model:

It has been already established in our *in vitro* lipotoxicity model that wrightia hydro-ethanolic extract improved deregulated mitochondrial parameters by phosphorylating AMPK α at the location of Threonine 172. In order to confirm WTEC's involvement in AMPK α activation, we wanted to assess phospho-172(Thr) AMPK α expression in HFD model of fatty liver disease. Immunohistochemistry was performed and the result

revealed that expression of this metabolic regulator was much higher in WTEC 500 dose group of mice while several fold reduction was seen in HFD-fed mice compared to control (Figure 18A). Protein expression of transcription factor PPAR α (regulator of lipid metabolism) and CPT1A (fatty acid β -oxidation), CD36 (fatty acid uptake) and MFN1 (mitochondrial fusion regulator) was checked in liver tissue homogenates. P62 is a major protein in autophagy pathway downstream of LC3B and its degradation gives a picture of autophagic flux. WTEC treatment manifested a significant increase in increment of autophagic flux compared to diminished effect in HFD group, re-establishing its involvement in augmented autophagy clearance process(Figure 18B).

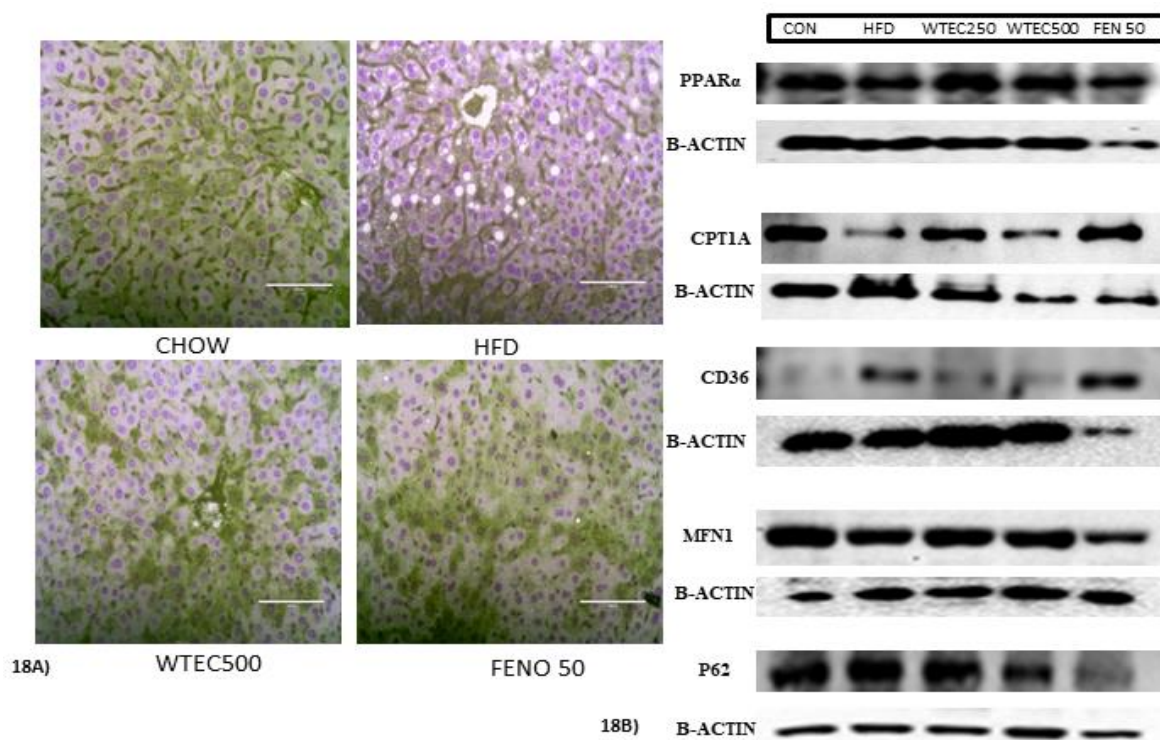


Figure 18: **AMPK α is responsible for WTEC's potential in curing mitochondrial anomalies in NAFLD:** Immunohistochemistry was done to check the expression of phosphor-AMPK α (Thr172) in liver tissue sections in control, High fat group (HFD), Wrightia hydro-ethanolic extract dose of 500mg/kg bodyweight (WTEC500) and fenofibrate fed mice. (18A) Protein expression profile were checked for lipid metabolism genes like (PPAR α , CPT1A and CD36), mitochondrial fusion (MFN1) and autophagic flux (P62) by western blotting. Protein expression was normalized to β -actin.

7.3. Discussion:

Over the past decade we can see an exponential surge in metabolic diseases like Type2 diabetes, fatty liver disease, obesity, pancreatitis, Wilson disease, Graucher disease. Nonalcoholic fatty liver disease is turning to be a global threat because of linked co morbidities like hepatocellular carcinoma, cardiovascular disease and diabetes. NAFLD originates from liver stress injury caused by increase fat accumulation in liver, surge in

cellular oxidant status, insulin resistance, obesity and high load of circulating free fatty acids in system. Hepatic stress often gets resonated in deregulation of lipid homeostasis resulting in generation of oxidative stress and mitochondrial abnormalities. Dysfunctional mitochondrial respiratory chain and diminished oxidative phosphorylation subsequently halts the fatty acid oxidation process while engaging in higher fatty acid uptake and secretion of low density lipoprotein molecules in circulatory system. Higher lipid intake with reduced oxidation results in generation of large lipid droplets and overproduction of mitochondrial ROS. This process in turn translates into net energy crisis, alteration of mitochondrial morphology as well as dynamics and disruption of mitophagy and autophagy processes.

Wrightia tinctoria hydro-ethanolic extract (WTEC) has already been established as a potent antioxidant formulation as well as have an efficient glucose uptake promoting effect. In this part of our study we concentrated on assessing the effect of this extract on debilitated mitochondrial features upon facing lipotoxic stress like NAFLD. Saturated fatty acid overload in hepatoma cells like HepG2 and high fat diet (60%Kcal) feeding in mice serves as a well-established model for lipotoxicity studies. Enhanced lipid accumulation results in generation of ROS and subsequently causes a dip in mitochondrial membrane potential due to depreciated proton leak which was efficiently rescued by WTEC. Palmitic acid treatment in HepG2 cells disrupts the mitochondrial bio-energetic efficiency by destroying mitochondrial respiratory chain(MRC) and OXPHOS enzymes, at the same time cause a substantial increment in glycolysis process. WTEC in dose range of 1 to 10 $\mu\text{g/ml}$ improves the expression of mitochondrial complex II, III and IV in HepG2 cells, rescues the depreciated basal and maximal respiration rate and increases ATP production. Glycolysis rate and glycolytic capacity was also reduced in response to WTEC treatment resulting in overall restoration of mitochondrial respiratory features. WTEC 250mg/kg bodyweight and 500mg/kg doses also rescued the diminished activities of mitochondrial TCA cycle and MRC enzymes as seen by colorimetric enzyme activity assays. PA treatment causes mitochondrial fragmentation as evident from confocal microscopy on HepG2 cells using mitotracker dyes but intriguingly WTEC treatment reverses this phenotype and the normal fibrillar network of mitochondria is re-established. Quantitation of mitochondrial size by different treatments validated this claim.

Altered mitochondrial dynamics by increase in fission process with reduced biogenesis and disturbed fusion is another signature characteristic of NAFLD. We wanted to explore this mechanistic pathway as we speculated WTEC involvement in improving mitochondrial biogenesis and restoring deregulated mitochondrial dynamics. Indeed when we checked PGC1 α and TFAM expression level in PA treated hepatoma cells, mRNA and protein level increased significantly compared to palmitate group. WTEC fed mice group also showed increase in SIRT1 expression in liver section. SIRT1, a major

regulator of lipid metabolism and mitochondrial biogenesis also showed a reduction in expression in palmitate treated cells and HFD fed mice. WTEC treatment in both cases improved the condition by up regulating SIRT1 expression. DRP1 and phosphorylation on its serine 616 residue is an important mandate for mitochondrial fragmentation by fission process. WTEC dose dependently abrogated this phosphorylation status and improved the diminished pphspho-DRP1/totalDRP1 ratio. Hydro-ethanolic extract with a dose of 5 and 10 µg/ml positively modulated the fusion protein expression MFN 1 and 2. Thus we can suggest that WTEC when given lipotoxic stress increases mitochondrial biogenesis and inhibits mitochondrial fragmentation creating a fused network of mitochondria and restores ATP balance (Bio-energetic homeostasis).

Not only prevention of fragmentation process but a well-regulated clearance of damaged mitochondria by efficient mitophagy and autophagy process helps in maintenance of cellular homeostasis. In NAFLD, obesity and associated metabolic diseases this regulation often gets disturbed. In fatty liver this inefficiency translates into increased ROS generation, inflammation leading to progression towards steatohepatitis. We checked for this aspect in mitochondrial dysfunction and evaluated effect of WTEC in this process if any. Surprisingly WTEC improved the mitophagy process as seen by increase in PARKIN and PINK1 expression. Not only these when we did a detailed time kinetic study we knew in the early hours after PA treatment (4 to 12 hour) WTEC enhances PARKIN expression and in later time (18-24 Hours) a surge in LC3B expression as well as LC3B-mitochondrial colocalization increases. This interesting data suggests a well regulated involvement of WTEC mediated mitophagy-autophagy mechanism ultimately resulting in amelioration of mitochondrial dysfunction and improvement of nonalcoholic fatty liver disease.

AMPK α being the major metabolic regulator of cell regulates mitochondrial biogenesis and autophagy process. Upon checking the expression of this master regulator we saw an increase in the phosphorylation status of Threonine 172 residue of AMPK α while it was severely reduced in palmitate group and HFD mice. WTEC dose dependently increased this expression and when it was blocked by AMPK inhibitor compound C, all the good effect vanished. Inhibition of AMPK α resulted in decreased expression of SIRT1, PPAR α as well as LC3B, suggesting the activity of *Wrightia tinctoria* hydro-ethanolic extract is regulated by AMPK α .

Thus from these experiments involving *in vitro* and *in vivo* model of NAFLD, we can suggest that *Wrightia* hydro-ethanolic extract (WTEC) showed a promising effect in alleviating mitochondrial dysfunction and associated metabolic perturbations in fatty liver by increasing mitochondrial biogenesis, maintaining dynamics and improving mitophagy process.

Chapter 3

Role of *Wrightia tinctoria* seedpod extracts in mitigating inflammation and characterization of compounds:

8.1. Introduction:

Inflammation has been playing a pivotal role in the pathophysiology of plethora of diseases and emerges as a potential risk factor in the development and progression of several pathogenic manifestations. Starting from Cancer, Arthritis, Chronic obstructive pulmonary diseases, Diabetes, Alzheimer's, and Parkinson's to emerging as the main pathogenic factor in various bacterial, and viral infestations in the human body (Tsalamandris et al., 2019; Alfaddagh et al., 2020). Inflammation has long been in the background or forerunner in the expansion or maturation of ailments and is also involved in various physiological processes maintaining cellular homeostasis hence posing a great challenge to the medical research fraternity. Nuclear factor kappa-B (NF- κ B), P38MAPK, STAT-like transcription factors and their gene products like COX-2, PGE2, various cytokines and chemokines like TNF- α , IL-1, IL-6, IL-8, IL-10 and C-reactive protein (CRP) to name a few, are the major effectors controlling the whole circuit of inflammatory network in the human body. Inflammation is a major driver of the propagation of NAFLD towards NASH and subsequent cirrhosis of the liver. Several intra and extra-hepatic alterations and complicated metabolic abnormalities cause a surge in inflammation by means of overactive immune effector cells. Various synthetic chemical compounds are majorly prescribed to mitigate the acute and chronic effects like steroids, immunosuppressants, analgesics, and non-steroidal anti-inflammatory drugs (NSAIDs) which bear a plethora of side effects and remission chances. So to limit the uses of these synthetic pills often researchers point out alternative and traditional medicine to harvest the best possible pharmacogenic effect with minimal complications. Plants like *Curcuma longa*, *Zinzibar officinalis*, and *Rosamarinus officinalis* to name a few which is long been used as a potent sources of anti-inflammatory phytoconstituents (Rodríguez-Yoldi, 2021, Azeez & Lunghar, 2021, Shimoda et al., 2010). *Wrightia tinctoria* is a well-acknowledged medicinal herb mainly used in psoriasis, jaundice, diarrhea, and diabetes in Ayurvedic and traditional medicine (Anusharaj; et al., 2013). Some researchers have also pointed out the anti-inflammatory properties of its leaves and bark but no such literature was found giving mechanistic evidence of this plant's seedpod which is often consumed by the Asian population as a herbal medicine (Aleykutty et al., 2011).

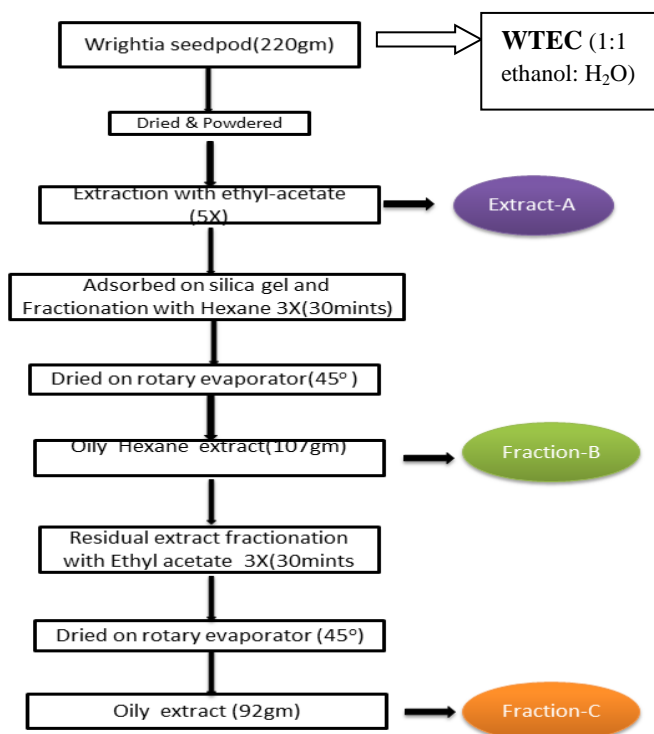
In previous sections, we have reported about the hepato-protective, lipid-lowering, and insulin resistance mitigating properties of wrightia seedpods along with providing a mechanism of action largely exploring the effect on mitochondrial physiology and metabolism. Here in this part we will embark on inspecting the anti-inflammatory potential of seedpods of this plant and try to decipher the identity of the phyto-compounds mainly exerting its therapeutic effect. While screening different seedpod extracts we observed a good response from non-polar fraction of the seeds showing effects against oxidative and nitrosative stress while being non-cytotoxic against

hepatoma cells. Here we will engage to investigate the anti-inflammatory role and possible mechanism of action of extracts of wrightia seedpods and dig towards the exploration of responsible phyto-constituents, giving us a certain lead about the development of a therapeutic lead against pathogenic pro-inflammatory conditions.

8.2. Results:

8.2.1. Extraction and isolation procedure of extracts from *Wrightia* seed pods:

To explore the anti-inflammatory effects of the seed pods we wanted to play around the polarity of solvents for the extraction process increasing the efficacy of partitioning and enrichment of the constituting phyto-compounds. Besides the already bio-active hydro-ethanolic (50:50) extract (WTEC) we employed extraction with ethyl acetate and the fractionation with hexane and the residual with ethyl acetate again to get the most of the non-polar compositions. The extraction process is depicted in the flowchart.



In short, the seed pods were ground into a coarse powder and extracted with ethyl acetate. The filtrate was combined and evaporated to obtain a greenish oily extract. A portion of the extract was adsorbed on silica gel (100-200 mesh) and eluted with hexane and ethyl acetate to obtain a hexane and ethyl acetate fraction. The eluent was dried and

Ext-A: Initial ethyl acetate extract

Fr-B: Hexane fraction

Fr-c: Ethyl acetate extract

8.2.2. Evaluation of cytotoxicity of seedpod extracts in macrophage cells by MTT assay:

The RAW264.7 macrophage cell line was employed to measure the cell viability in order to assess the cytotoxic effect of the extract and fractions using MTT assay. The results demonstrate that in a broad range of concentrations between 10µg/ml and

500µg/ml for 24 hours, none of the three extracts or fractions had any detectable cytotoxic impact. In most of the doses till 200µg/ml $\geq 90\%$ viability was seen and at the highest concentrations (500 µg/ml) some loss of viability (15-20%) was observed with respect to untreated control. (**Figure 1A**) So following these data on macrophage cells with no such significant toxicity or inhibition of growth ($IC_{50} > 500 \mu\text{g/ml}$) wrightia extracts were termed as safe and further exploration of bioactivities was conducted.

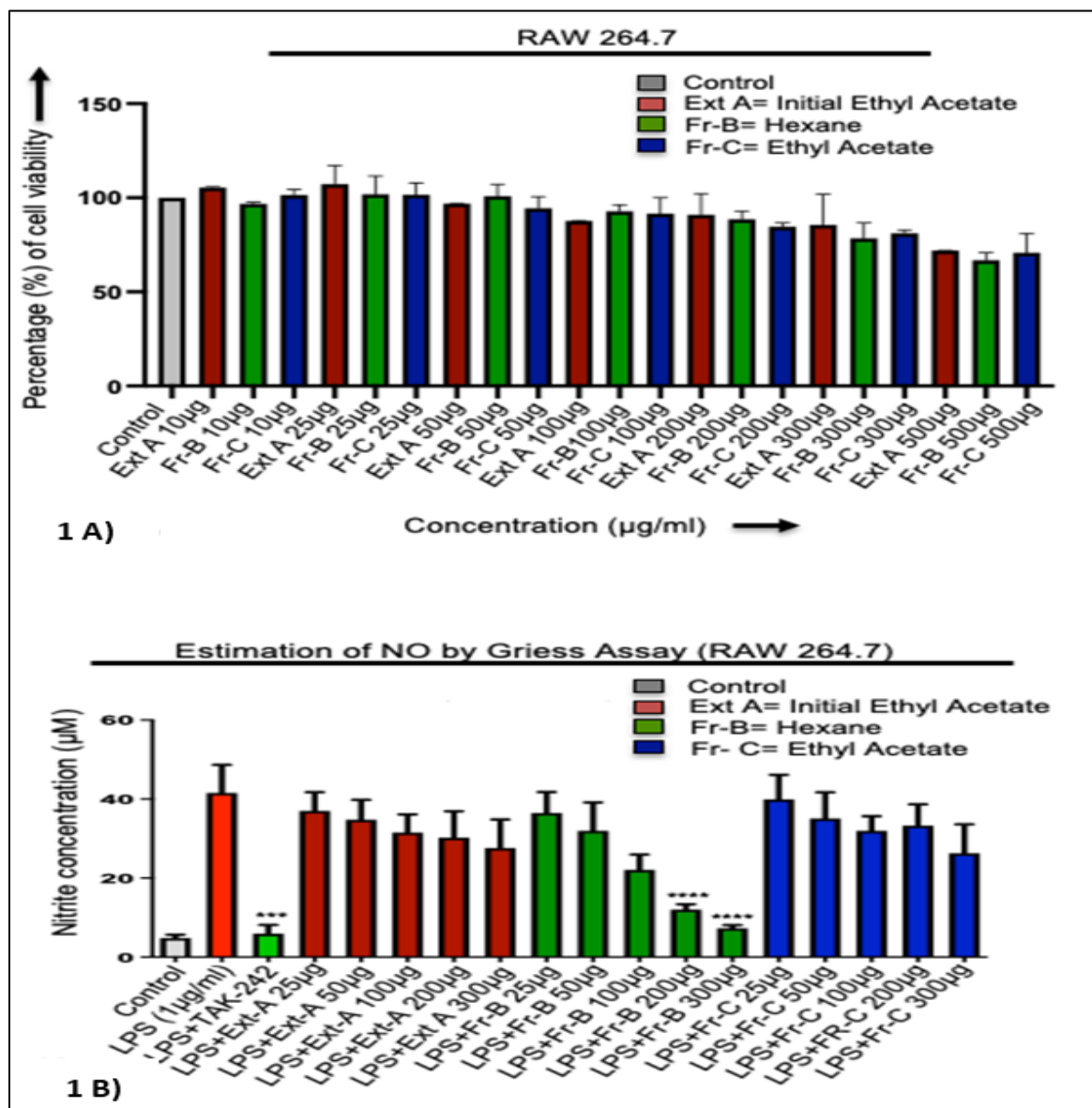


Figure 1: Evaluation of cytotoxicity of Initial ethyl acetate extract (Ext-A), Hexane fraction (Fr-B) and Ethyl acetate fraction (Fr-C) on RAW264.7 macrophage cells by MTT assay. B) Estimation of nitric oxide formation inhibitory potential of three extract and fractions by Griess assay. Data are expressed as mean \pm SEM and significance was calculated using one way ANOVA **** $P < 0.0001$, *** $P < 0.001$, ** $P < 0.01$, * $P < 0.05$, ns= non-significant

Using Griess reagent on RAW264.7 murine macrophage cells, we first examined the effect of the extract/fractions on suppression of cellular nitrates and nitrites (RNS) generated by LPS (*E. Coli* LPS, Sigma) stimulation (1µg/ml) for 22 hours. A standard curve was created using a variety of sodium nitrite concentrations, and a decrease in RNS level was found to be connected with a decrease in cellular nitrite level. According to our results, the hexane (Fr-B) fraction pre-treatment considerably lowers RNS production with an IC₅₀ dose of 139.83 µg/ml in comparison to the other fraction (Fr-C; IC₅₀: 428.71 µg/ml) and ethyl acetate extract (Ex-A; IC₅₀: 422.93 µg/ml). (**Figure 1B**)

8.2.3. Role in inhibition of total cellular oxidative stress:

The inflammatory signaling pathway is primarily regulated by reactive oxygen species (ROS) such as superoxide and H₂O₂, as well as reactive nitrogen species (RNS) such as nitrates, nitrites, and peroxy nitrites. This is particularly relevant when it comes to NFκB activation. We used DCFH-DA flow cytometry to measure the total cellular ROS level after pre-treating cells with the extract/fraction and 16 hours after LPS treatment. The outcome demonstrates that, in RAW264.7 macrophage cells, Fr-B dramatically decreased the amount of total cellular ROS at a dose of 200µg/ml (Fig 2A). But Ex-A and Fr-C did not reduce so as effectively, suggesting that Fr-B is typically more effective. TAK242, a TLR-4 inhibitor was introduced as a positive control which effectively reduced the ROS production as monitored by reduced fluorescence with respect to LPS group. (**Figure 2A**)

As a result of Fr-B's strong ability to reverse the increased levels of ROS and RNS that were caused by LPS, we looked into the expression levels of proinflammatory cytokines such as IL1 beta. We chose the dose of 200 µg/ml for further confirmatory anti-inflammatory investigations as the IC₅₀ dose of Fr-B was found to be 139.83 µg/ml in the Griess Assay (inhibition of RNS), which was also validated by the DCFH-DA assay (inhibition of ROS).

8.2.4. Evaluation of reduction in pro-inflammatory cytokines expression by ELISA and RT-PCR:

Inflammatory cytokines are the main effectors of aggravated immune responses. Real-time qPCR analysis was employed to verify the intracellular mRNA expression for IL-1β. After 16 hours of LPS induction, Fr-B (200 µg/ml) treatment significantly reduced the production of pro-inflammatory cytokines, such as IL1 beta, in RAW264.7 macrophage cells (**Figure 2C**). A sandwich ELISA technique was also used to determine the amount of secreted IL-1beta protein in the cultured cell supernatants after respective stimulations and pretreatment with fractions for 6 hours. Upon subjecting RAW264.7 cells to LPS induction (1µg/ml) for 6 hours, the results show a significant drop in the concentration of secreted IL-1beta protein expression with respect to increased expression in LPS stimulated cells (**Figure 2B**). TAK242 2µM was employed as positive control which countered the LPS effect by several folds as a TLR-4 inhibitor.

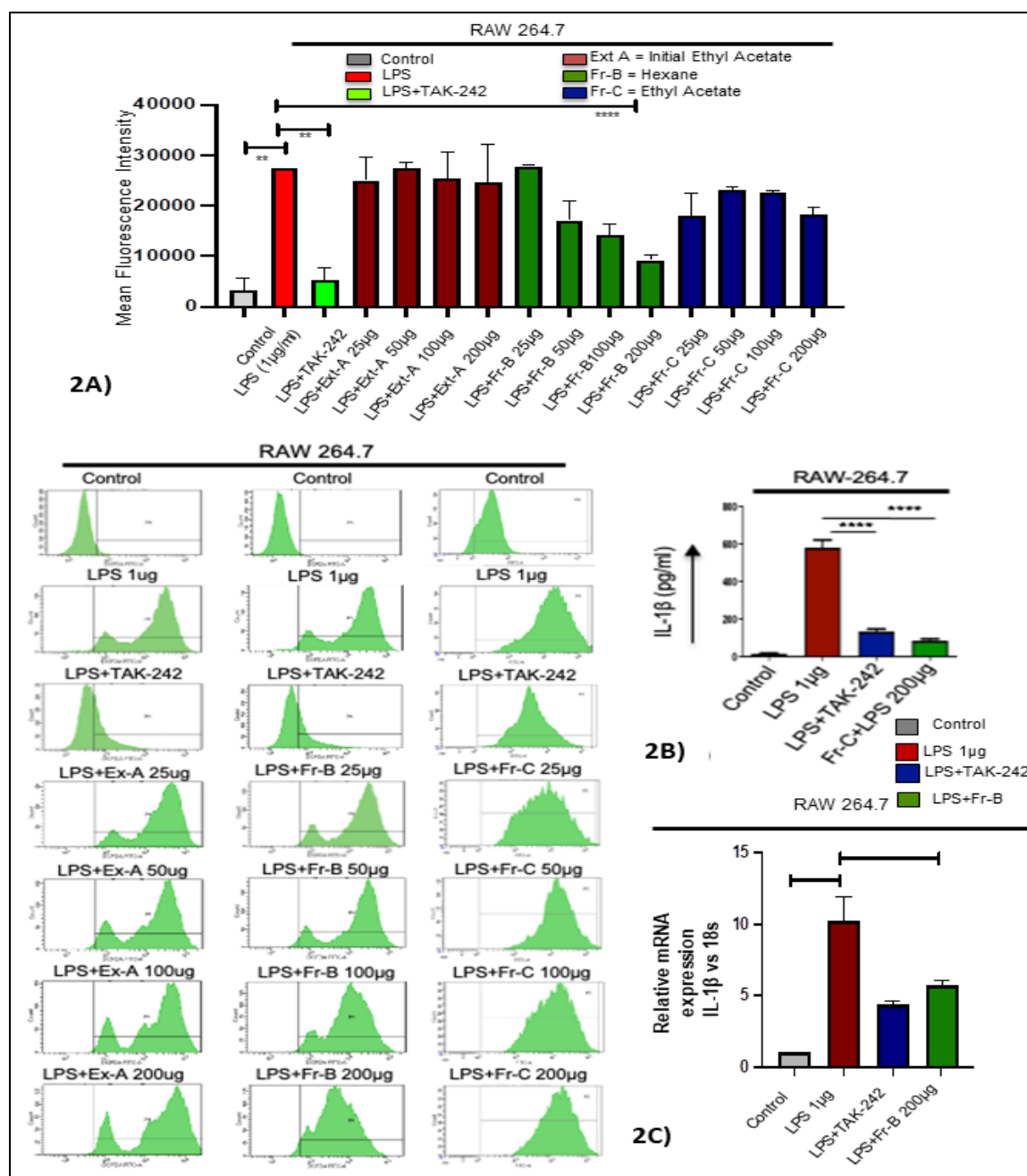
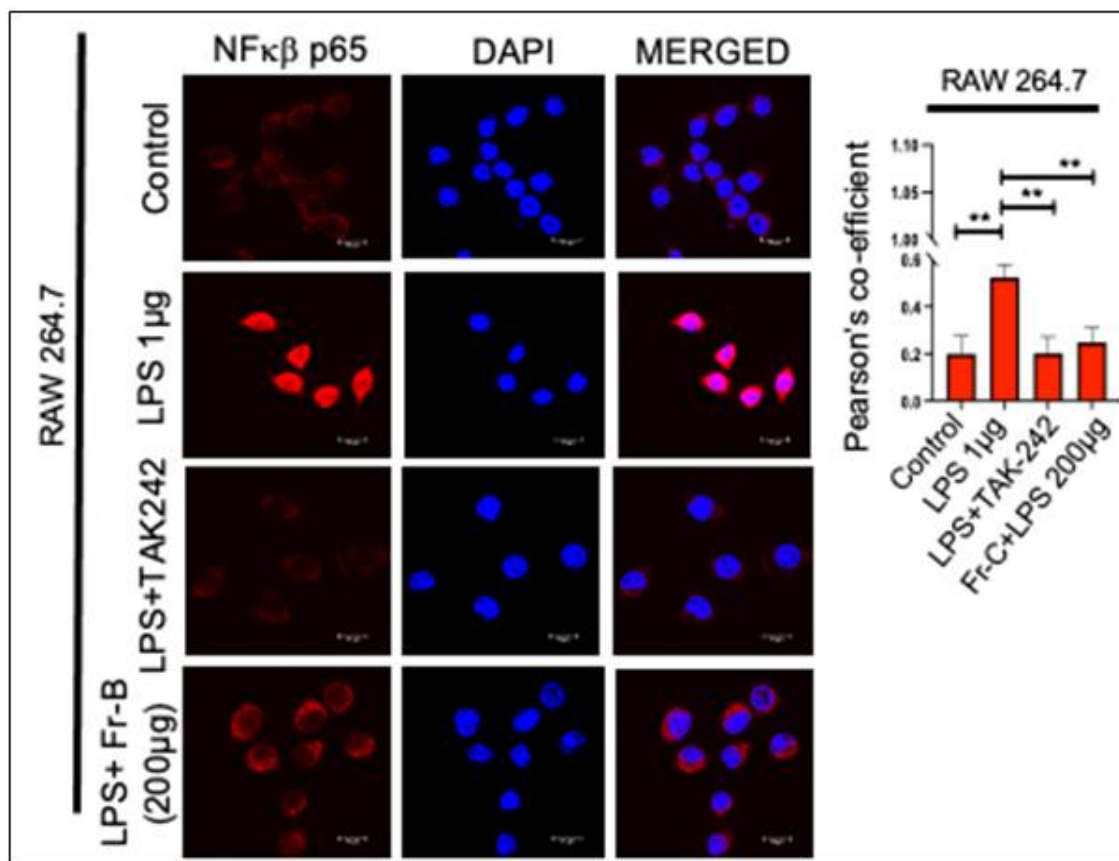


Figure 2: 2A) Estimation of total cellular ROS by DCFHDA fluorescent probe in LPS treated macrophage cells after pretreating with extract/fractions. 2B) Quantification of secreted IL-1 β from RAW264.7 cell culture sup after pretreating with Fr-B and stimulation with LPS by ELISA technique 2C) Quantification of intracellular IL-1 β mRNA by real time PCR technique in RAW cells. Data are expressed as mean \pm SEM and significance was calculated using one way ANOVA ****P<0.0001, ***P<0.001, **P<0.01, *P<0.05, ns= non-significant

Previous studies have shown that LPS operates via a route regulated by TLR4, in which NF κ B plays a key transcriptional role in the downstream signaling cascade of

inflammation. Following proteasomal degradation-induced activation, NF κ B p65 translocates into the nucleus where it controls the transcription of many inflammatory pathway genes, inducing the release of proinflammatory cytokines such as TNF alpha, IL-6, and IL1beta. In accordance with this, we examined the impact on the total expression of NF κ B by administering hexane (Fr-B) fraction (200 μ g/ml) to RAW264.7 cells and stimulating them with LPS (1 μ g/ml) for 16hours. Confocal microscopy analysis of the cells revealed a notable suppression of expression and nuclear translocation in RAW264.7 cells. (**Figure 3A**)



3A)

Figure 3: Detection of NF κ B expression and nuclear translocation by confocal microscopy in RAW 264.7 macrophage cells after LPS stimulation for 16 hours with pre-treated Fr-B (200 μ g/ml) Data are expressed as mean \pm SEM and significance was calculated using one way ANOVA
 ****P<0.0001, ***P<0.001, **P<0.01, * P<0.05, ns= non-significant

8.2.5. Anti-inflammatory activities of hydro-ethanolic extract (50:50) of wrightia seedpods:

Wrightia hydro-ethanolic extracts (WTEC) showed notable effects in improving mitochondrial health while simultaneously augmenting the hepato-protective role by altering metabolic status and cellular homeostasis. While inflammation plays a crucial role in the expansion of the deleterious effects of steatotic fatty liver disease a proper evaluation of the anti-inflammatory role by reduction in aggravated cytokine responses simultaneously managing the regulatory transcription factor NF κ B expression as well as translocation to the nucleus. The expression of NF κ B and subsequent secretion of pro-inflammatory cytokines like IL1 β and IL-6 were tested in HepG2 cells upon palmitic acid-mediated lipotoxic stress.

Concentrations of secreted cytokines in cell soup after stimulation with PA in WTEC pretreated hepatoma cells were measured by ELISA where fenofibrate was used as a reference drug. Palmitic acid induced 3.5 fold and 2.5 fold increase in IL1 β and IL-6 concentration respectively. Pretreatment with different doses of hydro-ethanolic extracts reduced the secretion of pro-inflammatory cytokines. WTEC at doses of 1 and 5 μ g/ml decreased almost 65% and 87% of secretion of IL1 β related to the palmitate group whereas it decreased 72% and 94% of IL-6 secretion. **(Figure 4A,B)** Fenofibrate, a PPAR alpha agonist and a reference drug for NAFLD at a dose of 25 μ M attenuated 65% of inflammatory cytokine IL1 β . NF κ B, being the central modulator of the inflammatory signaling pathway acts as a crucial transcription factor altering the expression and secretion of several pro or anti-inflammatory signals. So evaluations of this milestone regulator give an overall estimate of the inflammatory milieu inside the cell and simultaneously validate the role of extracts in maintaining the immune-redox balance after any pathological inflammatory insult. After 400 μ M of saturated fatty acid stimulation due to lipid overload a TLR-4 mediated and IRE1 α mediated response is generated which translates into elevated NF κ B expression(3.5 fold) as measured by intracellular mRNA by RT-PCR but different doses of WTEC dose-dependently decreased 60-75% of expression compared to fat stimulation(**Figure 4C**). The protein expression level was also checked in treated cell lysate which also corroborated the same trend as mRNA by decreasing the protein level of NF κ B dose-dependently. Besides transcription and protein expression of this transcription factor (NF κ B), a nuclear translocation of a stimulatory effector fragment of this protein (p65-NF κ B) broadly manages the downstream gene regulation of immune pathways. So we checked the nuclear translocation of the effector p65 subunit by confocal microscopy in HepG2 cells after pretreatment with WTEC followed by PA stimulation for 24 hours **(Figure 4D)**. A significant portion of NF κ B signal seemed to translocate inside the nucleus as measured by Pearson's correlation co-efficient but treatment with WTEC significantly abrogated

the translocation as well as overall NF κ B expression signal at par with fenofibrate (**Figure 4E**), thus establishing its anti-inflammatory effect by regulating NF κ B.

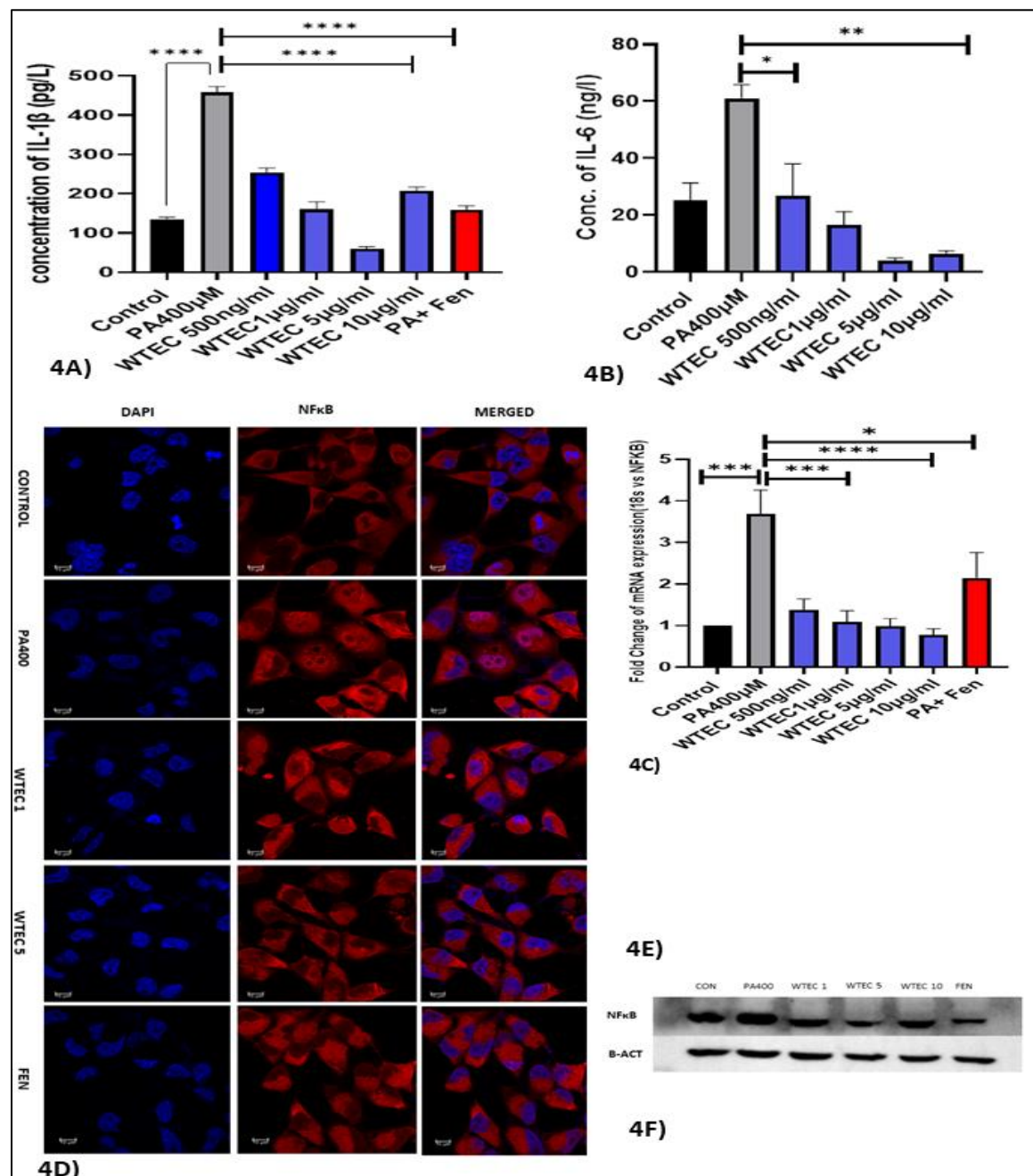


Figure 4: A,B) Estimation of secreted IL-1 β and IL-6 concentration from HepG2 culture supernatant after employing fatty acid stress with PA (400 μ M) for 24 hours with pretreatment of WTEC (1 μ g/ml and 5 μ g/ml) concentration by ELISA method C) Relative mRNA expression detected by qPCR analysis of NF κ B gene in HepG2 cells. D) Confocal image showing nuclear translocation and expression of NF κ B tagged with alexa fluor 633 E) western blot images showing the expression profile of NF κ B after treatment with increasing concentration of WTEC. Data are expressed as mean \pm SEM and significance was calculated using one way ANOVA ****P<0.0001, ***P<0.001, **P<0.01, *P<0.05, ns= non-significant

8.2.6. Characterization of phytoconstituents present in hexane fraction (Fr-B) and hydro-ethanolic extract of *Wrightia tinctoria*:

The non-polar active hexane fraction was subjected to GC-MS analysis and further characterization was done by ^1H NMR at 600 MHz and ^{13}C NMR at 150 MHz.

For the GC-MS study, mass spectrum data were recorded for the investigation using a Shimadzu GC-MS model GC-2010 plus and a GCMS-QP2020 mass spectrometer. An SH-Rtx-5 capillary column was used for the analyses, and helium was employed as the carrier gas. The sample was inserted into the GC inlet at a split ratio of 1:20 and a temperature of 270°C. At 70 eV, compounds were ionized using the electron ionization mechanism.

The NMR spectra were acquired using CDCl_3 as the solvent (δH 7.26, δC 77.22 ppm) on a Bruker Ultrashield 600 MHz (^1H at 600 MHz and ^{13}C at 150 MHz) spectrometer. Chemical shifts are presented in parts per million (ppm) with reference to 0.0 ppm for tetramethylsilane (TMS), which was employed as the internal standard. Chemical shifts documented in the literature (Lie Ken Jie et al., 1997; Park et al., 2014; Sung Ok Lee et al., 2004; Uranga et al., 2016; Knothe & Kenar, 2004; Alexandri et al., 2017) further corroborated the presence of the compounds proposed by GC-MS.

The GC-MS analysis indicated the existence of some significant peaks, which comparing the reference were marked as mainly octadecanoic acid ethyl ester, hexadecanoic acid, ethyl hexadecanoate, 9,12-octadecanoic acid, 9,12,15-octadecatrienoic acid, ethyl linoleate, and 9,12,15-octadecatrienoic acid ethyl ester as summarized in the chart. (GC-MS analysis part of work is taken from the Ph.D. thesis titled "Understanding the mechanism of insulin resistance and its downstream complications" by Eshani Karmakar, Dept of Biochemistry, University of Calcutta as a reference to show the presence of compounds speculated for non-polar hexane fraction) (**Figure 5A, B**).

Fr-B's NMR spectroscopic investigation helped to confirm the identity of the compounds tentatively indicated by GC-MS analysis. Fr-B's ^{13}C -NMR spectrum showed the existence of recognized compounds at δC 179.28-172.89 (-COOH or COOR; R= -CH₃ or -CH₂-CH₃), 131.99-127.19 (-C=C-), 68.98, 62.13 (-COOR; -CH₃ or -CH₂-CH₃), and 34.78-14.18 (-CH₂- or -CH₂-CH₃). According to Knothe & Kenar, 2004, Lie Ken Jie et al., 1997, Uranga et al., 2016, Alexandri et al., 2017, the ^1H -NMR spectra showed similar signals at δH 5.399-5.239 (-CH=CH-), 4.300-4.119 (-COOR; -CH₃ or -CH₂-CH₃), and 2.803-0.668 (-CH₂- or -CH₂-CH₃) (**Figure 6A,B**).

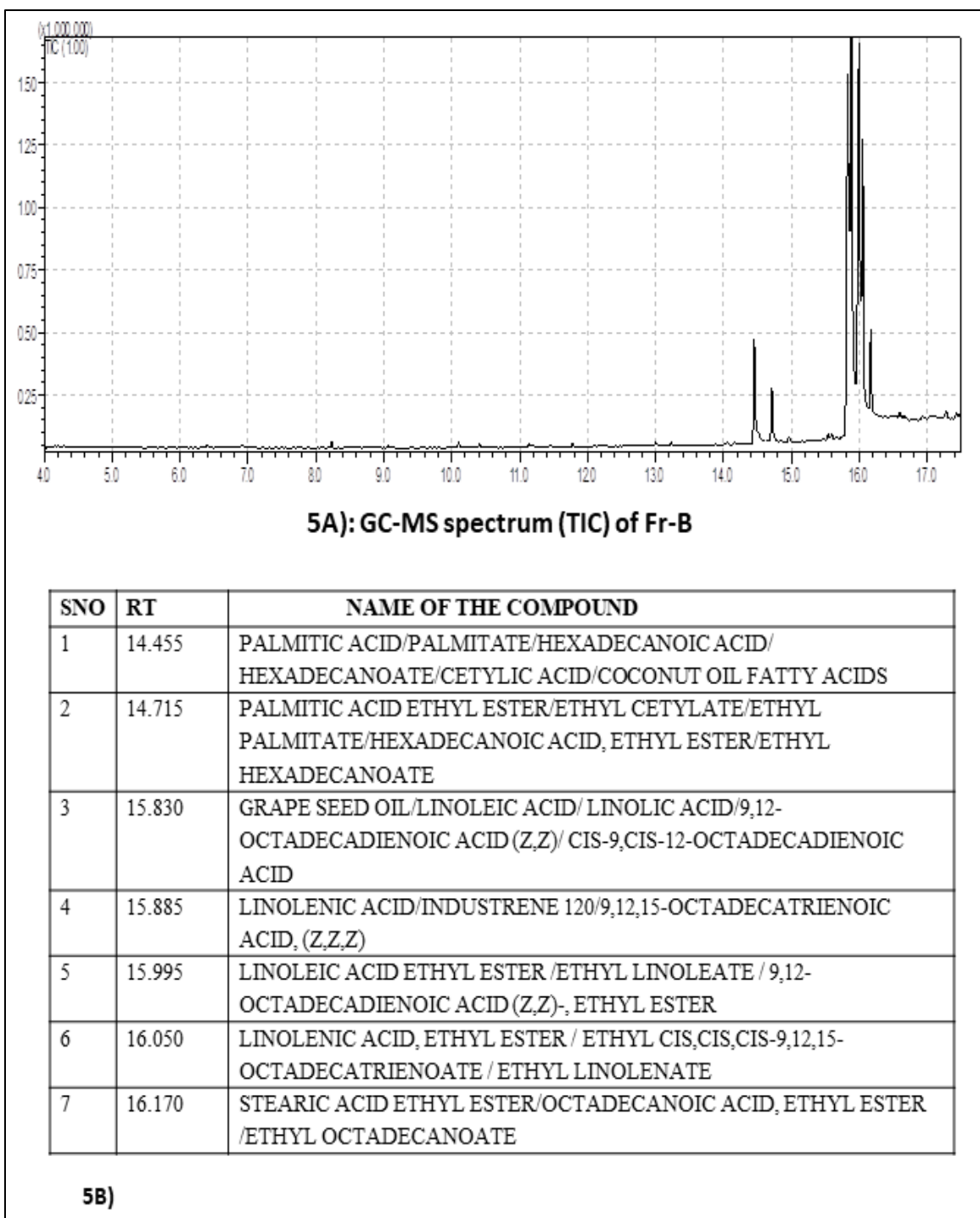


Figure 5: A) GC-MS spectrum (TIC) of Fr-B (Hexane fraction) B) List of compounds as matched from similarity check profile of GC-MS profile analysis non polar hexane fraction (GCMS profile and data for compiled list were taken from Karmakar, Das et al 2023 doi: 10.1080/14786419.2022.2146688. for reference.

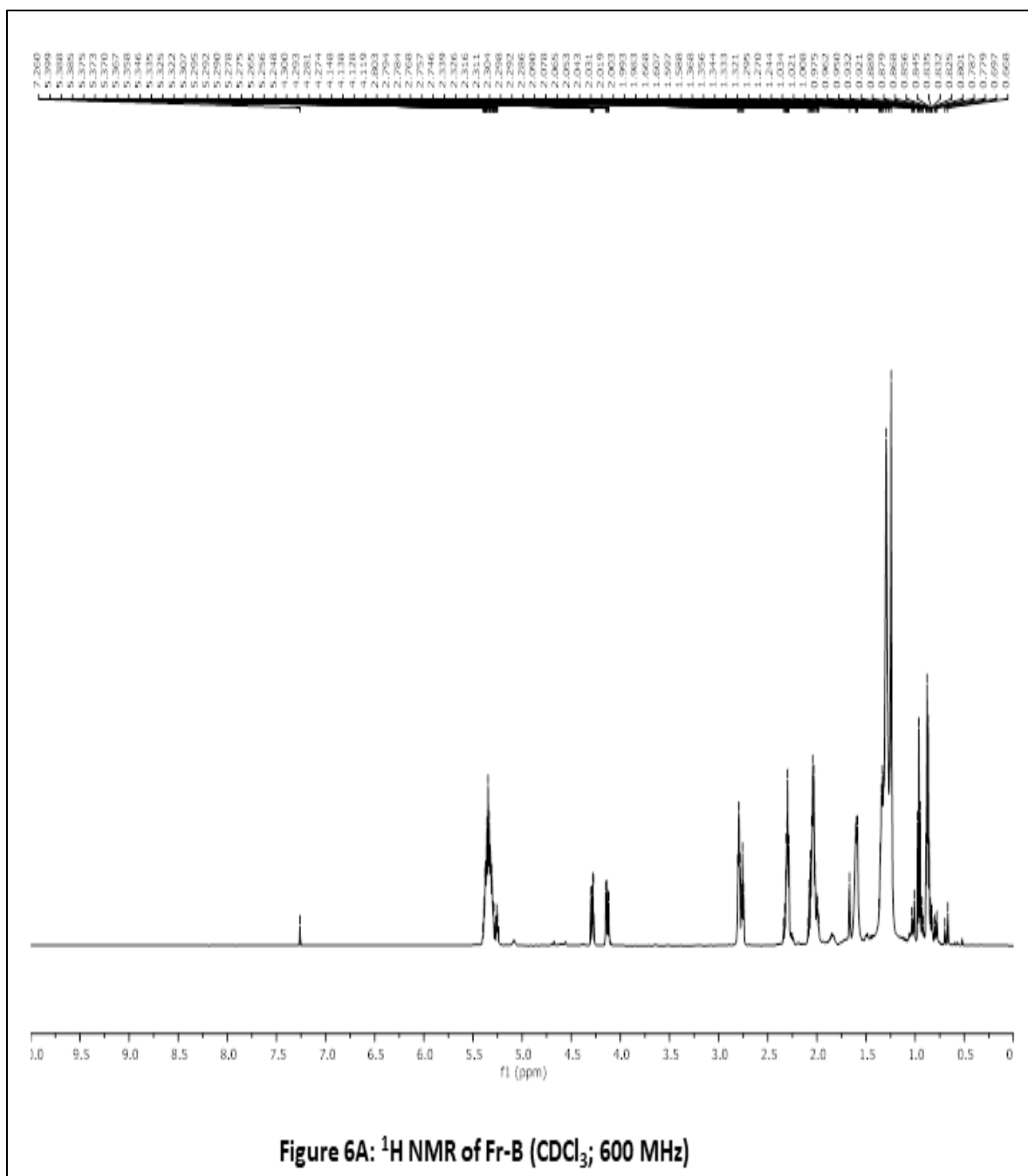


Figure 6A: ^1H NMR (CDCl_3 ; 600 MHz) profile of of Fr-B (Hexane fraction)

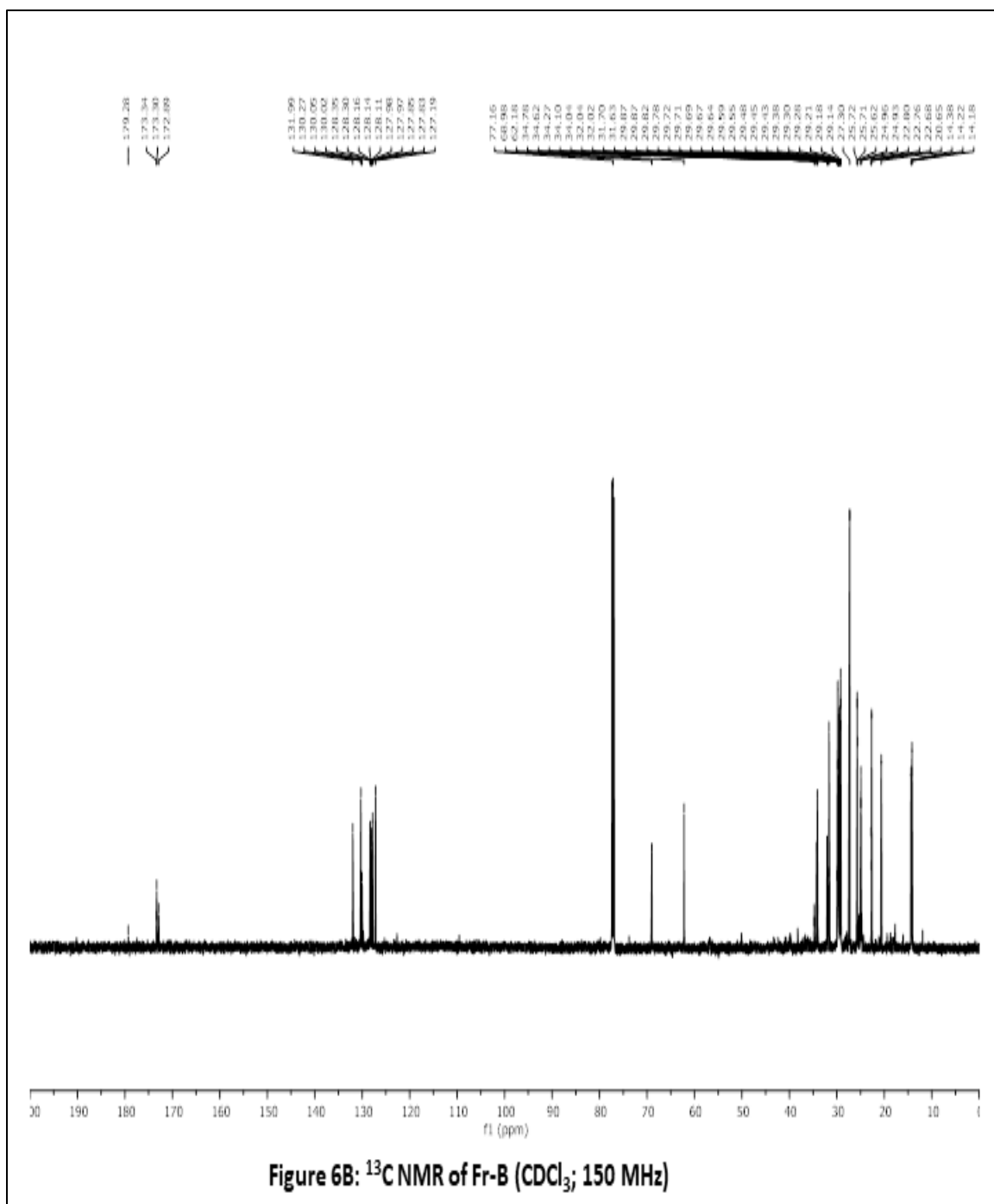


Figure 6B: ^{13}C NMR (CDCl_3 ; 150 MHz) profile of Fr-B (Hexane fraction)

8.2.7. Characterizations of wrightia hydro-ethanolic extract (WTEC) and identification of probable compounds responsible for effect:

Hydro-ethanolic extract (WTEC) of *Wrightia tinctoria* was the most potent one among all the extracts tested in our experiments to alleviate the effect of lipotoxic stress in hepatoma culture and in-vivo NAFLD model. The overall characterization of this extract by orbitrap mass spectrometer and possible identification by NMR was done to pinpoint the responsible class of compounds probably exerting the already testified bio-activity.

Methods:

Extraction: Coarsely powdered seeds of *Wrightia tinctoria* were successively extracted with the solvents of increasing polarity i.e. hexane, ethanol, ethanol-water (50:50 v/v), and water (48 hrs). The obtained extracts were evaporated under reduced pressure at 45-48°C to obtain solvent-free residues. **HPLC Method:** The obtained fractions were analyzed by HPLC (Ascentis RP18, 25 cm x 4.6 mm, 5 µm Supelco column; mobile phase A: water containing 0.1 % formic acid and B: acetonitrile, 0-1 min 90:10 v/v; 1-20 min 5:95 v/v; 20-25 min 5:95 v/v; 25-26 min 90:10 v/v and 25-30 min 90:10 v/v at 254 and 210 nm. **LC-MS conditions:** *UPLC conditions:* Ultimate 3000 Thermoscientific Quaternary pump, C18 Hypersil Gold column, 1.9 µm, 100 x 2.1 mm. **Spectroscopic Analysis:** The NMR analysis was performed on either 400 MHz (Jeol) NMR spectrometer using D₂O as solvent and tetramethylsilane (TMS) as an internal standard.

Results:

Based on the preliminary in-vitro evaluation the ethanol-water fraction was selected for further analysis such as LC-MS (**Figure 7A-D**) and ¹H-NMR (Figure 8) to retrieve information about the chemical constituents present. The ¹H-NMR spectrum of ethanol-water fraction displayed distinct signals at δ_H 6.3-7.6 corresponding phenolics alongside a bunch of signals in the range of δ_H 3.0-4.0 indicating the presence of aliphatic hydroxyl groups possibly due to the presence of polysaccharides. The presence of a large amount of polysaccharides could be explained by the polarity of the solvent used for extraction. In support, the LC-MS analysis indicated the presence of compounds in the molecular weight range of ~ 300-400 (**Figure 8**). It is pertinent to mention that most of the polyphenolic compounds display molecular weight in the same range. This observation collectively indicated that the ethanol-water fraction contains phenolic compounds and thus could be explored further for its potential to combat high-fat diet-induced NAFLD.

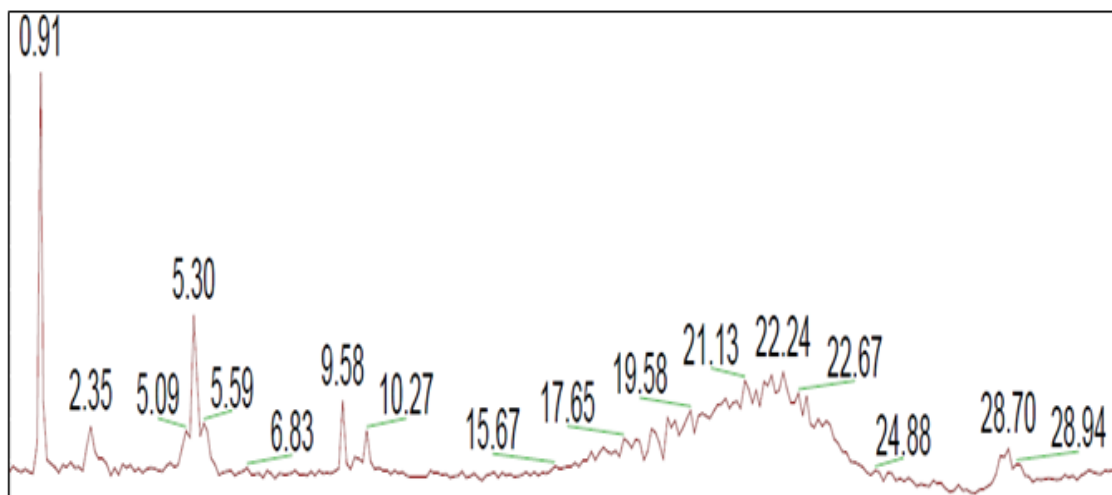
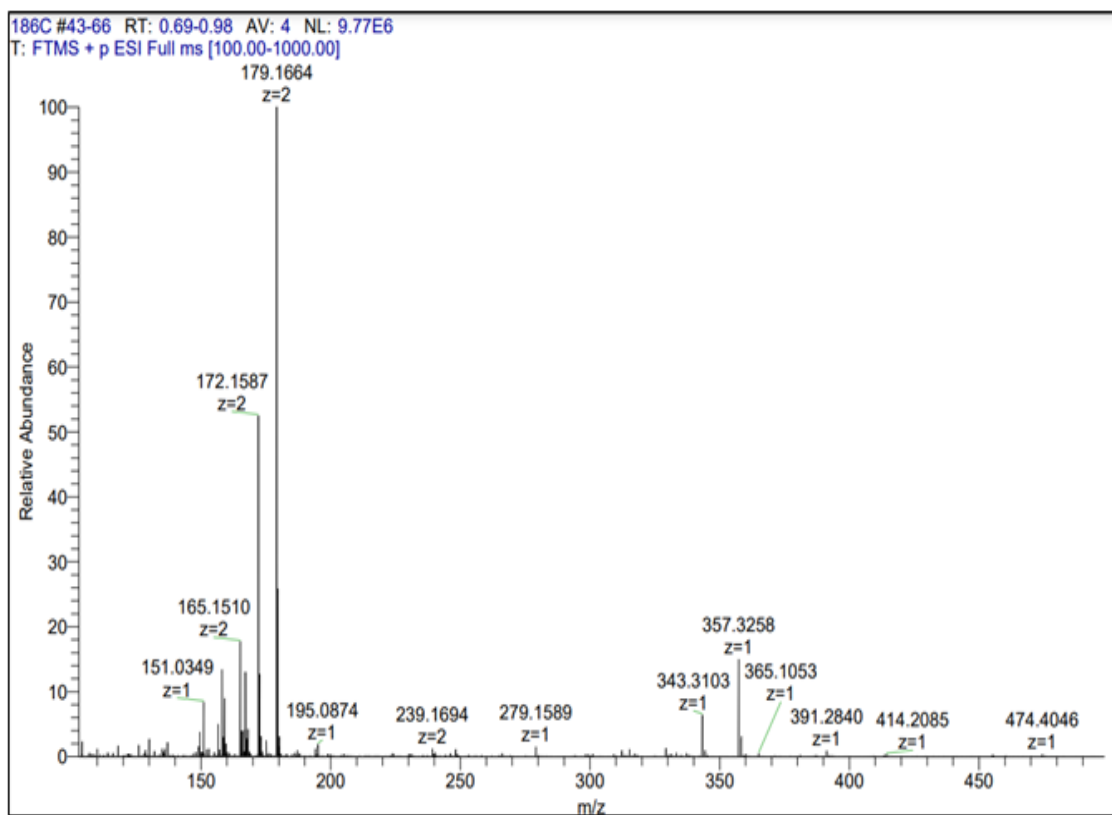
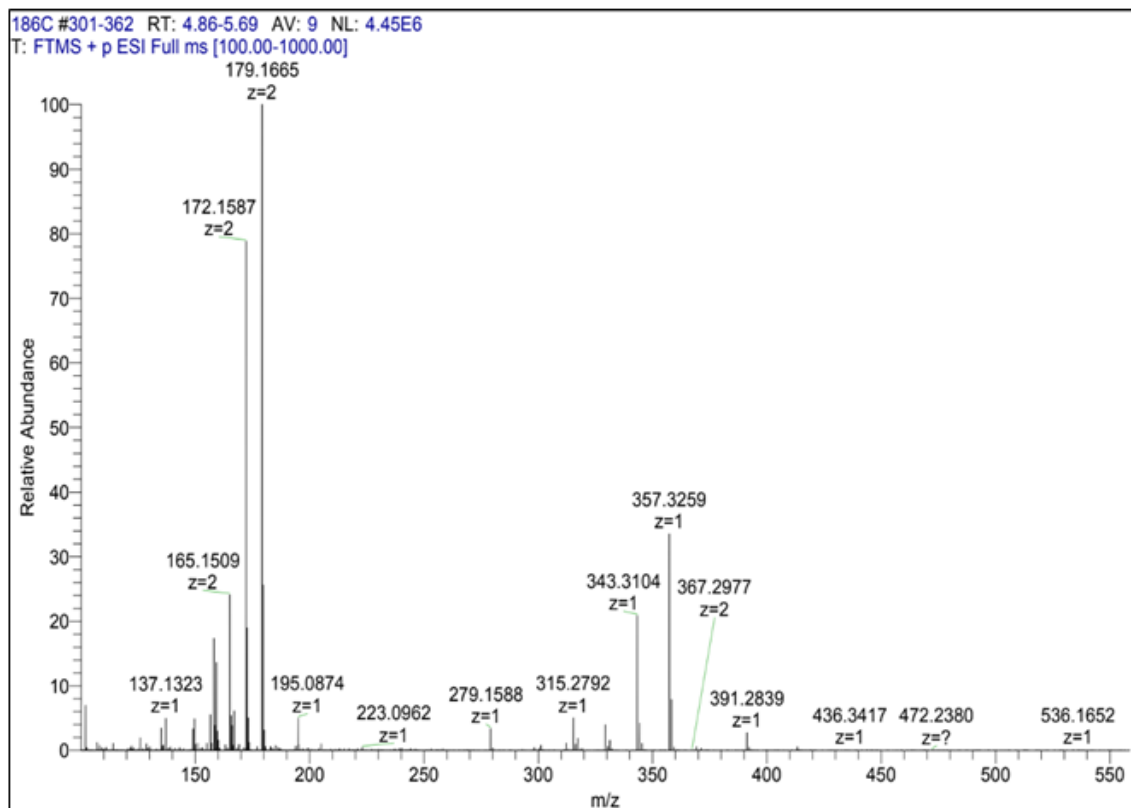
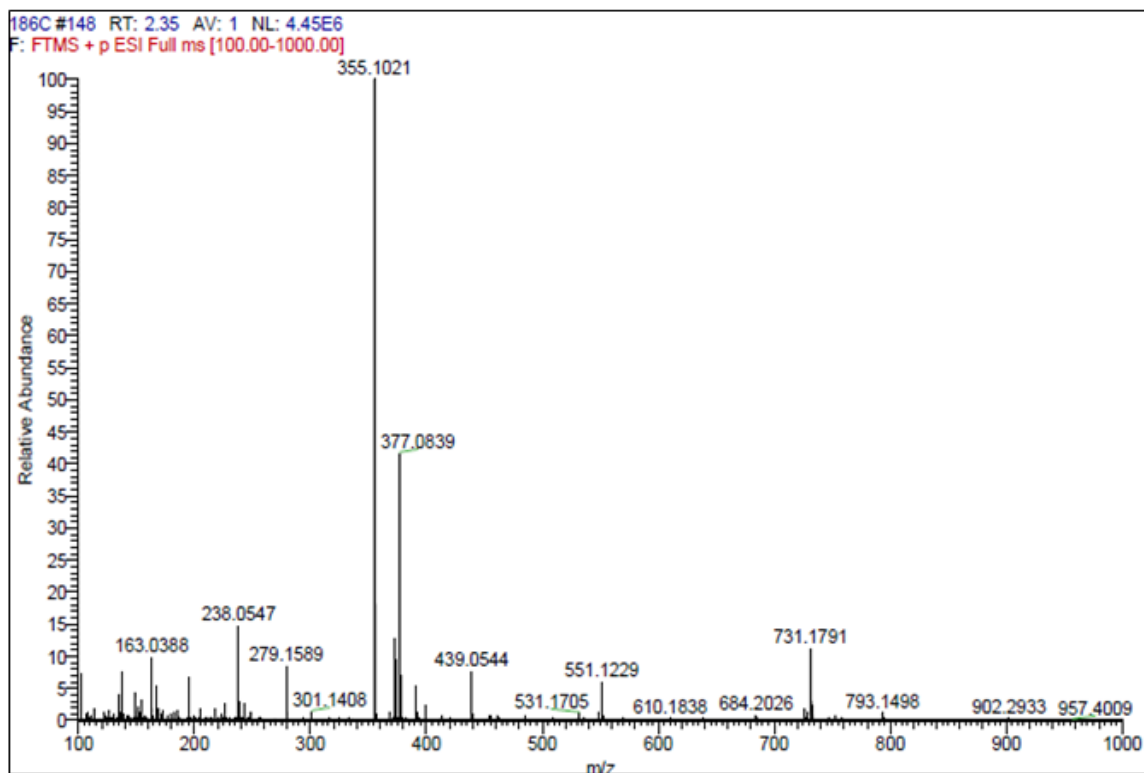


Figure 7A: TIC of ethanol-water fraction



7B)

Figure 7: TIC of ethanol-water fraction , analysis by LC-MS spectrometry using Orbitrap mass analyzer



7C)

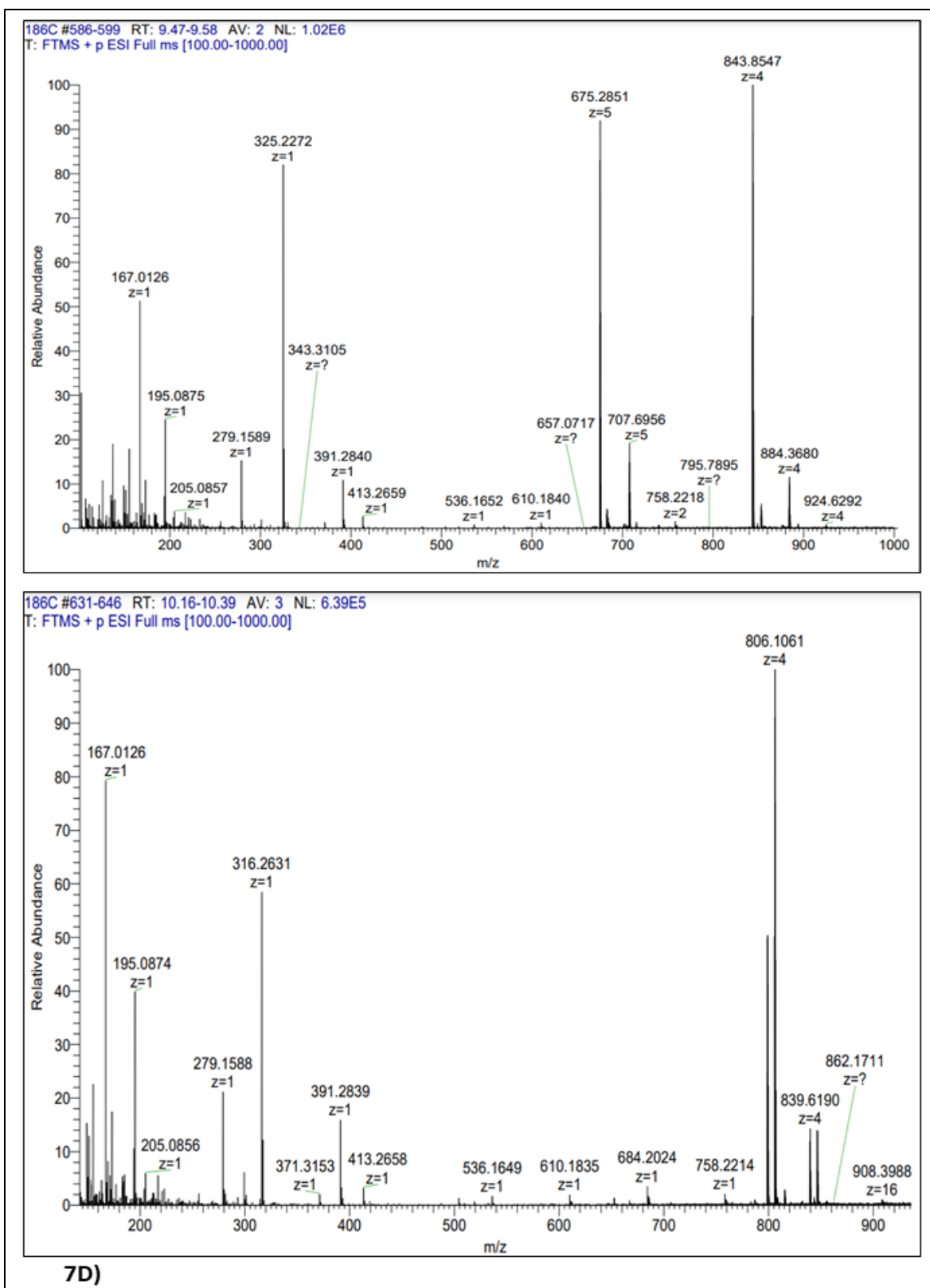


Figure 7 B-D) Major peak analysis of different R_T (0.69-0.98, 2.35, 4.88-5.69, 9.47-9.58, 10.16-10.39) in LC-MS profile of WTEC

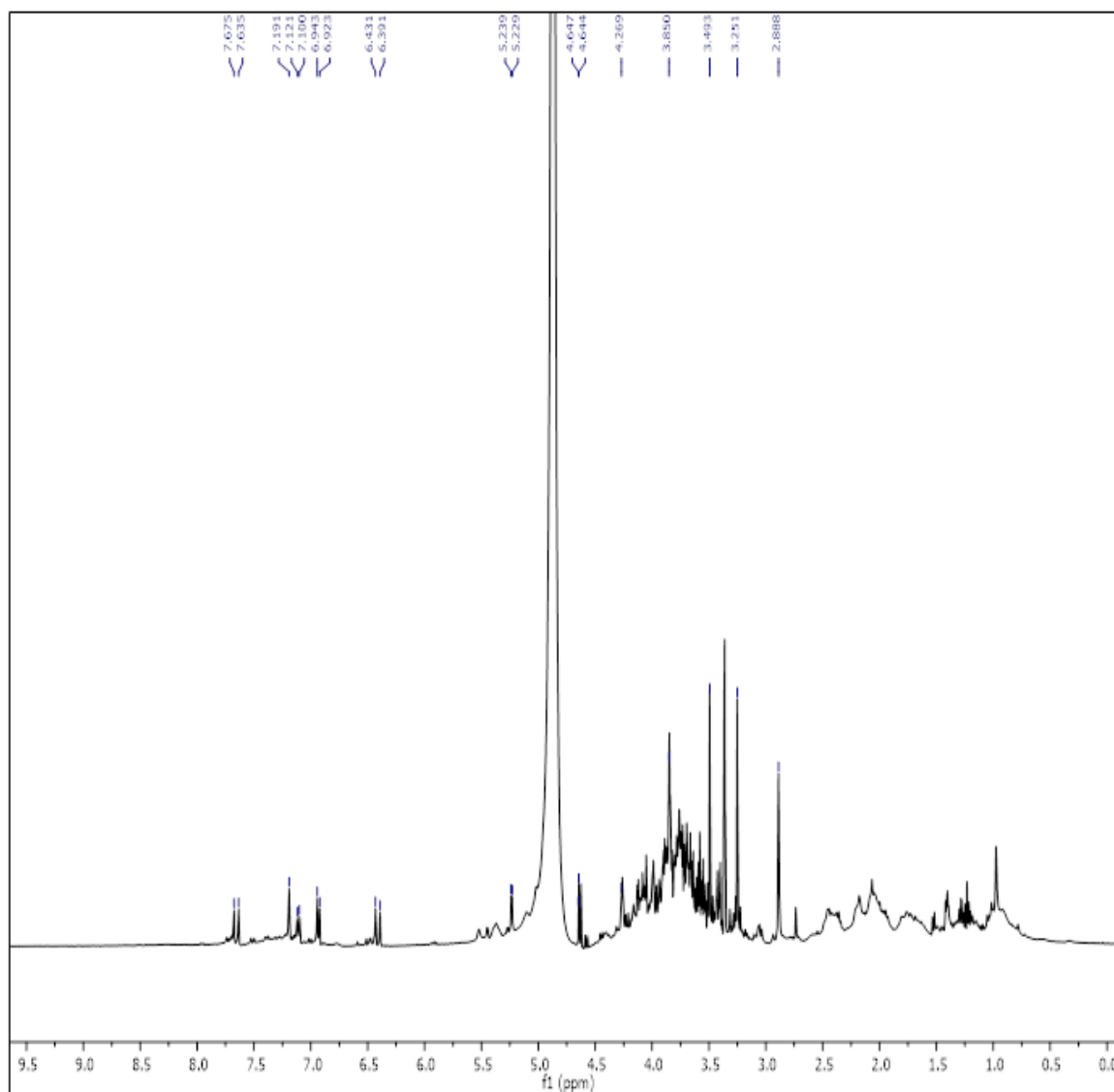


Figure 8: ^1H -NMR profile of ethanol-water fraction (WTEC)

8.3. Discussion:

Wrightia seedpods have already shown potential in reducing the pathogenic effects mediated by lipid overload in in-vitro and in-vivo animal models of NAFLD. Besides improving the mitochondrial health and altering its dynamics it has exerted a hepatoprotective role mediated by AMPK alpha and regulating the mitochondrial turnover and autophagy. Inflammation plays a pivotal role in exacerbating the pathogenicity of NAFLD and also directs its propagation toward NASH and further hepatic complications.

From the results of our experiments Fr-B (Hexane fraction) and hydroethanolic extract (WTEC) emerged as the potent formulations mitigating the ill effects of inflammation by curbing the ROS, and RNS generation, reducing the expression and secretion of immune-effectors like IL1 beta, IL-6 and also halting the translocation of pro-inflammatory nodal transcription factor NF κ B towards nucleus. While characterizing the constituents of the fraction and the extract some interesting leads were found.

Exploration of phytoconstituents demonstrates that in HepG2 and RAW264.7 cells, the hexane fraction (Fr-B) derived from ethyl acetate extract (Ex-A) shows a promising effect in suppressing the inflammatory response triggered by LPS and PA-mediated model of inflammation. Given that poly-unsaturated fatty acids (PUFA) such as 9,12-octadecanoic acid (linoleic acid), and 9,12,15-octadecatrienoic acid (α -linolenic acid), ethyl linoleate is found in good amounts in Fr-B and these have been well established to function as anti-inflammatory mediators protecting against inflammation (Pauls et al., 2018, Kolar et al., 2019, Reifen et al., 2015), we speculate that the aforementioned compounds may be responsible for exerting the anti-inflammatory properties.

When digging into the hydro-ethanolic extract by mass spectrometry and subsequent NMR studies we speculated presence of polyphenolic compounds within a mass range of 300-400 could be responsible for its therapeutic activity against fatty liver disease and associated metabolic abnormalities. Further exploration of separate peaks and identification of specific compounds elucidating their structure could pave an interesting avenue towards the establishment of a new therapeutic lead against lipid overload-mediated metabolic disorder and associated inflammatory conditions like NAFLD, and NASH.

General Discussion

Lipids are multifaceted molecules involved in plethora of structural and functional activities inside cells apart from acting as storage unit of energy. Lipid moieties are integral part of cell membrane, controls membrane dynamics, fluidity and also work as messengers in different physiological process like cell proliferation, fibrosis, hormonal regulation, inflammation and energy metabolism (Suryadevara et al., 2020, Carbone et al., 2019). Deregulation in lipid metabolism is linked with several pathogenic manifestation mainly obesity, diabetes, atherosclerosis, NAFLD and cancer. Nonalcoholic fatty liver disease is the most common form chronic liver disease and accounts for affecting nearly 25-40% of global population. Pathogenesis often stems from imbalance in *de novo* lipogenesis, fatty acid oxidation and fatty acid uptake resulting in net aggregation of fat depots inside hepatic cells. Characterization of NAFLD is generally noted as $\geq 5\%$ fat accumulation in hepatocytes with little or no intake of alcohol. Different class of lipid molecules exert different effects on fatty liver pathogenesis. Saturated fatty acid like palmitic acid, trans fatty acids, sphingolipids, diacylglycerols majorly contributes for initiation and progression of the disease whereas omega-3 poly unsaturated and monounsaturated fatty acids diminish disease severity (Gowda et al., 2023). Apart from *de novo* lipogenesis, adipose tissue lipolysis and diet are the primary source of fatty acids in liver (Donnelly et al., 2005). Obesity, insulin resistance and dyslipidaemia all risk factors work together and contribute in net surge of free fatty acid in the circulatory system which critically exceed the oxidation capacity of hepatic cells. This surfeit of lipid moieties forms intracellular aggregates and further deteriorates metabolic regulation resulting in development of metabolic syndrome. Pathological level of lipid accumulation if left untreated can activate hepatic inflammation and proceed towards steatohepatitis(NASH), cirrhosis and subsequently hepatocellularcarcinoma(HCC)(Gu Juanjuan et al., 2016). In most of the cases fatty liver goes asymptomatic until progression to later stage and have general overlapping symptoms with common liver problems. This ambush makes diagnosis and treatment of this ailment very challenging. Currently no FDA recommended drug is available as therapeutics apart from some PPAR agonists like rosiglitazone, pioglitazone so clinicians rely on some Type 2 diabetes pill along with dietary and lifestyle changes (Lange et al., 2022). This paves the way to the introduction of our study as ‘to explore the deregulated metabolic function and search for a therapeutic lead against non-alcoholic fatty liver disease’.

Mitochondria are considered the power generator of cell and account for almost 18% of hepatic volume. ATP generation along with regulation of metabolic signalling and nutrient oxidation is the prime function of this organelle. Maintenance of intricate balance between mitochondrial biogenesis, mitochondrial dynamics and mitochondrial autophagy is essential for establishment of mitochondrial homeostasis. Dysfunction in mitochondria can originate from genetic mutations of mitochondrial DNA (mtDNA) or can be acquired due to drug abuse, infection, lifestyle and environmental condition.

Diabetes mellitus and deafness (MIDD), Leigh syndrome, mitochondrial myopathy, dementia are examples of mitochondrial genetic defect whereas Parkinson's disease, Alzheimer's disease, Type 2 diabetes, cancer are indirectly linked with mitochondrial distress. Several researches have linked mitochondrial dysfunction with pathogenesis of NAFLD (Dabravolski et al., 2021) and it was also validated from affected liver tissue of suspected NAFLD patients (Gusdon et al., 2014). Exact mechanism deciphering the role of mitochondrial distress in development of NAFLD is still not clear however a surge in fatty acid delivery to liver, reduced fatty acid oxidation (FAO), increased *de novo* lipogenesis in association with dysfunctional electron transport chain (ETC) are considered to be the main causal factors. Altered lipid metabolism and debilitated mitochondrial respiration engender a surge in mitochondrial ROS and hepatic oxidative stress followed by hepatic injury and disease manifestation.

Traditional medicine practices like Ayurveda, unani, siddha and many indigenous tribal practices are a goldmine of possibilities for therapeutic research yet to be properly explored. Taking a cue from this we initiated a search for a lead against NAFLD. After consulting with experts and exhaustive literature study we zeroed upon a herbal plant named *Wrightia tictoria* or 'Indrajao' by common name. Root, leaves, stem bark and seeds, every part of this plant has medicinal properties but generally powdered or intact seeds are recommended for diabetes and jaundice treatment in Ayurvedic medicine (Anusharaj; et al., 2013). Some preliminary research literature is there documenting the anti-diabetic and anti-oxidant potential of these plant but no detailed mechanistic study is pursued. This dearth of knowledge instigated us to verify the potential of seedpods of this plant in treatment of NAFLD specially concentrating on mitochondrial parameters. Palmitic acid mediated lipotoxic stress in HepG2 (hepatoma) cells mimic the intra-hepatic scenario of fatty liver disease while high fat diet feeding in animal gives a direct perspective of non alcoholic fatty liver disease.

We started with elaborate extraction procedure taking an account of the polarity of solvents. Starting from non-polar hexane to most polar water it was divided in four categories. Hexane extract (WTEA), 100% ethanolic extract (WTEB), 50:50 hydro-ethanolic extract (WTEC), and aqueous extract (WTED). Firstly, cytotoxicity was checked in HepG2 cells with broad range of concentration with or without lipotoxic stress. Results clearly delineates that itself this extract poses no severe threat to hepatic cells but with introduction with palmitate the picture changes. In WTEA and WTEB we see a dip in overall viability with WTEB showing more toxic effect with increasing concentration. On the other hand WTEC and WTED greatly manage the toxic impact and shows hepatic protection against palmitate induced lipo-toxicity. Antioxidant activity was present in all four extracts but WTEC showed the most potent radical scavenging activity followed by WTED, WTEA and WTEB. Total cellular reactive oxygen species (ROS) was evaluated after pre-treatment with all four extracts HepG2 and RAW264.7

macrophages using PA and lipopolysaccharide (TLR-4 inducer) as stimulation. Inhibition of nitric oxide production was also checked in macrophage cells. The results clearly depict the oxidative stress mitigation properties of this extracts. WTEB showed some cytotoxicity in $> 50\mu\text{g/ml}$ doses otherwise every extract showed dose dependent decrease in the ROS production. Accumulated fat droplets in hepatic cells are the major driving factor for initiating disease pathophysiology. So we checked whether WT extracts can alleviate lipid accumulation and indeed we were surprised to see that each four extract showed good response. Analysing the results we could see that WTEC, amid all four extract showed the most potent and dose dependent activity while WTEB exhibited some toxicity, so further we concentrated on the rest three. As insulin resistance (IR) is often associated with disturbed metabolic signalling and glucose homeostasis, a significant elevation of IR often noted in fatty liver cases. As a result glucose uptake is severely impeded in liver, muscle and adipose tissue developing further crisis of energy. We saw the wrightia extracts showed commendable effect in increasing the glucose uptake capacity in PA treated HepG2 cells and among three extracts, WTEC at 1-5 $\mu\text{g/ml}$ doses exhibited the best effect. So summarizing all this data we chose wrightia hydro-ethanolic extract (WTEC) in the dose range of 1 to 25 $\mu\text{g/ml}$ as the most potent bio-active formulation and proceeded for further molecular studies targeting fatty liver disease. *In vivo* acute oral toxicity tests were carried out with WTEC to exclude the chances of acute toxicity with high oral doses. As wrightia seeds are already consumed by general people we were optimistic about its safety profile. But still a study with high oral doses with our specific formulation will certainly endorse the potentiality of this extract and unfold safe passage towards further mechanistic study. 3500mg/kg bodyweight doses of WTEC didn't produce any significant biochemical or haematological alteration. Liver, spleen and kidney tissue histology revealed no such abnormalities, except from mild neutrophilic infiltration in spleen tissues. So upon completion of this detailed screening and safety experiments we were satisfied and hopeful for further exploration of the bio-active principles of WTEC in liver lipotoxicity.

Lipid overload mediated hepatic stress often generates diminished mitochondrial respiration followed by decrease in net ATP yield and aggravated superoxide mediated oxidative stress. Effect of different doses of WTEC was checked in recovery of mitochondrial bioenergetics function in response to palmitate or HFD mediated fatty liver model. Extracellular acidification rate is a well acknowledged tool for estimation of cellular glycolysis rate and capacity whereas cellular oxygen consumption rate provide us a holistic picture of mitochondrial oxidative phosphorylation (OXPHOS). Introduction of palmitic acid induced lipotoxic stress in HepG2 cells significantly reduced basal and maximal respiration as well as ATP production. WTEC treatment doses 5-10 $\mu\text{g/ml}$ greatly salvaged this decrease and protected cell from ATP deficiency. In fatty liver a surge in overall glycolysis process is observed to overcome the ATP deficit, resulting in increased glycolysis rate and extracellular acidification by lactate overproduction. This

salvaging effect in turn results in toxicity so we did check the effect of WTEC on glycolytic parameters and interestingly we saw a dip in glycolysis rate following extract treatment. Further individual mitochondrial respiratory chain complex expression was evaluated and we report an increase in COM III, II and COMIV expression with wrightia treatment when incubated simultaneously with palmitic acid. TCA cycle and MRC enzyme activity was checked in HFD treated mice and compared with 250 and 500 mg/kg dose of WTEC in animal model. WTEC efficiently rescued the HFD mediated debilitation of enzymatic activity of succinate dehydrogenase, pyruvate dehydrogenase and citrate synthase activity. Cytochrome –C oxidoreductase enzyme of MRC was dose dependently activated in extract fed group where 500mg/kg dose showed excellent effect comparable to drug control fenofibrate (50mg/kg). So depending on this data we can surely comment that WTEC improves mitochondrial bio-energetic efficiency in fatty liver scenario.

Mitochondrial morphology and structural features were also evaluated employing Mitotracker red fluorescent dye and atomic force microscopy. Mitochondrial imaging by confocal microscopy yielded an interesting result where a plenty of fragmented small sized mitochondria (0.5 to 1.5 μm size) were seen in Palmitate treated HepG2 cells on the contrary untreated control contained long fibrillar network($\geq 2.5 \mu\text{m}$ size) of filamentous mitochondria. WTEC in 5 and 10 $\mu\text{g/ml}$ dose showed a commendable rescue in the PA mediated fragmentation. Atomic force microscopy of isolated mitochondria from cultured HepG2 cells also validated the protective effect of WTEC in maintaining mitochondrial topographic features eliminating PA induced obnoxious effect like roundedness, swelling and loss of cristae structure.

Mitochondrial quality control process is maintained by tight co-ordination between biogenesis, dynamics and mitophagy. AMPK is the master regulator of mitochondrial homeostasis regulating these three major processes. SIRT1 and PGC1 α are two main downstream effector of mitochondrial biogenesis. PGC1 α is a major transcriptional co-activator and interacts with mitochondrial transcription factor TFAM to regulate mtDNA replication and transcription, subsequently enhancing mitochondrial mass and energy metabolism process. We wanted to check the fate of this three major protein with WTEC treatment in lipid distressed cells and HFD tissue. The level of mRNA and protein expression of SIRT1, PGC1 α and TFAM were activated in response to increasing dose of WTEC suggesting a positive regulation. Confocal microscopy images also corroborated the induction of mitochondrial biogenesis by WTEC via activation of SIRT1-PGC1 α and TFAM.

Co-ordinated fission and fusion process is a fundamental mechanism to maintain mitochondrial homeostasis according to metabolic requirement. In obesity, fatty liver disease this dynamic interchange gets disintegrated resulting in energy distress.

Numerous studies has reported an increase in mitochondrial fission process in response to lipid stress and subsequent loss of trans-membrane potential and increased ROS. DRP1 and phosphorylation of its 616 residue is the major requisite for fission process whereas a co-ordinated activation of MFN1 and MFN2 in mitochondrial outer, inner membrane respectively maintains mitochondrial fusion. With PA or HFD treatment a rise in DRP1 and ph-DRP1 (Serine 616) expression and a higher ph-DRP1 (Ser616)/DRP1 ratio was observed along with a concomitant dip in MFN1 and 2 levels. WTEC 1 to 10 µg/ml efficiently reversed this phenomenon and resulted in lowered fission and restoration of longer, filamentous mitochondria.

In NAFLD, with progression in severity of disease hepatocytes are stacked with fragmented and mechanically damaged mitochondria population. Mitophagy is a protective mechanism which maintains efficient clearance of damaged mitochondria and hinders progression of NAFLD. PARKIN and PINK1 are two major protein regulating mitophagy. PINK1 generally accumulates on the damaged mitochondria and in turn activates ubiquitin ligase activity of PARKIN and subsequent accumulation on dysfunctional mitochondria and their degradation. LC3B mediates the fusion of mitophagy tagged mitochondria with autophagosome while p62 binds directly with LC3B and itself gets degraded during the autophagy process. P62 acts as an adaptor protein linking ubiquitinated protein with autophagosome and further degradation by lysosome. Together LC3B and p62 expression level serves as an indicator of autophagic flux. Potential of WTEC in regulation of mitophagy was evaluated. PARKIN and PINK1 expression was checked together with LC3B and p62 to get a total picture of dysfunctional mitochondrial clearance. After 24 hour treatment with palmitic acid in HepG2 cells parkin and co-treatment with different doses of WTEC we can find a far better response in activation of mitophagy with our wrightia hydro-ethanolic extract. LC3B and PINK1 level was significantly raised along with PARKIN justifying the mitophagy modulating effect of WTEC. To get a clear picture on the regulation of mitophagy we did a time kinetic study with simultaneously labelling PARKIN, LC3B and mitochondria. Upon analysis of confocal microscopy results we interpreted that during 4hour time point no such elevation of PARKIN was seen in WTEC group apart from the highest dose of 10 µg/ml with minimal activation of LC3B. At 12 hour after PA stimulation PARKIN level got significantly increased in WTEC treated cells compared to PA treated lipotoxic group. LC3B levels seem to be increasing with some effect was prominent in highest dose group. LC3B-PARKIN colocalization also increased significantly. At 18hour time point PARKIN and LC3B expression in lipotoxic group seem to increase compared to control group as a response to salvage the damaging effect of high saturated fat. In WTEC treatment group elevation of expression was not significant to PA group but LC3B-PARKIN localisation was increased significantly. At 24 hour after palmitate treatment WTEC showed a commendable increment in LC3B response but PARKIN level showed no further significant change. To specifically

determine the damaged mitochondria specific clearance potential of WTEC we studied the correlation coefficient, overlap coefficient and co-localization rate between LC3B and mitochondria at different time point. Till 4hour no such co-localization was prominent but after 4 hour to 12hr we see an increase in co-localization rate, overlap and Pearson's coefficient. At 24 hour we see a significant enhancement of mitochondria-LC3B (autophagy marker) co-localization rate as well as accumulation of LC3B puncta formation in fragmented mitochondria signifying a damaged mitochondria specific degradation by WTEC.

AMPK α is central regulator different avenues of mitochondrial quality control process. SIRT1, PPAR α , PGC1 α and LC3B all are downstream effector genes of AMPK α signalling pathway for cellular metabolic homeostasis. We checked for AMPK expression and activation by phosphorylation status on Threonine-172 position. Interestingly WTEC 1, 5 and 10 μ g/ml of doses effectively increased the phosphorylation status thus participating in AMPK mediated regulation. To ensure this mechanism we introduced AMPK inhibitor with WTEC AND PA treatment. Intriguingly we notice a marked reduction in SIRT1, PPAR α and LC3B expression with inhibitor treatment whereas WTEC at same doses without the inhibitor dose dependently increased this expression. In animal NAFLD model, WTEC treated liver tissue immunohistochemistry against AMPK α phosphor-Thr172 also validated this data by increasing the expression when compared to lowered expression in HFD liver. So we can confirm that WTEC show its potential against mitochondrial dysfunction by activation of AMPK α .

Aggregation of excess lipid due to deregulated lipid metabolism transforms the hepatic metabolic environment towards NAFLD/NASH. An increased fatty acid uptake from circulation, diminished fatty acid oxidation with increased *de novo* lipogenesis converts the hepatic metabolic milieu towards elevated oxidative stress and mitochondrial dysfunction. So we focused on the effect of WTEC doses on regulation of lipid metabolism genes. PPAR α is the central regulator of lipid metabolism, expression of this gene along with fatty acid oxidation marker CPT1A was checked in animal HFD model and hepatoma cells respectively. WTEC was seen to increase both gene expressions by significant level comparable to PPAR α agonist fenofibrate. CD36 and SREBP1 level was also checked in liver tissue and differentiated 3T3 adipocytes respectively. WTEC pre-treated adipocytes when co-incubated with PA, resulted in an increment of expression in SREBP1 whereas a dip in expression was seen in PA treated cells. Fatty acid uptake was greatly reduced by inhibiting CD36 as evidenced by reduced expression in liver tissue and palmitate treated hepatoma cells certifies the lipid stress lowering activity of WTEC. This inhibition of lipid accumulation was rechecked by oil Red O staining and BODIPY neutral fat droplet staining, which revalidated the de-escalation of lipid aggregation by WTEC. In HFD mediated NAFLD model hepatic steatosis along with epididymal adipocyte cells size were checked in WTEC dose group along with fenofibrate drug

control. WTEC 250mg/kg and 500mg/kg dose dependently reduced hepatic steatosis and decreased the inflated cell size of EPF tissue and improved overall NAS score. Elevation of collagen deposition and exacerbated lipid markers are hallmark of fatty liver disease which worsen with disease severity. WTEC 500mg/kg dose group showed very minimal collagen deposition compared to HFD group animals and also bettered haematological parameters like fasting blood glucose, triglyceride, and cholesterol and LDL levels. Together analysing all this data we can certainly conclude about the beneficial effect of *Wrightia tinctoria* hydro-ethanolic extract in ameliorating non-alcoholic fatty liver by mitigating mitochondrial dysfunction and enhancing lipid metabolism parameters.

Exacerbated inflammation plays an integral role in progression of fatty liver disease towards NASH and further on. Apart from checking the anti-inflammatory effect of WTEC we wanted to explore further extraction with a less polar solvent. Already hexane extract (WTEA) showed promising anti-oxidant and ROS, RNS inhibiting capacity which provoked us to extract with ethyl acetate and then further fractionated by hexane. Upon checking the anti-inflammatory activity we saw hexane fraction of ethyl acetate extract showed potent activity like decreasing ROS production, Nitrite inhibition and lowering of pro-inflammatory cytokine expression. NF κ B is the central transcription factor regulating various signalling pathways promoting inflammation. Expression of NF κ B was alleviated and nuclear translocation of this transcription factor was blocked by hexane fraction as validated in LPS treated macrophage and PA treated hepatoma cells. WTEC hydro-ethanolic extract also showed significant decrease in NF κ B mRNA level and protein expression with impeded IL1, IL-6 cytokine secretion. Thus to conclude modulating the expression of NF κ B, wrightia seedpod manifests its anti-inflammatory activity.

Characterization of compounds present in the hexane fraction and hydro-ethanolic extract of wrightia was done. Gas chromatography was employed to identify the compounds of Fr-B (Hexane fraction). The main peaks corresponded to mainly with poly and mono unsaturated fatty acids namely ethyl hexadecanoate, ethyl linoleate, 9, 12-octadecanoic acid, 9,12,15-octadecatrienoic acid, 9,12,15-octadecatrienoic acid ethyl ester, and octadecanoic acid ethyl esters. This enrichment of poly unsaturated fatty acids like ω -3 and ω -6 PUFA makes hexane fraction an important phyto-source to alleviate uncontrolled inflammation. ^{13}C -NMR spectrum and ^1H -NMR spectrum also validated this data. WTEC was also analyzed by mass spectrometry and subsequently by ^1H -NMR. The hydro-ethanolic extract's ^1H -NMR spectrum showed distinct signals at δH 6.3–7.6, which corresponds to phenolics, combined with a large number of signals in the δH 3.0–4.0 region, which suggested the presence of aliphatic hydroxyl groups, probably because of polysaccharides. All of these findings suggested that the ethanol-water fraction contained phenolic chemicals that could be responsible for its potential bio-activity against mitochondrial dysfunction and reversing the altered lipid metabolism in non-alcoholic fatty liver disease.

Bibliography

A

- Abdelmalek, M. F., Sanderson, S. O., Angulo, P., Soldevila-Pico, C., Liu, C., Peter, J., Keach, J., Cave, M., Chen, T., McClain, C. J., & Lindor, K. D. (2009). Betaine for nonalcoholic fatty liver disease: Results of a randomized placebo-controlled trial. *Hepatology*, 50(6), 1818–1826. <https://doi.org/10.1002/hep.23239>
- Acharya, P., Chouhan, K., Weiskirchen, S., & Weiskirchen, R. (2021). Cellular Mechanisms of Liver Fibrosis. *Frontiers in Pharmacology*, 12. <https://doi.org/10.3389/fphar.2021.671640>
- Aithal, G. P., Thomas, J. A., Kaye, P. V., Lawson, A., Ryder, S. D., Spendlove, I., Austin, A. S., Freeman, J. G., Morgan, L., & Webber, J. (2008). Randomized, Placebo-Controlled Trial of Pioglitazone in Nondiabetic Subjects With Nonalcoholic Steatohepatitis. *Gastroenterology*, 135(4), 1176–1184. <https://doi.org/10.1053/j.gastro.2008.06.047>
- Akinyemiju, T., Abera, S., Ahmed, M., Alam, N., Alemayohu, M. A., Allen, C., Al-Raddadi, R., Alvis-Guzman, N., Amoako, Y., Artaman, A., Ayele, T. A., Barac, A., Bensenor, I., Berhane, A., Bhutta, Z., Castillo-Rivas, J., Chitheer, A., Choi, J.-Y., Cowie, B., ... Fitzmaurice, C. (2017). The Burden of Primary Liver Cancer and Underlying Etiologies From 1990 to 2015 at the Global, Regional, and National Level. *JAMA Oncology*, 3(12), 1683. <https://doi.org/10.1001/jamaoncol.2017.3055>
- Akter, S. (2022). Non-alcoholic Fatty Liver Disease and Steatohepatitis: Risk Factors and Pathophysiology. *Middle East Journal of Digestive Diseases*, 14(2), 167–181. <https://doi.org/10.34172/mejdd.2022.270>
- Anand, S. S., Hawkes, C., de Souza, R. J., Mente, A., Dehghan, M., Nugent, R., Zulyniak, M. A., Weis, T., Bernstein, A. M., Krauss, R. M., Kromhout, D., Jenkins, D. J. A., Malik, V., Martinez-Gonzalez, M. A., Mozaffarian, D., Yusuf, S., Willett, W. C., & Popkin, B. M. (2015). Food Consumption and its Impact on Cardiovascular Disease: Importance of Solutions Focused on the Globalized Food System. *Journal of the American College of Cardiology*, 66(14), 1590–1614. <https://doi.org/10.1016/j.jacc.2015.07.050>
- Anavi, S., Eisenberg-Bord, M., Hahn-Obercyger, M., Genin, O., Pines, M., & Tirosh, O. (2015). The role of iNOS in cholesterol-induced liver fibrosis. *Laboratory Investigation*, 95(8), 914–924. <https://doi.org/10.1038/labinvest.2015.67>
- Alexandri, E., Ahmed, R., Siddiqui, H., Choudhary, M., Tsiafoulis, C., & Gerothanassis, I. (2017). High Resolution NMR Spectroscopy as a Structural and Analytical Tool for Unsaturated Lipids in Solution. *Molecules*, 22(10), 1663. <https://doi.org/10.3390/molecules22101663>
- Aleykutty, N. A., Bindu, A. R., Sangeetha, S., & Jiljit, G. (2011). Evaluation of Anti-inflammatory and Analgesic Activity of *Wrightia Tinctoria* Leaves. *Journal of Biologically Active Products from Nature*, 1(1), 33–41. <https://doi.org/10.1080/22311866.2011.10719071>
- Alfaddagh, A., Martin, S. S., Leucker, T. M., Michos, E. D., Blaha, M. J., Lowenstein, C. J., Jones, S. R., & Toth, P. P. (2020). Inflammation and cardiovascular disease: From mechanisms to therapeutics. *American Journal of Preventive Cardiology*, 4, 100130. <https://doi.org/10.1016/j.ajpc.2020.100130>
- Anusharaj, Chandrashekar, R., Adake, P., Rao, S. N., & Santanusaha, S. (2013). WRIGHTIA TINCTORIA: AN OVERVIEW. *Journal of Drug Delivery and Therapeutics*, 3(2). <https://doi.org/10.22270/jddt.v3i2.444>

- Arroyave-Ospina, J. C., Wu, Z., Geng, Y., & Moshage, H. (2021). Role of Oxidative Stress in the Pathogenesis of Non-Alcoholic Fatty Liver Disease: Implications for Prevention and Therapy. *Antioxidants*, 10(2), 174. <https://doi.org/10.3390/antiox10020174>
- Ayala, A., Muñoz, M. F., & Argüelles, S. (2014). Lipid Peroxidation: Production, Metabolism, and Signaling Mechanisms of Malondialdehyde and 4-Hydroxy-2-Nonenal. *Oxidative Medicine and Cellular Longevity*, 2014, 1–31. <https://doi.org/10.1155/2014/360438>
- Ayonrinde, O. T. (2021). Historical narrative from fatty liver in the nineteenth century to contemporary NAFLD - Reconciling the present with the past. *JHEP Reports : Innovation in Hepatology*, 3(3), 100261. <https://doi.org/10.1016/j.jhepr.2021.100261>
- Azeez, T. B., & Lunghar, J. (2021). Antiinflammatory effects of turmeric (*Curcuma longa*) and ginger (*Zingiber officinale*). In *Inflammation and Natural Products* (pp. 83–102). Elsevier. <https://doi.org/10.1016/B978-0-12-819218-4.00011-0>

B

- Bartlett, K., & Eaton, S. (2004). Mitochondrial β -oxidation. *European Journal of Biochemistry*, 271(3), 462–469. <https://doi.org/10.1046/j.1432-1033.2003.03947.x>
- Begriche, K., Massart, J., Robin, M.-A., Bonnet, F., & Fromenty, B. (2013). Mitochondrial adaptations and dysfunctions in nonalcoholic fatty liver disease. *Hepatology*, 58(4), 1497–1507. <https://doi.org/10.1002/hep.26226>
- Berná, G., & Romero-Gomez, M. (2020). The role of nutrition in non-alcoholic fatty liver disease: Pathophysiology and management. *Liver International*, 40(S1), 102–108. <https://doi.org/10.1111/liv.14360>
- Blum, T. B., Hahn, A., Meier, T., Davies, K. M., & Kühlbrandt, W. (2019). Dimers of mitochondrial ATP synthase induce membrane curvature and self-assemble into rows. *Proceedings of the National Academy of Sciences*, 116(10), 4250–4255. <https://doi.org/10.1073/pnas.1816556116>
- Borra, R. J. H., Salo, S., Dean, K., Lautamäki, R., Nuutila, P., Komu, M., & Parkkola, R. (2009). Nonalcoholic Fatty Liver Disease: Rapid Evaluation of Liver Fat Content with In-Phase and Out-of-Phase MR Imaging. *Radiology*, 250(1), 130–136. <https://doi.org/10.1148/radiol.2501071934>
- Bril, F., Biernacki, D. M., Kalavalapalli, S., Lomonaco, R., Subbarayan, S. K., Lai, J., Tio, F., Suman, A., Orsak, B. K., Hecht, J., & Cusi, K. (2019). Role of Vitamin E for Nonalcoholic Steatohepatitis in Patients With Type 2 Diabetes: A Randomized Controlled Trial. *Diabetes Care*, 42(8), 1481–1488. <https://doi.org/10.2337/dc19-0167>
- Buzzetti, E., Pinzani, M., & Tsochatzis, E. A. (2016). The multiple-hit pathogenesis of non-alcoholic fatty liver disease (NAFLD). *Metabolism*, 65(8), 1038–1048. <https://doi.org/10.1016/j.metabol.2015.12.012>

C

- Carbone, F., Lattanzio, M. S., Minetti, S., Ansaldo, A. M., Ferrara, D., Molina-Molina, E., Belfiore, A., Elia, E., Pugliese, S., Palmieri, V. O., Montecucco, F., & Portincasa, P. (2019). Circulating CRP Levels Are Associated with Epicardial and Visceral Fat Depots in Women with Metabolic Syndrome Criteria. *International Journal of Molecular Sciences*, 20(23), 5981. <https://doi.org/10.3390/ijms20235981>

- Cave, M. C., Clair, H. B., Hardesty, J. E., Falkner, K. C., Feng, W., Clark, B. J., Sidey, J., Shi, H., Aqel, B. A., McClain, C. J., & Prough, R. A. (2016). Nuclear receptors and nonalcoholic fatty liver disease. *Biochimica et Biophysica Acta (BBA) - Gene Regulatory Mechanisms*, 1859(9), 1083–1099. <https://doi.org/10.1016/j.bbagr.2016.03.002>
- Chadt, A., & Al-Hasani, H. (2020). Glucose transporters in adipose tissue, liver, and skeletal muscle in metabolic health and disease. *Pflügers Archiv - European Journal of Physiology*, 472(9), 1273–1298. <https://doi.org/10.1007/s00424-020-02417-x>
- Chalasani, N., Younossi, Z., Lavine, J. E., Charlton, M., Cusi, K., Rinella, M., Harrison, S. A., Brunt, E. M., & Sanyal, A. J. (2018). The diagnosis and management of nonalcoholic fatty liver disease: Practice guidance from the American Association for the Study of Liver Diseases. *Hepatology*, 67(1), 328–357. <https://doi.org/10.1002/hep.29367>
- Chalifoux, O., Faerman, B., & Mailloux, R. J. (2023). Mitochondrial hydrogen peroxide production by pyruvate dehydrogenase and α -ketoglutarate dehydrogenase in oxidative eustress and oxidative distress. *Journal of Biological Chemistry*, 299(12), 105399. <https://doi.org/10.1016/j.jbc.2023.105399>
- Chau, M. D. L., Gao, J., Yang, Q., Wu, Z., & Gromada, J. (2010). Fibroblast growth factor 21 regulates energy metabolism by activating the AMPK–SIRT1–PGC-1 α pathway. *Proceedings of the National Academy of Sciences*, 107(28), 12553–12558. <https://doi.org/10.1073/pnas.1006962107>
- Chen, J., Deng, X., Liu, Y., Tan, Q., Huang, G., Che, Q., Guo, J., & Su, Z. (2020). Kupffer Cells in Non-alcoholic Fatty Liver Disease: Friend or Foe? *International Journal of Biological Sciences*, 16(13), 2367–2378. <https://doi.org/10.7150/ijbs.47143>
- Chretien, D., Pourrier, M., Bourgeron, T., S  n  , M., R  tig, A., Munnich, A., & Rustin, P. (1995). An improved spectrophotometric assay of pyruvate dehydrogenase in lactate dehydrogenase contaminated mitochondrial preparations from human skeletal muscle. *Clinica Chimica Acta*, 240(2), 129–136. [https://doi.org/10.1016/0009-8981\(95\)06145-6](https://doi.org/10.1016/0009-8981(95)06145-6)
- Corrales, P., Vidal-Puig, A., & Medina-G  mez, G. (2018). PPARs and Metabolic Disorders Associated with Challenged Adipose Tissue Plasticity. *International Journal of Molecular Sciences*, 19(7), 2124. <https://doi.org/10.3390/ijms19072124>
- D**
- Dabravolski, S. A., Bezsonov, E. E., & Orekhov, A. N. (2021). The role of mitochondria dysfunction and hepatic senescence in NAFLD development and progression. *Biomedicine & Pharmacotherapy*, 142, 112041. <https://doi.org/10.1016/j.biopha.2021.112041>
- David, D., & Eapen, C. E. (2021). What Are the Current Pharmacological Therapies for Nonalcoholic Fatty Liver Disease? *Journal of Clinical and Experimental Hepatology*, 11(2), 232–238. <https://doi.org/10.1016/j.jceh.2020.09.001>
- Degli Esposti, D., Hamelin, J., Bosselut, N., Saffroy, R., Sebah, M., Pommier, A., Martel, C., & Lemoine, A. (2012). Mitochondrial Roles and Cytoprotection in Chronic Liver Injury. *Biochemistry Research International*, 2012, 1–16. <https://doi.org/10.1155/2012/387626>
- Delli Bovi, A. P., Marciano, F., Mandato, C., Siano, M. A., Savoia, M., & Vajro, P. (2021). Oxidative Stress in Non-alcoholic Fatty Liver Disease. An Updated Mini Review. *Frontiers in Medicine*, 8, 595371. <https://doi.org/10.3389/fmed.2021.595371>

- Demine, Renard, & Arnould. (2019). Mitochondrial Uncoupling: A Key Controller of Biological Processes in Physiology and Diseases. *Cells*, 8(8), 795. <https://doi.org/10.3390/cells8080795>
- DERVARTANIAN, D. V., & VEEGER, C. (1964). STUDIES ON SUCCINATE DEHYDROGENASE. I. SPECTRAL PROPERTIES OF THE PURIFIED ENZYME AND FORMATION OF ENZYME-COMPETITIVE INHIBITOR COMPLEXES. *Biochimica et Biophysica Acta*, 92, 233–247. <http://www.ncbi.nlm.nih.gov/pubmed/14249115>
- Dhanabal Sp, Baskar Ananda Raj, N. Muruganantham, Praveen Tk, & Raghu Ps. (2012). Screening of Wrightia tinctoria leaves for Anti psoriatic activity. *Hygeia.J.D.Med*, 4 (1).
- Di Mauro, S., Scamporrino, A., Filippello, A., Di Pino, A., Scicali, R., Malaguarnera, R., Purrello, F., & Piro, S. (2021). Clinical and Molecular Biomarkers for Diagnosis and Staging of NAFLD. *International Journal of Molecular Sciences*, 22(21), 11905. <https://doi.org/10.3390/ijms22111905>
- Diao, L., Auger, C., Konoeda, H., Sadri, A.-R., Amini-Nik, S., & Jeschke, M. G. (2018). Hepatic steatosis associated with decreased β -oxidation and mitochondrial function contributes to cell damage in obese mice after thermal injury. *Cell Death & Disease*, 9(5), 530. <https://doi.org/10.1038/s41419-018-0531-z>
- Divakar Madhu.C, & Devi. S Lakshmi. (2011). Antiulcer activity of Wrightia tinctoria (Roxb.) R.Br. *Der Pharmacia Sinica*, 2 (2), 355–360.
- Dongiovanni, P., Anstee, Q., & Valenti, L. (2013). Genetic Predisposition in NAFLD and NASH: Impact on Severity of Liver Disease and Response to Treatment. *Current Pharmaceutical Design*, 19(29), 5219–5238. <https://doi.org/10.2174/13816128113199990381>
- Donnelly, K. L., Smith, C. I., Schwarzenberg, S. J., Jessurun, J., Boldt, M. D., & Parks, E. J. (2005). Sources of fatty acids stored in liver and secreted via lipoproteins in patients with nonalcoholic fatty liver disease. *The Journal of Clinical Investigation*, 115(5), 1343–1351. <https://doi.org/10.1172/JCI23621>
- Dorn, G. W., & Kitsis, R. N. (2015). The Mitochondrial Dynamism-Mitophagy-Cell Death Interactome. *Circulation Research*, 116(1), 167–182. <https://doi.org/10.1161/CIRCRESAHA.116.303554>

E

- Edmunds, L. R., Xie, B., Mills, A. M., Huckestein, B. R., Undamatla, R., Murali, A., Pangburn, M. M., Martin, J., Sipula, I., Kaufman, B. A., Scott, I., & Jurczak, M. J. (2020). Liver-specific Prkn knockout mice are more susceptible to diet-induced hepatic steatosis and insulin resistance. *Molecular Metabolism*, 41, 101051. <https://doi.org/10.1016/j.molmet.2020.101051>
- Ezhilarasan, D., & Lakshmi, T. (2022). A Molecular Insight into the Role of Antioxidants in Nonalcoholic Fatty Liver Diseases. *Oxidative Medicine and Cellular Longevity*, 2022, 1–15. <https://doi.org/10.1155/2022/9233650>

F

- Fabbrini, E., Sullivan, S., & Klein, S. (2010). Obesity and nonalcoholic fatty liver disease: Biochemical, metabolic, and clinical implications. *Hepatology*, 51(2), 679–689. <https://doi.org/10.1002/hep.23280>
- Ferramosca, A., di Giacomo, M., & Zara, V. (2017). Antioxidant dietary approach in treatment of fatty liver: New insights and updates. *World Journal of Gastroenterology*, 23(23), 4146. <https://doi.org/10.3748/wjg.v23.i23.4146>

- Francisco, V., Sanz, M. J., Real, J. T., Marques, P., Capuozzo, M., Ait Eldjoudi, D., & Gualillo, O. (2022). Adipokines in Non-Alcoholic Fatty Liver Disease: Are We on the Road toward New Biomarkers and Therapeutic Targets? *Biology*, 11(8). <https://doi.org/10.3390/biology11081237>
- Friedman, J. R. (2022). Mitochondria from the Outside in: The Relationship Between Inter-Organelle Crosstalk and Mitochondrial Internal Organization. *Contact*, 5, 251525642211332. <https://doi.org/10.1177/25152564221133267>
- Fukunishi, S., Sujishi, T., Takeshita, A., Ohama, H., Tsuchimoto, Y., Asai, A., Tsuda, Y., & Higuchi, K. (2014). Lipopolysaccharides accelerate hepatic steatosis in the development of nonalcoholic fatty liver disease in Zucker rats. *Journal of Clinical Biochemistry and Nutrition*, 54(1), 39–44. <https://doi.org/10.3164/jcbrn.13-49>
- G**
- Galloway, C. A., Lee, H., Brookes, P. S., & Yoon, Y. (2014). Decreasing mitochondrial fission alleviates hepatic steatosis in a murine model of nonalcoholic fatty liver disease. *American Journal of Physiology-Gastrointestinal and Liver Physiology*, 307(6), G632–G641. <https://doi.org/10.1152/ajpgi.00182.2014>
- Ganga Rao Battu, L. N. Rajeswari Dodda, Ramadevi Devarakonda, & Heera Battu. (2018). PHYTOCHEMICAL AND PHARMACOLOGICAL STUDIES ON WRIGHTIA TINCTORIA. *JOURNAL OF PHARMACY AND PHARMACEUTICAL SCIENCES*, 562–585.
- Geng, Y., Faber, K. N., de Meijer, V. E., Blokzijl, H., & Moshage, H. (2021). How does hepatic lipid accumulation lead to lipotoxicity in non-alcoholic fatty liver disease? *Hepatology International*, 15(1), 21–35. <https://doi.org/10.1007/s12072-020-10121-2>
- Giorgio, V., Prono, F., Graziano, F., & Nobili, V. (2013). Pediatric non alcoholic fatty liver disease: old and new concepts on development, progression, metabolic insight and potential treatment targets. *BMC Pediatrics*, 13(1), 40. <https://doi.org/10.1186/1471-2431-13-40>
- Godoy-Matos, A. F., Silva Júnior, W. S., & Valerio, C. M. (2020). NAFLD as a continuum: from obesity to metabolic syndrome and diabetes. *Diabetology & Metabolic Syndrome*, 12, 60. <https://doi.org/10.1186/s13098-020-00570-y>
- Gowda, D., Shekhar, C., B. Gowda, S. G., Chen, Y., & Hui, S.-P. (2023). Crosstalk between Lipids and Non-Alcoholic Fatty Liver Disease. *Livers*, 3(4), 687–708. <https://doi.org/10.3390/livers3040045>
- Goyal, N., & Srivastava, V. M. L. (1995). Oxidation and reduction of cytochrome c by mitochondrial enzymes of *Setaria cervi*. *Journal of Helminthology*, 69(1), 13–17. <https://doi.org/10.1017/S0022149X00013778>
- Grewal, T., & Buechler, C. (2022). Emerging Insights on the Diverse Roles of Proprotein Convertase Subtilisin/Kexin Type 9 (PCSK9) in Chronic Liver Diseases: Cholesterol Metabolism and Beyond. *International Journal of Molecular Sciences*, 23(3), 1070. <https://doi.org/10.3390/ijms23031070>
- Gu Juanjuan, Yao min, Yo denbing, & Yao Dengfu. (2016). Nonalcoholic Lipid Accumulation and Hepatocyte Malignant Transformation. *Journal of Clinical and Translational Hepatology*, 4(2). <https://doi.org/10.14218/JCTH.2016.00010>
- Gusdon, A. M., Song, K., & Qu, S. (2014). Nonalcoholic Fatty Liver Disease: Pathogenesis and Therapeutics from a Mitochondria-Centric Perspective. *Oxidative Medicine and Cellular Longevity*, 2014, 1–20. <https://doi.org/10.1155/2014/637027>

H

- Hassani Zadeh, S., Mansoori, A., & Hosseinzadeh, M. (2021). Relationship between dietary patterns and non-alcoholic fatty liver disease: A systematic review and meta-analysis. *Journal of Gastroenterology and Hepatology*, 36(6), 1470–1478. <https://doi.org/10.1111/jgh.15363>
- Heida, A., Gruben, N., Catrysse, L., Koehorst, M., Koster, M., Kloosterhuis, N. J., Gerding, A., Havinga, R., Bloks, V. W., Bongiovanni, L., Wolters, J. C., van Dijk, T., van Loo, G., de Bruin, A., Kuipers, F., Koonen, D. P. Y., & van de Sluis, B. (2021). The hepatocyte IKK:NF- κ B axis promotes liver steatosis by stimulating de novo lipogenesis and cholesterol synthesis. *Molecular Metabolism*, 54, 101349. <https://doi.org/10.1016/j.molmet.2021.101349>
- Hernández-Alvarez, M. I., Sebastián, D., Vives, S., Ivanova, S., Bartoccioni, P., Kakimoto, P., Plana, N., Veiga, S. R., Hernández, V., Vasconcelos, N., Peddinti, G., Adrover, A., Jové, M., Pamplona, R., Gordaliza-Alaguero, I., Calvo, E., Cabré, N., Castro, R., Kuzmanic, A., ... Zorzano, A. (2019). Deficient Endoplasmic Reticulum-Mitochondrial Phosphatidylserine Transfer Causes Liver Disease. *Cell*, 177(4), 881–895.e17. <https://doi.org/10.1016/j.cell.2019.04.010>
- Higuchi, N., Kato, M., Shundo, Y., Tajiri, H., Tanaka, M., Yamashita, N., Kohjima, M., Kotoh, K., Nakamuta, M., Takayanagi, R., & Enjoji, M. (2008). Liver X receptor in cooperation with SREBP-1c is a major lipid synthesis regulator in nonalcoholic fatty liver disease. *Hepatology Research*, 38(11), 1122–1129. <https://doi.org/10.1111/j.1872-034X.2008.00382.x>
- Hotamisligil, G. S., Arner, P., Caro, J. F., Atkinson, R. L., & Spiegelman, B. M. (1995). Increased adipose tissue expression of tumor necrosis factor- α in human obesity and insulin resistance. *The Journal of Clinical Investigation*, 95(5), 2409–2415. <https://doi.org/10.1172/JCI117936>
- Houten, S. M., Violante, S., Ventura, F. V., & Wanders, R. J. A. (2016). The Biochemistry and Physiology of Mitochondrial Fatty Acid β -Oxidation and Its Genetic Disorders. *Annual Review of Physiology*, 78(1), 23–44. <https://doi.org/10.1146/annurev-physiol-021115-105045>
- Huang, Y., Lang, H., Chen, K., Zhang, Y., Gao, Y., Ran, L., Yi, L., Mi, M., & Zhang, Q. (2020). Resveratrol protects against nonalcoholic fatty liver disease by improving lipid metabolism and redox homeostasis via the PPAR α pathway. *Applied Physiology, Nutrition, and Metabolism*, 45(3), 227–239. <https://doi.org/10.1139/apnm-2019-0057n>
- Huh, Y., Cho, Y. J., & Nam, G. E. (2022). Recent Epidemiology and Risk Factors of Nonalcoholic Fatty Liver Disease. *Journal of Obesity & Metabolic Syndrome*, 31(1), 17–27. <https://doi.org/10.7570/jomes22021>

I

- Iizuka, K., Bruick, R. K., Liang, G., Horton, J. D., & Uyeda, K. (2004). Deficiency of carbohydrate response element-binding protein (ChREBP) reduces lipogenesis as well as glycolysis. *Proceedings of the National Academy of Sciences of the United States of America*, 101(19), 7281–7286. <https://doi.org/10.1073/pnas.0401516101>
- Ishihara, N., Nomura, M., Jofuku, A., Kato, H., Suzuki, S. O., Masuda, K., Otera, H., Nakanishi, Y., Nonaka, I., Goto, Y., Taguchi, N., Morinaga, H., Maeda, M., Takayanagi, R., Yokota, S., & Mihara, K. (2009). Mitochondrial fission factor Drp1 is essential for embryonic development and synapse formation in mice. *Nature Cell Biology*, 11(8), 958–966. <https://doi.org/10.1038/ncb1907>

J

- Jain, P. S., Bari, S. B., & Surana, S. J. (2011). Acute Oral Toxicity of *Abelmoschus manihot* and *Wrightia tinctoria* in Mice. *Pharmacognosy Journal*, 3(25), 78–81. <https://doi.org/10.5530/pj.2011.25.14>
- JASIRWAN, C. O. M., LESMANA, C. R. A., HASAN, I., SULAIMAN, A. S., & GANI, R. A. (2019). The role of gut microbiota in non-alcoholic fatty liver disease: pathways of mechanisms. *Bioscience of Microbiota, Food and Health*, 38(3), 81–88. <https://doi.org/10.12938/bmfh.18-032>
- Jump, D. B., Lytle, K. A., Depner, C. M., & Tripathy, S. (2018). Omega-3 polyunsaturated fatty acids as a treatment strategy for nonalcoholic fatty liver disease. *Pharmacology & Therapeutics*, 181, 108–125. <https://doi.org/10.1016/j.pharmthera.2017.07.007>
- K**
- Kale, N., Rathod, S., More, S., & Shinde, N. (2021). Phyto-Pharmacological Profile of *Wrightia tinctoria*. *Asian Journal of Research in Pharmaceutical Sciences*, 301–308. <https://doi.org/10.52711/2231-5659.2021.00047>
- Kamal, S., Khan, M. A., Seth, A., Cholankeril, G., Gupta, D., Singh, U., Kamal, F., Howden, C. W., Stave, C., Nair, S., Satapathy, S. K., & Ahmed, A. (2017). Beneficial Effects of Statins on the Rates of Hepatic Fibrosis, Hepatic Decompensation, and Mortality in Chronic Liver Disease: A Systematic Review and Meta-Analysis. *American Journal of Gastroenterology*, 112(10), 1495–1505. <https://doi.org/10.1038/ajg.2017.170>
- Kanwal, F., Kramer, J. R., Li, L., Dai, J., Natarajan, Y., Yu, X., Asch, S. M., & El-Serag, H. B. (2020). Effect of Metabolic Traits on the Risk of Cirrhosis and Hepatocellular Cancer in Nonalcoholic Fatty Liver Disease. *Hepatology*, 71(3), 808–819. <https://doi.org/10.1002/hep.31014>
- Kausar, S., Wang, F., & Cui, H. (2018). The Role of Mitochondria in Reactive Oxygen Species Generation and Its Implications for Neurodegenerative Diseases. *Cells*, 7(12). <https://doi.org/10.3390/cells7120274>
- Kawai, T., Autieri, M. V., & Scalia, R. (2021). Adipose tissue inflammation and metabolic dysfunction in obesity. *American Journal of Physiology-Cell Physiology*, 320(3), C375–C391. <https://doi.org/10.1152/ajpcell.00379.2020>
- Khan, N., Ali, A., Qadir, A., Ali, A., Warsi, M. H., Tahir, A., & Ali, A. (2021). GC-MS Analysis and Antioxidant Activity of *Wrightia tinctoria* R.Br. Leaf Extract. *Journal of AOAC International*, 104(5), 1415–1419. <https://doi.org/10.1093/jaoacint/qsab054>
- Khyade Mahendra, & Malpani DJM. (2014). *Wrightia tinctoria* R. Br.-a review on its ethnobotany, pharmacognosy and pharmacological profile. *Journal of Coastal Life Medicine*. <https://doi.org/10.12980/JCLM.2.2014C1221>
- Kitada, T., Asakawa, S., Hattori, N., Matsumine, H., Yamamura, Y., Minoshima, S., Yokochi, M., Mizuno, Y., & Shimizu, N. (1998). Mutations in the parkin gene cause autosomal recessive juvenile parkinsonism. *Nature*, 392(6676), 605–608. <https://doi.org/10.1038/33416>
- Kleiner, D. E., Brunt, E. M., van Natta, M., Behling, C., Contos, M. J., Cummings, O. W., Ferrell, L. D., Liu, Y.-C., Torbenson, M. S., Unalp-Arida, A., Yeh, M., McCullough, A. J., & Sanyal, A. J. (2005). Design and validation of a histological scoring system for nonalcoholic fatty liver disease. *Hepatology*, 41(6), 1313–1321. <https://doi.org/10.1002/hep.20701>

- Knebel, B., Haas, J., Hartwig, S., Jacob, S., Köllmer, C., Nitzgen, U., Muller–Wieland, D., & Kotzka, J. (2012). Liver-Specific Expression of Transcriptionally Active SREBP-1c Is Associated with Fatty Liver and Increased Visceral Fat Mass. *PLoS ONE*, 7(2), e31812. <https://doi.org/10.1371/journal.pone.0031812>
- Knothe, G., & Kenar, J. A. (2004). Determination of the fatty acid profile by ¹H-NMR spectroscopy. *European Journal of Lipid Science and Technology*, 106(2), 88–96. <https://doi.org/10.1002/ejlt.200300880>
- Kodama, Y., Kisseleva, T., Iwaisako, K., Miura, K., Taura, K., De Minicis, S., Österreicher, C. H., Schnabl, B., Seki, E., & Brenner, D. A. (2009). c-Jun N-terminal Kinase-1 From Hematopoietic Cells Mediates Progression From Hepatic Steatosis to Steatohepatitis and Fibrosis in Mice. *Gastroenterology*, 137(4), 1467–1477.e5. <https://doi.org/10.1053/j.gastro.2009.06.045>
- Koek, G. H., Liedorp, P. R., & Bast, A. (2011). The role of oxidative stress in non-alcoholic steatohepatitis. *Clinica Chimica Acta*, 412(15–16), 1297–1305. <https://doi.org/10.1016/j.cca.2011.04.013>
- Kolar, M. J., Konduri, S., Chang, T., Wang, H., McNerlin, C., Ohlsson, L., Härröd, M., Siegel, D., & Saghatelian, A. (2019). Linoleic acid esters of hydroxy linoleic acids are anti-inflammatory lipids found in plants and mammals. *Journal of Biological Chemistry*, 294(27), 10698–10707. <https://doi.org/10.1074/jbc.RA118.006956>
- Kumar, A., Chinnathambi, S., Kumar, M., & Pandian, G. N. (2023). Food Intake and Colorectal Cancer. *Nutrition and Cancer*, 75(9), 1710–1742. <https://doi.org/10.1080/01635581.2023.2242103>
- Kumar D Lakshman, Rao. K. N. V. B. D. (2011). Anti oxidation activity of Wrightia tinctoria Roxb bark and Schrebera swietenoides Roxb bark extract. *Journal of Pharmacy Research*, 396–397.
- Kumar, J. K., & Sinha, A. K. (2004). Resurgence of natural colourants: a holistic view. *Natural Product Research*, 18(1), 59–84. <https://doi.org/10.1080/1057563031000122112>
- Kuramoto, K., & He, C. (2022). Degradative and Non-Degradative Roles of Autophagy Proteins in Metabolism and Metabolic Diseases. *Frontiers in Cell and Developmental Biology*, 10. <https://doi.org/10.3389/fcell.2022.844481>
- Kwanten, W. J., Martinet, W., & Francque, S. M. (2016). Autophagy in Non-Alcoholic Fatty Liver Disease (NAFLD). In *Autophagy in Current Trends in Cellular Physiology and Pathology*. InTech. <https://doi.org/10.5772/64534>

L

- Lakhia, R., Yheskel, M., Flaten, A., Quittner-Strom, E. B., Holland, W. L., & Patel, V. (2018). PPAR α agonist fenofibrate enhances fatty acid β -oxidation and attenuates polycystic kidney and liver disease in mice. *American Journal of Physiology-Renal Physiology*, 314(1), F122–F131. <https://doi.org/10.1152/ajprenal.00352.2017>
- Lange, N. F., Graf, V., Caussy, C., & Dufour, J.-F. (2022). PPAR-Targeted Therapies in the Treatment of Non-Alcoholic Fatty Liver Disease in Diabetic Patients. *International Journal of Molecular Sciences*, 23(8), 4305. <https://doi.org/10.3390/ijms23084305>
- Le, M. H., Yeo, Y. H., Li, X., Li, J., Zou, B., Wu, Y., Ye, Q., Huang, D. Q., Zhao, C., Zhang, J., Liu, C., Chang, N., Xing, F., Yan, S., Wan, Z. H., Tang, N. S. Y., Mayumi, M., Liu, X., Liu, C., ... Nguyen, M. H. (2022). 2019 Global NAFLD Prevalence: A Systematic Review and Meta-analysis. *Clinical Gastroenterology and Hepatology*, 20(12), 2809–2817.e28. <https://doi.org/10.1016/j.cgh.2021.12.002>

- Lee, J., Hong, S.-W., Kim, M.-J., Moon, S. J., Kwon, H., Park, S. E., Rhee, E.-J., & Lee, W.-Y. (2022). Dulaglutide Ameliorates Palmitic Acid-Induced Hepatic Steatosis by Activating FAM3A Signaling Pathway. *Endocrinology and Metabolism*, 37(1), 74–83. <https://doi.org/10.3803/EnM.2021.1293>
- Legaki, A.-I., Moustakas, I. I., Sikorska, M., Papadopoulos, G., Velliou, R.-I., & Chatzigeorgiou, A. (2022). Hepatocyte Mitochondrial Dynamics and Bioenergetics in Obesity-Related Non-Alcoholic Fatty Liver Disease. *Current Obesity Reports*, 11(3), 126–143. <https://doi.org/10.1007/s13679-022-00473-1>
- Leoni, S., Tovoli, F., Napoli, L., Serio, I., Ferri, S., & Bolondi, L. (2018). Current guidelines for the management of non-alcoholic fatty liver disease: A systematic review with comparative analysis. *World Journal of Gastroenterology*, 24(30), 3361–3373. <https://doi.org/10.3748/wjg.v24.i30.3361>
- Li, M., Gong, W., Wang, S., & Li, Z. (2022). Trends in body mass index, overweight and obesity among adults in the USA, the NHANES from 2003 to 2018: a repeat cross-sectional survey. *BMJ Open*, 12(12), e065425. <https://doi.org/10.1136/bmjopen-2022-065425>
- Lie Ken Jie, M. S. F., Pasha, M. K., & Alam, M. S. (1997). Synthesis and nuclear magnetic resonance properties of all geometrical isomers of conjugated linoleic acids. *Lipids*, 32(10), 1041–1044. <https://doi.org/10.1007/s11745-997-0134-9>
- Long, J.-K., Dai, W., Zheng, Y.-W., & Zhao, S.-P. (2019). miR-122 promotes hepatic lipogenesis via inhibiting the LKB1/AMPK pathway by targeting Sirt1 in non-alcoholic fatty liver disease. *Molecular Medicine*, 25(1), 26. <https://doi.org/10.1186/s10020-019-0085-2>
- M**
- Ma, Y., Lee, G., Heo, S.-Y., & Roh, Y.-S. (2021). Oxidative Stress Is a Key Modulator in the Development of Nonalcoholic Fatty Liver Disease. *Antioxidants*, 11(1), 91. <https://doi.org/10.3390/antiox11010091>
- Mailloux, R. J. (2020). An Update on Mitochondrial Reactive Oxygen Species Production. *Antioxidants*, 9(6), 472. <https://doi.org/10.3390/antiox9060472>
- Mansouri, A., Gattolliat, C.-H., & Asselah, T. (2018). Mitochondrial Dysfunction and Signaling in Chronic Liver Diseases. *Gastroenterology*, 155(3), 629–647. <https://doi.org/10.1053/j.gastro.2018.06.083>
- Mantovani, A., & Dalbeni, A. (2021). Treatments for NAFLD: State of Art. *International Journal of Molecular Sciences*, 22(5), 2350. <https://doi.org/10.3390/ijms22052350>
- Mariani, S., Fiore, D., Basciani, S., Persichetti, A., Contini, S., Lubrano, C., Salvatori, L., Lenzi, A., & Gnessi, L. (2015). Plasma levels of SIRT1 associate with non-alcoholic fatty liver disease in obese patients. *Endocrine*, 49(3), 711–716. <https://doi.org/10.1007/s12020-014-0465-x>
- Martín-Fernández, M., Arroyo, V., Carnicero, C., Sigüenza, R., Busta, R., Mora, N., Antolín, B., Tamayo, E., Aspichueta, P., Carnicero-Frutos, I., Gonzalo-Benito, H., & Aller, R. (2022). Role of Oxidative Stress and Lipid Peroxidation in the Pathophysiology of NAFLD. *Antioxidants*, 11(11), 2217. <https://doi.org/10.3390/antiox11112217>
- Mattson, M. P. (2009). Roles of the lipid peroxidation product 4-hydroxynonenal in obesity, the metabolic syndrome, and associated vascular and neurodegenerative disorders. *Experimental Gerontology*, 44(10), 625–633. <https://doi.org/10.1016/j.exger.2009.07.003>

- Mendez-Sanchez, N., Cruz-Ramon, V. C., Ramirez-Perez, O. L., Hwang, J. P., Barranco-Fragoso, B., & Cordova-Gallardo, J. (2018). New Aspects of Lipotoxicity in Nonalcoholic Steatohepatitis. *International Journal of Molecular Sciences*, 19(7). <https://doi.org/10.3390/ijms19072034>
- Mihaylova, M. M., & Shaw, R. J. (2011). The AMPK signalling pathway coordinates cell growth, autophagy and metabolism. *Nature Cell Biology*, 13(9), 1016–1023. <https://doi.org/10.1038/ncb2329>
- Molina, A. J. A., Wikstrom, J. D., Stiles, L., Las, G., Mohamed, H., Elorza, A., Walzer, G., Twigg, G., Katz, S., Corkey, B. E., & Shirihai, O. S. (2009). Mitochondrial Networking Protects β -Cells From Nutrient-Induced Apoptosis. *Diabetes*, 58(10), 2303–2315. <https://doi.org/10.2337/db07-1781>
- Montecucco, F., & Mach, F. (2008). Does Non-Alcoholic Fatty Liver Disease (NAFLD) Increase Cardiovascular Risk? *Endocrine, Metabolic & Immune Disorders-Drug Targets*, 8(4), 301–307. <https://doi.org/10.2174/187153008786848268>
- Morio, B., Panthou, B., Bassot, A., & Rieusset, J. (2021). Role of mitochondria in liver metabolic health and diseases. *Cell Calcium*, 94, 102336. <https://doi.org/10.1016/j.ceca.2020.102336>
- Moslehi, A., & Hamidi-zad, Z. (2018). Role of SREBPs in Liver Diseases: A Mini-review. *Journal of Clinical and Translational Hepatology*, 6(3), 1–7. <https://doi.org/10.14218/JCTH.2017.00061>
- Mota, M., Banini, B. A., Cazanave, S. C., & Sanyal, A. J. (2016). Molecular mechanisms of lipotoxicity and glucotoxicity in nonalcoholic fatty liver disease. *Metabolism*, 65(8), 1049–1061. <https://doi.org/10.1016/j.metabol.2016.02.014>

N

- Nagalakshmi¹, H. S., Das, A., & Bhattacharya, S. (2012). In vitro Antimicrobial Properties and Phytochemical Evaluation of Mature Seed Extracts of *Wrightia tinctoria* R. Br. *Pure and Applied Microbiology*, 6(3), 1273–1279.
- Napolitano, G., Fasciolo, G., & Venditti, P. (2021). Mitochondrial Management of Reactive Oxygen Species. *Antioxidants*, 10(11), 1824. <https://doi.org/10.3390/antiox10111824>
- Nassir, F. (2014). Role of mitochondria in alcoholic liver disease. *World Journal of Gastroenterology*, 20(9), 2136. <https://doi.org/10.3748/wjg.v20.i9.2136>
- Nicholas, D. A., Proctor, E. A., Agrawal, M., Belkina, A. C., Van Nostrand, S. C., Panneerseelan-Bharath, L., Jones, A. R., Raval, F., Ip, B. C., Zhu, M., Cacicedo, J. M., Habib, C., Sainz-Rueda, N., Persky, L., Sullivan, P. G., Corkey, B. E., Apovian, C. M., Kern, P. A., Lauffenburger, D. A., & Nikolajczyk, B. S. (2019). Fatty Acid Metabolites Combine with Reduced β Oxidation to Activate Th17 Inflammation in Human Type 2 Diabetes. *Cell Metabolism*, 30(3), 447–461.e5. <https://doi.org/10.1016/j.cmet.2019.07.004>

O

- Obika, M., & Noguchi, H. (2012). Diagnosis and evaluation of nonalcoholic fatty liver disease. *Experimental Diabetes Research*, 2012, 145754. <https://doi.org/10.1155/2012/145754>
- Orasanu, G., Ziouzenkova, O., Devchand, P. R., Nehra, V., Hamdy, O., Horton, E. S., & Plutzky, J. (2008). The Peroxisome Proliferator-Activated Receptor- γ Agonist Pioglitazone Represses Inflammation in a Peroxisome Proliferator-Activated Receptor- α -Dependent Manner In Vitro and In Vivo in Mice. *Journal of the American College of Cardiology*, 52(10), 869–881. <https://doi.org/10.1016/j.jacc.2008.04.055>

P

- Palma, R., Pronio, A., Romeo, M., Scognamiglio, F., Ventriglia, L., Ormando, V. M., Lamazza, A., Pontone, S., Federico, A., & Dallio, M. (2022). The Role of Insulin Resistance in Fueling NAFLD Pathogenesis: From Molecular Mechanisms to Clinical Implications. *Journal of Clinical Medicine*, 11(13). <https://doi.org/10.3390/jcm11133649>
- Park, S. Y., Seetharaman, R., Ko, M. J., Kim, D. Y., Kim, T. H., Yoon, M. K., Kwak, J. H., Lee, S. J., Bae, Y. S., & Choi, Y. W. (2014). Ethyl linoleate from garlic attenuates lipopolysaccharide-induced pro-inflammatory cytokine production by inducing heme oxygenase-1 in RAW264.7 cells. *International Immunopharmacology*, 19(2), 253–261. <https://doi.org/10.1016/j.intimp.2014.01.017>
- Pauls, S. D., Rodway, L. A., Winter, T., Taylor, C. G., Zahradka, P., & Aukema, H. M. (2018). Anti-inflammatory effects of α -linolenic acid in M1-like macrophages are associated with enhanced production of oxylipins from α -linolenic and linoleic acid. *The Journal of Nutritional Biochemistry*, 57, 121–129. <https://doi.org/10.1016/j.jnutbio.2018.03.020>
- Pawlak, M., Lefebvre, P., & Staels, B. (2015). Molecular mechanism of PPAR α action and its impact on lipid metabolism, inflammation and fibrosis in non-alcoholic fatty liver disease. *Journal of Hepatology*, 62(3), 720–733. <https://doi.org/10.1016/j.jhep.2014.10.039>
- Pérez-Carreras, M. (2003). Defective hepatic mitochondrial respiratory chain in patients with nonalcoholic steatohepatitis. *Hepatology*, 38(4), 999–1007. <https://doi.org/10.1053/jhep.2003.50398>
- Perumpail, B., Li, A., John, N., Sallam, S., Shah, N., Kwong, W., Cholankeril, G., Kim, D., & Ahmed, A. (2018). The Role of Vitamin E in the Treatment of NAFLD. *Diseases*, 6(4), 86. <https://doi.org/10.3390/diseases6040086>
- Pfluger, P. T., Herranz, D., Velasco-Miguel, S., Serrano, M., & Tschöp, M. H. (2008). Sirt1 protects against high-fat diet-induced metabolic damage. *Proceedings of the National Academy of Sciences*, 105(28), 9793–9798. <https://doi.org/10.1073/pnas.0802917105>
- Pinyopornpanish, K., Leerapun, A., Pinyopornpanish, K., & Chattipakorn, N. (2021). Effects of Metformin on Hepatic Steatosis in Adults with Nonalcoholic Fatty Liver Disease and Diabetes: Insights from the Cellular to Patient Levels. *Gut and Liver*, 15(6), 827–840. <https://doi.org/10.5009/gnl20367>
- Pipitone, R. M., Ciccioli, C., Infantino, G., La Mantia, C., Parisi, S., Tulone, A., Pennisi, G., Grimaudo, S., & Petta, S. (2023). MAFLD: a multisystem disease. *Therapeutic Advances in Endocrinology and Metabolism*, 14, 20420188221145548. <https://doi.org/10.1177/20420188221145549>
- Podszun, M. C., Alawad, A. S., Lingala, S., Morris, N., Huang, W.-C. A., Yang, S., Schoenfeld, M., Rolt, A., Ouwerkerk, R., Valdez, K., Umarova, R., Ma, Y., Fatima, S. Z., Lin, D. D., Mahajan, L. S., Samala, N., Violet, P.-C., Levine, M., Shamburek, R., ... Rotman, Y. (2020). Vitamin E treatment in NAFLD patients demonstrates that oxidative stress drives steatosis through upregulation of de-novo lipogenesis. *Redox Biology*, 37, 101710. <https://doi.org/10.1016/j.redox.2020.101710>
- Poeta, M., Pierri, L., & Vajro, P. (2017). Gut-Liver Axis Derangement in Non-Alcoholic Fatty Liver Disease. *Children (Basel, Switzerland)*, 4(8). <https://doi.org/10.3390/children4080066>
- Ponnusamy, K., Petchiammal, C., Mohankumar, R., & Hopper, W. (2010). In vitro antifungal activity of indirubin isolated from a South Indian ethnomedicinal plant *Wrightia tinctoria* R. Br. *Journal of Ethnopharmacology*, 132(1), 349–354. <https://doi.org/10.1016/j.jep.2010.07.050>

Puengel, T., Lefere, S., Hundertmark, J., Kohlhepp, M., Penners, C., Van de Velde, F., Lapauw, B., Hoorens, A., Devisscher, L., Geerts, A., Boehm, S., Zhao, Q., Krupinski, J., Charles, E. D., Zinker, B., & Tacke, F. (2022). Combined Therapy with a CCR2/CCR5 Antagonist and FGF21 Analogue Synergizes in Ameliorating Steatohepatitis and Fibrosis. *International Journal of Molecular Sciences*, 23(12), 6696. <https://doi.org/10.3390/ijms23126696>

Q

Qiao, Y., Li, X., Zhang, X., Xiao, F., Zhu, Y., Fang, Z., & Sun, J. (2019). Hepatocellular iNOS protects liver from NASH through Nrf2-dependent activation of HO-1. *Biochemical and Biophysical Research Communications*, 514(2), 372–378. <https://doi.org/10.1016/j.bbrc.2019.04.144>

Quinn, P. M. J., Moreira, P. I., Ambrósio, A. F., & Alves, C. H. (2020). PINK1/PARKIN signalling in neurodegeneration and neuroinflammation. *Acta Neuropathologica Communications*, 8(1), 189. <https://doi.org/10.1186/s40478-020-01062-w>

R

Raj R, Kumar Saravana, & R. Gandhimathi. (2009). Hypoglycemic and hypolipidemic activity of Wrightia tinctoria L. in alloxan induced diabetes in albino wistar rats. *Pharmacologyonline*, 3, 550–559.

Ramanathan, R., Ali, A. H., & Ibdah, J. A. (2022). Mitochondrial Dysfunction Plays Central Role in Nonalcoholic Fatty Liver Disease. *International Journal of Molecular Sciences*, 23(13), 7280. <https://doi.org/10.3390/ijms23137280>

Rani M. Sandhya, Pippalla Rao S, Krishna Mohan G, & Gangaraju M. (2012). ANTI-DIABETIC ACTIVITY OF METHANOLIC AND ETHYL ACETATE EXTRACTS OF WRIGHTIA TINCTORIA R.BR. FRUIT. *IJPSR*, 3(10), 3861–3866.

Raza, S., Rajak, S., Singh, R., Zhou, J., Sinha, R. A., & Goel, A. (2023). Cell-type specific role of autophagy in the liver and its implications in non-alcoholic fatty liver disease. *World Journal of Hepatology*, 15(12), 1272–1283. <https://doi.org/10.4254/wjh.v15.i12.1272>

Reifen, R., Karlinsky, A., Stark, A. H., Berkovich, Z., & Nyska, A. (2015). α -Linolenic acid (ALA) is an anti-inflammatory agent in inflammatory bowel disease. *The Journal of Nutritional Biochemistry*, 26(12), 1632–1640. <https://doi.org/10.1016/j.jnutbio.2015.08.006>

Reusch, V. M., & Burger, M. M. (1974). Distribution of Marker Enzymes between Mesosomal and Protoplast Membranes. *Journal of Biological Chemistry*, 249(16), 5337–5345. [https://doi.org/10.1016/S0021-9258\(19\)42369-7](https://doi.org/10.1016/S0021-9258(19)42369-7)

Riazi, K., Azhari, H., Charette, J. H., Underwood, F. E., King, J. A., Afshar, E. E., Swain, M. G., Congly, S. E., Kaplan, G. G., & Shaheen, A.-A. (2022). The prevalence and incidence of NAFLD worldwide: a systematic review and meta-analysis. *The Lancet Gastroenterology & Hepatology*, 7(9), 851–861. [https://doi.org/10.1016/S2468-1253\(22\)00165-0](https://doi.org/10.1016/S2468-1253(22)00165-0)

Rodriguez-Ramiro, I., Vauzour, D., & Miniñane, A. M. (2016). Polyphenols and non-alcoholic fatty liver disease: impact and mechanisms. *Proceedings of the Nutrition Society*, 75(1), 47–60. <https://doi.org/10.1017/S0029665115004218>

Rodríguez-Yoldi, M. J. (2021). Anti-Inflammatory and Antioxidant Properties of Plant Extracts. *Antioxidants*, 10(6), 921. <https://doi.org/10.3390/antiox10060921>

Rolfe, D. F., & Brown, G. C. (1997). Cellular energy utilization and molecular origin of standard metabolic rate in mammals. *Physiological Reviews*, 77(3), 731–758. <https://doi.org/10.1152/physrev.1997.77.3.731>

Rong, L., Zou, J., Ran, W., Qi, X., Chen, Y., Cui, H., & Guo, J. (2023). Advancements in the treatment of non-alcoholic fatty liver disease (NAFLD). *Frontiers in Endocrinology*, 13. <https://doi.org/10.3389/fendo.2022.1087260>

S

Sakhuja, P. (2014). Pathology of alcoholic liver disease, can it be differentiated from nonalcoholic steatohepatitis? *World Journal of Gastroenterology*, 20(44), 16474. <https://doi.org/10.3748/wjg.v20.i44.16474>

Sami, W., Ansari, T., Butt, N. S., & Hamid, M. R. A. (2017). Effect of diet on type 2 diabetes mellitus: A review. *International Journal of Health Sciences*, 11(2), 65–71.

Saponaro, C., Gaggini, M., & Gastaldelli, A. (2015). Nonalcoholic fatty liver disease and type 2 diabetes: common pathophysiologic mechanisms. *Current Diabetes Reports*, 15(6), 607. <https://doi.org/10.1007/s11892-015-0607-4>

Sato, S., Jung, H., Nakagawa, T., Pawlosky, R., Takeshima, T., Lee, W.-R., Sakiyama, H., Laxman, S., Wynn, R. M., Tu, B. P., MacMillan, J. B., De Brabander, J. K., Veech, R. L., & Uyeda, K. (2016). Metabolite Regulation of Nuclear Localization of Carbohydrate-response Element-binding Protein (ChREBP). *Journal of Biological Chemistry*, 291(20), 10515–10527. <https://doi.org/10.1074/jbc.M115.708982>

Schrader, M., Costello, J., Godinho, L. F., & Islinger, M. (2015). Peroxisome-mitochondria interplay and disease. *Journal of Inherited Metabolic Disease*, 38(4), 681–702. <https://doi.org/10.1007/s10545-015-9819-7>

Schrepfer, E., & Scorrano, L. (2016). Mitofusins, from Mitochondria to Metabolism. *Molecular Cell*, 61(5), 683–694. <https://doi.org/10.1016/j.molcel.2016.02.022>

Schwenzer, N. F., Springer, F., Schraml, C., Stefan, N., Machann, J., & Schick, F. (2009). Non-invasive assessment and quantification of liver steatosis by ultrasound, computed tomography and magnetic resonance. *Journal of Hepatology*, 51(3), 433–445. <https://doi.org/10.1016/j.jhep.2009.05.023>

Shimoda, H., Shan, S.-J., Tanaka, J., Seki, A., Seo, J.-W., Kasajima, N., Tamura, S., Ke, Y., & Murakami, N. (2010). Anti-Inflammatory Properties of Red Ginger (*Zingiber officinale* var. Rubra) Extract and Suppression of Nitric Oxide Production by Its Constituents. *Journal of Medicinal Food*, 13(1), 156–162. <https://doi.org/10.1089/jmf.2009.1084>

Shum, M., Ngo, J., Shirihai, O. S., & Liesa, M. (2021). Mitochondrial oxidative function in NAFLD: Friend or foe? *Molecular Metabolism*, 50, 101134. <https://doi.org/10.1016/j.molmet.2020.101134>

Singh, R., Wang, Y., Xiang, Y., Tanaka, K. E., Gaarde, W. A., & Czaja, M. J. (2009). Differential effects of JNK1 and JNK2 inhibition on murine steatohepatitis and insulin resistance. *Hepatology*, 49(1), 87–96. <https://doi.org/10.1002/hep.22578>

Sinha, A., & Bankura, B. (2023). Prevalence of nonalcoholic fatty liver disease in type 2 diabetes mellitus patients from the Eastern region of India. *Diabetes Epidemiology and Management*, 12, 100161. <https://doi.org/10.1016/j.deman.2023.100161>

- Smeuninx, B., Boslem, E., & Febbraio, M. A. (2020). Current and Future Treatments in the Fight against Non-Alcoholic Fatty Liver Disease. *Cancers*, 12(7), 1714. <https://doi.org/10.3390/cancers12071714>
- Smith, B. K., Marcinko, K., Desjardins, E. M., Lally, J. S., Ford, R. J., & Steinberg, G. R. (2016). Treatment of nonalcoholic fatty liver disease: role of AMPK. *American Journal of Physiology-Endocrinology and Metabolism*, 311(4), E730–E740. <https://doi.org/10.1152/ajpendo.00225.2016>
- Srere, P. A. (1969). [1] *Citrate synthase* (pp. 3–11). [https://doi.org/10.1016/0076-6879\(69\)13005-0](https://doi.org/10.1016/0076-6879(69)13005-0)
- Sulaiman, S. A., Dorairaj, V., & Adrus, M. N. H. (2022). Genetic Polymorphisms and Diversity in Nonalcoholic Fatty Liver Disease (NAFLD): A Mini Review. *Biomedicines*, 11(1). <https://doi.org/10.3390/biomedicines11010106>
- Sumida, Y., & Yoneda, M. (2018). Current and future pharmacological therapies for NAFLD/NASH. *Journal of Gastroenterology*, 53(3), 362–376. <https://doi.org/10.1007/s00535-017-1415-1>
- Sung Ok Lee, Sang Zin Choi, & Kang Ro Lee. (2004). Phytochemical Constituents of the Aerial Parts from *Aster hispidus*. *Natural Product Sciences*, 10(6), 335–340.
- Suomalainen, A., & Battersby, B. J. (2018). Mitochondrial diseases: the contribution of organelle stress responses to pathology. *Nature Reviews Molecular Cell Biology*, 19(2), 77–92. <https://doi.org/10.1038/nrm.2017.66>
- Suryadevara, V., Ramchandran, R., Kamp, D. W., & Natarajan, V. (2020). Lipid Mediators Regulate Pulmonary Fibrosis: Potential Mechanisms and Signaling Pathways. *International Journal of Molecular Sciences*, 21(12), 4257. <https://doi.org/10.3390/ijms21124257>

T

- Takahashi, Y. (2014). Histopathology of nonalcoholic fatty liver disease/nonalcoholic steatohepatitis. *World Journal of Gastroenterology*, 20(42), 15539. <https://doi.org/10.3748/wjg.v20.i42.15539>
- Tanwar, S., Rhodes, F., Srivastava, A., Trembling, P. M., & Rosenberg, W. M. (2020). Inflammation and fibrosis in chronic liver diseases including non-alcoholic fatty liver disease and hepatitis C. *World Journal of Gastroenterology*, 26(2), 109–133. <https://doi.org/10.3748/wjg.v26.i2.109>
- Teng, M. L., Ng, C. H., Huang, D. Q., Chan, K. E., Tan, D. J., Lim, W. H., Yang, J. D., Tan, E., & Muthiah, M. D. (2023). Global incidence and prevalence of nonalcoholic fatty liver disease. *Clinical and Molecular Hepatology*, 29(Suppl), S32–S42. <https://doi.org/10.3350/cmh.2022.0365>
- Thibaut, R., Gage, M. C., Pineda-Torra, I., Chabrier, G., Venteclef, N., & Alzaid, F. (2022). Liver macrophages and inflammation in physiology and physiopathology of non-alcoholic fatty liver disease. *The FEBS Journal*, 289(11), 3024–3057. <https://doi.org/10.1111/febs.15877>
- Tsalamandris, S., Antonopoulos, A. S., Oikonomou, E., Papamikroulis, G.-A., Vogiatzi, G., Papaioannou, S., Deftereos, S., & Tousoulis, D. (2019). The Role of Inflammation in Diabetes: Current Concepts and Future Perspectives. *European Cardiology Review*, 14(1), 50–59. <https://doi.org/10.15420/ecr.2018.33.1>

U

- Uranga, C. C., Beld, J., Mrse, A., Córdova-Guerrero, I., Burkart, M. D., & Hernández-Martínez, R. (2016). Data from mass spectrometry, NMR spectra, GC–MS of fatty acid esters produced by *Lasiodiplodia theobromae*. *Data in Brief*, 8, 31–39. <https://doi.org/10.1016/j.dib.2016.05.003>

V

- Viola, A., Munari, F., Sánchez-Rodríguez, R., Scolaro, T., & Castegna, A. (2019). The Metabolic Signature of Macrophage Responses. *Frontiers in Immunology*, 10. <https://doi.org/10.3389/fimmu.2019.01462>
- von Holstein-Rathlou, S., BonDurant, L. D., Peltekian, L., Naber, M. C., Yin, T. C., Claflin, K. E., Urizar, A. I., Madsen, A. N., Ratner, C., Holst, B., Karstoft, K., Vandenbeuch, A., Anderson, C. B., Cassell, M. D., Thompson, A. P., Solomon, T. P., Rahmouni, K., Kinnamon, S. C., Pieper, A. A., ... Potthoff, M. J. (2016). FGF21 Mediates Endocrine Control of Simple Sugar Intake and Sweet Taste Preference by the Liver. *Cell Metabolism*, 23(2), 335–343. <https://doi.org/10.1016/j.cmet.2015.12.003>

W

- Wahlang, B., Jin, J., Beier, J. I., Hardesty, J. E., Daly, E. F., Schneggelberger, R. D., Falkner, K. C., Prough, R. A., Kirpich, I. A., & Cave, M. C. (2019). Mechanisms of Environmental Contributions to Fatty Liver Disease. *Current Environmental Health Reports*, 6(3), 80–94. <https://doi.org/10.1007/s40572-019-00232-w>
- Wainwright, P., & Byrne, C. (2016). Bidirectional Relationships and Disconnects between NAFLD and Features of the Metabolic Syndrome. *International Journal of Molecular Sciences*, 17(3), 367. <https://doi.org/10.3390/ijms17030367>
- Wang, J., Conti, D. V., Bogumil, D., Sheng, X., Nouredin, M., Wilkens, L. R., Le Marchand, L., Rosen, H. R., Haiman, C. A., & Setiawan, V. W. (2021). Association of Genetic Risk Score With NAFLD in An Ethnically Diverse Cohort. *Hepatology Communications*, 5(10), 1689–1703. <https://doi.org/10.1002/hep4.1751>
- Wang, L., Klionsky, D. J., & Shen, H.-M. (2023). The emerging mechanisms and functions of microautophagy. *Nature Reviews Molecular Cell Biology*, 24(3), 186–203. <https://doi.org/10.1038/s41580-022-00529-z>
- Wang, Y., Tong, J., Chang, B., Wang, B.-F., Zhang, D., & Wang, B.-Y. (2014). Relationship of *SREBP-2* rs2228314 G>C Polymorphism with Nonalcoholic Fatty Liver Disease in a Han Chinese Population. *Genetic Testing and Molecular Biomarkers*, 18(9), 653–657. <https://doi.org/10.1089/gtmb.2014.0116>
- Wang, Y.-X. (2010). PPARs: diverse regulators in energy metabolism and metabolic diseases. *Cell Research*, 20(2), 124–137. <https://doi.org/10.1038/cr.2010.13>
- Wong, V. W., Chan, W., Chitturi, S., Chawla, Y., Dan, Y. Y., Duseja, A., Fan, J., Goh, K., Hamaguchi, M., Hashimoto, E., Kim, S. U., Lesmana, L. A., Lin, Y., Liu, C., Ni, Y., Sollano, J., Wong, S. K., Wong, G. L., Chan, H. L., & Farrell, G. (2018). Asia–Pacific Working Party on Non-alcoholic Fatty Liver Disease guidelines 2017—Part 1: Definition, risk factors and assessment. *Journal of Gastroenterology and Hepatology*, 33(1), 70–85. <https://doi.org/10.1111/jgh.13857>
- Wong, V. W.-S., Tse, C.-H., Lam, T. T.-Y., Wong, G. L.-H., Chim, A. M.-L., Chu, W. C.-W., Yeung, D. K.-W., Law, P. T.-W., Kwan, H.-S., Yu, J., Sung, J. J.-Y., & Chan, H. L.-Y. (2013). Molecular Characterization of the Fecal Microbiota in Patients with Nonalcoholic Steatohepatitis – A Longitudinal Study. *PLoS ONE*, 8(4), e62885. <https://doi.org/10.1371/journal.pone.0062885>
- Woodhouse, C. A., Patel, V. C., Singanayagam, A., & Shawcross, D. L. (2018). Review article: the gut microbiome as a therapeutic target in the pathogenesis and treatment of chronic liver disease. *Alimentary Pharmacology & Therapeutics*, 47(2), 192–202. <https://doi.org/10.1111/apt.14397>

Wu, Q.-J., Zhang, T.-N., Chen, H.-H., Yu, X.-F., Lv, J.-L., Liu, Y.-Y., Liu, Y.-S., Zheng, G., Zhao, J.-Q., Wei, Y.-F., Guo, J.-Y., Liu, F.-H., Chang, Q., Zhang, Y.-X., Liu, C.-G., & Zhao, Y.-H. (2022). The sirtuin family in health and disease. *Signal Transduction and Targeted Therapy*, 7(1), 402. <https://doi.org/10.1038/s41392-022-01257-8>

X

Xanthakos, S., Miles, L., Bucuvalas, J., Daniels, S., Garcia, V., & Inge, T. (2006). Histologic Spectrum of Nonalcoholic Fatty Liver Disease in Morbidly Obese Adolescents. *Clinical Gastroenterology and Hepatology*, 4(2), 226–232. [https://doi.org/10.1016/S1542-3565\(05\)00978-X](https://doi.org/10.1016/S1542-3565(05)00978-X)

Y

Younossi, Z. M., Golabi, P., de Avila, L., Paik, J. M., Srishord, M., Fukui, N., Qiu, Y., Burns, L., Afendy, A., & Nader, F. (2019). The global epidemiology of NAFLD and NASH in patients with type 2 diabetes: A systematic review and meta-analysis. *Journal of Hepatology*, 71(4), 793–801. <https://doi.org/10.1016/j.jhep.2019.06.021>

Z

Zelber-Sagi, S., Godos, J., & Salomone, F. (2016). Lifestyle changes for the treatment of nonalcoholic fatty liver disease: a review of observational studies and intervention trials. *Therapeutic Advances in Gastroenterology*, 9(3), 392–407. <https://doi.org/10.1177/1756283X16638830>

Zhang, X., Heredia, N. I., Balakrishnan, M., & Thrift, A. P. (2021). Prevalence and factors associated with NAFLD detected by vibration controlled transient elastography among US adults: Results from NHANES 2017–2018. *PLOS ONE*, 16(6), e0252164. <https://doi.org/10.1371/journal.pone.0252164>

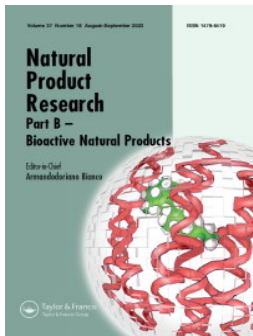
Zhao, Y., Zhou, Y., Wang, D., Huang, Z., Xiao, X., Zheng, Q., Li, S., Long, D., & Feng, L. (2023). Mitochondrial Dysfunction in Metabolic Dysfunction Fatty Liver Disease (MAFLD). *International Journal of Molecular Sciences*, 24(24), 17514. <https://doi.org/10.3390/ijms242417514>

Zhu, L., Wu, X., & Liao, R. (2023). Mechanism and regulation of mitophagy in nonalcoholic fatty liver disease (NAFLD): A mini-review. *Life Sciences*, 312, 121162. <https://doi.org/10.1016/j.lfs.2022.121162>

Zisser, A., Ipsen, D. H., & Tveden-Nyborg, P. (2021). Hepatic Stellate Cell Activation and Inactivation in NASH-Fibrosis—Roles as Putative Treatment Targets? *Biomedicines*, 9(4), 365. <https://doi.org/10.3390/biomedicines9040365>

Publications

1. Karmakar Eshani, **Prosenjit Das**, Priyanka Yatham, Deepak Kumar, Satinath Mukhopadhyay, and Sib Sankar Roy. 2022. “Seedpod Extracts of *Wrightia tinctoria* Shows Significant Anti-Inflammatory Effects in HepG2 and RAW-264.7 cell Lines.” *Natural Product Research* 37 (18): 3158–62. doi:10.1080/14786419.2022.2146688.
2. Eshani Karmakar, Nabanita Das, Bidisha Mukherjee, **Prosenjit Das**, Satinath Mukhopadhyay, and Sib Sankar Roy. 2023. Lipid-induced alteration in retinoic acid signaling leads to mitochondrial dysfunction in HepG2 and Huh7 cells. *Biochemistry and Cell Biology*. **101**(3): 220-234. <https://doi.org/10.1139/bcb-2022-0266>



Seedpod extracts of *Wrightia tinctoria* shows significant anti-inflammatory effects *in* HepG2 and RAW-264.7 cell lines

Eshani Karmakar, Prosenjit Das, Priyanka Yatham, Deepak Kumar, Satinath Mukhopadhyay & Sib Sankar Roy

To cite this article: Eshani Karmakar, Prosenjit Das, Priyanka Yatham, Deepak Kumar, Satinath Mukhopadhyay & Sib Sankar Roy (2023) Seedpod extracts of *Wrightia tinctoria* shows significant anti-inflammatory effects *in* HepG2 and RAW-264.7 cell lines, Natural Product Research, 37:18, 3158-3162, DOI: [10.1080/14786419.2022.2146688](https://doi.org/10.1080/14786419.2022.2146688)

To link to this article: <https://doi.org/10.1080/14786419.2022.2146688>



View supplementary material [↗](#)



Published online: 17 Nov 2022.



Submit your article to this journal [↗](#)



Article views: 262



View related articles [↗](#)



View Crossmark data [↗](#)

SHORT COMMUNICATION



Seedpod extracts of *Wrightia tinctoria* shows significant anti-inflammatory effects in HepG2 and RAW-264.7 cell lines

Eshani Karmakar^{a†}, Prosenjit Das^{a†}, Priyanka Yatham^{c†}, Deepak Kumar^c, Satinath Mukhopadhyay^b and Sib Sankar Roy^a

^aCell Biology & Physiology Division, CSIR-Indian Institute of Chemical Biology (IICB), Kolkata, India;

^bDepartment of Endocrinology and Metabolism, Institute of Post Graduate Medical Education and Research, Kolkata, India; ^cOrganic and Medicinal Chemistry Division, CSIR-Indian Institute of Chemical Biology (IICB), Kolkata, India

ABSTRACT

W. tinctoria, an Indian herb *Indrajao*, has significant therapeutic potential. While studies have highlighted the anti-inflammatory potential of the leaves and bark of this plant, similar efficacy of the seed-pods remains unexplored. We demonstrate significant anti-inflammatory effects of the hexane fraction (Fr-B) of ethyl acetate extract of the seedpods in reducing lipopolysaccharide and palmitate mediated inflammation in RAW264.7 macrophages and HepG2 cells. GC-MS and NMR profiling of Fr-B revealed the existence of hexadecanoic acid, ethyl hexadecanoate, 9,12-octadecanoic acid, 9,12,15-octadecatrienoic acid, 9,12,15-octadecatrienoic acid ethyl ester, ethyl linoleate and octadecanoic acid ethyl esters.

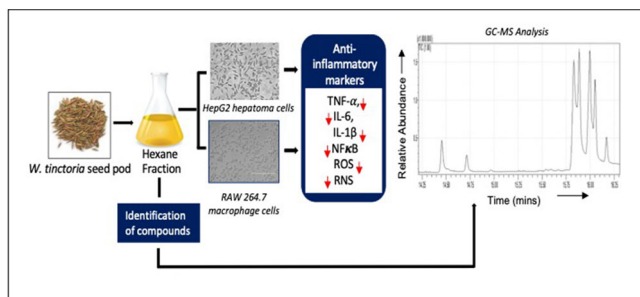
ARTICLE HISTORY

Received 29 August 2022

Accepted 4 November 2022

KEYWORDS

Wrightia tinctoria; lipopolysaccharide; palmitic acid; inflammation; fatty acids; HepG2RAW-264.7




1. Introduction

Research over several years positioned chronic inflammatory response as an underlying cause for a vast continuum of detrimental disorders ranging from diabetes, cardiovascular ailments, neurodegenerative disorders, and aggressive cancers (Glass et al. 2010; Koene et al. 2016). The obnoxious side effects of long-term application of anti-

CONTACT Sib Sankar Roy  sibsankar@iicb.res.in; Deepak Kumar  deepak@iicb.res.in

[†]Contributed equally: These authors have contributed equally and share first authorship

 Supplemental data for this article can be accessed online at <https://doi.org/10.1080/14786419.2022.2146688>

© 2022 Informa UK Limited, trading as Taylor & Francis Group

inflammatory drugs necessitated the requirement for herbal drugs with minimal toxicity. Since ancient times, plants served as a trustable source of therapeutic agents and several plant parts in the form of extract exhibited potential in preventing inflammation (Rodríguez-Yoldi 2021). Empirical evidence of such plants with significant therapeutic potential includes *Wrightia tinctoria* of the Apocynaceae family, which showed beneficial effects in treating diseases like jaundice, dysentery, haemorrhage, and psoriasis (Kumar and Sinha 2004; Anusharaj et al. 2013). While significant anti-inflammatory effects of the leaves and bark of this plant is already known, similar effects of its seedpods is yet to be reported. We studied the anti-inflammatory effects of seedpod extracts of this plant in RAW 264.7 and HepG2 cell lines, mediated by palmitate (PA) and lipopolysaccharide (LPS).

2. Results and discussion

2.1. Fractions of *W. tinctoria* seedpod exhibit anti-inflammatory properties

The anti-inflammatory effects of ethyl acetate extract (Ex-A) obtained from the seedpod and its fractions, hexane (Fr-B) and ethyl acetate (Fr-C) were evaluated in RAW264.7 (mouse macrophage cell line) and HepG2 (hepatoma cell line). The cytotoxic effects were evaluated by cell viability percentage using MTT assay. Data shows that each of the three extract/fractions possess no such significant cytotoxic effect at a concentration range of 10–300 µg/ml in both the cells (Figure S1A and B). Further we checked the effect of extract/fractions on inhibition of cellular nitrates, and nitrites (RNS) produced by LPS (*E. Coli* LPS, Sigma) stimulation (1 µg/ml) for 22 hr by using Griess reagent on RAW264.7 macrophage cells. A range of different concentrations of sodium nitrite was used to generate a standard curve and a reduction in the level of RNS was correlated with reduction in cellular nitrite level. Our data reveals that pre-treatment with hexane (Fr-B) fraction significantly reduces RNS generation with an IC_{50} of 139.83 µg/ml as compared to ethyl acetate extract (Ex-A; IC_{50} : 422.93 µg/ml) and other fraction (Fr-C; IC_{50} : 428.71 µg/ml) (Figure S2A). Subsequently, we estimated total cellular ROS level using DCFH-DA after pre-treating cells with the extract/fraction followed by LPS treatment for 16 hr. Fr-B significantly reduced the level of total cellular ROS at 200 µg/ml concentration in RAW264.7 macrophage cells (Figures 1A and S2B). However, Ex-A and Fr-C were not so effective in reducing ROS, thereby hinting at the overall efficacy of Fr-B. Since Fr-B showed a potent effect in reversing elevated ROS and RNS level upon induction by LPS, it prompted us to check the expression of proinflammatory cytokines IL-6, IL1 β , and TNF α (Table S1). Since the IC_{50} dose of Fr-B emerged as 139.83 µg/ml in case of Griess Assay (inhibition of RNS) which was also supported by DCFH-DA assay (inhibition of ROS), we selected the dose of 200 µg/ml for further confirmatory anti-inflammatory studies. The expression of intracellular protein levels of IL-6 and IL1 β was checked by flow cytometry treating HepG2 cells with PA (0.75 mM). The results indicate that in presence of PA, Fr-B (200 µg/ml) decreases IL6, IL1 β expression (Figure S3A). Subsequently, mRNA expression was checked by real-time qPCR in RAW264.7 macrophage cells which revealed a marked decrease in the expression of pro-inflammatory cytokines viz, IL1 β , TNF α (Figure 1B) and IL6 (Figure S3B) when treated with Fr-B (200 µg/ml) upon LPS induction for 16 hr.

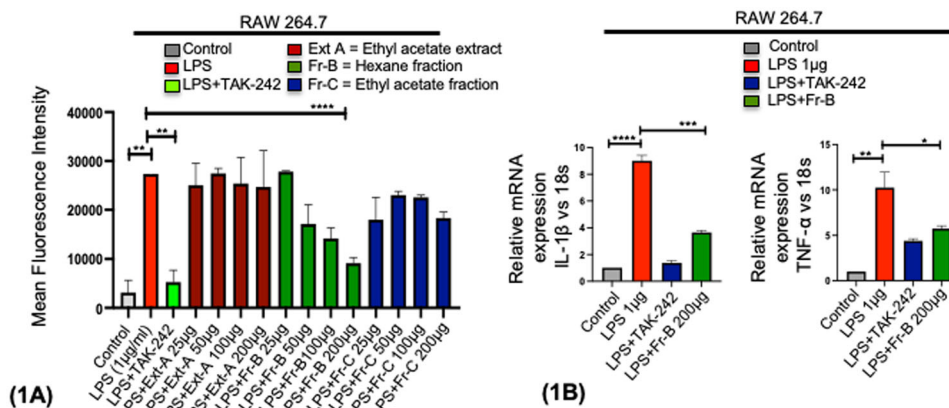


Figure 1. Anti-inflammatory effect of *W. tinctoria* seedpod extract and fractions in RAW 264.7 cells. (1A) Estimation of DCFH-DA in RAW 264.7 cells by flow cytometry. (1B) Relative mRNA expression detected by RT-qPCR analysis of the respective genes TNF α , IL-1 β . Experiments were performed in triplicate ($n = 3$). Data are expressed as mean \pm SEM and statistical significance was calculated using one way ANOVA (followed by Bonferroni Multiple Comparison Test) employing Graph Pad Prism (Version 9). The level of significance is calculated as $\alpha = 0.05$ (95% confidence interval). Data information: **** $p < 0.0001$, *** $p < 0.001$, ** $p < 0.01$, * $p < 0.05$.

Additionally, a decrease in secreted IL-1 β protein concentration was noticed on pre-treating RAW264.7 cells with Fr-B (200 μ g/ml) and stimulating with LPS for 6 hr (Figure S3C), measured by sandwich ELISA method. Studies earlier highlighted that LPS and saturated fatty acids like PA works through TLR4 mediated inflammatory pathway where NF κ B acts as a major transcription factor (Korbecki and Bajdak-Rusinek 2019). After activation by proteasomal degradation, NF κ B p65 translocate into the nucleus and regulates transcription of different set of genes, thereby triggering secretion of proinflammatory cytokines like TNF α , IL-6, and IL1 β (Liu et al. 2017). Consistent to this, we checked the effect on overall expression of NF κ B, treating both RAW264.7 and HepG2 cells with hexane (Fr-B) fraction (200 μ g/ml) stimulating with LPS and PA respectively. Confocal imaging of cells showed a marked reduction in overall expression of NF κ B in HepG2 cells and a prominent inhibition of expression as well as nuclear translocation in RAW264.7 cells, suggesting the plausible anti-inflammatory role of inhibition of NF κ B in pro-inflammatory signalling cascade (Figure S3D).

2.2. Identification of compounds by GC-MS analysis and NMR spectroscopy

The GC-MS analysis suggested the presence of 7 prominent peaks which were tentatively identified as hexadecanoic acid (Rt 14.455 min), ethyl hexadecanoate (Rt 14.715 min), 9,12-octadecanoic acid (Rt 15.830 Min), 9,12,15-octadecatrienoic acid (Rt 15.885 min), ethyl linoleate (Rt 15.995 Min), 9,12,15-octadecatrienoic acid ethyl ester (Rt 16.050 min), and octadecanoic acid ethyl ester (Rt 16.170 min) (Figures S4–S11) (Roussis et al. 2000; Asuming et al. 2005; Pino et al. 2005; Benkaci-Ali et al. 2007). The identification of these compounds was further ascertained by NMR spectroscopic analysis of Fr-B. The 13 C-NMR spectrum of Fr-B displayed at δ c 179.28–172.89 (–COOH or COOR; R= –CH $_3$ or –CH $_2$ –CH $_3$), 131.99–127.19 (–C=C–), 68.98, 62.13 (–COOR; –CH $_3$ or

$-\text{CH}_2-\text{CH}_3$), 34.78-14.18 ($-\text{CH}_2-$ or $-\text{CH}_2-\text{CH}_3$) suggesting the presence of identified compounds. In support the ^1H -NMR spectrum displayed corresponding signals at δ_{H} 5.399-5.239 ($-\text{CH}=\text{CH}-$), 4.300-4.119 ($-\text{COOR}$; $-\text{CH}_3$ or $-\text{CH}_2-\text{CH}_3$), 2.803-0.668 ($-\text{CH}_2-$ or $-\text{CH}_2-\text{CH}_3$) (Figures S12 and S13) (Jie et al. 1997; Kenar and Knothe 2004; Uranga et al. 2016; Alexandri et al. 2017).

3. Experimental

Supplementary file.

4. Conclusions

The present study highlights that hexane fraction (Fr-B) obtained from ethyl acetate extract (Ex-A) exhibits potential in inhibition of inflammatory response induced by LPS and PA in HepG2 and RAW264.7 cells. Since poly-unsaturated fatty acids (PUFA) are known to render protection against inflammation (Park et al. 2014; Pauls et al. 2018) we presume that the presence of the identified compounds might be responsible in delivering anti-inflammatory effects. It would be interesting to identify the anti-inflammatory effects of Fr-B in various animal models to substantiate the traditional uses and isolation of individual compound from the Fr-B and treating them separately or in combination in *in-vitro* and *in-vivo* models would further clarify its efficacy, dosing and therapeutic potential.

Disclosure statement

No potential conflict of interest was reported by the authors.

Funding

Instrumentation support from CIF division of the institute is appreciated. This work was supported by grants from in-house projects (CSIR-IICB).

References

- Alexandri E, Ahmed R, Siddiqui H, Choudhary MI, Tsiafoulis CG, Gerothanassis IP. 2017. High resolution NMR spectroscopy as a structural and analytical tool for unsaturated lipids in solution. *Molecules*. 22(10):1663.
- Anusharaj Chandrashekar R, Adake P, Rao SN, Santanusaha S. 2013. *Wrightia tinctoria*: an overview. *J Drug Deliv Ther*. 3:196–198.
- Asuming WA, Beauchamp PS, Descalzo JT, Dev BC, Dev V, Frost S, Ma CW. 2005. Essential oil composition of four *Lomatium Raf.* species and their chemotaxonomy. *Biochem Syst Ecol*. 33(1):17–26.
- Benkaci-Ali F, Baaliouamer A, Meklati BY, Chemat F. 2007. Chemical composition of seed essential oils from Algerian *Nigella sativa* extracted by microwave and hydrodistillation. *Flavour Fragr J*. 22(2):148–153.
- Glass CK, Saijo K, Winner B, Marchetto MC, Gage FH. 2010. Mechanisms underlying inflammation in neurodegeneration. *Cell*. 140(6):918–934.

- Jie MS, Pasha MK, Alam MS. 1997. Synthesis and nuclear magnetic resonance properties of all geometrical isomers of conjugated linoleic acids. *Lipids*. 32(10):1041–1044.
- Kenar JA, Knothe G. 2004. Determination of the fatty acid profile by ¹H-NMR spectroscopy. *Eur J Lipid Sci Technol*. 106(2):88–96.
- Koene RJ, Prizment AE, Blaes A, Konety SH. 2016. Shared risk factors in cardiovascular disease and cancers. *Circulation*. 133(11):1104–1114.
- Korbecki J, Bajdak-Rusinek K. 2019. The effect of palmitic acid on inflammatory response in macrophages: an overview of molecular mechanisms. *Inflamm Res*. 68(11):915–932.
- Kumar JK, Sinha AK. 2004. Resurgence of natural colourants: a holistic view. *Nat Prod Res*. 18(1): 59–84.
- Liu T, Zhang L, Joo D, Sun SC. 2017. NF-κB signaling in inflammation. *Signal Transduct Target Ther*. 2:17023.
- Park SY, Seetharaman R, Ko MJ, Kim DY, Kim TH, Yoon MK, Kwak JH, Lee SJ, Bae YS, Choi YW. 2014. Ethyl linoleate from garlic attenuates lipopolysaccharide-induced pro-inflammatory cytokine production by inducing heme oxygenase-1 in RAW264.7 cells. *Int Immunopharmacol*. 19(2):253–261.
- Pauls SD, Rodway LA, Winter T, Taylor CG, Zahradka P, Aukema HM. 2018. Anti-inflammatory effects of α-linolenic acid in M1-like macrophages are associated with enhanced production of oxylipins from α-linolenic and linoleic acid. *J Nutr Biochem*. 57:121–129.
- Pino JA, Mesa J, Muñoz Y, Martí MP, Marbot R. 2005. Volatile components from mango (*Mangifera indica* L.) cultivars. *J Agric Food Chem*. 53(6):2213–2223.
- Rodríguez-Yoldi MJ. 2021. Anti-inflammatory and antioxidant properties of plant extracts. *Antioxidants*. 10(6):921–924.
- Roussis V, Tsoukatou M, Petrakis PV, Chinou I, Skoula M, Harborne JB. 2000. Volatile constituents of four *Helichrysum* species growing in Greece. *Biochem Syst Ecol*. 28(2):163–175.
- Uranga CC, Beld J, Mrse A, Córdova-Guerrero I, Burkart MD, Hernández-Martínez R. 2016. Data from mass spectrometry, NMR spectra, GC-MS of fatty acid esters produced by *Lasiodiplodia theobromae*. *Data Brief*. 8:31–39.

Lipid-induced alteration in retinoic acid signaling leads to mitochondrial dysfunction in HepG2 and Huh7 cells

Eshani Karmakar^a, Nabanita Das^{a,b}, Bidisha Mukherjee^c, Prosenjit Das^a, Satinath Mukhopadhyay^c, and Sib Sankar Roy^{a,d}

^aCell Biology and Physiology Division, CSIR-Indian Institute of Chemical Biology, 4 Raja S. C. Mullick Road, Kolkata, 700032, India;

^bDepartment of Pharmacology and Toxicology, National Institute of Pharmaceutical Education and Research, Raebareli,

Bijnor-sisendi Road, Lucknow, Uttar Pradesh, 226002, India; ^cDepartment of Endocrinology and Metabolism, Institute of Post

Graduate Medical Education and Research, 244, A.J.C. Bose Road, Kolkata, 700020, India; ^dAcademy of Scientific & Innovative Research (AcSIR), India

Corresponding author: **Sib Sankar Roy** (email: sibsankar@iicb.res.in)

Abstract

A surfeit of mitochondrial reactive oxygen species (ROS) and inflammation serve as obligatory mediators of lipid-associated hepatocellular maladies. While retinoid homeostasis is essential in restoring systemic energy balance, its role in hepatic mitochondrial function remains elusive. The role of lecithin-retinol acyltransferase (LRAT) in maintenance of retinoid homeostasis is appreciated earlier; however, its role in modulating retinoic acid (RA) bioavailability upon lipid-imposition is unexplored. We identified LRAT overexpression in high-fat diet (HFD)-fed rats and palmitate-treated hepatoma cells. Elevation in LRAT expression depletes RA production and deregulates RA signaling. This altered RA metabolism enhances fat accumulation, accompanied by inflammation that leads to impaired mitochondrial function through enhanced ROS generation. Hence, LRAT inhibition could be a novel approach preventing lipid-induced mitochondrial dysfunction in hepatoma cells.

Key words: lipid, retinoic acid, PPAR α , mitochondrial dysfunction, HepG2 and Huh7 cells

Introduction

The ever-rising incidence of obesity, reaching epidemic proportions worldwide, strongly correlates with the elevation of circulating free fatty acids (FFA). A surfeit of plasma FFA and low-grade inflammation is a crucial determinant of insulin resistance (IR), and its associated hepatic disorders, which includes non-alcoholic fatty liver disease (NAFLD), steatosis or non-alcoholic steatohepatitis (NASH), and late cirrhosis (Tripathy et al. 2003; Arner and Rydén 2015). FFAs play an intricate role in the activation of various inflammatory pathways, posing lipotoxicity and inflammation as a common cause of obesity-driven hepatic disorders (Zhou et al. 2020). Based on the association of FFA-induced inflammation with type 2 diabetes (T2DM) the use of thiazolidinediones like rosiglitazone, pioglitazone came to the limelight (Heliövaara et al. 2007; Lin et al. 2014). Besides all the therapeutic approaches brought forward currently, recent findings highlighted the potential use of a synthetic retinoid, Fenretinide, against inflammation in preventing obesity and IR (Bikman et al. 2012; Mcilroy et al. 2013; Lin et al. 2016). This further substantiates the implication of vitamin-A or retinol in lipid-driven hepatic disorders. Besides the role of vitamin-A in tissue remodeling, immune function, and night vision (Barber et al. 2014; Huang et al. 2018), extensive research in recent days highlighted an alteration in vitamin-A or retinoic

acid (RA) homeostasis in diet-induced obesity and IR (Mody 2017).

Retinol, the active precursor of retinoid metabolism, undergoes a two-step oxidation process yielding retinaldehyde at first, which is then oxidized further to yield RA (Kedishvili 2016). The transcriptionally active metabolite of vitamin A (retinol), RA exist in several forms, the two most common being all-trans retinoic acid (atRA) and 9-*cis* RA. atRA and 9-*cis* RA functions through retinoid-x receptor (RXR) that heterodimerizes with retinoic acid receptor (RAR) (Byrne and Blaner 2013) and peroxisome proliferator-activated receptor (PPAR) (Ziouzenkova et al. 2007; Dawson and Xia 2012). While pharmacological intervention with retinol (Jeyakumar et al. 2006), retinaldehyde (Ziouzenkova et al. 2007), and atRA reduces body weight and adiposity in rodents, a retinol-deficient diet led to an upsurge in the fat mass of affected rodents (Mercader et al. 2006). The participation of RAR α and RAR γ in inhibiting adipocyte differentiation by inducing pre-adipocyte factor-1, a potent adipogenesis inhibitor, was highlighted earlier (Berry et al. 2012). Retinol-binding protein 4 (RBP4), a hepato-secretory protein that keeps retinol in the circulation, its level in the serum remains significantly elevated during IR (Fan et al. 2019). The uptake of retinol (holo-RBP4) obtained from the dietary retinoids is mediated through STRA6 receptor in the hepatocytes (Steinhoff

et al. 2021). Retinol, transported into the cell, is esterified in the form of retinyl palmitate by a retinol esterifying enzyme, lecithin-retinol acyltransferase (LRAT). Recent studies projected the involvement of LRAT in RBP4-mediated IR, and LRAT knockout obese mice are more glucose tolerant than those of the wild type (Marwarha et al. 2014). Predominantly, LRAT is essential for the cellular uptake of retinol from RBP4 and also for the maintenance of retinoid homeostasis (Amengual et al. 2012).

PPAR α , a predominant isoform in the liver, is a critical regulator of energy homeostasis and fatty acid oxidation (FAO) (Keller et al. 1993; Pawlak et al. 2015). Of note, hepatocyte-specific deletion of PPAR α leads to the development of steatosis in high-fat diet (HFD)-fed mice (Montagner et al. 2016). Consistently, impairment in FAO leading to excess fat accumulation in the liver is often associated with enhanced oxidative stress and mitochondrial dysfunction (Wajner and Amaral 2016; Bhatti et al. 2017). Extensive research over years revealed that mitochondria of NAFLD and NASH patients have altered morphology, reduced or mutated mtDNA content (Schroder et al. 2016; Dabrowski et al. 2021). Further, increased mitochondrial fission coincides with excessive reactive oxygen species (ROS) generation and apoptosis (Galloway et al. 2014). RA, besides its role in the retardation of steatosis, is a positive regulator of mitochondrial function in skeletal muscle and adipose tissue (Kim et al. 2014; Tourniaire et al. 2015). RA treatment enhances PPAR α -mediated FAO and reduces lipid biosynthesis in the liver of HFD-fed mice (Berry and Noy 2009; Amengual et al. 2010). atRA regulation is, therefore, plausibly mediated through PPAR α .

Considering the information in the backdrop, we aimed to study if LRAT under excess FFA influx could modulate the bioavailability of the cellular RA. However, the role of endogenous RA in maintaining mitochondrial functions in the hepatocytes and the mechanism thereof is still unclear. Our study indicates PA-induced elevated expression of LRAT could be associated with a reduction in endogenous RA synthesis and deregulated RA signaling. This alteration in the RA metabolism could lead to inflammation and mitochondrial dysfunction in the hepatoma cells.

Materials and methods

Animals

Male Sprague-Dawley rats, weighing 160–190 g, were obtained from our animal facility and maintained in a well-ventilated and temperature-controlled room supported by 12 h day/dark cycles. The animals were equally distributed and segregated into two groups. Both control and the study groups were fed with a standard diet and HFD (60 kcal fat content, Test diet, USA; Fig S1A) for 12 weeks (Das et al. 2017a). The tissues collected from the euthanized rats were snap-frozen in liquid N₂ and then transferred to 80 °C for subsequent experiments. All procedures involving experimental animals were performed in compliance with the Institutional Animal Ethics Committee regulations (CPCSEA, Govt. of India).

Histological studies

Paraffin-embedded liver tissues were sectioned (5 μ m thickness) in microtome (Leica RM2235, Germany) and stained with α -Smooth Muscle Actin (α -SMA), LRAT antibody. The bright-field colored images were captured using Andor iXON3 ultra EMCCD camera of Andor spinning disk confocal laser scanning microscope (Andor Technology plc, Belfast, Ireland; 40X (NA 0.75) magnification).

Cell culture and treatments

HepG2 and Huh7 (hepatoma) cells retained in Dulbecco Modified Eagle Medium and supplemented with 10% FBS, 100 U/L penicillin/streptomycin (Invitrogen) were maintained at 37 °C in 5% CO₂ humidified chamber. A stock solution of 2 mM palmitic acid (PA, Sigma-Aldrich) conjugated with BSA (Hi-Media; Cat# TC194) was prepared, from which working 0.75 mM concentration of PA was applied to serum-starved cells for 16 h (Dou et al. 2011; Shen et al. 2018). The cells were treated with PPAR- α agonist (fenofibrate (FEN), concentration 200 μ M, Sigma) and RXR- α agonist (9-*cis* RA, concentration 300 nM, Sigma; Sarang et al. 2014) for 16 h.

siRNA/plasmid transfection

1 \times 10⁶ cells seeded uniformly were grown overnight in 35 mm dishes and allowed to attain approximately 60% confluency for siRNA transfection using LRAT-specific siRNA (Santa Cruz Biotechnology) at a concentration of 20 nM/well. Similarly, for plasmid transfection, more than 80% (approx.) confluent cells were transfected using LRAT overexpression clone (GenScript) at a concentration of 1 μ g/well. Following the manufacturer's instructions, siRNA and plasmid transfection were performed employing Lipofectamine 2000 (Invitrogen) transfection reagent. After 48 h of transfection, the cells were harvested for downstream experiments. The siRNA-transfected cells were treated with PA for 16 h before harvesting. The control cells were transfected with scrambled siRNA (Ambion).

RNA isolation and quantitative PCR

Total RNA from the cell lines (HepG2 and Huh7) was isolated using an RNA isolation solution (RNAiso Plus, TaKaRa Bio) following the standard protocol (Das et al. 2017a). 0.5 μ g of RNA was used for cDNA preparation using the iScript kit (Bio-Rad). Relative expression level of specific genes were quantified by real-time PCR (Applied Biosystems 7500) upon normalizing to the housekeeping gene by using the SyBr Green kit (Bio-Rad). The relative gene expression was measured by the comparative CT method (Δ CT), where Δ CT is the CT of the target gene that was subtracted from the CT of the housekeeping gene. The "Fold" change in the Y-axis indicates the relative gene expression. After normalization with 18S rRNA, the relative mRNA level was expressed as fold induction concerning control, which is defined as 1 in cells/tissue samples with no treatment. Primers were designed using Primer Express 3 software (Applied Biosystem) and procured from Integrated DNA Technology. The sequences of the primers are mentioned in the table (Fig. S1B).

Immuno-cytochemistry followed by confocal microscopy

In a 6-well plate, 1×10^4 cells seeded on coverslips were grown overnight and subjected to synchronization in serum-free DMEM for 24 h, followed by 16 h of treatment with 0.75 mM PA. Preparation for microscopy was done following a standard protocol (Chowdhury et al. 2017) where cells were fixed with 4% paraformaldehyde for 10 min, followed by permeabilization for 5 min with 0.1% Triton X-100. Subsequently, cells were incubated in a 5% BSA blocking solution (in PBS) for 1 h and subsequently incubated with the primary antibody for 2 h. This step was followed by conjugation with secondary Alexa-Fluor 488/633-antibody (Invitrogen; dilution 1:400) for another 1.5 h. The cells were then stained with 0.25 $\mu\text{g/mL}$ DAPI for 5 min, followed by PBS wash. To visualize mitochondrial morphology, cells were stained with MitoTrackerTM Red FM (50 nM, Invitrogen; Waltham, Massachusetts, USA; Cat# M22425) for 20 min at 37 °C, post 48 h transfection and 16 h of PA treatment. Visualization and acquisition of the images were done employing the Leica confocal microscope SP8 (Leica Microscope Systems; Wetzlar, Germany; RRID: SCR_008960) with a 63X oil immersion objective lens (NA 1.4) and the Olympus BX51 microscope (Olympus; acquisition software cellSens; Shinjuku, Tokyo, Japan; RRID: SCR_013673) with a 40X (NA 0.75) objective lens. Image capture was done at room temperature.

HPLC and MS analysis of retinoic acid (RA)

The extraction of RA was done under a dim red light, as described earlier (Kane et al. 2014). Identification and quantification of RA were done with a Waters C18-Novapak reverse phase HPLC column (3.9 mm \times 150 mm). The column was equilibrated with 90% methanol: 10% 0.01 M acetic acid. After application of the sample in equilibrating buffer, a linear gradient was set up to 100% methanol for 15 min. The flow rate was 0.8 mL/min and the elution was followed at 350 nm. Standard RA (Sigma) was eluted as a single symmetrical peak with a retention time (R_t) = 6.25 ± 0.05 min. A calibration curve correlating the amount of RA applied (0–2 μg) and the area of the eluted peak was constructed where a linear dependency was observed. The fraction from HPLC was analyzed and further validated by a mass spectrometer with electrospray ionization (ESI) in negative mode. A mass of 299.38 (against $M^+ = 300.44$) confirmed the presence of RA. All data and graph generated for LC-MS was processed employing Mass Lynx V4.1 software. Following details for experimental setup are as follows: Instrument Specification: Xevo-G2 XS Q-ToF (Waters); LC-profile (UPLC): Acquity UPLC BEH C18 1.7 μm ; column: length 2.1 mm \times 100 mm; run time: 5 min; Method used: Gradient [80% Water, 80% water (0.1% Formic acid) + 20% Acetonitrile]; flow (mL/min): 0.4 mL/min; general operational settings: high pressure 8000–9000 psi; ESI = negative ion (sensitivity mode); source: capillary (kV) = 3.00, Sampling Cone-40, Source Offset-80; temperature (°C): source: 120, desolvation-350; gas flows: Cone Gas (L/h) = 50, desolvation gas (L/h) = 800.

Nuclear/cytosolic protein fraction isolation

Cells (approximately 2×10^6) were seeded in 60 mm dishes and cytoplasmic and nuclear fractions were isolated using ProteoJet Protein Extraction Kit (Fermentas) following the manufacturer's protocol. Immunoblotting was performed on isolated nuclear and cytoplasmic proteins using specific antibodies such as anti-NF κ B (cell signaling; Cat# C22B4 dilution 1:1000), anti-histone H3 (Cell Signaling Technology; Cat# 9715S; dilution 1:1000 used as a loading control for nuclear fraction), and anti-GAPDH (Genscript; Cat# A01622 dilution 1:1000 used as a loading control for cytosolic fraction). Chemo-luminescence detection was done with a Biospectrum Imaging system using UVP life science software.

Protein isolation and Western blotting

Preparation of the cell lysate and extraction of the proteins was performed using RIPA lysis buffer following the standard protocol (Nicholas et al. 2019). Proteins isolated from the cells were subjected to Western blotting with antibodies specific for the protein, viz., human anti-LRAT (Abcam; Cat# ab137304; dilution 1:1000). Detection of the chemiluminescent bands in the blot was done using an ECL detection reagent (Cat# 1705062, Bio-Rad) and the fold change was calculated using ImageJ software.

Intracellular protein detection using flow cytometry

Harvested cells (1×10^6) were fixed by the addition of 4% formaldehyde drop-wise with vigorous mixing and incubated at 37 °C for 10 min, followed by brief incubation on ice for 1 min. Centrifugation of the cells was done at 300 g for 5 min and the supernatant was discarded. Cells were resuspended in the PBS and permeabilized with drop-wise addition of chilled 90% methanol while stirring condition. This step was followed by incubation on the ice for 30 min, leaving the set up o/n at -20 °C. Next day cells were washed with PBS, then incubated using the respective primary antibodies anti-CRABPI/II (Santa Cruz; Cat# sc166897, dilution 1:400) anti-PPAR α (Sigma; Cat# P0369; dilution 1:400), anti-RAR β (Santa Cruz; Cat# sc552; dilution 1:400), anti-NF κ B (Cell Signaling; Cat# C22B4; dilution 1:400), anti-CPT1A (Santa Cruz; Cat# sc20514; dilution 1:100), anti-IL-6 (Santa Cruz; Cat# sc7920; dilution 1:400), anti-IL-1 β (Santa Cruz; Cat# sc7884; dilution 1:400), anti-MFN2 (Cell Signaling; Cat# D2D10; dilution 1:400), and anti-OPA (Santa Cruz; Cat# sc393296; dilution 1:400) for 2 h. Cells were subsequently washed with PBST buffer and further incubated with the respective FITC-tagged secondary antibodies (Santa Cruz; dilution 1:400) for 1 h at room temperature. After incubation, the cells were rinsed and resuspended in PBS for analysis using LSR Fortessa cell analyzer (BD Biosciences, RRID:SCR_013311). Non-specificity of the secondary antibody was verified by staining control cells with FITC-tagged mouse/rabbit secondary antibody (only) used in experiments detecting the intracellular protein level (Fig. S1C).

Bodipy 493/503 neutral lipid droplets staining

The cells were grown in a 35 mm culture dish under normal conditions overnight, followed by transfection with LRAT siRNA/overexpressing plasmid construct or treatment with 0.75 mM PA for 16 h. Excess media/serum was removed by washing with PBS. Further, the cells were stained with 2 μ M Bodipy (Invitrogen, Molecular Probes) dissolved in PBS and incubated at 37 °C in the dark for 15 min (Qiu et al. 2016). After washing with PBS for three times, the cells were immediately processed for the live imaging performed using a Leica confocal microscope SP8 (Leica Microscope Systems; Wetzlar, Germany; RRID: SCR_008960) with a 63X oil immersion objective lens (NA 1.4)

Fatty acid oxidation (FAO) by extracellular flux analyzer

PA treated or LRAT-siRNA or LRAT construct transfected cells were plated at a density of 30 000/well in a 24-well XF24 cell culture microplate (Seahorse Bioscience, North Billerica MA, USA) in DMEM medium containing 10% FBS and were kept in the CO₂ incubator for a consecutive 3 h. The assay was performed following the protocol mentioned earlier (Das et al. 2017b). Before the assay, the cells were washed twice with FAO Assay Medium (1X KHB Buffer supplemented with 2 mmol/L-glutamine) followed by incubation with the same assay medium in a non-CO₂ incubator for 1 h at 37 °C. Carbonyl-cyanide-4-(trifluoromethoxy)phenylhydrazone (FCCP, 1.6 μ M) was loaded into the first Injection Port A of the assay cartridge, followed by 12 min of instrument equilibration and calibration. 10–20 min before initiation of the assay, 75 μ L of XF Palmitate-BSA-FAO substrate was added to the appropriate wells. Further, normalization of protein employing Lowry's method was done once the assay was over. The FAO rate was measured by quantifying the oxygen consumption rate (OCR).

Cellular ROS measurement by DCFH-DA

A 60 mm covered glass-bottom dish was used to grow the cells. Approximately 1×10^6 cells were scraped and washed with PBS followed by staining with 2 μ M DCFH-DA (CM-H2DCFDA, Invitrogen, Molecular Probes Cat# C6827) for 15 min. Following this, three 5 min washes were performed. The stained cells were suspended in 300 μ L PBS and subjected to detection by flow cytometry (excitation/emission 488 nm/570 nm) using BD FACSDiva Software (RRID: SCR_001456).

Estimation of mitochondrial ROS generation by mitosox staining

Mitochondrial ROS was measured following the standard protocol. Approximately 1×10^6 cells grown in a 60 mm covered glass-bottom dish were scraped and washed with PBS. This step was followed by staining with 100 μ L of PBS containing Mitosox™ red (5 μ M) mitochondrial superoxide indicator (Invitrogen, Cat# M36008) at 37 °C for 20 min. Stained cells were washed twice with PBS by centrifugation at $300 \times g$ for 5 min each. The stained cells were then suspended in 300 μ L PBS and processed for detection by flow cytometry (excita-

tion/emission 488 nm/570 nm) employing BD FACSDiva Software.

Mitochondrial membrane potential by JC1 staining

1×10^6 cells were scraped and washed with PBS twice at an interval of 5 min. This step was followed by staining with PBS containing JC-1 (5 μ g/mL, Invitrogen, Molecular Probes) for 15 min at 37 °C. Stained cells were washed twice and suspended in PBS for detection by flow cytometry (Red Excitation/Emission 514 nm/529 nm; Green Excitation/Emission 485 nm/529 nm) using BD FACSDiva Software. The transition of red aggregates of JC1 to green monomeric form was utilized for the measurement of mitochondrial membrane potential.

Estimation of mitochondrial load using nonyl-acridine orange (NOA) and mito-tracker green (MTG)

The cells were seeded at a density of 1×10^6 and grown in a 60 mm round covered glass-bottom dish, washed with PBS repeatedly thrice at an interval of 5 min. Subsequently, cells were scraped and stained with 1 μ M nonyl acridine orange (NOA) (Invitrogen, Cat#A1372) for 30 min and 100 nM mito-tracker green (MTG) re-suspended in PBS, (Invitrogen, Cat#M7514) for another 10–15 min. Determination of green fluorescence intensity (490/516 nm) was done using a flow cytometer (BDFacs Diva Software) (Maftah et al. 1989).

Measurement of mitochondrial respiration by extracellular flux analyzer

Mitochondrial respiration was determined by measuring OCR utilizing XF-24 Extracellular Flux Analyzer (Seahorse Bioscience, North Billerica MA, USA) following standardized protocol (Gu et al. 2020). Treated or transfected cells were seeded in XF24 cell culture plates (Seahorse BioScience) at a density of 25 000/well and grown in a 100 μ L DMEM growth medium containing 10% FBS in a CO₂ incubator for 3 h. Immediately after cell adherence, 150 μ L of growth medium was added further and cells were maintained at 37 °C in the incubator. Before the start of the assay, the existing medium was replaced by a DMEM base medium supplemented with 25 mM glucose, 2 mM glutamine, and 1 mM sodium pyruvate (pH 7.4) and the plates were pre-incubated at 37 °C in a non-CO₂ incubator. After calibration, the plates were placed into the XF24 extracellular flux analyzer, and the OCR was evaluated by the sequential injection of 1 μ M oligomycin, 2 μ M FCCP, and 1 μ M rotenone/antimycin A. OCR was calculated by the Seahorse XF24 analyzer and the OCR values were normalized to total protein concentration following Lowry's method.

Statistical analysis

Using GraphPad Prism-5 software, all statistical analyses were performed. Data were expressed as the mean \pm S.E.M. Two-tailed Student's *t*-test was used to calculate the statistical significance when the number of groups was two, and one-way ANOVA (followed by Dunnett's and Tukey's test analysis)

was done when the number of groups was more than two. The experiments were repeated at least three times.

Results

LRAT overexpression was observed in HFD-fed animals and palmitic acid (PA) treated HepG2 and Huh7 cells

Sprague Dawley rats ($n = 4$ for each group) fed a 60% HFD ad libitum 12 consecutive weeks were used to study the pathophysiology of NAFLD. The HFD-fed rats became obese and hyperglycemic; the serum levels of cholesterol, triglyceride, alanine transaminase, and aspartate transaminase were also elevated (data published earlier, [Das et al. 2017a](#)). qPCR performed from the liver tissue of HFD-fed animals revealed a high LRAT mRNA expression compared to the controls ([Fig. 1A](#)). Immuno-histochemistry of HFD-fed rats' liver tissue revealed increased expression of fibrosis marker α -SMA as well as a significant increase in the LRAT expression ([Fig. 1B](#)).

Further to continue with the downstream mechanistic study *in vitro*, we considered human hepatoma cells (HepG2 and Huh7), which are proposed as alternative model for hepatocytes owing to their stable phenotype and retention of functional characteristics of differentiated hepatic cells ([Donato et al. 2013](#)). Since, PA is reported as a predominantly elevated saturated fatty acid in obese conditions, we continued our *in vitro* studies employing it. We found that treating hepatoma cells, HepG2 and Huh7 cells with 0.75 mM PA for 16 h significantly increased LRAT mRNA expression (qPCR analysis: [Figs. 1C, 1D](#)). Similarly, confocal microscopy ([Fig. 1E](#)) and FACS analysis ([Fig. 1F](#)) of HepG2 and Huh7 cells treated with 0.75 mM PA showed increased expression of LRAT. Additionally, Western blotting performed ([Fig. 1G](#)) revealed similar pattern of elevated LRAT expression in a dose-dependent manner.

LRAT downregulates retinoic acid (RA) production and the functional machinery of RA in PA-treated HepG2 and Huh7 cells

RA-metabolism is orchestrated by enzymatic network that tightly controls the conversion of retinol to RA. Since PA treatment enhances the expression of LRAT, the enzyme involved in the esterification of retinol, we aimed to check its impact on RA synthesis or its level in the cells. Initially the level of increase in LRAT mRNA expression was determined by transfecting or treating cells with LRAT overexpression plasmid (PL_LRAT) ([Fig. S2A and S2B](#)). Subsequently, it has been observed that PA treatment could effectively increase LRAT expression with a concomitant reduction in RA at the cellular level as quantified by HPLC ([Fig. 2A](#)) followed by mass spectrometric analysis ([Fig. S2C](#)). The cells were exposed to 4-IU retinol as substrate during the experiment, and the concentration of RA was found to be significantly lower in PA-mediated LRAT overexpressed cells ([Fig. 2B](#)). The intracellular lipid-binding protein, cellular retinoic acid binding protein II (CRABP II) mediates the delivery of atRA to the nuclear receptors ([Nelson et al. 2016](#); [Fischer-huchzermeyer et](#)

[al. 2017](#)). In line with this, we observed a marked reduction in CRABP-I/II expression both in PA-treated and LRAT overexpressed (PL_LRAT) cells. This change in the expression of CRABP-I/II was reverted by silencing LRAT in the presence of PA in HepG2 cells ([Fig. 2C](#)). Subsequently, a marked decrease in the transcription of Cytochrome P450 26A1 (Cyp26a1), a RA-responsive gene, was noticed in both PA-treated and LRAT overexpressed cells. LRAT silencing in presence of PA leads to marked upregulation of Cyp26a1 in HepG2 ([Fig. 2D](#)) and Huh7 cells ([Fig. 2E](#)).

Reduced activity of PPAR α due to LRAT-mediated depletion of RA leads to inflammation in HepG2 cells

To ascertain the downstream effect of PA-mediated disruption of RA-signaling, we looked at the expression of RA-responsive nuclear receptors, RAR β and PPAR α as well as their target genes, FGF21 and CPT1A which are involved in β -oxidation and glucose metabolism ([Li et al. 2013](#); [Amengual et al. 2019](#)). We observed downregulation of RAR β ([Fig. 3A](#)) and PPAR α ([Fig. 3B](#)) in HepG2 cells. Reduced expression of FGF21 revealed by qPCR was restored upon silencing LRAT ([Fig. 3C](#)). A similar pattern of CPT1A expression was observed upon flow cytometry analysis ([Fig. S2D](#)). In addition, PA-treated and LRAT overexpressed cells showed a significant reduction in PPAR α mRNA expression estimated by real-time qPCR ([Fig. S2E](#)). PPAR α inhibits inflammation during metabolic disorders by physically interacting with NF κ B ([Delerive et al. 1999](#); [Pawlak et al. 2015](#); [Korbecki et al. 2019](#)). Consistently, here we noticed LRAT knockdown could ameliorate PA-mediated inflammation ([Fig. 3D](#)), partially by reducing the activation of NF κ B as well as its translocation to the nucleus ([Fig. 3E](#)), as evidenced by Western blot analysis using nuclear and cytoplasmic fractions. Furthermore, this observation was corroborated by marked increase in the expression of pro-inflammatory cytokines like IL-1 β ([Fig. 3F](#)) and IL-6 ([Fig. 3G](#)), assessed by flow cytometry in both PA-treated and LRAT overexpressed HepG2 cells. Elevated levels of the proinflammatory markers were reverted upon LRAT silencing in the presence of PA.

PA-induced LRAT overexpression impairs mitochondrial function and enhances ROS generation in HepG2 and Huh7 cells

Chronic inflammation is intricately related to mitochondrial dysfunction ([Missiroli et al. 2020](#)). Since PA-induced overexpression of LRAT contributes to inflammation, we aimed to ascertain its impact on mitochondrial function. Impaired mitochondrial function disrupts FAO and further manifests excess fat deposition in the liver. Consistent with this, we observed that a reduced level of PPAR α both due to PA treatment and LRAT overexpression (PL_LRAT) led to reduced FAO as indicated by decreased OCR level in both HepG2 ([Fig. 4A](#)) and Huh7 cells ([Fig. S3A](#)). This in turn causes neutral fat deposition, as revealed by Bodipy staining ([Figs. 4B and S3B](#)). Furthermore, to ascertain the extent of mitochondrial damage in consequence of enhanced fat accumulation, we estimated cellular ROS generation by measuring Mitosox

Fig. 1. Upregulation of LRAT in HFD-fed animals and PA-treated hepatoma (HepG2 and Huh7) cells. (A) qPCR analysis shows fold change increase of LRAT mRNA expression in the liver tissue of obese vs control rats. (B) Immuno histochemical analysis performed using LRAT, α SMA anti-sera in the liver sections of obese vs control rats. LRAT mRNA level was quantified by qPCR in (C) HepG2, and (D) Huh7 cells treated with PA at 0.75 mM concentration for 16 h. (E) Representative confocal images of cells using LRAT antibody under different concentrations of PA in HepG2 and Huh7 cell line. (F) Detection of internal antigen through FACS analysis using LRAT antibody in HepG2 and Huh7 cells. Gating was done using unstained cells. (G) Western Blot performed to measure LRAT protein expression in HepG2 cells. Quantification of protein was done by ImageJ Software for each replicates and densitometry was performed on the basis of three independent experiments. Significance level was calculated by Student's *t*-test using Graph Pad Prism (Version 9). Data expressed as the mean \pm SEM. ****P* < 0.001, ***P* < 0.01, **P* < 0.05, ns = non-significant. Scale bars 100 μ m (B) and 20 μ m (E). α -SMA: α -Smooth Muscle Actin; LRAT: lecithin-retinol acyltransferase.

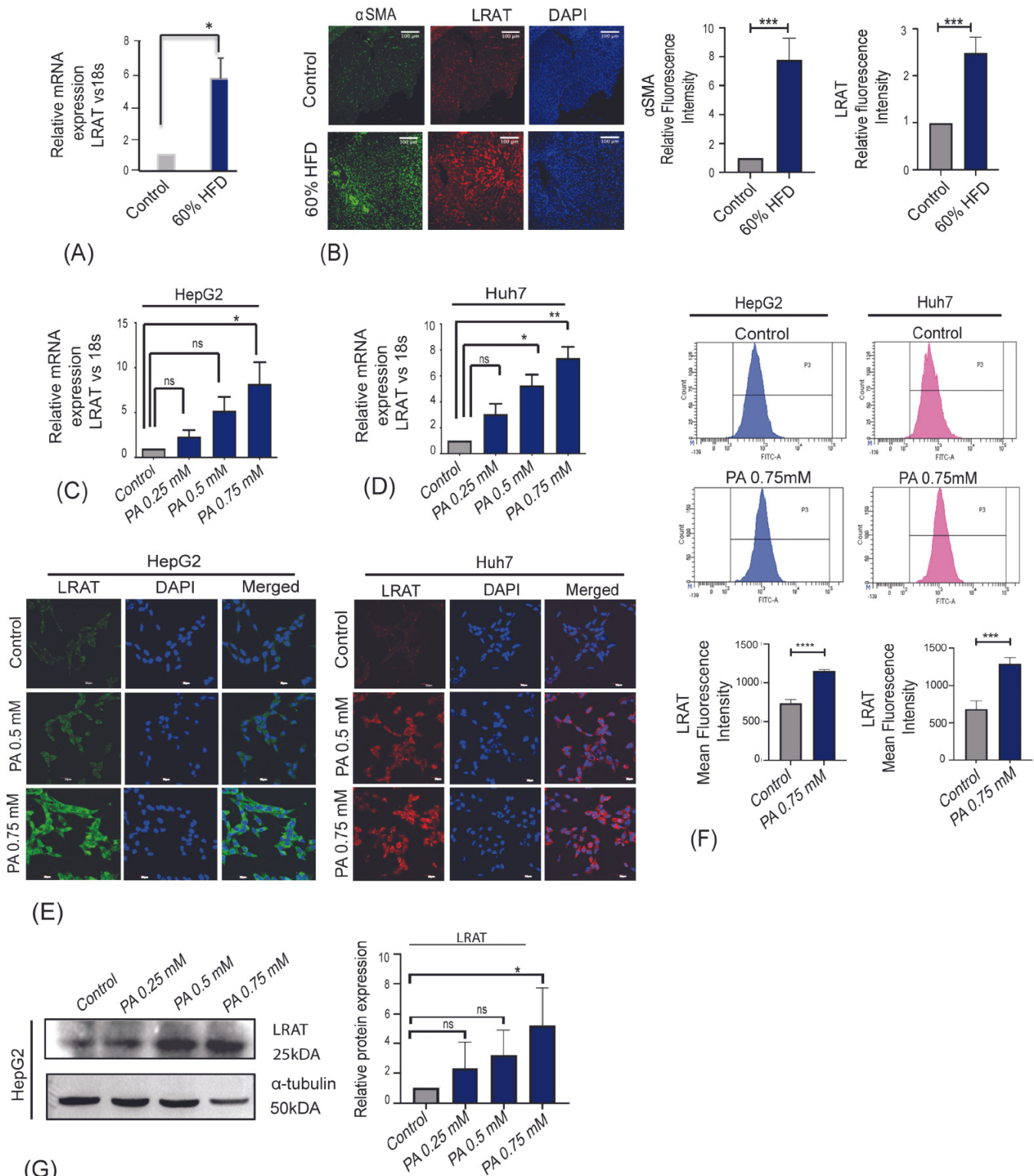
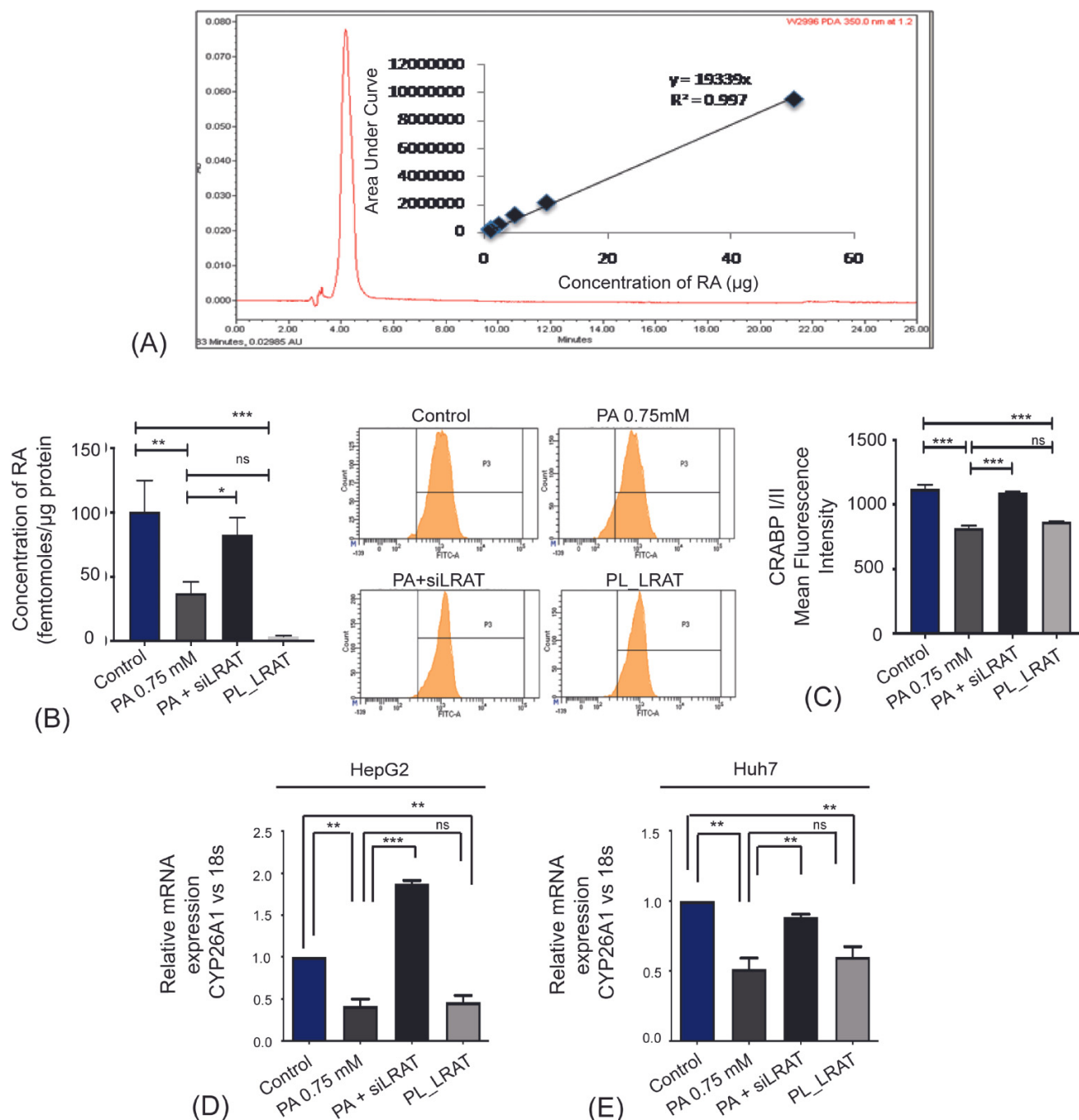


Fig. 2. RA biosynthesis in HepG2 cells is deregulated by PA, which is partially recovered by knockdown of LRAT. HepG2 cells were transfected with LRAT siRNA (PA + siLRAT) followed by PA-treatment (0.75 mM) or transfected by LRAT cDNA clone (PL-LRAT). (A) The RA was extracted and its levels were quantified using HPLC/UV and validated by mass spectrometry under 4IU retinol as substrate. (B) Bar represents quantification of RA levels in HepG2 cells. (C) Detection of internal antigen was done using antibody of CRABPI/II. Gating for FACS analysis was done using unstained cells. mRNA expression of CYP26A1 gene was quantified by qPCR in (D) HepG2 and (E) Huh7 cells. Data are expressed as the mean \pm SEM. *** P < 0.001, ** P < 0.01, * P < 0.05, ns = non-significant. LRAT: lecithin-retinol acyltransferase; PA: palmitic acid; RA: retinoic acid.



(Figs. 4C and S3C) and DCFDA levels (Figs. 4D and S3D). PA-mediated LRAT overexpression led to increased ROS generation, which was restored by siRNA-mediated LRAT knockdown. Additionally, reduced membrane potential was noted when compared to the control cells. This reduction in the mitochondrial membrane potential was retrieved when LRAT

was silenced in presence of PA (Fig. 4E), as indicated by the transition of red aggregates to the green monomeric form of JC1.

Elevated ROS production owing to excess FFA influx could initiate mitochondrial fragmentation leading to its dysfunction. Increased mRNA levels of fission gene FIS1 and de-

Fig. 3. Reduced RA synthesis disrupts the retinoid signaling pathway and induces inflammation. Detection of internal antigen performed through FACS Analysis using anti-body of (A) RAR β , (B) PPAR α , and (D) NF κ B in HepG2 cells. (C) mRNA levels of FGF21 in HepG2 cells was measured by qPCR. (E) Immuno-blots revealing protein expression of NF κ B in the cytosolic and nuclear fractions of HepG2 cells at indicated conditions, GAPDH, and Histone H3 used as a loading control for cytosolic and nuclear proteins, respectively. Densitometric analysis performed based on three replicates. Detection of internal antigen performed through FACS analysis using antibody of (F) IL1 β and (G) IL6 in HepG2 cells. Gating for FACS analysis was done using unstained cells. Data are expressed as the mean \pm SEM. **** P < 0.0001, *** P < 0.001, ** P < 0.01, * P < 0.05, ns = non-significant. Fold change for quantifying protein expression was calculated using ImageJ software. Same set of protein samples were loaded equally for the detection of α -tubulin, GAPDH, and Histone H3 used as a loading control. PPAR: peroxisome proliferator-activated receptor; RA: retinoic acid; RAR: retinoic acid receptor.

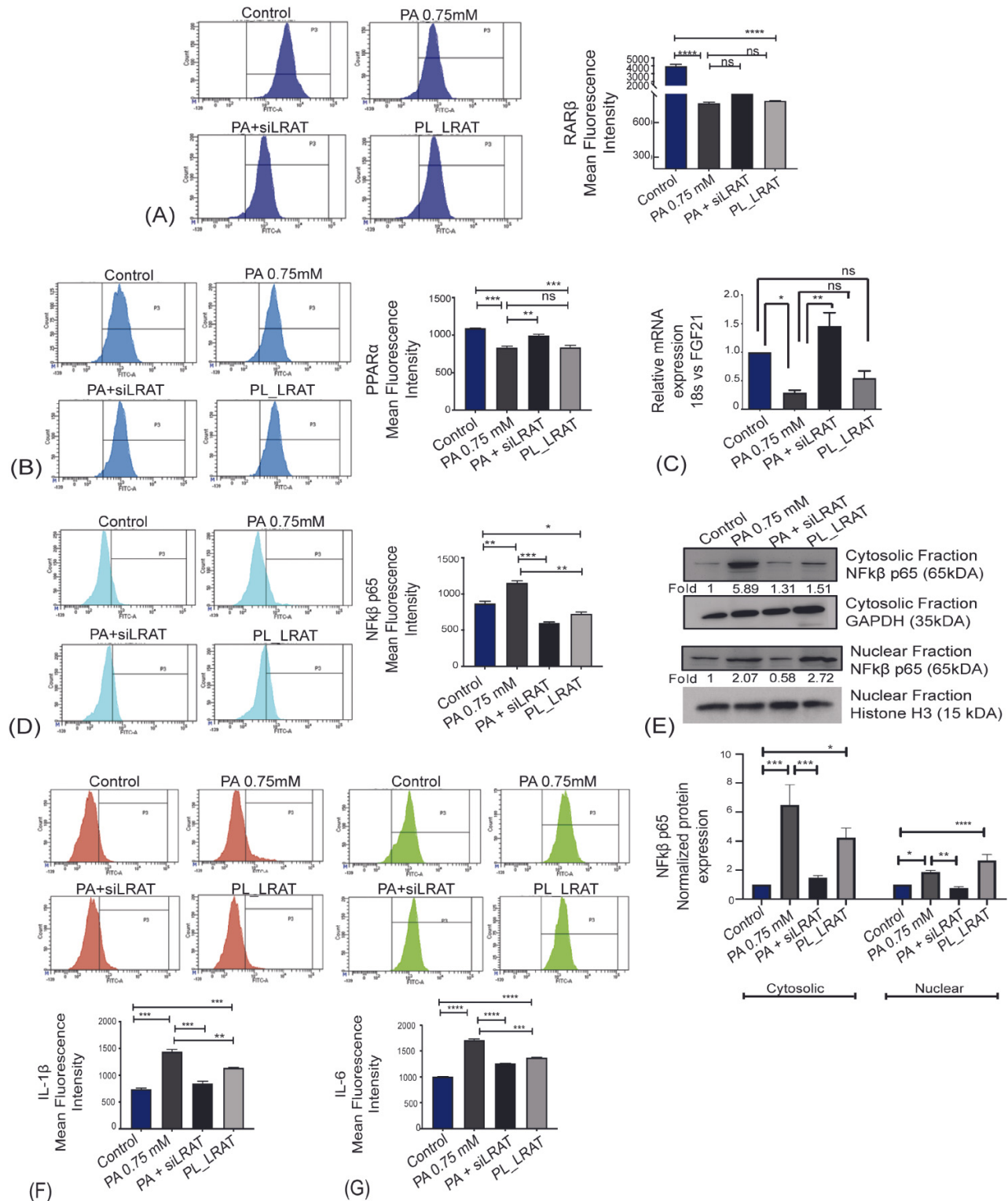
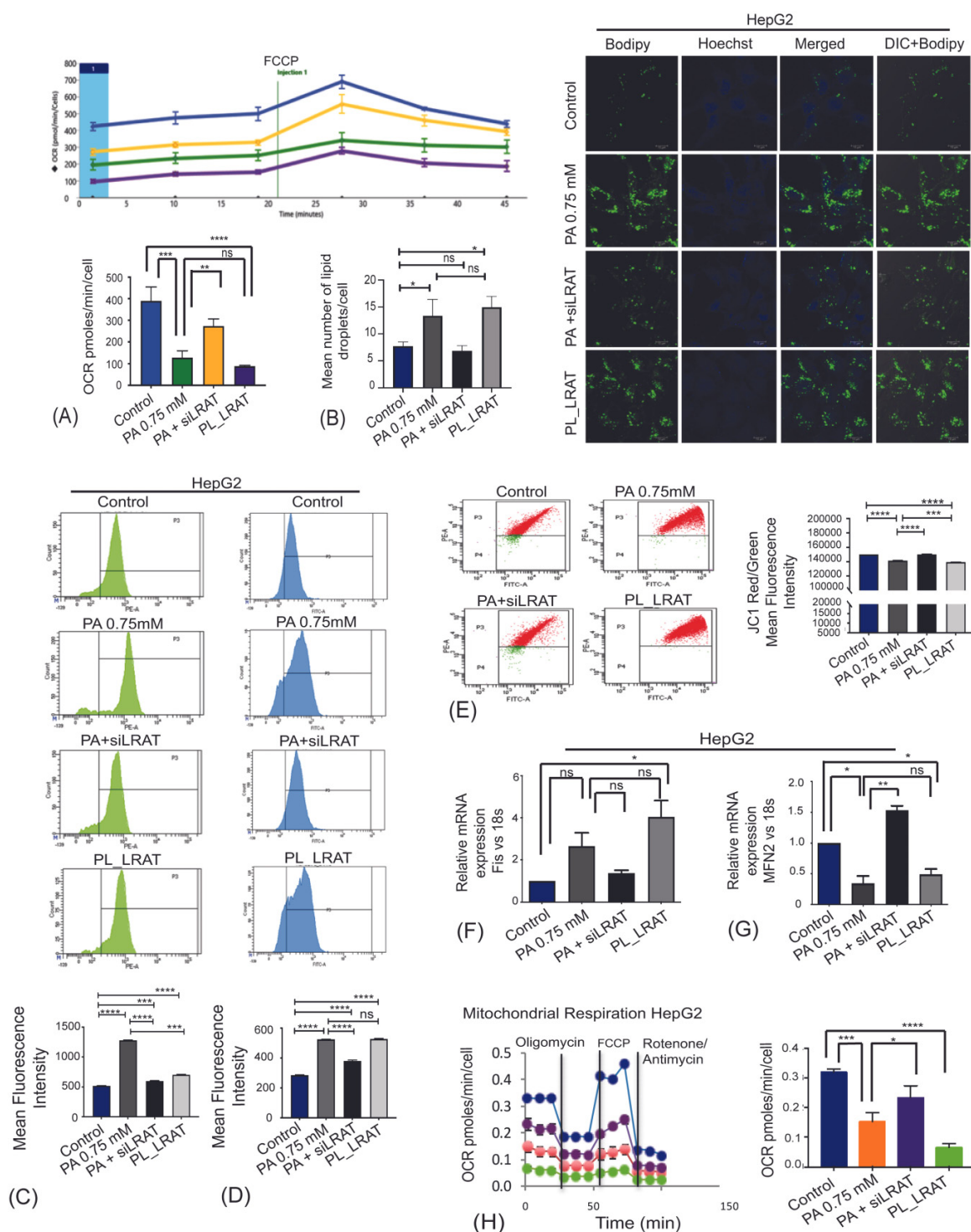


Fig. 4. PA-induced mitochondrial dysfunction could be rectified by silencing LRAT expression. HepG2 cells were treated with PA for 16 h and transfected either with siRNA of LRAT (siLRAT) or with LRAT overexpression clone followed by measurement of mitochondrial health parameters. (A) FAO was measured by OCR rate using Extracellular Flux Analyzer in HepG2 cells. (B) Neutral fat accumulation stained by Bodipy 493/503 dye was quantified and visualized under confocal microscope in HepG2 cell line. (C) Mitochondrial ROS generation measured by Mitosox in HepG2 cells, and (D) estimation of cellular ROS using DCFDA stain in HepG2 cells by flow cytometry. Gating for FACS analysis was done using unstained cells. (E) Mitochondrial membrane potential was measured by JC1 staining as shown by the transition of red/green fluorescence intensity ratio by flow cytometry analysis in HepG2 cells. The mRNA expression quantified by qPCR analysis of the indicated genes (F) FIS and (G) MFN2 in HepG2 cells were estimated after silencing LRAT/overexpressing LRAT (PA + siLRAT/PLRAT). (H) Mitochondrial respiration was measured by OCR in HepG2 cells. Data are expressed as the mean \pm SEM. **** $P < 0.0001$, *** $P < 0.001$, ** $P < 0.01$, * $P < 0.05$. Scale bar 10 μ m (B). FAO: fatty acid oxidation; LRAT: lecithin-retinol acyltransferase; OCR: oxygen consumption rate; PA: palmitic acid.



creased levels of mitochondrial fusion gene MFN2 were noted in PA-treated and LRAT overexpressed HepG2 (Figs. 4F, 4G) and Huh7 cells (Fig. S3E and S3F). Although flow cytometry in HepG2 cells showed reduced MFN2 expression (Fig. S3G) upon LRAT overexpression, we did not observe significant change in the expression level of OPA (Fig. S3H). Moreover, a mitochondrial morphological study performed using mitotracker red indicates increased mitochondrial fragmentation in both PA-treated and LRAT overexpressed cells. LRAT knockdown was found to partially reduce fragmentation (Fig. S3I). Elevated expression of MFN2 correlates with increased mitochondrial respiratory capacity (Mourier et al. 2015). Consistent with this, we noted a marked decrease in the mitochondrial respiration measured by OCR level overexpressing LRAT, which was significantly increased upon LRAT silencing in the presence of PA (Figs. 4H and S3J). Furthermore, we estimated mitochondrial mass using NOA (Fig. S3K) and MTG (Fig. S3L and S3M), where a significant depletion in mitochondrial mass was observed in PA treated and LRAT over expressed cells compared to the control cells. This alteration in the mitochondrial mass was restored upon siRNA-mediated LRAT knockdown in presence of PA. Furthermore, we found increased PINK1 expression in PA-treated and PL_LRAT overexpressed HepG2 cells, indicating a possibility of autophagic mitochondrial degradation in these cells (Fig. S3N).

Co-treatment with 9-*cis* retinoic acid (9-*cis* RA) and fenofibrate (FEN) normalized the PA-induced overexpression of LRAT

FEN is reported to be a well-known PPAR α -agonist (Nikam et al. 2018). Hence, we determined if combinatorial treatment with FEN and 9-*cis* RA could inhibit PA-mediated LRAT expression. qPCR analysis revealed that co-treatment with 9-*cis*RA (300 nM) and FEN (200 μ M) significantly decreases LRAT expression at the mRNA level both in HepG2 (Fig. 5A) and Huh7 (Fig. 5B) cell lines. Following that, confocal microscopy (Fig. 5C) revealed similar results, implying that PA-imposed LRAT over-expression could be possibly mediated through downregulation of PPAR α . Additionally, co-treatment with FEN and 9-*cis* RA decreases the expression of pro-inflammatory cytokines like IL-6 and IL-1B (Fig. S4A and S4B). Further, co-treatment of FEN and 9-*cis* RA restores impaired mitochondrial functions through significant increase in the mitochondrial OCR (Fig. S4C) and mitochondrial fusion proteins OPA and MFN2 in HepG2 cells (Fig. S4D and S4E).

Discussion

Mitochondria play a crucial role in maintaining energy metabolism and are noted to be a major site for FAO and oxidative phosphorylation (Wajner M et al. 2016). Abnormalities in mitochondrial structure and functions in the hepatic tissue of patients with NAFLD and NASH have been elucidated earlier (Ciaula et al. 2021; Galloway et al. 2021). Subsequently, loss of vitamin A homeostasis has been associated with NAFLD, steatosis, and depletion of “atRA” have been observed in liver of patients with NAFLD (Saeed et al. 2018; Zhong et al. 2019). atRA promotes mitochondrial biogenesis

and it functions mainly through downstream transcription factors PPAR and RAR (Tourniaire et al. 2015). Therefore, a depressed availability of atRA can contribute to mitochondrial dysfunction. However, most of the studies have been undertaken with exogenous the application of atRA; the availability of endogenous RA and its downstream consequences need to be studied further. The current study emphasizes the significance of RA bioavailability modulation and its implications in overcoming lipid-induced mitochondrial dysfunctions.

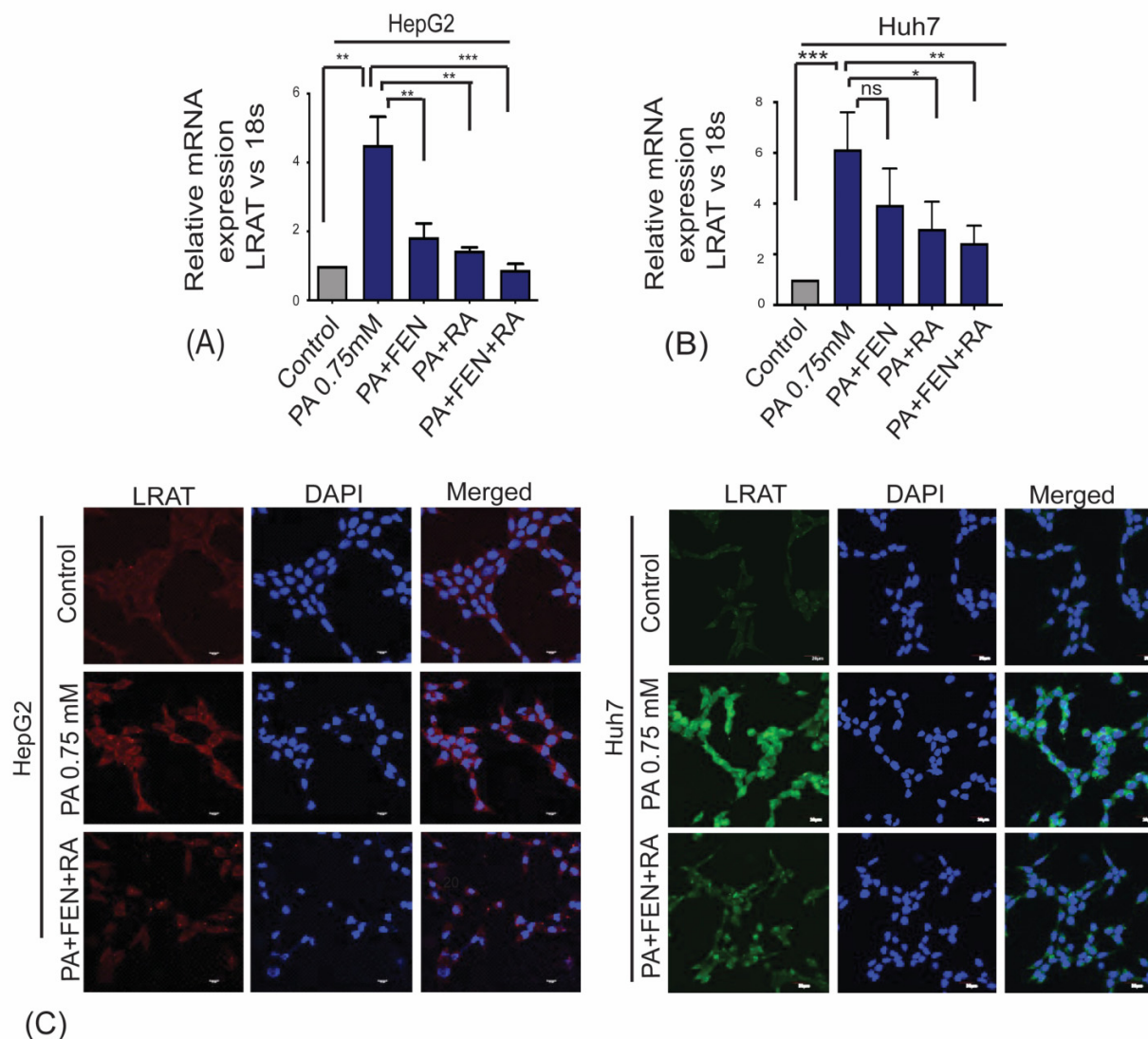
As reported earlier, storage and uptake of retinol is mainly controlled by the crucial enzyme LRAT (Amengual et al. 2012). LRAT is expressed both in hepatocytes and hepatic stellate cells (HSCs); however, its expression and specific activity are greater in the HSCs compared to the hepatocytes under normal and induction-free conditions (Bobowski-gerard et al. 2018; Saeed et al. 2018). Our report suggests that PA treatment induces LRAT expression in the hepatoma cells (HepG2 and Huh7), underscoring that in addition to the stellate cells, hepatocytes themselves contribute significantly to the total LRAT activity upon lipid enrichment (Saeed et al. 2021).

Studies in recent days have shown that a strong reduction in hepatic retinol increases fat accumulation in the liver of mice. Low hepatic retinol content and elevated retinyl esters level associates with impaired vitamin A metabolism, which in turn exacerbates inflammation and fibrosis (Saeed et al. 2021). Furthermore, obese mice display a reduction in the expression of RA-responsive nuclear receptors (RAR $\alpha/\beta/\gamma$) and impairment in vitamin A transcriptional signaling (Trasino et al. 2015). Consistent with this, our experimental outcome implies, PA-mediated LRAT overexpression reduces the synthesis of RA from retinol and we hypothesize that retinol is majorly driven towards esterification process.

Since RA is the ligand for nuclear receptor RXR, its depletion could result in reduced expression and transcriptional activity of PPAR α and RAR β that heterodimerize with it (Neerven et al. 2008; Wells and Chan 2009). LRAT-mediated reduction in RA impairs hetero-dimerization of PPAR α /RXR α , leading to the transcriptional repression of PPAR α itself by self-regulatory mechanisms along with its target genes. Again, the regulation of LRAT gene expression in the liver reportedly involves the presence of an RA-binding element (RARE) in its promoter (Gene 2010; Kun Cai1 and Lorraine J. Gudas, 2010). We speculate that there may be functional PPRE present in its promoter, and hence it could be possible that PPAR α negatively regulates the expression of LRAT upon binding to it. Hence, a feedback loop might exist between PPAR α and LRAT, where overexpression of the latter may reduce the repression of the former and vice versa.

Excess lipid-influx in hepatocytes causes the release of pro-inflammatory cytokines such as TNF α , IL-1 β , and IL-6 (Joshi-Barve et al. 2007). Our report suggests that PA-induced LRAT downregulates the expression of RA-responsive nuclear receptor, PPAR α , and thereby abrogates its inhibitory effect on NF κ B signaling, facilitating its nuclear entry. We identified LRAT as a plausible contributing factor in FFA-mediated derangement of retinoid homeostasis as well as lipid metabolism. PA-mediated repression of PPAR α may be a cause for LRAT upregulation. LRAT induces transcription of the pro-inflammatory genes like IL-1 β , IL-6 plausibly through

Fig. 5. Combinatorial effect of PPAR α agonist FEN and RXR agonist 9-*cis* RA on LRAT expression. HepG2 and Huh7 cells were treated with PA, 9-*cis*RA (300 nM) and FEN (200 μ M) to measure LRAT expression. (A, B) Relative mRNA expression of LRAT measured upon co-treatment of HepG2, Huh7 cells with FEN and 9-*cis* RA. (C) LRAT expression was monitored after co-treatment with FEN and 9-*cis*-RA by confocal microscopy in HepG2 and Huh7 cells. Data are expressed as the mean \pm SEM. *** P < 0.001, ** P < 0.01, * P < 0.05, ns = non-significant. Scale bars 10 μ m (HepG2), 20 μ m (Huh7) (C). FEN: fenofibrate; LRAT: lecithin-retinol acyltransferase; PPAR: proliferator-activated receptor; RA: retinoic acid; RXR: retinoid-x receptor.



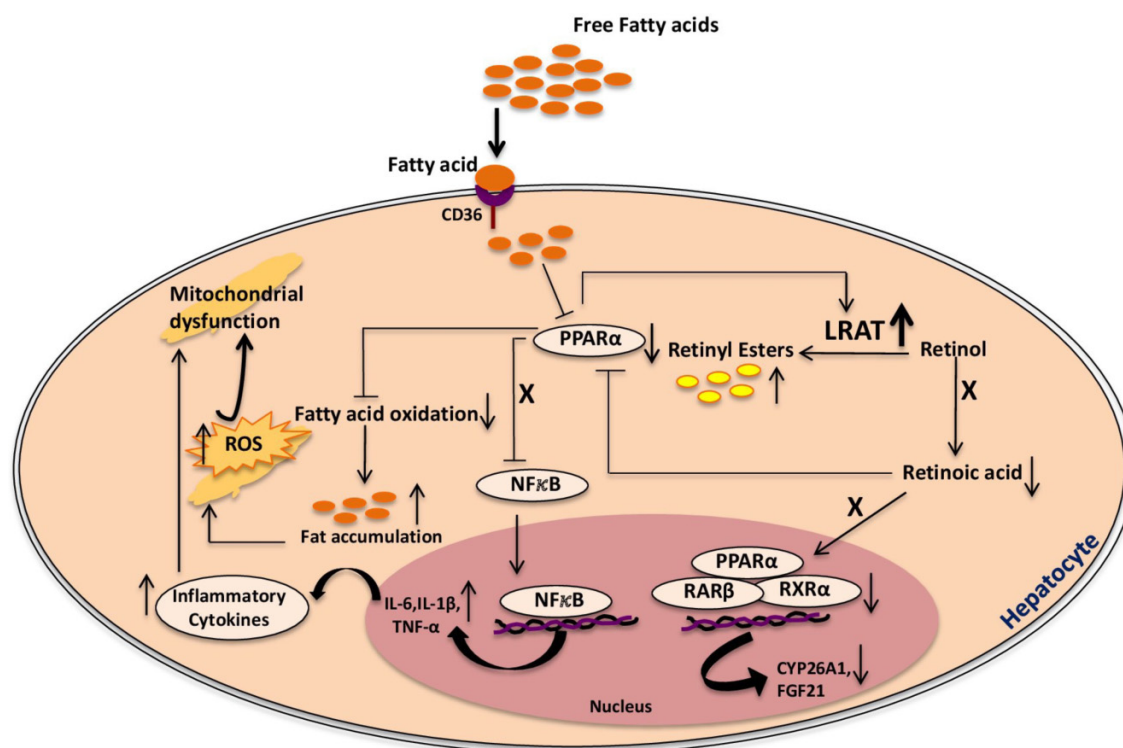
translocation of NF κ B to the nucleus, which thereby highlights its participation in obesity-mediated inflammation (Fig. 3). However, the dynamics behind this translocation is not yet clear and needs further experimentation.

Previous research found that retinoid metabolizing enzymes play a role in hepatic lipogenesis and β -oxidation (Quiroga et al. 2012; Amengual et al. 2019). PPAR α regulates lipid-metabolizing genes such as CPT1A, FGF21 that favor lipid catabolism over neutral lipid storage (Amengual et al. 2019). Recent studies have shown FGF21 as a direct target of RAR β in addition to nuclear receptors like PPAR α and RORs (Badman et al. 2007; Li et al. 2013). Subsequently, extensive research has shown FGF21 to hold considerable promise owing to its potential in reducing liver fat mass and allevi-

ating hepatic injury by suppressing inflammation (Tillman and Rolph 2020). Our study indicates that lipid-induced differential expression of retinoid metabolizing enzymes LRAT regulates liver fat accumulation upon PPAR α downregulation and that in turn might reduce the expression of its target genes FGF21 and CPT1A. FEN serves as ligand for PPAR α and the latter functions in conjugation with RXR of which 9-*cis*-RA is a ligand (Nikam et al. 2018). Our study indicates that co-administration of FEN and 9-*cis*-RA restores perturbed retinoid homeostasis caused by FFA-induced upregulation of LRAT (Fig. 5).

In our earlier studies also, we demonstrated mitochondrial FAO rate to be downregulated owing to excess fatty acid influx (Das et al. 2017). The present study reveals that

Fig. 6. Schematic representation of lipid-induced altered retinoid metabolism leading to impairment of mitochondrial function in the hepatoma cell. Saturated fatty acid (PA) induced LRAT overexpression leads to reduced expression of RA responsive nuclear receptors $RAR\beta$ and $RXR\alpha$ and its heterodimerising partner $PPAR\alpha$, leading to deregulation of RA signaling. Alteration in RA metabolism followed by reduced expression of $PPAR\alpha$ attenuates FAO and enhances lipid/fat accumulation in the hepatoma cell. Additionally, repression in $PPAR\alpha$ transcriptional activity followed by PA-induced LRAT overexpression abrogates sequestration of cytosolic $NF\kappa B$ and enhances the transcription of the pro-inflammatory cytokines IL-6 and IL-1 β . PA driven LRAT overexpression favor fat deposition associated with inflammation, together which induces elevated ROS production leading to mitochondrial dysfunction in the hepatoma cells. FAO: fatty acid oxidation; LRAT: lecithin-retinol acyltransferase; PA: palmitic acid; RA: retinoic acid.



lipid-mediated overexpression of LRAT in hepatoma cells hampered mitochondrial bioenergetics potential. Depressed bio-energetic functions could be correlated with increased ROS generation, lowered mitochondrial membrane potential, and increased mitochondrial fission. Detrimental effects that were shown to incur elevated ROS and potentiate mitochondrial DNA damage were reflected by a decrease in mitochondrial mass (Yang et al. 2019). Consistent with this, in the present study, we observed PA-driven LRAT overexpression leading to reduction in the mitochondrial mass. Subsequent studies revealed autophagic degradation of mitochondria as an important regulatory mechanism in controlling both mitochondrial mass and quality (Melser et al. 2015). Our experimental observations suggest that increased expression of autophagic marker PINK1 in both PA-treated and PL_LRAT overexpressed cells may contribute to reduction in mitochondrial mass in these cells. Furthermore, our results correlate well with the earlier report on retinoids' mediated enhancement of mitochondrial genes and functions (Everts and Berdanier 2002). Precisely, LRAT reduces the formation of RA and thereby abrogates mitochondrial function (Fig 4). Therefore, lipid-induced mitochondrial dysfunction

occurs through abrogated retinol metabolic pathway (Fig. 6).

In conclusion, our study shows significant role of LRAT in lipid-induced inflammation. We could identify LRAT as important player in the FFA-mediated derangement of retinoid homeostasis and signaling pathways. LRAT may, therefore, serve as a therapeutic target for reversing impaired retinoid-signaling pathway that contribute to mitochondrial health. Co-administration of FEN and 9-*cis*-RA abrogated disrupted retinoid homeostasis and signaling caused by FFA-induced upregulation of LRAT. Since the metabolic effects of LRAT silencing appear to improve lipid metabolism, a putative LRAT blocker may have a significant impact on ameliorating lipid-induced mitochondrial dysfunction. Our work strongly suggests LRAT inhibition as a promising option to treat obesity-associated hepatosteatosis. In addition, LRAT may serve as a biomarker for diagnosis of obesity-induced NAFLD.

Acknowledgements

Tanmoy Dalui, Debalina Chakraborty (flow cytometry), Sounak Bhattacharya (confocal microscopy), and Soumik

Laha (Mass Spectrometry) of IICB Central Instrumentation Facilities are highly acknowledged for their technical support. Debasish Bhattacharyya and Kanika Sharma of CSIR-IICB are highly acknowledged for their assistance in HPLC. The technical assistance of Prabir Kumar Dey is highly acknowledged. Other members of the SSR laboratory are acknowledged for their cooperation.

Author declaration

We confirm that the manuscript has been read and approved by all named authors and that there are no other persons who satisfied the criteria for authorship but are not listed. We further confirm that the order of the authors listed in the manuscript has been approved by all of us. We further confirm that the work is original and is not currently under review with any other journal or has not been accepted or published anywhere else.

Article information

History dates

Received: 19 August 2022

Accepted: 13 January 2023

Accepted manuscript online: 14 February 2023

Version of record online: 9 March 2023

Copyright

© 2023 The Author(s). Permission for reuse (free in most cases) can be obtained from [creativecommons.org](https://creativecommons.org/licenses/by/4.0/).

Data availability

Data are available on request from the corresponding author.

Author information

Author ORCIDs

Sib Sankar Roy <https://orcid.org/0000-0002-6117-1546>

Author notes

Eshani Karmakar and Nabanita Das contributed equally and share first authorship.

Author contributions

Conceptualization: EK, ND, SM, SSR

Data curation: EK, ND

Formal analysis: EK, ND, BM, PD

Funding acquisition: SSR

Investigation: SM, SSR

Methodology: EK, ND, BM, PD

Project administration: SM, SSR

Supervision: SM, SSR

Validation: BM, PD, SM, SSR

Visualization: SSR

Writing – original draft: EK, ND

Writing – review & editing: EK, ND

Competing interests

No potential conflicts of interest including financial or personal relationships relevant to this article were reported by the authors that could have appeared to influence the work.

Funding

We thankfully acknowledge the Council of Scientific and Industrial Research (CSIR, Govt. of India) for intramural funding and SERB, Govt. of India (EMR/2016/002/578), for providing the grant. EK (award No. IF150404) is the recipient of the DST Inspire fellowship. ND (award No. 31/002(0889/2011-EMR-1) was a recipient of a fellowship from CSIR.

Ethical approval for animal studies

All animal experiments were approved by institutional animal ethics committee, CSIR-Indian Institute of Chemical Biology, India, (Registration No: 147/GO/ReBi/S/99/CPSCEA) following the guidelines of Committee for the Purpose of Control and Supervision of Experiments on Animals (CPCSEA), Govt. of India.

Supplementary material

Supplementary data are available with the article at <https://doi.org/10.1139/bcb-2022-0266>.

Reference

- Amengual, J., Golczak, M., Palczewski, K., and Lintig, J. Von. 2012. Lecithin: retinol acyltransferase is critical for cellular uptake of vitamin A from serum retinol-binding protein. *J. Biol. Chem.* **287**(29): 24216–24227. doi:[10.1074/jbc.M112.353979](https://doi.org/10.1074/jbc.M112.353979). PMID: [22637576](https://pubmed.ncbi.nlm.nih.gov/22637576/).
- Amengual, J., Petrov, P., Bonet, M.L., Ribot, J., and Palou, A. 2019. Induction of carnitine palmitoyl transferase 1 and fatty acid oxidation by retinoic acid in HepG2 cells. *Int. J. Biochem. Cell Biol.* **44**(11): 2019–2027. doi:[10.1016/j.biocel.2012.07.026](https://doi.org/10.1016/j.biocel.2012.07.026).
- Amengual, J., Ribot, J., Bonet, M.L., and Palou, A. 2010. Retinoic acid treatment enhances lipid oxidation and inhibits lipid biosynthesis capacities in the liver of mice. *Cell. Physiol. Biochem.* **25**: 657–666. doi:[10.1159/000315085](https://doi.org/10.1159/000315085). PMID: [20511711](https://pubmed.ncbi.nlm.nih.gov/20511711/).
- Arner, P., and Rydén, M. 2015. Fatty acids, obesity and insulin resistance. *Obes. Facts* **8**(2): 147–155. doi:[10.1159/000381224](https://doi.org/10.1159/000381224). PMID: [25895754](https://pubmed.ncbi.nlm.nih.gov/25895754/).
- Badman, M.K., Pissios, P., Kennedy, A.R., Koukos, G., and Flier, J.S. 2007. Hepatic fibroblast growth factor 21 is regulated by PPAR α and is a key mediator of hepatic lipid metabolism in ketotic states. *Cell. Metab.* **5**: 426–437. doi:[10.1016/j.cmet.2007.05.002](https://doi.org/10.1016/j.cmet.2007.05.002). PMID: [17550778](https://pubmed.ncbi.nlm.nih.gov/17550778/).
- Barber, T., Esteban-Pretel, G., Marín, M.P., and Timoneda, J. 2014. Vitamin A deficiency and alterations in the extracellular matrix. *Nutrients* **6**(11): 4984–5017. doi:[10.3390/nu6114984](https://doi.org/10.3390/nu6114984). PMID: [25389900](https://pubmed.ncbi.nlm.nih.gov/25389900/).
- Berry, D.C., Desantis, D., Soltanian, H., Croniger, C.M., and Noy, N. 2012. Retinoic acid upregulates preadipocyte genes to block adipogenesis and suppress diet-induced obesity. *Diabetes* **61**: 1112–1121. doi:[10.2337/db11-1620](https://doi.org/10.2337/db11-1620). PMID: [22396202](https://pubmed.ncbi.nlm.nih.gov/22396202/).
- Berry, D.C., and Noy, N. 2009. All-trans-retinoic acid represses obesity and insulin resistance by activating both peroxisome proliferation-activated receptor β/δ and retinoic acid receptor. *Mol. Cell. Biol.* **29**(12): 3286–3296. doi:[10.1128/mcb.01742-08](https://doi.org/10.1128/mcb.01742-08). PMID: [19364826](https://pubmed.ncbi.nlm.nih.gov/19364826/).
- Bhatti, J.S., Bhatti, G.K., and Reddy, P.H. 2017. Mitochondrial dysfunction and oxidative stress in metabolic disorders—a step towards mitochondria based therapeutic strategies. *Biochim. Biophys. Acta Mol. Basis Dis.* **1863**(5): 1066–1077. doi:[10.1016/j.bbadis.2016.11.010](https://doi.org/10.1016/j.bbadis.2016.11.010).
- Bikman, B.T., Guan, Y., Shui, G., Siddique, M.M., Holland, W.L., Kim, J.Y., et al. 2012. Fenretinide prevents lipid-induced insulin resistance by blocking ceramide biosynthesis. *J. Biol. Chem.* **287**(21): 17426–17437. doi:[10.1074/jbc.M112.359950](https://doi.org/10.1074/jbc.M112.359950). PMID: [22474281](https://pubmed.ncbi.nlm.nih.gov/22474281/).

- Bobowski-gerard, M., Zummo, F.P., Staels, B., and Lefebvre, P. 2018. Retinoids issued from hepatic stellate cell lipid droplet loss as potential signaling molecules orchestrating a multicellular liver injury response. *Cell* 7(137): 1–7. doi:10.3390/cells7090137.
- Byrne, S.M.O., and Blaner, W.S. 2013. Retinol and retinyl esters: biochemistry and physiology. *J. Lipid Res.* 54: 1731–1743. doi:10.1194/jlr.R037648. PMID: 23625372.
- Chowdhury, S.R., Ray, U., Chatterjee, B.P., and Roy, S.S. 2017. Targeted apoptosis in ovarian cancer cells through mitochondrial dysfunction in response to *Sambucus nigra* agglutinin. *Cell Death Dis.* 8(5): 2762–2712. doi:10.1038/cddis.2017.77.
- Ciaula, D.A., Passarella, S., Shanmugam, H., and Portincasa, P. 2021. Nonalcoholic fatty liver disease (NAFLD). Mitochondria as players and targets of therapies?. *Int. J. Mol. Sci.* 22(10): 5375. doi:10.3390/ijms22105375. PMID: 34065331.
- Das, N., Mandala, A., Bhattachajee, S., Mukherjee, D., Bandyopadhyay, D., and Roy, S.S. 2017a. Dietary fat proportionately enhances oxidative stress and glucose intolerance followed by impaired expression of the genes associated with mitochondrial biogenesis. *Food Funct.* 8(4): 1577–1586. doi:10.1039/c6fo01326k. PMID: 28282095.
- Das, N., Mandala, A., Naaz, S., Giri, S., Jain, M., Bandyopadhyay, D., et al. 2017b. Melatonin protects against lipid-induced mitochondrial dysfunction in hepatocytes and inhibits stellate cell activation during hepatic fibrosis in mice. *J. Pineal Res.* 62(4): 1–21. doi:10.1111/jipi.12404.
- Dabrowski, A.S., Bezsonov, E.E., Baig, S.M., and Orekhov, N.A. 2021. Mitochondrial mutations and genetic factors determining NAFLD risk. *Int. J. Mol. Sci.* 22: 4459. doi:10.3390/ijms22094459. PMID: 33923295.
- Dou, X., Wang, Z., Yao, T., and Song, Z. 2011. Cysteine aggravates palmitate-induced cell death in hepatocytes. *Life Sci.* 89(23–24): 878–885. doi:10.1016/j.lfs.2011.09.022. PMID: 22008477.
- Dawson, I.M., and Xia, Z. 2012. The retinoid X receptors and their ligands. *Biochim. Biophys. Acta* 1821(1): 21–56. doi:10.1016/j.bbailip.2011.09.014.
- Delerive, P., Bosscher, K. De, Besnard, S., Berghe, W. Vanden, Peters, J.M., Gonzalez, F.J., et al., 1999. Peroxisome proliferator-activated receptor- α negatively regulates the vascular inflammatory gene response by negative cross-talk with transcription factors NF- κ B and AP-1. *J. Biol. Chem.* 274(45): 32048–32054. doi:10.1074/jbc.274.45.32048. PMID: 10542237.
- Donato, T.M., Ramiro, J., and Gomez-Lechon, J.M. 2013. Hepatic cell lines for drug hepatotoxicity testing: limitations and strategies to upgrade their metabolic competence by gene engineering. *Curr. Drug Metab.* 14: 946–968. doi:10.2174/1389200211314090002. PMID: 24160292.
- Everts, H.B., and Berdanier, C.D. 2002. Regulation of mitochondrial gene expression by retinoids. *IUBMB Life* 42: 45–49. doi:10.1080/15216540290114216.
- Fan, J., Yin, S., Lin, D., Liu, Y., Chen, N., Bai, X., et al. 2019. Association of serum retinol-binding protein 4 levels and the risk of incident type 2 diabetes in subjects with prediabetes. *Diabetes Care* 42(8): 1574–1581. doi:10.2337/dc19-0265. PMID: 31186297.
- Fischer-huchzermeyer, S., Dombrowski, A., Hagel, C., Mautner, V.F., Schittenhelm, J., and Harder, A. 2017. The cellular retinoic acid binding protein 2 promotes survival of malignant peripheral nerve sheath tumor cells. *Am. J. Pathol.* 187(7): 1623–1632. doi:10.1016/j.ajpath.2017.02.021. PMID: 28502478.
- Galloway, C.A., Lee, H., Brookes, P.S., and Yoon, Y. 2014. Decreasing mitochondrial fission alleviates hepatic steatosis in a murine model of nonalcoholic fatty liver disease. *Am. J. Physiol. Gastrointest. Liver Physiol.* 307(19): 632–641. doi:10.1152/ajpgi.00182.2014.
- Gene, A.L. 2010. An essential set of basic DNA response elements is required for receptor-dependent transcription of the lecithin:retinol acyltransferase (Lrat) gene. *Arch. Biochem. Biophys.* 489(1–2): 1–9. doi:10.1016/j.abb.2009.08.001.
- Gu, X., Ma, Y., Liu, Y., and Wan, Q. 2020. Measurement of mitochondrial respiration in adherent cells by Sea Horse XF96 Cell Mito Stress Test. *STAR Protoc.* 2(1): 100245, 1–2713. doi:10.1016/j.xpro.2020.100245.
- Heliövaara, M.K., Herz, M., Teppo, A.M., Leinonen, E., and Ebeling, P. 2007. Pioglitazone has anti-inflammatory effects in patients with type 2 diabetes. *J. Endocrinol. Invest.* 30(4): 292–297. doi:10.1007/BF03346296. PMID: 17556865.
- Huang, Z., Liu, Y., Qi, G., Brand, D., and Zheng, S. 2018. Role of vitamin A in the immune system. *J. Clin. Med.* 7(9): 258. doi:10.3390/jcm7090258. PMID: 30200565.
- Jeyakumar, S.M., Vajreswari, A., and Giridharan, N.V. 2006. Chronic dietary vitamin A supplementation regulates obesity in an obese mutant WNI/Ob rat model. *Obesity* 14(1): 52–59. doi:10.1038/oby.2006.7. PMID: 16493122.
- Joshi-Barve, S., Barve, S.S., Amancherla, K., Gobejishvili, L., Hill, D., Cave, M., et al. 2007. Palmitic acid induces production of proinflammatory cytokine interleukin-8 from hepatocytes. *Hepatology* 46(3): 823–830. doi:10.1002/hep.21752. PMID: 17680645.
- Kane, M.A., Folias, A.E., Wang, C., and Napoli, J.L. 2014. Quantitative profiling of endogenous retinoic acid in vivo and in vitro by tandem mass spectrometry. *Anal. Chem.* 80(5): 1702–1708. doi:10.1021/ac702030.
- Kedishvili, N.Y. 2016. Retinoic acid synthesis and degradation. *Subcell. Biochem.* 81: 127–161. doi:10.1007/978-94-024-0945-1_5. PMID: 27830503.
- Keller, H., Dreyer, C., Medin, J., Mahfoudi, A., Ozato, K., and Wahli, W. 1993. Fatty acids and retinoids control lipid metabolism through activation of peroxisome proliferator-activated receptor-retinoid X receptor heterodimers. *Proc. Natl. Acad. Sci. U.S.A.* 90(6): 2160–2164. doi:10.1073/pnas.90.6.2160. PMID: 8384714.
- Kim, S.C., Kim, C.K., Axe, D., Cook, A., Lee, M., Li, T., et al. 2014. All-trans-retinoic acid ameliorates hepatic steatosis in mice by a novel transcriptional cascade. *Hepatology* 59(5): 1750–1760. doi:10.1002/hep.26699. PMID: 24038081.
- Korbecki, J., Bobiński, R., and Dutka, M. 2019. Self-regulation of the inflammatory response by peroxisome proliferator activated receptors. *Inflamm. Res.* 68(6): 443–458. doi:10.1007/s00011-019-01231-1. PMID: 30927048.
- Cai, K., and Gudas, L.J. 2010. Retinoic acid receptors and GATA transcription factors activate the transcription of the human lecithin:retinol acyltransferase gene. *Int. J. Biochem. Cell Biol.* 41(3): 546–553. doi:10.1016/j.biocel.2008.06.007.
- Li, Y., Walsh, K., Gao, B., and Zang, M. 2013. Retinoic acid receptor stimulates hepatic induction of fibroblast growth factor 21 to promote fatty acid oxidation and control whole-body energy homeostasis in mice. *J. Biol. Chem.* 288(15): 10 490–10 504. doi:10.1074/jbc.M112.429852. PMID: 23430257.
- Lin, C.F., Young, K.C., Bai, C.H., Yu, B.C., Ma, C.T., Chien, Y.C., et al. 2014. Rosiglitazone regulates anti-inflammation and growth inhibition via PTEN. *BioMed Res. Int.* 2014: 787924. doi:10.1155/2014/787924. PMID: 24757676.
- Lin, C.H., Lee, S.Y., Zhang, C.C., Du, Y.F., Hung, H.C., Wu, H.T., and Ou, H.Y. 2016. Fenretinide inhibits macrophage inflammatory mediators and controls hypertension in spontaneously hypertensive rats via the peroxisome proliferator-activated receptor gamma pathway. *Drug Des. Dev. Ther.* 10: 3591–3597. doi:10.2147/DDDT.S114879. PMID: 27843299.
- Maftah, A., Petit, J.M., Ratinaud, M.H., and Julien, R. 1989. 10-N nonyl-acridine orange: a fluorescent probe which stains mitochondria independently of their energetic state. *Biochem. Biophys. Res. Commun.* 164(1): 185–190. doi:10.1016/0006-291X(89)91700-2. PMID: 2478126.
- Marwarha, G., Berry, D.C., Croniger, C.M., and Noy, N. 2014. The retinol esterifying enzyme LRAT supports cell signaling by retinol-binding protein and its receptor STRA6. *Faseb. J.* 28(26–34). doi:10.1096/fj.13-234310.
- McIlroy, G.D., Delibegovic, M., Owen, C., Stoney, P.N., Shearer, K.D., McCaffery, P.J., and Mody, N. 2013. Fenretinide treatment prevents diet-induced obesity in association with major alterations in retinoid homeostatic gene expression in adipose, liver, and hypothalamus. *Diabetes* 62: 825–836. doi:10.2337/db12-0458. PMID: 23193184.
- Melser, S., Lavie, J., and Benard, G. 2015. Mitochondrial degradation and energy metabolism. *Biochim. Biophys. Acta* 1858: 2812–2821. doi:10.1016/j.bbamcr.2015.05.010.
- Mercader, J., Ribot, J., Murano, I., Felipe, F., Cinti, S., and Bonet, M.L. 2006. Remodeling of white adipose tissue after retinoic acid administration in mice. *Endocrinology* 147(11): 5325–5332. doi:10.1210/en.2006-0760. PMID: 16840543.
- Missiroli, S., Genovese, I., Perrone, M., Vezzani, B., Vitto, V.A.M., and Giorgi, C. 2020. The role of mitochondria in inflammation: from cancer to neurodegenerative disorders. *J. Clin. Med.* 9(3): 740. doi:10.3390/jcm9030740.

- Mody, N. 2017. Alterations in vitamin A/retinoic acid homeostasis in diet-induced obesity and insulin resistance. *Proc. Natl. Acad. Sci. U.S.A.* **76**(4): 597–602. doi:[10.1017/S0029665117001069](https://doi.org/10.1017/S0029665117001069).
- Montagner, A., Polizzi, A., Fouché, E., Ducheix, S., Lippi, Y., Lasserre, F., et al. 2016. Liver PPAR α is crucial for whole-body fatty acid homeostasis and is protective against NAFLD. *Hepatology* **65**: 1202–1214. doi:[10.1136/gutjnl-2015-310798](https://doi.org/10.1136/gutjnl-2015-310798).
- Mourier, A., Motori, E., Brandt, T., Lagouge, M., Atanassov, I., Galinier, A., et al. 2015. Mitofusin 2 is required to maintain mitochondrial coenzyme Q levels. *J. Cell Biol.* **208**(4): 429–442. doi:[10.1083/jcb.201411100](https://doi.org/10.1083/jcb.201411100). PMID: [25688136](https://pubmed.ncbi.nlm.nih.gov/25688136/).
- Nelson, C.H., Peng, C., Lutz, J.D., Yeung, C.K., Zelter, A., and Isoheranen, N. 2016. Direct protein–protein interactions and substrate channeling between cellular retinoic acid binding proteins and CYP26B1. *FEBS Lett.* **590**: 2527–2535. doi:[10.1002/1873-3468.12303](https://doi.org/10.1002/1873-3468.12303). PMID: [27416800](https://pubmed.ncbi.nlm.nih.gov/27416800/).
- Neerven, S., Kampmann, E., and Mey, J. 2008. RAR/RXR and PPAR/RXR signaling in neurological and psychiatric diseases. *Prog. Neurobiol.* **85**(4): 433–451. doi:[10.1016/j.pneurobio.2008.04.006](https://doi.org/10.1016/j.pneurobio.2008.04.006). PMID: [18554773](https://pubmed.ncbi.nlm.nih.gov/18554773/).
- Nicholas, D.A., Proctor, E.A., Agrawal, M., Belkina, A.C., Van Nostrand, S.C., Panneerseelan-Bharath, L., et al. 2019. Fatty acid metabolites combine with reduced β oxidation to activate Th17 inflammation in human type 2 diabetes. *Cell Metab.* **30**(3): 447–461.e5. doi:[10.1016/j.cmet.2019.07.004](https://doi.org/10.1016/j.cmet.2019.07.004). PMID: [31378464](https://pubmed.ncbi.nlm.nih.gov/31378464/).
- Nikam, A., Patankar, V.J., and Abuja, M. 2018. The PPAR α agonist fenofibrate prevents formation of protein aggregates (Mallory-Denk bodies) in a murine model of steatohepatitis-like hepatotoxicity. *Sci. Rep.* **8**. Article ID: 12964. doi:[10.1038/s41598-018-31389-3](https://doi.org/10.1038/s41598-018-31389-3). PMID: [30154499](https://pubmed.ncbi.nlm.nih.gov/30154499/).
- Pawlak, M., Lefebvre, P., and Staels, B. 2015. Molecular mechanism of PPAR α action and its impact on lipid metabolism, inflammation and fibrosis in non-alcoholic fatty liver disease. *J. Hepatol.* **62**(3): 720–733. doi:[10.1016/j.jhep.2014.10.039](https://doi.org/10.1016/j.jhep.2014.10.039). PMID: [25450203](https://pubmed.ncbi.nlm.nih.gov/25450203/).
- Qiu, B., and Simon, M.C. 2016. Bodipy 493/503 staining of neutral lipid droplets for microscopy and quantification by flow cytometry. *Bio. Protoc.* **6**(17): 1–6. doi:[10.21769/BioProtoc.1912](https://doi.org/10.21769/BioProtoc.1912). PMID: [27642615](https://pubmed.ncbi.nlm.nih.gov/27642615/).
- Quiroga, A.D., Li, L., Tr, M., Nelson, R., Proctor, S.D., and Harald, K. 2012. Deficiency of carboxylesterase 1/esterase-x results in obesity, hepatic steatosis, and hyperlipidemia. *Hepatology* **56**(202272): 2188–2198. doi:[10.1002/hep.25961](https://doi.org/10.1002/hep.25961). PMID: [22806626](https://pubmed.ncbi.nlm.nih.gov/22806626/).
- Saeed, A., Bartuzi, P., Heegsma, J., Dekker, D., Kloosterhuis, N., de Bruin, A., et al. 2021. Impaired hepatic vitamin A metabolism in NAFLD mice leading to vitamin A accumulation in hepatocytes. *Cell. Mol. Gastroenterol. Hepatol.* **11**(1): 309–325. doi:[10.1016/j.jcmgh.2020.07.006](https://doi.org/10.1016/j.jcmgh.2020.07.006). PMID: [32698042](https://pubmed.ncbi.nlm.nih.gov/32698042/).
- Saeed, A., Dullaart, R.P.F., Schreuder, T.C.M.A., Blokzijl, H., and Faber, K.N. 2018. Disturbed vitamin A metabolism in non-alcoholic fatty liver disease (NAFLD). *Nutrients* **10**(29): 1–25. doi:[10.3390/nu10010029](https://doi.org/10.3390/nu10010029).
- Sarang, Z., Joos, G., Garabuczi, E., Ruh1, R., Gregory, D.C., and Szondy, Z. 2014. Macrophages engulfing apoptotic cells produce nonclassical retinoids to enhance their phagocytic capacity. *J. Immunol.* **192**: 5730–5738. doi:[10.4049/jimmunol.1400284](https://doi.org/10.4049/jimmunol.1400284). PMID: [24850721](https://pubmed.ncbi.nlm.nih.gov/24850721/).
- Schroder, T., Kucharczyk, D., Bär, F., Pagel, R., Derer, S., Jendrek, S.T., et al. 2016. Mitochondrial gene polymorphisms alter hepatic cellular energy metabolism and aggravate diet-induced non-alcoholic steatohepatitis. *Mol. Metab.* **5**(4): 283–295. doi:[10.1016/j.molmet.2016.01.010](https://doi.org/10.1016/j.molmet.2016.01.010). PMID: [27069868](https://pubmed.ncbi.nlm.nih.gov/27069868/).
- Steinboff, J.S., Lass, A., and Schupp, M. 2021. Biological functions of RBP4 and its relevance for human diseases. *Front. Physiol.* **12**: 1–15. doi:[10.3389/fphys.2021.659977](https://doi.org/10.3389/fphys.2021.659977).
- Tillman, E.J., and Rolph, T. 2020. FGF21: an emerging therapeutic target for non-alcoholic steatohepatitis and related metabolic diseases. *Front. Endocrinol.* **11**(Article 601290): 1–25. doi:[10.3389/fendo.2020.601290](https://doi.org/10.3389/fendo.2020.601290).
- Tourniaire, F., Musinovic, H., Gouranton, E., Astier, J., Marcotorchino, J., Arreguin, A., et al. 2015. All-trans retinoic acid induces oxidative phosphorylation and mitochondria biogenesis in adipocytes. *J. Lipid Res.* **56**: 1100–1109. doi:[10.1194/jlr.M053652](https://doi.org/10.1194/jlr.M053652). PMID: [25914170](https://pubmed.ncbi.nlm.nih.gov/25914170/).
- Trasino, S.E., Tang, X.H., Jessurun, J., and Gudas, L.J. 2015. Obesity leads to tissue, but not serum vitamin A deficiency. *Sci. Rep.* **5**: 1–10. doi:[10.1038/srep15893](https://doi.org/10.1038/srep15893).
- Tripathy, D., Dandona, P., Aljada, A., Dhindsa, S., Mohanty, P., Ghanim, H., and Syed, T. 2003. Elevation of free fatty acids induces inflammation and impairs vascular reactivity in healthy subjects. *Diabetes* **52**(12): 2882–2887. doi:[10.2337/diabetes.52.12.2882](https://doi.org/10.2337/diabetes.52.12.2882). PMID: [14633847](https://pubmed.ncbi.nlm.nih.gov/14633847/).
- Wajner, M., and Amaral, A.U. 2016. Mitochondrial dysfunction in fatty acid oxidation disorders: Insights from human and animal studies. *Biosci. Rep.* **36**(1): 1–13. doi:[10.1042/BSR20150240](https://doi.org/10.1042/BSR20150240).
- Wells, R.A., and Chan, L.S.A. 2009. Cross-talk between PPARs and the partners of RXR: a molecular perspective. *PPAR Res.* **2009**. Article ID: 925309. doi:[10.1155/2009/925309](https://doi.org/10.1155/2009/925309). PMID: [20052392](https://pubmed.ncbi.nlm.nih.gov/20052392/).
- Yang, L., Wei, J., Sheng, F., and Li, P. 2019. Attenuation of palmitic acid-induced lipotoxicity by chlorogenic acid through activation of SIRT1 in hepatocytes. *Mol. Nutr. Food Res.* **63**(14): 1–12. doi:[10.1002/mnfr.201801432](https://doi.org/10.1002/mnfr.201801432).
- Zhong, G., Kirkwood, J., Jae, K., Tjota, N., Jeong, H., and Isoherranen, N. 2019. Characterization of vitamin A metabolome in human livers with and without non-alcoholic fatty liver disease. *J. Pharmacol. Exp. Ther.* **370**: 92–103. doi:[10.1124/jpet.119.258517](https://doi.org/10.1124/jpet.119.258517). PMID: [31043436](https://pubmed.ncbi.nlm.nih.gov/31043436/).
- Zhou, H., Urso, C.J., and Jadeja, V. 2020. Saturated fatty acids in obesity-associated inflammation. *J. Inflamm. Res.* **13**: 1–14. doi:[10.2147/JIR.S229691](https://doi.org/10.2147/JIR.S229691). PMID: [32021375](https://pubmed.ncbi.nlm.nih.gov/32021375/).
- Ziouzenkova, O., Orasanu, G., Sharlach, M., Akiyama, T.E., Joel, P., Viereck, J., et al. 2007. Retinaldehyde represses adipogenesis and diet-induced obesity. *Nat. Med.* **13**(6): 695–702. doi:[10.1038/nm1587](https://doi.org/10.1038/nm1587). PMID: [17529981](https://pubmed.ncbi.nlm.nih.gov/17529981/).